Cape Peninsula University of Technology

POLYCYCLIC AROMATIC HYDROCARBONS (PAHs) IN THE DIEP AND PLANKENBURG RIVERS AND POTENTIAL REMEDIATION USING CHARRED *Vitis vinifera* (GRAPE) LEAF LITTER

by

ADETUNJI AJIBOLA AWE

Thesis submitted in fulfilment of the requirements for the degree

Doctor of Philosophy: Chemistry

in the Faculty of Applied Sciences

at the Cape Peninsula University of Technology

Supervisor: Prof Opeolu, BO
Co- Supervisors: Prof Fatoki, OS, Dr Jackson, VA and Aprf Snyman, RG

Cape Town
December 2019

DECLARATION

I, Awe, Adetunji Ajibola declare that the content of this thesis represents my own unaided work, and that the thesis has not previously been submitted for academic examination towards any qualification. Furthermore, it represents my own opinions and not necessarily those of the Cape Peninsula University of Technology.

Signed **Date**

ABSTRACT

Occurrence of polycyclic aromatic hydrocarbons (PAHs) in freshwater systems may aggravate the water crisis currently being experienced in the Western Cape province of South Africa. However, there is dearth of data on the levels of PAHs, necessary for effective assessment of water quality as well as remediation strategies. This study therefore assessed levels of PAHs in two important freshwater systems in the Western Cape Province, South Africa. The potential of grape leaf litter for PAH abatement was also investigated.

A solid-phase extraction - gas chromatography - flame ionisation detection (SPE-GC-FID) method was developed to simultaneously determine the 16 United States Environmental Protection Agency (US EPA) priority PAHs in environmental samples. Levels of 16 US EPA priority PAHs were assessed in water, sediment and plants from seven selected sites on the Diep and Plankenburg Rivers. Seasonal variations of some water quality parameters and PAHs levels in water and sediment samples were determined from the selected sites. Activated carbons produced from *Vitis vinifera* (grape) leaf litter were utilised for PAH-remediation.

The SPE-GC-FID method developed for the 16 US EPA priority PAHs determination gave acceptable linearity ($R^2 > 0.999$). Instrument detection limits ranged between 0.02 and 0.04 µg/mL and instrument quantification limits of between 0.06 and 0.13 µg/mL. Recovery studies were also acceptable (70.35 - 100.83%) with the exception of naphthalene that had lower recoveries.

The average ∑16 PAHs detected in water samples at a given site, over a one-year period ranged from 73.90 to187.11 µg/L. The highest PAHs levels were detected in water samples from industrial areas of both rivers; chrysene (Chy) followed by benzo[a]anthracene (BaA) were the most abundant PAHs detected in water samples. Higher PAHs levels were detected in sediment samples relative to water samples; the average ∑16 PAHs detected in sediment samples at a given site, over a one-year period ranged from 6.048 to 39.656 µg/g. PAHs levels were also highest in sediment samples from industrial areas of the two rivers; benzo[b]fluoranthene (BbF) followed by benzo[k]fluoranthene (BkF) were the most abundant PAHs detected in sediment samples. The average ∑16 PAHs detected in plant samples [*Phragmites australis* (common reed) and *Eichhornia crassipes* (water hyacinth)] at a given site, ranged between 62.11 and 226.72 µg/g. Highest levels of PAHs were therefore detected in plant samples, suggesting possible bioaccumulation of PAHs in plant tissues. The bioaccumulation of PAHs by the plants also indicates the phytoremediation potential of these plants for PAHs remediation.

The levels of PAHs measured in water and sediment samples were subjected to probabilistic risk assessment to predict the possibility of regulatory values being exceeded. The average percentage exceedence of 63.26 and 42.81 were obtained for PAHs in water samples of the Diep

and Plankenburg Rivers respectively, while the corresponding average percentage exceedence obtained for sediment samples were 63.71 and 77.20.

Vitis vinifera (grape) leaf litter showed enormous prospect as precursor for activated carbon. The yield of activated carbons obtained from grape leaf litter ranged from 44.65 to 58.40% and the Brunauer-Emmett-Teller (BET) surface area of up to 616.60 m^2/g was obtained for activated carbons. The estimated adsorption capacities of the $ZnCl_2$ and H_3PO_4 activated carbons for phenanthrene removal from aqueous solutions were 94.12 and 89.13 mg/g respectively.

The environmental samples analysed were heavily contaminated with the 16 US EPA priority PAHs and the probabilistic risk assessment suggested risks of the carcinogenic PAHs at the levels measured in the environment. *Vitis vinifera* leaf litter, showed enormous potential as renewable precursor for activated carbon production, capable of removing varied contaminants from wastewater.

Keywords: PAHs; Adsorption; Activated carbon; GC-FID; Freshwater; *Vitis vinifera*; Western Cape.

ACKNOWLEDGEMENTS

I wish to thank:

- The God almighty, for the gift of life and the grace for the journey.
- Prof BO Opeolu, my supervisor for her kindness, support and encouragement.
- Prof OS Fatoki, Prof RG Snyman and Dr VA Jackson, my co-supervisors and Dr Olatunji; for their support and immense contributions to the project.
- Mr Joshua Adekunle Awe and Mrs Elizabeth Arinola Awe, my parents, for being my pillar of support. I am so blessed to have you to call dad and mom.
- Mr Tony Wagbafor and family, for the love, support and encouragement.
- Adebayo, Temilola and Omotola Kolade, my siblings and their spouses (Titilayo, Ifewumi and Fiyinfoluwa respectively); for their love.
- Chief MO Awe, Mrs Omolara Ojo, Dr Olusegun Oguntoke, Mrs Oluwakemi Oyedokun, Mr Ade Emmanuel Toke, my uncles and aunts; for their prayers, support and encouragement.
- Mr David Kok, Prof Merrill Wicht, Mr Jacobs and all the staff of the Department of Chemistry, for their kindness and technical support.
- Mr Ademola Rabiu and Prof Tunde Ojumu, for giving me access to their laboratory.
- Bamidele, Oluwadara, Oputu, Michael, Wole, Justino and all other colleagues, for making the journey bearable.
- Olwethu Bonke, Okuhle September, Joyce Pankendem Olpa and all other students for the kind assistance.
- Mrs Erere Wagbafor-Awe, my jewel, for the love, peace, support and loyalty. I love you.

DEDICATION

This work is dedicated to the sweet memory of my grandmother, Madam Victoria Omobola Awe.
(1914/07/16 - 2016/07/28)

TABLE OF CONTENTS

DECLARATION ... **ii**
ABSTRACT ... **iii**
ACKNOWLEDGEMENTS ... **v**
DEDICATION ... **vi**
TABLE OF CONTENTS ... **vii**
LIST OF FIGURES ... **x**
LIST OF TABLES ... **xii**
LIST OF APPENDICES ... **xiv**
GLOSSARY ... **xv**

CHAPTER ONE ... **1**
INTRODUCTION ... **1**
1.1 Background ... 1
1.2 Problem statement ... 5
1.3 Broad objective of the research ... 6
1.4 Limitation of the Study ... 6

CHAPTER TWO ... **7**
LITERATURE REVIEW ... **7**
2.1 Polycyclic Aromatic Hydrocarbons (PAHs) ... 7
2.1.1 Background Information on the 16 US EPA Priority PAHs ... 11
2.2 Sources of PAHs in the aquatic environment ... 22
2.3 Routes of exposure and toxicity of PAHs to aquatic organisms ... 26
2.4 Routes of exposure and toxicity of PAHs to humans ... 30
2.5 Occurrence and distribution of PAHs in aquatic environments ... 36
2.6 Extraction of PAHs from environmental matrices ... 39
2.6.1 Extraction of PAHs from water samples ... 39
2.6.2 Extraction of PAHs from solid matrices ... 43
2.7 Analysis of PAHs ... 48
2.8 Evidence and monitoring of PAHs in South African environment ... 51
2.9 Remediation of PAHs ... 53
2.9.1 Conventional remediation methods for PAHs ... 53
2.9.2 Remediation of PAHs using nanoparticles ... 58
2.9.3 Bioremediation of PAHs ... 58
2.10 Adsorption remediation technology ... 76

2.10.1 Adsorption isotherm models 76
2.10.2 Adsorption kinetic models 79
2.11 Diep River 83
2.12 Plankenburg River 83

CHAPTER 3 84
METHODOLOGY 84
3.1 Method of analysis 84
3.1.1 Chemicals 84
3.1.2 Method development on GC-FID 84
3.1.3 Extraction and SPE clean-up of PAHs from samples 86
3.1.4 Method validation 87
3.2 Study area 89
3.2.1 The Diep River sites 89
3.2.2 The Plankenburg River sites 91
3.3 Sampling and sample pre-treatment 93
3.3.1 Sampling and pre-treatment of water 93
3.3.2 Sampling and pre-treatment of sediment 93
3.3.3 Sampling and pre-treatment of plant samples 94
3.4 Quality assurance and quality control steps 94
3.5 Analysis of grape leaf litter 95
3.5.1 Determination of moisture content 95
3.5.2 Determination of ash content 95
3.5.3 Crude fibre content determination 96
3.5.4 Elemental analysis 96
3.6 Production and characterisation of activated carbons 97
3.6.1 Adsorbent preparation 97
3.6.2 Adsorbent characterisation 98
3.7 Adsorption studies 98
3.7.1 Optimisation of parameters 99
3.7.2 Adsorption Isotherms 100
3.7.3 Kinetic studies 103
3.8 Analysis of data 103

CHAPTER 4 104
RESULTS AND DISCUSSION 104
4.1 GC-FID method optimisation and validation 104
4.1.1 Chromatographic separation 104
4.1.2 Linearity, detection limit and quantification limit 104
4.1.3 Precision 107
4.1.4 Recovery of PAHs 108
4.2 Water quality parameters of the Diep and Plankenburg Rivers water samples 111
4.2.1 Temperature 111
4.2.2 pH 112
4.2.3 Electrical conductivity (EC) 114
4.2.4 Total dissolved solids (TDS) 115
4.2.5 Salinity 117
4.3 Levels of PAHs in the Diep and Plankenburg Rivers 120
4.3.1 Levels of PAHs in surface water samples 120
4.3.2 Levels of PAHs in sediment samples 135
4.3.3 Levels of PAHs in plant samples of the Diep and Plankenburg Rivers 146
4.3.4 Probabilistic risk assessment of PAHs in water and sediment samples 155
4.4 Remediation of PAHs from aqueous solution 161
4.4.1 Characterisation of adsorbents produced from *V. vinifera* leaf litter 161
4.4.2 Adsorption of phenanthrene on obtained activated carbons 169

CHAPTER 5 196
CONCLUSIONS AND RECOMMENDATIONS 196
5.1 Conclusions 196
5.2 Recommendations 198
REFERENCES 199
APPENDICES 232

LIST OF FIGURES

Figure 2.1: Structures of the two to four ringed US EPA priority PAHs obtained with CambridgeSoft ChemDraw Ultra 12.0 Wizard 9
Figure 2.2: Structures of the five to six ringed US EPA priority PAHs obtained with CambridgeSoft ChemDraw Ultra 12.0 Wizard 10
Figure 2.3: Uptake and elimination pathways of toxicant by organisms [Adapted from: Mackay & Fraser (2000)] 27

Figure 3.1: Map showing the sampling sites at the Diep River 90
Figure 3.2: Map showing the sampling sites at the Plankenburg River 92

Figure 4.1: Chromatogram of the 16 US EPA priority PAHs 105
Figure 4.2: Seasonal variations and annual average levels of 16 US EPA priority PAHs in water samples of the Diep River 121
Figure 4.3: Annual distribution of 16 US EPA PAHs in water samples of the Diep River 123
Figure 4.4: Fractions of PAHs in water samples of the Diep River 125
Figure 4.5: Seasonal variations and annual average levels of 16 US EPA priority PAHs in water samples of the Plankenburg River 127
Figure 4.6: Annual distribution of 16 US EPA PAHs in water samples of the Plankenburg River 129
Figure 4.7: Fractions of PAHs in water samples of the Plankenburg River 130
Figure 4.8: Seasonal variations and annual average levels of 16 US EPA priority PAHs in water samples of the Diep and Plankenburg Rivers 131
Figure 4.9: Fractions of PAHs in water samples of the Diep and Plankenburg Rivers 132
Figure 4.10: Seasonal variations and annual average levels of 16 US EPA PAHs in sediment samples of the Diep River 136
Figure 4.11: Annual distribution of 16 US EPA PAHs in sediment samples of the Diep River 137
Figure 4.12: Fractions of PAHs in sediment samples of the Diep River 138
Figure 4.13: Seasonal variations and annual average levels of 16 US EPA priority PAHs in sediment samples of the Plankenburg River 140
Figure 4.14: Annual distribution of 16 US EPA priority PAHs in sediment samples of the Plankenburg River 141
Figure 4.15: Fractions of PAHs in sediment samples of the Plankenburg River 142
Figure 4.16: Seasonal variations and annual average levels of 16 US EPA priority PAHs in sediment samples of the Diep and Plankenburg Rivers 144
Figure 4.17: Occurrence of PAHs in *P. australis* tissues of the Diep River (site DB) 149

Figure 4.18: Occurrence of PAHs in *P. australis* tissues of the Plankenburg River 153
Figure 4.19: Fractions of PAHs in plant samples of the Diep and Plankenburg Rivers.....154
Figure 4.20: BET isotherm plots for nitrogen adsorption capacity of produced activated carbons 165
Figure 4.21: FTIR spectra of produced chars vs raw biomass.....167
Figure 4.22: Scanning electron micrographs of produced activated carbons, charred and raw biomass (magnification: x1000 vs x5000) 168
Figure 4.23: Effect of solution pH on phenanthrene adsorption using activated carbons.....170
Figure 4.24: Effect of adsorbent dosage on phenanthrene removal using activated carbons..172
Figure 4.25: Effect of initial concentration of phenanthrene on activated carbons' efficiency...175
Figure 4.26: SEM images of activated carbons before and after adsorption of phenanthrene from aqueous solution.....178
Figure 4.27a: Langmuir adsorption isotherm plots for phenanthrene removal using activated carbons (ZAac, ZBac and PAac).....180
Figure 4.27b: Freundlich adsorption isotherm plots for phenanthrene removal using activated carbons (ZAac, ZBac and PAac)……..181
Figure 4.27c: Temkin adsorption isotherm plots for phenanthrene removal using activated carbons (ZAac, ZBac and PAac)……..182
Figure 4.27d: Dubinin-Radushkevich adsorption isotherm plots for phenanthrene removal using activated carbons (ZAac, ZBac and PAac)……..184
Figure 4.28: Effect of contact time on phenanthrene adsorption using activated carbons 186
Figure 4.29a: Pseudo-first order adsorption kinetic plots for phenanthrene removal using activated carbons (ZAac, ZBac and PAac).....188
Figure 4.29b: Pseudo-second order adsorption kinetic plots for phenanthrene removal using activated carbons (ZAac, ZBac and PAac).....190
Figure 4.29c: Elovich adsorption kinetic plots for phenanthrene removal using activated carbons (ZAac, ZBac and PAac) 192
Figure 4.29d: Weber Morris intraparticle diffusion adsorption kinetic plots for phenanthrene removal using activated carbons (ZAac, ZBac and PAac).....194
Figure 4.30: Intra particle diffusion kinetics for phenanthrene removal using activated carbons 195

LIST OF TABLES

Table 2.1: Properties of the 16 US EPA Priority PAHs 8
Table 2.2: Toxic equivalent factors (TEFs) for the 16 US EPA priority PAHs 18
Table 2.3: PAH ratios used for pyrogenic and petrogenic source assignment 25
Table 2.4: PAH Content in Food 31
Table 2.5: Detected levels of PAHs in different food samples 32
Table 2.6: A summary of methods used to analyse PAHs in water samples 42
Table 2.7: A summary of methods used to analyse PAHs in sediment samples 45
Table 2.8: A summary of methods used to analyse PAHs in plant samples 47
Table 2.9: Summary of conventional remediation approaches utilised for PAH-degradation 54
Table 2.10: Phytoremediation approaches for PAH-degradation 60
Table 2.11: Bioreactors utilised for PAH-degradation 65
Table 2.12: Biosorption approaches for PAHs remediation 71
Table 3.1: Specifications and the operating conditions of the GC-FID 85
Table 3.2: Description of sampling sites of the Diep River 89
Table 3.3: Description of sampling sites of the Plankenburg River 91

Table 4.1: Calibration data and linearity for the 16 US EPA Priority PAHs 106
Table 4.2: Repeatability and reproducibility of GC-FID analysis of 16 US EPA priority PAHs 107
Table 4.3: Average percentage recovery of the 16 US EPA priority PAHs from milli-Q water 109
Table 4.4: Percentage recovery of PAHs in plant and sediment samples (n = 3) 110
Table 4.5a: Seasonal variation of temperature (^{o}C) in the Diep River water samples 112
Table 4.5b: Seasonal variation of temperature (^{o}C) in the Plankenburg River water samples 112
Table 4.6a: Seasonal variation of pH values in the Diep River water samples 114
Table 4.6b: Seasonal variation of pH values in the Plankenburg River water samples 114
Table 4.7a: Seasonal variation of electrical conductivity (µS/cm) values in the Diep River water samples 115
Table 4.7b: Seasonal variation of electrical conductivity (µS/cm) values in the Plankenburg River water samples 115
Table 4.8a: Seasonal variation of TDS (mg/L) values in the Diep River water samples 116
Table 4.8b: Seasonal variation of TDS (mg/L) values in the Plankenburg River water samples 116
Table 4.9a: Seasonal variation of salinity (mg/L) in the Diep River water samples 118
Table 4.9b: Seasonal variation of salinity (mg/L) in the Plankenburg River water samples 118
Table 4.10: Correlation matrix of water quality parameters measured on site 119
Table 4.11: Fractions of PAHs congeners in water samples of the Diep River 124

Table 4.12: Fractions of PAHs congeners in water samples of the Plankenburg River.....129
Table 4.13: Annual average concentrations of PAHs in water samples of the Diep and Plankenburg Rivers 133
Table 4.14: Regulatory threshold limits of PAHs in sediment and water for the protection of aquatic life.....134
Table 4.15: Fractions of PAHs congeners in sediment samples of the Diep River 138
Table 4.16: Fractions of PAHs congeners in sediment samples of the Plankenburg River.....142
Table 4.17: Annual average concentrations of PAHs in sediment samples of the Diep and Plankenburg Rivers 145
Table 4.18a: Levels of PAHs (mean (n = 3) ± SD) in *E. crassipes* samples of the Diep River.147
Table 4.18b: Levels of PAHs (mean (n = 3) ± SD) in *P. australis* tissues of the Diep River……...148
Table 4.19a: Levels of PAHs (mean (n = 3) ± SD) in *P. australis* tissues of the Plankenburg River (sites PA and PB) 151
Table 4.19b: Levels of PAHs (mean (n = 3) ± SD) in *P. australis* tissues of the Plankenburg River (sites PC and PD).....152
Table 4.20a: Summary of statistics of the tests of the Weibull distribution of the annual concentrations (µg/L) of PAHs in water samples of the Diep River 156
Table 4.20b: Summary of statistics of the tests of the Weibull distribution of the annual concentrations (µg/L) of PAHs in water samples of the Plankenburg River……157
Table 4.21a: Summary of statistics of the tests of the Weibull distribution of the annual concentrations (µg/g) of PAHs in sediment samples of the Diep River.....159
Table 4.21b: Summary of statistics of the tests of the Weibull distribution of the annual concentrations (µg/g) of PAHs in sediment samples of the Plankenburg River……160
Table 4.22: Ash, moisture, crude fibre and atomic elements of raw grape leaf litter 161
Table 4.23: Yield, burn-off, attrition and elemental composition of the chars.....163
Table 4.24: Textural properties of produced activated carbons 164
Table 4.25: Effect of aqueous solution pH on phenanthrene removal using activated carbons170
Table 4.26: Effect of adsorbent dosage on phenanthrene removal from solution using activated carbons.....173
Table 4.27: Effect of initial concentration on phenanthrene removal from solution using activated carbons.....176
Table 4.28: Langmuir, Freundlich, Temkin and Dubinin-Radushkevich isotherm constants for the adsorption of phenanthrene onto activated carbons obtained from *V. vinifera* 183
Table 4.29: Adsorption kinetics parameters for the removal of phenanthrene from aqueous solution using activated carbons obtained from *V. vinifera*.....193

LIST OF APPENDICES

Appendix A: Calibration plots for the 16 US EPA priority PAHs....232
Appendix B: Pictures from sampling sites....234
Appendix C1: Seasonal occurrence (average ±SD) of PAHs in the Diep River water samples (sites DA and DB)....235
Appendix C2: Seasonal occurrence (average ±SD) of PAHs in the Diep River water samples (site DC)....236
Appendix D: ANOVA statistical analysis (multivariate tests) of data from the Diep River water samples....237
Appendix E1: Seasonal occurrence (average ±SD) of PAHs in the Plankenburg River water samples (sites PA and PB)....238
Appendix E2: Seasonal occurrence (average ±SD) of PAHs in the Plankenburg River water samples (sites PC and PD)....239
Appendix F: ANOVA statistical analysis (multivariate tests) of data from the Plankenburg River water samples....240
Appendix G1: Seasonal occurrence (average ±SD) of PAHs in the Diep River sediment samples (sites DA and DB)....241
Appendix G2: Seasonal occurrence (average ±SD) of PAHs in the Diep River sediment samples (site DC)....242
Appendix H1: Seasonal occurrence (average ±SD) of PAHs in the Plankenburg River sediment samples (sites PA and PB)....243
Appendix H2: Seasonal occurrence (average ±SD) of PAHs in the Plankenburg River sediment samples (sites PC and PD)....244
Appendix I: ANOVA statistical analysis (multivariate tests) of data from the Diep and Plankenburg River sediment samples (compound Vs sites)....245
Appendix J: ANOVA statistical analysis (multivariate tests) of data from the Diep and Plankenburg River sediment samples (compound Vs seasons)....246
Appendix K: Sediment physicochemical properties....247
Appendix L: Weibull plots of PAHs levels in water samples from the Diep and Plankenburg Rivers....248
Appendix M: Weibull plots of PAHs levels in sediments from the Diep and Plankenburg Rivers....250

GLOSSARY

Acy	Acenaphthylene
AHR	Aryl Hydrocarbon Receptor
Ant	Anthracene
AOAC	Association of Official Analytical Chemists
ASE	Accelerated Solvent Extraction
BaA	Benzo[a]anthracene
BaP	Benzo[a]pyrene
BbF	Benzo[b]fluoranthene
BET	Brunauer-Emmett-Teller
BgP	Benzo[g, h, i]perylene
BkF	Benzo[k]fluoranthene
Can	Acenaphthene
CAS	Chemical abstracts service
CCME	Canadian Council of Ministers of the Environment
Chy	Chrysene
C PAHs	Carcinogenic polycyclic aromatic hydrocarbons
CPE	Cloud point extraction
CSTR	Continuous stirred-tank reactors
CYP	Cytochrome P450
DBA	Dibenzo[a, h]anthracene
DCM	Dichloromethane
DEAT	Department of Environmental Affairs and Tourism
DL	Detection limit
DLLME	Dispersive liquid-liquid micro-extraction
DNA	Deoxyribonucleic acid
DWAF	Department of Water Affairs and Forestry
DWEL	Drinking water equivalent level
EC	Electrical conductivity
EDS	Energy-dispersive spectroscopy
EFSA	European food safety authority
ELISA	Enzyme-linked immuno-sorbent assay
EPA	Environmental protection agency
FBB	Fluidised-bed bioreactor
FID	Flame ionisation detector

FLD	Fluorescence detector
Flt	Fluoranthene
Flu	Fluorene
FPF	Fish potency factor
FTIR	Fourier transform infrared
FWS	Free-water surface
GC	Gas chromatography
HMW	High molecular weight
HPLC	High pressure liquid chromatography
HSDB	Hazardous substances data bank
IARC	International Agency for Research on Cancer
ICH	International Council for Harmonisation
IcP	Indeno[1, 2, 3-cd]pyrene
ICSC	International chemical safety cards
LC	Liquid chromatography
LEDs	Light-emitting diodes
LLE	Liquid-liquid extraction
LMW	Lower molecular weight
LPME	Liquid-phase micro-extraction
MASE	Microwave-assisted solvent extraction
MCL	Maximum contaminant level
MS	Mass spectrophotometer
Nap	Naphthalene
NCBI	National Centre for Biotechnology Information
NP	Nitropyrene
NTP	National toxicology program
OLEDs	Organic light-emitting diodes
OPAHs	Oxygenated polycyclic aromatic hydrocarbons
PAHs	Polycyclic aromatic hydrocarbons
PCR	Polymerase chain reaction
PDMS	Polydimethylsiloxane
Phe	Phenanthrene
POPs	Persistent organic pollutants
PVC	Polyvinyl chloride
Pyr	Pyrene

QL	Quantification limit
RfD	Reference dose
RSD	Relative standard deviation
SBSE	Stir bar sorptive extraction
SDME	Single-drop micro-extraction
SEM	Scanning electron micrograph
SFE	Supercritical fluid extraction
SLE	Solid-liquid extraction
SLME	Supported-liquid membrane extraction
SPE	Solid-phase extraction
SPMD	Semipermeable membrane device
SPME	Solid-phase micro-extraction
SSF	Subsurface flow
TDS	Total dissolved solids
TEF	Toxic equivalent factor
TPPBs	Two-phase partitioning bioreactors
TSS	Total suspended solid
UAE	Ultrasound-assisted extraction
UATR	Universal attenuated total reflectance
USAEME	Ultrasound-assisted emulsification-micro-extraction
US EPA	United states environmental protection agency
UV	Ultraviolet
WHO	World health organisation

CHAPTER ONE
INTRODUCTION

1.1 Background

As water is essential to human existence, the aquatic system is of immense importance. Contamination thus limits its availability as a resource, which could possibly result in human health problems, reduced biodiversity, environmental degradation, hunger and poverty, amongst others. Amongst these contaminants are Polycyclic Aromatic Hydrocarbons (PAHs) (Christensen & Arora, 2007).

Polycyclic aromatic hydrocarbons are persistent organic chemical compounds, which are found to be ubiquitous environmental contaminants (Sun *et al*., 2009). PAHs are of environmental concern, as they have been shown to be carcinogenic, mutagenic and teratogenic (Yamada *et al*., 2003). PAHs' persisting and highly hydrophobic (lipophilic) nature, results in their bioaccumulation in aquatic organisms. They have been shown to display acute toxicity and sub-lethal effects on aquatic organisms (Olivella *et al*., 2006; Cardellicchio *et al*., 2007; Boitsov *et al*., 2009).

Polycyclic aromatic hydrocarbons are not listed in the Stockholm Convention on persistent organic pollutants (POPs) [a treaty South Africa signed] but are covered by the POPs-Protocol under the United Nations Economic Commission for Europe's Convention on Long Range Transboundary Air Pollution (Choi *et al*., 2009; Quinn *et al*., 2009). The Stockholm Convention on POPs is a global treaty to protect human health and the environment from chemicals that remain intact in the environment for long periods of time (Choi *et al*., 2009).The United States Environmental Protection Agency (US EPA) listed 16 PAHs as priority pollutants in wastewaters and 24 in soils, sediments, hazardous solid waste and ground water (Christensen & Bzdusek, 2005; US EPA, 2014) based on their potential health hazards to animals and humans. Degger *et al*. (2011a) reported on the widespread contamination of the marine environment of South Africa by PAHs. Lipid weight PAHs levels of 0.29 to 2.10 µg/g in mussels and 0.26 to 0.72 µg/g in semi-permeable-membrane-devices (SPMDs) were reported. Nieuwoudt *et al*. (2011) on the other hand reported on the widespread contamination of aquatic environment of South Africa by PAHs. The sediment samples were reported to be the most impacted with PAHs and levels ranged between 0.112 to 61.764 µg/g. Both studies stressed the fact that there is paucity of data on PAHs in South Africa and the need for more extensive data on PAHs in aquatic systems of South Africa was highlighted. Data on contaminants are crucial in identifying pollution sources, mapping out clean up strategies,

meeting environmental management and policy objectives as well as formulating policy and guidelines for freshwater ecosystems.

PAHs have multiple anthropogenic (combustion of fossil fuel and biomass as well spillage of petroleum products) and natural sources (forest fires, volcanic emissions, and natural oil seeps amongst others), and are easily and widely dispersed through air and water, resulting in their global presence and impact on humans' and aquatic biota's health, air and water quality and other environmental media [soils, sediments, flora and fauna amongst others] (Ravindra *et al*., 2008; Wang *et al*., 2014). Asia and Africa have particularly high PAHs burden, because of heavy reliance on combustion of solid fuels for cooking and heating (Ravindra *et al*., 2008; Lea-Langton *et al*., 2018). This burden is exacerbated with lack of proper guidelines and regulations for PAHs, which is evident in the unabated oil spillage and gas flaring occurrences reported by Ejiba *et al*. (2016). PAHs have been detected in various environmental matrices, reported detected levels as far back as the 80's and 90's ranged from ng/L to µg/L in surface water samples and 1000 to 10000 µg/kg in river sediments, up to g/kg in soil close to industrial areas, up to 200 µg/kg in smoked food (fish and meat), up to 400 µg/kg in food crop grown on contaminated soil and up to up to 950 ng/m^3 in ambient air (near oil processing plant) amongst others (WHO, 1998a). In more recent years, levels of PAHs monitored in the different compartments (water, sediment and biota) of the aquatic ecosystems worldwide had been reported; ∑18 PAHs that ranged from 3749 to 22324 µg/kg in surface sediments [USA] (Kim *et al*., 2018), ∑15 PAHs from 910 to 1520 ng/L, 404 to 883 ng/g, 397 to 1935 ng/g, and 1585 to 3539 ng/g in surface water, surface sediment, soil and leaf samples respectively [China] (Li *et al*., 2010a), ∑16 PAHs from 105 to 513 ng/g in fish tissue (bighead carp and silver carp fishes) [China] (Zhao *et al*., 2014b), ∑16 PAHs from 2886 to 5482 ng/g in surface sediment [Iran] (Abdollahi *et al*., 2013), ∑10 PAHs from 13.17 to 26.38 mg/L and from 27.10 to 55.93 mg/kg in surface water and sediment samples [South Africa] (Edokpayi *et al*., 2016) and ∑16 PAHs from 3.75 to 22.30 mg/kg [across northern France and Belgium] (Rabodonirina *et al*., 2015) amongst others. The sediment compartment has received tremendous attention relative to others (e.g. surface water and plant). Dissolved pollutants in water are however more bioavailable to effect toxicity relative to those in sediments and accumulated levels in plants threatens dietary quality (a key factor in epidemiology) (Neff *et al*., 2005; Abdel-Shafy & Mansour, 2016). Hence, this study provides data on levels of the 16 US EPA priority PAHs in sediments, water and plants.

The capabilities of PAHs causing acute (eye and dermal irritation, acute haemolysis and nausea amongst others), sub-chronic (growth inhibition, mortality, diarrhoea and severe anaemia amongst others) and chronic (cancer, silicosis and chronic bronchitis amongst others) toxicities on sufficiently exposed organisms have also been reported (WHO, 1998a; Machado *et al*., 2014).

Various organisms *in vivo*/*in vitro* and human *in vitro* assays have confirmed the deleterious effects of PAHs which include genotoxicity, carcinogenicity and embryotoxicity amongst others (Ma & Lu, 2007; Machado *et al*., 2014; Ajayi *et al*., 2016; Santos *et al*., 2018a). The guppy, *Poecilia vivipara* (widely distributed fish in most of the tropical and subtropical world) was utilised by Machado *et al*. (2014), the fish expressed oxidative stress and DNA damage on phenanthrene exposure for just 96 h.

The toxic nature of PAHs had prompted various international, national and state agencies to formulate guidelines and regulations, to reduce environmental PAH-levels, as well as limit human PAH-exposures. The reduction in the detected levels of some individual PAH has since been observed, even though five-fold increase were observed over a 150-year period in the total PAHs levels in soils and sediments (WHO, 1998a). Agencies that have given guidelines and regulations on PAHs include International Agency for Research on Cancer (IARC), World Health Organisation (WHO), Occupational Safety and Health Administration (OSHA), Environmental Protection Agency (EPA) and National Institute for Occupational Safety and Health (NIOSH) amongst others [Agency for Toxic Substances and Disease Registry (ATSDR), 1995]. The EPA for example, gave carcinogenic classification, probable effect level, maximum contaminant level in various environmental media, procedure of analysis and proposed remediation strategies amongst others for priority PAHs.

To assess environmental quality, monitor health-effects and ascertain the suitability of food for consumption, PAHs have been quantified by various techniques (chromatographic and biotic) (Poster *et al*., 2006; Ye *et al*., 2009). The liquid and gas chromatography (LC and GC) are the commonly utilised techniques for the measurement of PAHs, however the GC is preferred based on selectivity, resolution, sensitivity and analysis time (Poster *et al*., 2006). Fast GC, with reduced analysis time for PAHs are often limited to flame ionisation detector (FID), electron capture detector (ECD) and time-of-flight mass spectrometry (TOF-MS) detection methods, having good detector response (Poster *et al*., 2006). Therefore, GC-FID, GC-ECD and GC-TOF-MS are the techniques that are easily adaptable for the routine separation, detection and quantification of PAHs extracted from environmental matrices.

To ensure healthy ecosystems, enormous resources have been and are being channelled into remediating PAH-impacted aquatic ecosystems worldwide, especially as a result of oil spillage (Shahriari & Frost, 2008). However, the aquatic ecosystems have not been rid of these recalcitrant contaminants. Wastewater treatment prior to discharge into aquatic ecosystems and clean-up of aquatic ecosystems that have been impacted with PAHs from anthropogenic (oil spillage,

domestic, industrial and vehicular combustion of material for energy) and natural sources (forest and prairie fires, green waste, volcanic eruption) are often achieved at astronomical costs (Shahriari & Frost, 2008; De-Gisi *et al*., 2016; Grubesic *et al*., 2017). These exorbitant costs (infrastructural and associated costs) cannot be maintained by developing countries for which the feeding, sanitation, basic infrastructural needs and other socio-economical needs are already proving to be challenging. Therefore, researchers are focusing on achieving cleaner freshwater ecosystems through affordable and sustainable technologies, involving the use of agricultural waste biomass and microorganisms (Calheiros *et al*., 2012; Reungoat *et al*., 2012; Matamoros *et al*., 2016).

Wastewater consists of diverse contaminants that cannot be addressed efficiently by a single remediation approach (Reungoat *et al*., 2012). The concurrent application of more than one remediation approach for wastewater treatment is receiving particular attention to enhance the efficient removal/remediation of contaminants, as well as their by-products (Bollmann *et al*., 2016; Mujtaba & Lee, 2017). The use of adsorbents in remediation processes in combination with microorganism, have gained increased popularity (Mujtaba & Lee, 2017; Louis *et al*., 2018; Lefèvre *et al*., 2018). Production of adsorbents that could replace expensive and conventional adsorbents currently available now, for wastewater treatment becomes imperative. Activated carbon (which can be produced from agricultural waste biomass) has been described as one of the most promising adsorbents used in wastewater treatment due to its high surface area and high capacity for organic pollutants removal from water (Louis *et al*., 2018).

Grapes were first cultivated in Mediterranean countries over thousands of years ago, (Spinelli *et al*., 2012). The cultivation of grape is now common all over the world, surface covered with vineyards amounted to almost eight million hectares worldwide, as at 2008 and often represents a very profitable endeavour (Spinelli *et al*., 2012). The total harvest of *Vitis vinifera* (grape) worldwide is about 60 million metric tons per year and about 80% of the harvest being utilised in wineries (Lafka *et al*., 2007). In South Africa, 101,259 hectares (ha) of land are used for grape wine cultivation, which places South Africa at 14th place in terms of hectares used for wine grape production and the 7th largest producer of wine in the world (Siphugu & Terry, 2011). Consequently, wastes from wineries could serve as precursors for agricultural based activated carbons. This provides an opportunity to explore the possible utilisation of this resource for the abatement of recalcitrant PAHs, in a way that will provide environmental and economic benefits, as well as reducing the problems associated with their disposal. This informed the production of activated carbons from leaf litter for PAH removal from water.

1.2 Problem statement

South Africa is a semi-arid country with shortage of freshwater resources having only 8.6% of rainfall available as surface water (Department of Environmental Affairs and Tourism (DEAT), 2006) and the annual major dam levels for City of Cape Town (a major city of the Western Cape Province) has been monitored at 37.4% in 2017 (www.capetown.gov.za). Pollution of this scarce resource by PAH-containing substances could have far reaching negative implications on the water resources of the country. Water is indeed a crucial ecological resource perhaps after air; contaminated surface water may percolate to the aquifer through infiltration and direct input from sinking streams (Ruggieri *et al*., 2017).

Polycyclic aromatic hydrocarbons (PAHs) being mutagenic, carcinogenic and teratogenic have been reported to be the most dangerous of all anthropogenic contaminants released into the environment (Degger *et al*., 2011b). The aquatic system is the ultimate repository of human waste (Chakraborty *et al*., 2016) and as such, environmental water resources need to be continually monitored for these pollutants. The high lipophilic and persistent nature of PAHs result in their transport through the food chain (Olivella *et al*., 2006; Chen *et al*., 2011), predisposing humans and animals to the negative impacts of these toxic chemicals.

Crop cultivation in South Africa depends largely on irrigation. Thus, irrigating with PAH-contaminated water may result in food-shortage as PAHs absorbed by plants has been shown to inhibit plant growth and development (Tomar & Jajoo, 2014).

Abatement and control of these pollutants depend largely on temporal and spatial distribution data of these PAHs. Hence, the present study is imperative as it seeks to provide data on the levels of 16 US EPA PAHs in water, plant and sediment samples in Rivers of Western Cape Province facing acute shortage of freshwater resources. These data are needed to effectively control the release of PAHs into aquatic environments. The need for remediation strategies of wastewater, including biosorption, also becomes imperative to prevent the pollution of receiving waters, for sustainable use of freshwater resources for agricultural, recreational and domestic activities.

This study therefore aimed at developing a GC-FID method for the simultaneous analysis of the 16 priority US EPA PAHs in water, sediment and plant samples. Spatial and seasonal variations of the compounds were monitored in surface water and sediment samples over a 12 months period. The uniqueness of this study lies in the fact that it will provide the baseline data on levels of 16 priority PAHs in plant samples around industrial, residential and agricultural areas of the City

of Cape Town. The potential of activated carbons produced from grape leaf litter for possible remediation capabilities of PAHs in water was also investigated.

1.3 Broad objective of the research

The broad objective of this study was therefore to assess levels of PAHs in the Diep and Plankenburg Rivers and possible abatement of the compounds using activated carbons derived from grape leaf litter.

The specific objectives are:

1. To assess the spatial and seasonal occurrence of the 16 US EPA priority PAHs in the Diep and Plankenburg Rivers.
2. To examine the distribution of the 16 US EPA priority PAHs between the rivers' compartments (water and sediment).
3. To determine the possibility of the 16 US EPA priority PAHs accumulation in plants [*Eichhornia crassipes* (water hyacinth) and *Phragmites australis* (common reed)].
4. To determine the potential of activated carbons produced from grape leaf litter for PAH removal.

1.4 Limitation of the Study

Remediation studies were carried out as batch experiments only; flow through systems were not investigated.

CHAPTER TWO
LITERATURE REVIEW

2.1 Polycyclic Aromatic Hydrocarbons (PAHs)

Polycyclic aromatic hydrocarbons (PAHs) are compounds of two or more fused arene structures, made up of hydrogen and carbon. The low hydrogen-to-carbon ratio in PAH-compounds makes them the most stable form of hydrocarbons, which occur in complex mixtures rather than single compounds in the environment (Ravindra *et al*., 2008). PAHs are produced in the environment primarily by incomplete combustion of organic materials originating from anthropogenic sources, while natural processes like volcanic eruption and forest fire also contribute to ambient PAH-levels (Okuda *et al*., 2010).

There are numerous PAH compounds and they differ based on the number and position of aromatic rings, and the location of substituents on the basic ring structure. Mobile PAH compounds from two-ringed (naphthalene) to seven-ringed (coronene) range have attracted environmental concerns over the years. This is because they are carcinogenic, mutagenic, tetratogenic, endocrine-distruptive and have a global environmental spread (Eisler, 1987; Bixian *et al*., 2001; Okuda *et al*., 2010). The best known compound of PAH is benzo[a]pyrene with five rings, being the first chemical carcinogen to be discovered (Ravindra *et al*., 2008).

Humans are generally exposed to the adverse effects of PAHs through dermal, oral and inhalation pathways (Wakefield, 2007). The United State Environmental Protection Agency (US EPA) has classified 16 of these PAHs as priority pollutants (US EPA, 2014). Information about these 16 priority US EPA PAH compounds is given in Table 2.1 and the structures of these PAHs shown in Figures 2.1 and 2.2.

Table 2.1: Properties of the 16 US EPA Priority PAHs

PAH	Abbreviation	CAS number	Chemical Formula	Number of fused rings	Molecular weight	Partition Coefficient log(K_{OW})	Solubility in water (mg/L)	Carcinogenic potency classification
Naphthalene	Nap	91-20-3	$C_{10}H_8$	2	128.2	3.28	3.10E+01	2B
Acenaphthylene	Acy	208-96-8	$C_{12}H_8$	3	152.2	4.07	1.60E+01	3
Acenaphthene	Can	83-32-9	$C_{12}H_{10}$	3	154.2	3.98	4.24E+00	3
Fluorene	Flu	86-73-7	$C_{13}H_{10}$	3	166.2	4.18	1.98E+00	3
Phenanthrene	Phe	85-01-8	$C_{14}H_{10}$	3	178.2	4.45	1.10E+00	3
Anthracene	Ant	120-12-7	$C_{14}H_{10}$	3	178.2	4.45	4.34E-02	3
Fluoranthene	Flt	206-44-0	$C_{16}H_{10}$	4	202.3	4.90	2.06E-01	3
Pyrene	Pyr	129-00-0	$C_{16}H_{10}$	4	202.3	4.88	1.35E-01	3
Benzo[a]anthracene	BaA	56-55-3	$C_{18}H_{12}$	4	228.2	5.61	9.40E-03	2B
Chrysene	Chy	218-01-9	$C_{18}H_{12}$	4	228.3	5.16	1.60E-03	2B
Benzo[b]fluoranthene	BbF	205-99-2	$C_{20}H_{12}$	5	252.3	6.04	1.50E-03	2B
Benzo[k]fluoranthene	BkF	207-08-9	$C_{20}H_{12}$	5	252.3	6.06	8.00E-04	2B
Benzo[a]pyrene	BaP	50-32-8	$C_{20}H_{12}$	5	252.3	6.06	1.62E-03	1
Benzo[g, h, i]perylene	BgP	191-24-2	$C_{22}H_{12}$	6	276.3	6.50	2.60E-04	3
Indeno[1,2,3-cd]pyrene	IcP	193-39-5	$C_{22}H_{12}$	6	276.3	6.58	2.20E-05	2B
Dibenzo[a, h]anthracene	DBA	53-70-3	$C_{22}H_{14}$	5	278.4	6.84	2.49E-03	2B

Adapted from National Centre for Biotechnology Information (NCBI) [2005]; Ferrarese *et al.* (2008); International Agency on Research on Cancer (IARC) [2016]

International Agency on Research on Cancer (IARC) Classification:
Group 1: Carcinogenic to humans. **Group 2A**: Probably Carcinogenic to humans.
Group 2B: Possibly Carcinogenic to humans. **Group 3**: Not classified as to its Carcinogenicity to humans.
Group 4: Probably not Carcinogenic to humans

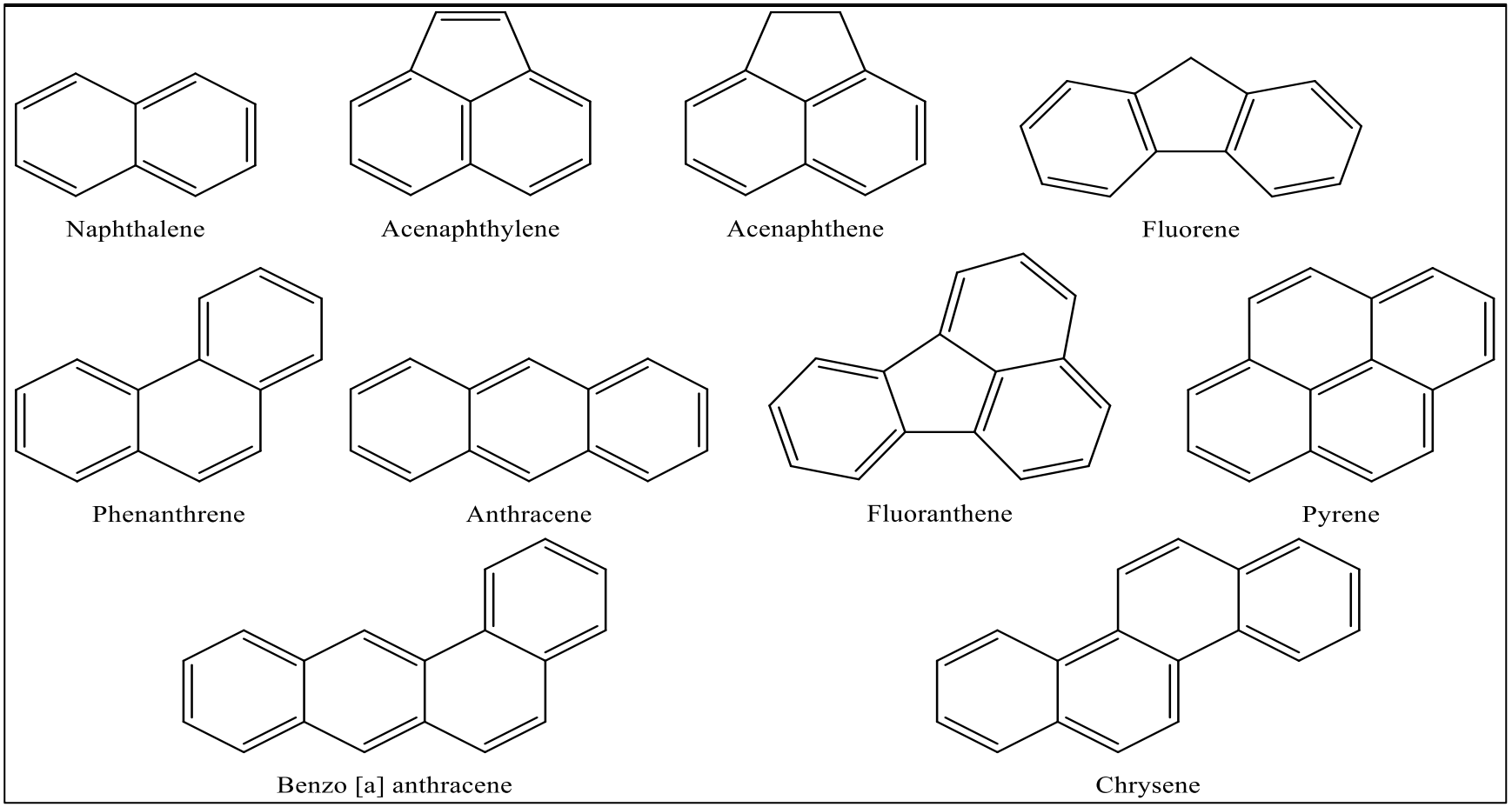

Figure 2.1: Structures of the two to four ringed US EPA priority PAHs obtained with CambridgeSoft ChemDraw Ultra 12.0 Wizard

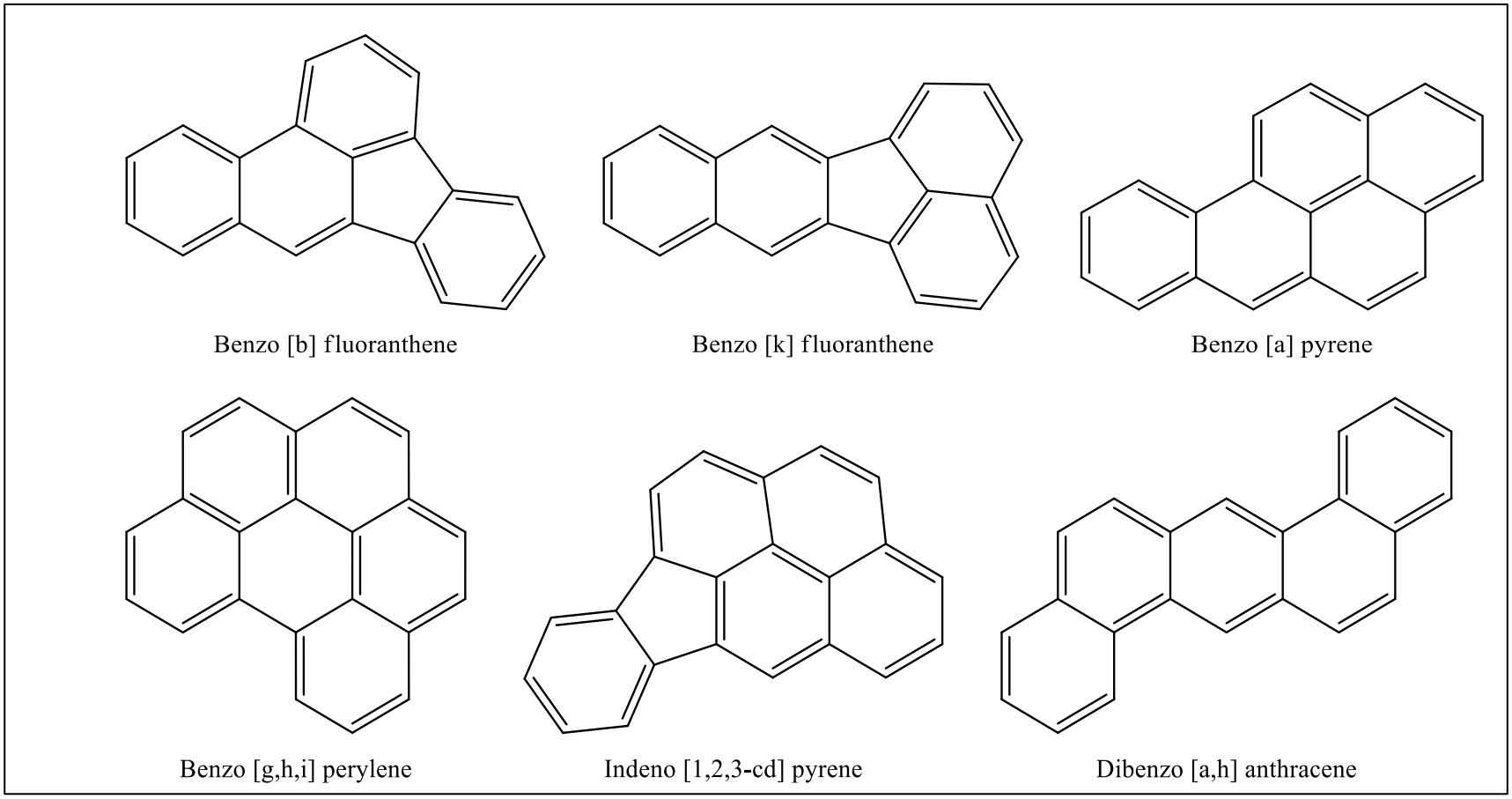

Figure 2.2: Structures of the five to six ringed US EPA priority PAHs obtained with CambridgeSoft ChemDraw Ultra 12.0 Wizard

2.1.1 Background Information on the 16 US EPA Priority PAHs

2.1.1.1 Naphthalene ($C_{10}H_8$): Nap

This is the smallest of the PAHs, consisting of only two fused benzene rings with a characteristic strong odour that smells like tar. It is also known as naphthene, naphthelin, white tar and tar camphor (International Agency for Research on Cancer (IARC), 2002). It has a relative molecular mass of 128.17, occurs as white monoclinic crystals with a boiling-point of 217.9^{o}C and has a melting point of 80.2^{o}C. It is slightly soluble in water (31 - 34 mg/L at room temperature), soluble in methanol and ethanol, but highly soluble in benzene, acetone, carbon disulphide, diethyl ether and chloroform (Lide & Miline, 1996; O'Neil, 2001). Naphthalene is volatile at room temperature and sublimes substantially at temperature above its melting-point (O'Neil, 2001). It occurs naturally in fossil fuels (coal tar and crude oil) and it is also found in cigarette smoke, car exhaust and other smoke of organic origin (Gervais *et al*., 2010). Naphthalene is used as moth repellent, in the production of azo dyes, surfactants and dispersants, tanning agents, toilet deodorant blocks, as well as insecticides (O'Neil, 2001). Naphthalene is largely employed commercially in the manufacturing of chemicals like phthalic anhydride used as softeners in polyvinyl chloride (PVC) plastics (O'Neil, 2001; Gervais *et al*., 2010).

Diarrhoea, fever, tachycardia, tachypnoea, painful urination, dermal and eye irritation, cataracts, acute haemolysis and haemolytic anaemia amongst others are some of the adverse effects of acute exposure to naphthalene in humans. Long term exposure, could possibly result in cancer, based on an animal study (IARC, 2002; Wakefield, 2007; Gervais *et al*., 2010). Though classified as group 2B (Table 2.1), it could influence the toxicity and carcinogenicity of PAHs mixtures through an array of interactions, which could eventually lead to either enhancement or inhibition of the metabolic activation of a carcinogenic PAH to a mutagenic form (Spink *et al*., 2008).

2.1.1.2 Acenaphthylene ($C_{12}H_8$): Acy

This can be described as a naphthalene molecule with an additional C_2H_2 unit attachment, resulting in a three-ringed structure. It is also known as cyclopenta[de]naphthalene and acenaphthalene with a relative molecular mass of 152.19. It is a colourless or yellow crystalline powder with a melting point between 92 – 93^{o}C, a boiling point between 265 – 275^{o}C and unlike most PAHs, does not fluorescence (National Center for Biotechnology Information (NCBI), 2004). It has a solubility of 16.1 mg/L in water at room temperature, and is soluble in alcohol, ether and benzene (Hazardous Substances Data Bank (HSDB), 1983). It has a flash point of 122.2^{o}C, and

produces acrid smoke and irritating fumes when decomposed by heat (HSDB, 1983). Acenaphthylene is highly reactive with all atmospheric oxidants such as OH and NO_3 radicals, Cl atoms and O_3 due to the presence of the C_2H_2 unit which makes it relatively unique amongst PAHs (Riva *et al*., 2016). Based on its reactivity, it can undergo thermal/photo dimerisation to produce heptacyclene dimers (Santos *et al*., 2006). Like most PAHs, it occurs naturally in coal tar and crude oil. It can be produced and released into to the environment as products of combustion caused by natural fire resulting from lightening, volcanic activities and spontaneous combustion (NCBI, 2004; HSDB, 1983). Acenaphthylene is used in the production of dyes, plastics, fungicides, insecticides, pesticides, resins and also employed in biochemical or cancer research (NCBI, 2004; Santos *et al*., 2006). Acenaphthylene is capable of causing eye, skin and respiratory tract irritation, chronic cough, bronchitis, and bronchogenic; however its carcinogenic ability has not been established (HSDB, 1983). Occupational exposure is the most probable route of human exposure, but significant daily intake of acenaphthylene has been shown in studies of human population diet (Martorell *et al*., 2012). The daily intake of dietary acenaphthylene estimated from the standard meal of a male adult (bodyweight of 70 kg) was found to be the highest (12.7 µg/day) of the 16 priority US EPA PAHs investigated by the study.

2.1.1.3 Acenaphthene ($C_{12}H_{10}$): Can

Structurally, acenaphthene is like acenaphthylene, differing only by having the central double-bond in the five-membered ring structure replaced by a single bond (Figure 2.1), giving structural stability to acenaphthene. This also makes acenaphthene incompatible with strong oxidising agents, such as ozone and chlorinating agents. It forms crystalline complexes with desoxycholic acids (Thorwirth *et al*., 2007; National Toxicology Program (NTP), 1992), and is also known as 1, 2-dihydroacenaphthylene, naphthyleneethylene, and 1, 8-ethylenenaphthalene with a relative molecular weight of 154.20. It is a white needle like crystal with a melting point of 93.6^{o}C, a boiling point of 279^{o}C and a flash point of 135^{o}C (NCBI, 2004). It is readily soluble in benzene and toluene, slightly soluble in alcohol and chloroform and poorly soluble in water (0.4 mg/100 mL) (International Chemical Safety Cards (ICSC), 2006). Acenaphthene can be derived from coal tar and is largely employed in the production of dyes, plastics, pharmaceuticals, insecticides as well as fungicides (NCBI, 2004). Acenaphthene is also used as an intermediate to produce naphthalic acids, naphthalic anhydride and acenaphthylene. Irritation of the eyes, skin and mucous membranes are forms of its physiological effects and if swallowed, could result in acute vomiting (HSDB, 1983). This compound is very toxic to aquatic organisms and capable of causing long-term effects in the aquatic system, such as morphological alterations and reduction in aquatic population (Peterson & Bain, 2004). Also, human exposure have been linked with cancer and

cardiovascular diseases (ICSC, 2006). Its ability to produce nuclear and cytological changes in microbial and plant species have also been established (NCBI, 2005).

2.1.1.4 Fluorene ($C_{13}H_{10}$): Flu

This is also known as 9H-Fluorene, Diphenylenemethane, ortho-Biphenylenemethane, Fluoren and 2,3-Benzindene with a relative molecular weight of 166.22. It occurs as white leaflets, sublimes under vacuum and when impure fluorescent (NTP, 1992). It has a boiling point of 295^{o}C, melting point of 116 - 117^{o}C, highly soluble in benzene, ether, hot alcohol and acetone, but insoluble in water (NCBI, 2004). Fluorene is said to be a major component of the total environmental PAHs with tobacco smoking being the major route of human exposure. Human exposure through inhalation of polluted air, and ingestion of food and water contaminated by combustion effluents also occurs (IARC, 1983). Fluorene can be produced in the following ways: i). the reaction of acetylene and hydrogen in red-hot tube; ii). boiling charcoal with fuming HNO_3; iii). palladium-catalysed boiling of 2,2'-Dibromodiphenylmethane with hydrazine hydrate; and iv). zinc reduction of diphenylene ketone (NCBI, 2004). It is used as a petroleum component but is largely utilised as the precursor to other fluorene compounds used in the production of pharmaceuticals, dyes, thermoset plastics, pesticides and in recent years, in the production of luminophores for their applications in light-emitting diodes (LEDs) (NCBI, 2004; Guo *et al*., 2011). While there are no evidence to suggest that fluorene has carcinogenic properties, it could cause numerous non-cancer effects with chronic exposure such as; eye and dermal irritation, eye and dermal photosensitivity, bronchitis, leukoplakia and erythema amongst others (HSDB, 1983).

2.1.1.5 Phenanthrene ($C_{14}H_{10}$): Phe

This PAH is also known as Ravatite; a tricyclic aromatic hydrocarbon which occurs as colourless monoclinic crystals with a faint aromatic smell and exhibits blue fluorescence in solution (NTP, 1992). It has a relative molecular weight of 178.23, boiling point of 340^{o}C, melting point of 101^{o}C, flash point of 171^{o}C and sublimes. Phenanthrene is soluble in organic solvents such as ethanol, benzene and acetone but has a solubility of 1.15 mg/L in water at 25^{o}C (NCBI, 2004). Phenanthrene is one of the most abundant PAHs (major constituent of crude oil and coal tar) and represents the semi-volatile organic compounds in the environment (Zhao *et al*., 2016). Under ambient conditions, it can undergo photochemical reactions forming more polar oxygenated and nitro-forms. Compounds of higher hydrophilicity that can be easily reabsorbed in the alveolus, and the quinone form contributes to oxidative stress (Zhao *et al*., 2016). Phenanthrene can be used in the production of dyes, drugs and explosives, as well as in carbon black feed stock and as a

precursor for phenanthrenequinone which is largely employed in the syntheses of dyes, agrochemicals and preservatives (NCBI, 2004). Phenanthrene has been detected in various environmental matrices such as coastal estuaries and marine sediment, drinking water. It has been reported to be an abundant PAH in fresh- and brackish water as well as in seafood and aquatic organisms (Dailianis *et al*., 2014; Machado *et al*., 2014). The potential of phenanthrene causing neurotoxicity, endocrine- and reproductive disruption, cytotoxicity, genotoxicity, oxidative damage and growth impairment in fish has been reported by Machado *et al*. (2014). The potential toxicity of phenanthrene has earned it a classification of priority pollutant as well as one of the most aggressive contaminants in numerous countries (Machado *et al*., 2014).

2.1.1.6 Anthracene ($C_{14}H_{10}$): Ant

This is the parent molecule for tricyclic aromatic hydrocarbons made of three benzene rings joined side by side, also known as paranaphthalene, anthracin, green oil and anthracen. It occurs as white to yellow solid, colourless when pure, darkens in sunlight, has a faint aromatic smell and can be derived from coal tar. It has a molecular weight of 178.23, boiling point of 342^{o}C, melting point of 218^{o}C, and flash point of 121^{o}C (NCBI, 2005), is soluble in ethanol, methanol, benzene, chloroform, and toluene, slightly soluble in acetone but have a solubility of 1.29 mg/L in distilled water at 25^{o}C. Anthracene can be easily oxidised to anthraquinone which is a very important fine chemical employed in the production of dyes, pigments and hydrogen peroxide (Wang *et al*., 2015a; Ghosh *et al*., 2016). Anthraquinone is also employed to enhance the Kraft process in paper production and as signalling unit in molecular sensors (Wang *et al*., 2015a; Ghosh *et al*., 2016). Anthracene forms the base of a number of commercially available colourants as the core is anthraquinone with multiple substitutes (Langdon-jones & Pope, 2014). Also, several compounds derived from anthracene are utilised for their photo-physics, rich redox properties and biological significance and have found application in organometallic chemistry, biological imaging, DNA binding, sensing, and actinide coordination chemistry (Langdon-jones & Pope, 2014).

As a chronic pollutant, anthracene has been detected in various natural environments and its potential to bioaccumulate in aquatic organisms is high with organisms expressing oxidative stress and neurotoxicity (Chevremont *et al*., 2013; Palanikumar *et al*., 2012).

2.1.1.7 Fluoranthene ($C_{16}H_{10}$): Flt

Fluoranthene poses a significant threat to aquatic ecosystems as it is a major fraction of PAH burden in aquatic environments and evidence of its toxicity to aquatic organisms has been reported (Zezulka *et al*., 2013). Fluoranthene is classified as a non-alternant PAH, having a fusion

of naphthalene and benzene unit joined by a five-membered ring (Figure 2.1) and it is also known as 1,2-Benzanaphthene, with a molecular weight of 202.26. It is a structural isomer of pyrene, but less thermodynamically stable compared to pyrene, which is an alternant PAH (Monte *et al*., 2012). Fluoranthene is obtainable as light yellow or colourless fine crystals, having a boiling point of 384^{o}C, melting point of 111^{o}C, soluble in non-polar solvents and practically insoluble in water (NCBI, 2004).

In the atmosphere, fluoranthene can undergo a gas-phase reaction with NO_3/NO_2 to predominantly generate 2-nitrofluoranthene. The nitrated derivatives could possibly be more life threatening as they have been shown to exhibit increased mutagenicity at concentrations lower than that of the parent fluoranthene (Wang *et al*., 2015b). Also, toxicity of fluoranthene and increased toxicity of photo-modified fluoranthene (more polar and hence, more bioavailable) has been expressed in plant with decreased growth, chlorophyll content and protein synthesis (Tomar & Jajoo, 2015). Thus, fluoranthene contamination may be a risk factor for food security.

2.1.1.8 Pyrene ($C_{16}H_{10}$): Pyr

Pyrene consist of four ortho- and peri-fused arene rings (Figure 2.1), resulting in a flat aromatic system and the parent class of peri-fused PAH. Pyrene is also known as benzo[def]phenanthrene and can be obtained as a solid in various forms having a pale yellow colour or colourless when pure with a molecular weight of 202.25 (NCBI, 2005). Pyrene is capable of exhibiting blue fluorescence while in solid form and in solution, has a boiling point of 404^{o}C, melting point of 156^{o}C, is soluble in ethanol, ethyl ether, benzene, toluene and carbon disulphide, slightly soluble in carbon tetrachloride but virtually insoluble in water with a solubility of 0.135 mg/L at 25^{o}C (HSDB, 1983; IARC, 1983).

Like most PAHs, pyrene and its derivatives are commercially used to produce dye and dye precursors (Zhang *et al*., 2012). In recent years, the unique fluorescent properties of pyrene has resulted in its use in sensor probes for the detection of guest molecules (O_2 or NH_3), organic molecules and metals (Pinheiro *et al*., 2014). This application has resulted in low cost, high sensitivity, selectivity and versatility in the diagnostic detection of cysteine, which plays a pivotal role in varieties of biological processes and whose elevated levels are associated with several adverse effects, such as neurotoxicity, Parkinson's disease, Alzheimer's disease, and adverse pregnancy outcomes, amongst others (Rani & John, 2016).

The reaction of pyrene with nitrogen oxides yields nitro derivatives with 1-nitropyrene(NP), 1,6-diNP and 1,8-diNP shown to be of major importance as they are possibly carcinogenic and

mutagenic to humans (Miet *et al*., 2009). Also, the developmental toxicity of low-level pyrene to aquatic organisms has been established (Zhang *et al*., 2012).

2.1.1.9 Benzo[a]anthracene ($C_{18}H_{12}$): BaA

Benzo[a]anthracene is a crystalline PAH made-up of four fused arene rings (Figure 2.1). It occurs as colourless leaflets, plates or powder and exhibits a greenish-yellow fluorescence. It is also known as tetraphene, benzanthrene and naphthanthracene. It has a boiling point of 435^{o}C, melting point of 167^{o}C, dissolves readily in benzene, soluble in acetone and diethyl ether, sparingly soluble in acetic acid and virtually insoluble in water (NCBI, 2004; IARC, 1983). Benzo[a]anthracene reacts with nitrogen oxides to give the nitro derivatives and also undergo Diels-Alder, catalytic hydrogenation, oxidation (giving quinones and diols) reactions (IARC, 1983). Being a luminogenic molecule, it could be employed in sensors, bioimaging and organic light-emitting diodes, amongst others (Maity *et al*., 2016).

It is highly hydrophobic (log K_{ow} = 5.6-5.9), has a high propensity to bioaccumulate in lipid-rich tissues and also, accumulate in aquatic sediments round the world contributing up to 10% of the total PAH-content (Le Bihanic *et al*., 2015). It has been shown to be carcinogenic, having a 2B classification; possibly carcinogenic to humans by IARC (Table 2.1) and B2 classification; probable human carcinogen by US EPA (US EPA, 1990). Its metabolite, 3,4-diol-1,2-epoxide is more potent at effecting cytotoxicity and genotoxicity in humans as shown via the *in vitro* hepatocyte culture system (Song *et al*., 2012). It is also toxic to marine phytoplankton, causing reduction in photosynthetic efficiency and population biomass (Othman *et al*., 2012). Therefore, it could exert toxic effects on exposed organisms either as the parent compound or by its metabolic products.

2.1.1.10 Chrysene ($C_{18}H_{12}$): Chy

This is a crystalline solid, having a symmetrical structure made up of four fused arene rings (Figure 2.1) with two Bay-regions that are highly reactive for the formation of potent carcinogenic species (Xiu *et al*., 2016). It is also known as 1,2-benzophenanthrene and benzo[a]phenanthrene with a molecular weight of 228.29. Chrysene derives its name from chrysos (gold) based on its golden-yellow colour when first obtained in its impure state, due to tetracene (chrysene isomer) impurities. However, at high levels of purity; it is colourless, has strong blue fluorescence, boiling point of 448^{o}C and a melting point of 254 – 256^{o}C (NCBI, 2004; IARC, 1983). It is moderately soluble in benzene, slightly soluble in alcohol, ether, carbon bisulfide, glacial acetic acid and acetone and virtually insoluble in water with a solubility of 1.89 x 10^{-3} mg/L at 25^{o}C (HSDB, 1983; IARC, 1983).

Chrysene has been utilised as fluorescer and materials that contain chrysene are largely employed for wood preservation (creosote), roof coatings, electrode caking materials amongst others. Chrysene is classified 2B by IARC (Table 2.1) and forms part of the “dirty-four-PAH” (benzo[a]anthracene, chrysene, benzo[b]fluoranthene and benzo[a]pyrene) whose sum is concluded by European Food Safety Authority (EFSA) to be the most suitable indicator for PAHs in food in order to minimise health risks from dietary PAHs exposure (Xiu *et al*., 2016).

Also, chrysene can undergo oxidation reaction to yield oxides, diols and quinones; and yields nitro derivatives from reaction with nitrogen oxides (Murray *et al*., 1996; IARC, 1983). The 6-nitrochrysene derivative has a toxic equivalent factor (TEF) of 10 compared to the parent compound having TEF of 0.01 (Albinet *et al*., 2008), which is suggestive of a more potent derivative causing various toxic effects. Its ability to accumulate and metabolise in aquatic organisms have been shown, within which toxic effect (oxidative damage) was exerted (Ren *et al*., 2015; Xiu *et al*., 2016).

2.1.1.11 Benzo[b]fluoranthene ($C_{20}H_{12}$): BbF

This is a colourless non-alternant PAH congener, consisting of five fused rings (Figure 2.2), is also known as Benzo[e]acephenanthrylene; 3,4-benzofluoranthene; 2,3-Benzofluoranthene with a molecular weight of 252.32. It has a boiling point of 481^{o}C; melting point of 168^{o}C; is readily soluble in benzene; slightly soluble in acetone and virtually insoluble in water (HSDB, 1983; IARC, 1983). It can undergo oxidation reactions with atmospheric oxidants generating more toxic compounds such as nitro-BbF and oxygenated BbF derivatives (Zhang *et al*., 2014).

It is one of the most toxic PAHs with a toxic equivalent factor (TEF) of 0.1 (Table 2.2). The high toxicity of BbF was shown by Xiu *et al*. (2014), who reported that BbF was accumulated and metabolised in an aquatic organism in which lipid peroxidation, protein oxidation and DNA damage occurred with potency just below that of BaP. Also, the potential of BbF at low doses to cause dysfunctional male reproductive system in humans that are maternally exposed to low dosage has been shown, as male mice that were maternally exposed expressed dysregulated sperm function (Kim *et al*., 2011).

Table 2.2: Toxic equivalent factors (TEFs) for the 16 US EPA priority PAHs

PAH	TEFs[a]	TEFs[b]	TEFs[b]
Naphthalene	-	-	0.001
Acenaphthylene	0.001	-	0.001
Acenaphthene	0.001	-	0.001
Fluorene	0.001	-	0.001
Phenanthrene	0.001	-	0.001
Anthracene	0.01	-	0.01
Fluoranthene	0.001	-	0.001
Pyrene	0.001	-	0.001
Benzo[a]anthracene	-	0.1	0.1
Chrysene	-	0.01	0.01
Benzo[b]fluoranthene	-	0.1	0.1
Benzo[k]fluoranthene	-	0.1	0.1
Benzo[a]pyrene	-	1	1
Benzo[g, h, i]perylene	-	0.01	0.01
Indeno[1,2,3-cd]pyrene	-	0.1	0.1
Dibenzo[a, h]anthracene	-	1	1

[a] Data by Malcom and Dobson (1994), Adapted from Kim *et al*. (2013)
[b] Data by Doornaert and Pichard (2003), Adapted from Albinet *et al.* (2008)
[c] Data by Nisbet and LaGoy (1992), Adapted from Fang *et al.* (2004)

2.1.1.12 Benzo[k]fluoranthene ($C_{20}H_{12}$): BkF

This is a pale-yellow needle-shaped PAH, made-up of five fused rings (Figure 2.2), also known as 8,9-benzofluoranthene, 11,12-benzofluoranthene, dibenzo[b, jk]fluorene and is an isomer of BbF with a molecular weight of 252.31, boiling point of 480^{o}C and melting point of 215.7^{o}C (IARC, 1983). It is soluble in benzene, acetic acid and ethanol, but insoluble in water (IARC, 1983). Derivatives are formed upon its reaction with strong oxidising agents, electrophiles, peroxides, nitrogen oxides and sulphur oxides (NTP, 1992).

Its possible utilisation in optical sensors for *in situ*, selective, sensitive and simple determination of nitro-aromatic compound species which are of great environmental concern has been explored (Patra & Mishra, 2001). In that, its fluorescence can be quenched by the formation of nitro derivatives. Also, its possible use in materials for blue-green emissive organic light-emitting diodes (OLEDs) with improved luminescence spectra has been demonstrated (Lee *et al*., 2013).

The TEF of BkF (0.1) is the same as that of BbF, just second to that of BaP (Table 2.2). This is indicative of a highly toxic PAH, which can also be metabolised into more potent mutagens and carcinogens like dihydrodiol epoxide and orthoquinone (Spink *et al*., 2008). Pan *et al*. (2005) also indicated that BkF could be bioaccumulated, bio-transformed and eventually effect changes in normal cellular functions and antioxidant damage in exposed organisms.

2.1.1.13 Benzo[a]pyrene ($C_{20}H_{12}$): BaP

This is a high molecular weight PAH, consisting of five fused arene rings (Figure 2.2), having a crystalline structure and a molecular weight of 252.31 (NCBI, 2004). It has a boiling point of 310-312^{o}C and melting point of 178^{o}C; is readily soluble in chloroform; soluble in ether, xylene, toluene and benzene; slightly soluble in methanol and ethanol; and virtually insoluble in water (IARC, 1983; NCBI, 2004).

It is one of the most potent mutagenic and carcinogenic PAHs, as it is the only PAH classified as group 1 by IARC (Table 2.1) with a TEF of 1 (Table 2.2). Also, it can be readily adsorbed in tissues and metabolised by cytochrome P450 enzymes to yield ultimate potent PAH mutagens (Spink *et al*., 2008; Guo *et al*., 2017). The deleterious properties of BaP such as embryo-toxicity, teratogenicity, colonic-toxicity, cytotoxicity and genotoxicity have been presented (Kazerouni *et al*., 2001; Genies *et al*., 2013; Ajayi *et al*., 2016; Jiang *et al*., 2016; Muthusamy *et al*., 2016). These hazardous properties have been shown to be enhanced by co-exposure with other toxicants (Guo *et al*., 2017; Huang *et al*., 2016a; Muthusamy *et al*., 2016).

Hence, occupational human exposure, passive and active smoking, ingestion via food and water and inhalation via polluted air are important exposure pathways (Yao *et al*., 2016). This is a concerning, because BaP has the highest carcinogenic capability of all the 16 priority pollutant PAHs.

2.1.1.14 Benzo[g, h, i]perylene ($C_{22}H_{12}$): BgP

This is a pale yellow-green crystalline solid, made-up of six peri-condensed rings (Figure 2.2), with a molecular weight of 276.33. It is also known as 1,12-benzoperylene having a boiling point of 550^{o}C and a melting point of 278^{o}C (NCBI, 2005). BgP solubility in water is very poor (2.60×10^{-4} mg/L), but soluble in 1,4-dioxane, dichloromethane, benzene and acetone (IARC, 1983). Like some other PAHs, it is a constituent of products such as creosote, tar paints, water proof membranes and serves as intermediates in dye production (IARC, 1983).

Amongst the 16 priority PAHs, BgP has been reported to be the most detected PAH contaminant in the atmosphere and serves as a potent tracker of pollution from gasoline combustion (Amador-Muñoz *et al*., 2013; Amador-Muñoz *et al*., 2011; Guzmán-Torres *et al*., 2009). Although classified in group 3 (Table 2.1) and lacking a "classic" Bay-region needed for the formation of ultimate mutagens (Platt *et al*., 2008), BgP has been shown to synergistically promote the deleterious effects of BaP (Cherng *et al*., 2001). Also, the mutagenicity of BgP has been reported through the formation of 3,4-arene oxide metabolites responsible for BgP DNA adducts formation (Platt *et al*., 2008).

2.1.1.15 Indeno[1,2,3-cd]pyrene ($C_{22}H_{12}$): IcP

This is a yellow plate or needle-shaped solid high-molecular-weight (HMW) PAH with a six condensed rings structure (Figure 2.2). It is also known as ortho-phenylenepyrene, with a molecular mass of 276.33 and exhibits greenish-yellow fluorescence (IARC, 1983). It has a boiling point of 536^{o}C; melting point of 164^{o}C; insoluble in water but soluble in organic solvents (NCBI, 2005).

It is highly toxic; classified in group 2B as a possible human carcinogen (IARC, 2016) (Table 2.1) and having a TEF of 0.1, similar to the TEF value for BkF (Table 2.2). Barron *et al.* (2004) reported on the possible high potency of IcP, as the fish potency factor (FPF) reported for IcP and BkF are consistently high compared to that of other PAHs. Though IcP is a non-alternant PAH and lacking in Bay-region, IcP mutagenic metabolites have been identified elsewhere (Rice *et al*., 1985).

2.1.1.16 Dibenzo[a, h]anthracene ($C_{20}H_{14}$): DBA

Structurally, composed of five fused arene rings (Figure 2.2) and occurs as colourless plates or leaflets with a molecular weight of 278.35 (IARC, 1983). It is also known as benzo[k]tetraphene and has a boiling point of 524^{o}C; melting point of 267^{o}C; poor water solubility (2.49 x 10^{-3} mg/L); slight solubility in diethyl ether and ethanol; good solubility in benzene, xylene, toluene, cyclohexane and most organic solvent (IARC, 1983; NCBI, 2005).

Dibenzo[a, h]anthracene has the highest octanol-water partition coefficient (log K_{ow}) at 6.84 (Table 2.1) of the 16 priority US EPA PAHs, signifying very high lipophilicity (Ferrarese *et al*., 2008). High log K_{ow} show the tendency of chemical to remain sorbed onto organics (Ferrarese *et al*., 2008). This is a highly toxic PAH, classified in group 2B by IARC (Table 2.1) and have the same TEF (1) as BaP as shown in Table 2.2. It can be metabolically transformed by enzymes into more potent carcinogens and mutagens as reported by Shou *et al.* (1996) and Wood *et al.* (1978). DBA is highly potent in effecting tumours even at a low doses and the 3,4-dihydrodiol metabolite has been reported to be highly tumorigenic (Buening *et al*., 1979).

2.2 Sources of PAHs in the aquatic environment

Polycyclic aromatic hydrocarbons are environmental pollutants that have been detected in environmental matrices (water, sediments, and biota) from aquatic ecosystems (Patrolecco *et al*., 2010; Pérez-Fernández *et al*., 2015; Gu *et al*., 2016). They are introduced into the aquatic environment from natural and anthropogenic sources. Natural sources of PAHs include forest fires, volcanic emissions, natural oil seeps, coal deposits, plant debris and certain biological (biogenic) processes (Grueiro-Noche *et al*., 2010; Orecchio, 2010). The biosynthesis of PAHs naturally by plants and microbes are grouped as biological sources of PAHs (Wilcke *et al*., 2000).

Anthropogenic sources of PAHs in aquatic environments can be grouped into pyrogenic and petrogenic; where pyrogenic PAHs are composed mainly of high molecular weight PAHs and the petrogenic PAHs are composed mainly of low molecular weight PAHs (Dong & Lee, 2009). Pyrogenic sources include the combustion of fossil fuel such as which occurs in automobiles, power plants, industries that burn coal and petroleum, and waste incinerators, amongst others (Dong & Lee, 2009). Petrogenic sources include crude oil and petroleum products such as kerosene, petrol, diesel, lubricating oil, and asphalt (Boonyatumanond *et al*., 2007). PAHs derived from anthropogenic sources have been shown to enter aquatic systems through direct discharges, run-off and atmospheric deposition (dry/wet deposition, air-water gaseous exchanges) (Bouloubassi *et al*., 2006). Those sourced from atmospheric deposition and biological activities are removed from surface water by sorption on particles that subsequently undergo downward settling into the sediment (Bouloubassi *et al*., 2006). The sediment compartment of aquatic systems serves as a sink for the PAHs that do not undergo dilution, evaporation and biodegradation in surface water. Sediments therefore constitute an important source of information regarding the sequence of contaminant input events into aquatic systems (Quiroz *et al*., 2005; Hu *et al*., 2010; Barakat *et al*., 2011).

The PAHs sourced from atmospheric deposition are emitted into the environment from sources which include stationary (domestic and industrial), mobile, agricultural, and natural sources (Ravindra *et al*., 2008). Domestic sources of PAHs are mainly from the combustion and pyrolysis of wood, oil, coal, garbage or other organic substances for heating, cooking and for waste disposal purposes. Industries are sources of anthropogenic PAHs emission from various activities such as aluminum and coke production, iron and steel production, rubber tyre manufacturing, cement manufacturing, bitumen and coal exploration amongst others. The 1998 Aarhus Protocol on POPs that came to force in 2003, recommended four PAHs (benzo[b]fluoranthene, benzo[k]fluoranthene, benzo[a]pyrene and Indeno[1,2,3-cd]pyrene) as indicators for stationary

PAHs emission sources (UNECE (United Nations Economic Commission for Europe), 1998). Mobile PAH emission are sourced from vehicles such as ships, boats, automobiles, aircrafts, helicopters, trains and others which are equipped with either a compression or spark ignition internal combustion engines (Cheruyiot *et al*., 2015). PAHs emission from agricultural sources have been shown to be primarily from open burning of agricultural biomass under sub-optimum combustion conditions to dispose crop and forest residue as well as for land preparation (Ravindra *et al*., 2008). The emission of PAHs from natural occurrences such as forest, woodland and moorland fires (as a result of lightning or spontaneous combustion of dry fuel), volcanic eruption, diagenesis process in fossil fuel formation, microbes and plants biosynthesis and cosmic dust also arises (Ravindra *et al*., 2008; Cheruyiot *et al*., 2015; Pérez-Fernández *et al*., 2015).

2.2.1 Source apportionment

The entry of PAHs into the aquatic systems is from multiple sources. To control the release of PAHs into an aquatic system, it is essential to identify the prime source of the contaminating PAHs. Criteria exist that allow scientists to apportion PAHs that enter aquatic systems from pyrogenic or petrogenic sources. The examination of the 5-ringed PAHs for instance, could be used to distinguish petrogenic from pyrogenic PAHs (Abdel-Shafy & Mansour, 2016). The 5-ringed PAHs are more prevalent in petrogenic relative to pyrogenic PAHs, because the formation of the 5-ringed PAH is more favoured by the extensive time required for petroleum hydrocarbon formation. Whereas, the formation of the more stable 6-ringed PAH is favoured with the rapidness with which pyrolysis takes place (Abdel-Shafy & Mansour, 2016). Advances have been and are being made in the identification of PAHs sources as well as distinguishing pyrogenic- from petrogenic PAHs.

Ahrens & Depree (2010) employed compositional signature and diagnostic PAH isomer ratios to distinguish pyrogenic PAHs from coal tar and petrogenic PAHs from bitumen, which were reported to be the parent sources of PAHs in sediments of the aquatic system. To apportion PAH sources, Yan *et al.* (2006) utilised the following ratios: Flt / (Flt + Pyr) or Flt / 202 ratio (202 is the sum of Flt and Pyr masses); Ant / (Ant + Phe) or Ant / 178 ratio; BaA / (BaA + Chy) or BaA / 228 ratio; C_0 / $(C_0 + C_1)_{P/A}$ ratio, where C_0 is parent PAHs with mass I78 (sum of Phe and Ant masses) and C_1 is alkyl homologues at the same mass; C_0 / $(C_0 + C_1)_{F/P}$ ratio, where C_0 is parent PAHs with mass 202 (sum of Flu and Pyr masses) and IcP / (IcP + BgP) ratio. Yunker *et al.* (2002) selected PAH ratios that best exhibited the potential to differentiate natural and anthropogenic PAH sources. They suggested that a good knowledge of the relative thermodynamic stability of different parent PAHs, the distinctive characteristics of PAH sources, and compositional changes in PAH between

source and sediment (such as the relative stability of different PAH isomers and PAHs from various sources) are the keys to selecting PAH ratios for source apportionment.

PAHs sourced from fossil fuels, liquid-fuel combustion and solid-fuel (biomass/coal) combustion can be distinguished by four-ring and larger parent PAH ratios; whereas PAHs sourced from petroleum combustion can be distinguished by having smaller parent PAHs ratios and $C_0 / (C_0 + C_1)$ ratios. The differentiation approach is based on differences in the relative stability of PAHs under low and high temperature regimes (Yunker *et al.,* 2012). A higher Phe/Ant ratio (>10) is proposed to indicate petrogenic pollution, while a proposed ratio of <10 indicates a pyrogenic source, since Phe is more thermodynamically stable than Ant. Similarly, Pyr is more thermodynamically stable than Flt and they are often associated with each other in natural matrices. A pyrogenic source is inferred when there is predominance of Flt over Pyr; while it is petrogenic source when Pyr is more abundant than Flt (Li *et al*., 2012).

The use of diagnostic ratios of PAH isomer pairs that show an inverse abundance relationship in different source materials presents a precise method for source assignment. The use of a ratio of one isomer to the sum of its isomer concentration is often preferred, because it gives less variability than using the simple ratio of two isomers. Preferred ratios for PAHs source assignment include those that have the less thermodynamically stable isomer in the numerator, so that ratios increase as combustion input increases for ease of comparison (Yunker *et al*., 2012; Yunker *et al*., 2002; Yan *et al*., 2006; Ahrens & Depree, 2010).

The presence of high molecular weight (HMW, four- to six- rings) PAHs have been associated with pyrolytic sources, whereas lower molecular weight (LMW, two- to three-rings) PAHs have been associated with petrogenic sources. A ratio of LMW/HMW >1 generally indicates a petrogenic origin of pollution; whereas a ratio of<1, indicates that the PAHs have a pyrolytic origin (Aldarondo-Torres *et al*., 2010). PAH ratios used for pyrogenic and petrogenic assignment are highlighted in Table 2.3.

Table 2.3: PAH ratios used for pyrogenic and petrogenic source assignment

PAH Ratio	Petroleum origin value range	Pyrogenic origin value range		Mixed origin value range	Reference
		Liquid fossil fuel combustion	Biomass combustion		
Phe / Ant	>15	<10	<10	10 - 15	Ruiz *et al.* (2011)
Ant / (Ant + Phe)	<0.10	>0.10	>0.10		Ruiz *et al.* (2011); Yunker *et al.* (2012)
Flt / Pyr	<1	>1	>1		Ruiz *et al.* (2011)
Flt / (Flt + Pyr)	<0.40	0.40-0.50	>0.50		Liu *et al.* (2008); Ruiz *et al.* (2011); Yunker *et al*. (2012)
BaA / (BaA + Chy)	<0.20	>0.35	>0.35	0.20 - 0.35	Yunker *et al*. (2002); Ruiz *et al*. (2011)
BaA / Chy	>2	<2	<2		Kuppusamy *et al*. (2017)
BaP / (BaP + Chy)	< 0.3	0.3 – 0.7	0.07 – 0.24 (coal)		Kuppusamy *et al*. (2017)
IcP / (IcP + BgP)	<0.20	0.20-0.50	>0.50		Ruiz *et al*. (2011); Yunker *et al*. (2012); Keshavarzifard *et al*. (2014)
IcC / (IcC + BgP)	<0.10	0.10-0.30	>0.30		Yunker *et al*. (2012)
DjA / (DjA + DhA)	<0.25	0.25-0.60	>0.60		Yunker *et al*. (2012)
Pic / (DhA + Pic)	<0.20	0.20-0.50	>0.50		Yunker *et al*. (2012)
1,7 / (2,6+1,7)-DMP	0.45 - 0.80	<0.45	>0.70	0.45 - 0.70	Yunker *et al*. (2012)
M-Phe / Phe	>1	<1	<1		Garrigues *et al*. (1995)
∑ LMW PAHs / ∑ HMW PAHs	2 - 6 (fresh petroleum) >1	<1	<1		Kuppusamy *et al*. (2017)

PAH Ratio	Value range	Emission origin	Reference
BaP / BgP	> 0.6	Traffic	Kuppusamy *et al*. (2017)
BbF / BkF	2.5 - 3	Aluminium smelter	Kuppusamy *et al*. (2017)
Phe / Ant	2 – 8	Vehicle	Kuppusamy *et al*. (2017)

Parent PAHs in the ratio are Phenanthrene (Phe), anthracene (Ant), fluoranthene (Flt), benzo [a]anthracene (BaA), chrysene (Chy), indeno[1,2,3-cd] pyrene (IcP), benzo[g, h, i]perylene (BgP), indeno[7,1,2,3-cdef]chrysene (IcC), dibenzo [a, j] anthracene (DjA), dibenzo [a, c/a, h]anthracene (DhA), picene (Pic), 1,7 and 2,6-dimethylphenanthrenes (DMP) and M-Phe = the sum of 3-methylphenanthrene, 2-methylphenanthrene, 9-methylphenanthrene and 1-methylphenanthrene.

2.3 Routes of exposure and toxicity of PAHs to aquatic organisms

An improved understanding regarding exposure routes of aquatic ecosystems to PAHs has become essential as it has been found that the level of toxicity could be affected by the exposure route of PAH (Van Veld *et al*., 1997). Aquatic organisms have also been sufficiently utilised as biomarkers and to investigate the probable toxic effects (especially fish) of PAHs on humans (Carls *et al*., 2008; Machado *et al*., 2014; Xiu *et al*., 2016). Fishes have long been identified as suitable alternatives to rodents in carcinogenesis studies or as supplementary models based on their availability, economy, latency of tumorigenic response, and ease of exposure and maintenance (Hawkins *et al*., 1988).

Aquatic organisms can be exposed to PAHs through contaminated food, water and sediment, with the intestine and gills being the dominant exposure routes in fish (Van Veld *et al*., 1997; Baumard *et al*., 1998). There is a relationship between bioavailability of PAHs to aquatic organisms and their water solubilities. Solubilities also depend on factors such as: lipid levels, organic carbon, sediment surface area, dissolved organic matter, dissolved or suspended material, salinity, hydrogen ion concentration and octanol-water partition coefficient (Meodor *et al*., 1995; Baumard *et al*., 1998; Ter Laak *et al*., 2009). Feeding habits and habitat also play a role in toxicant exposure to these organisms (Baumard *et al*., 1998). Figure 2.3 gives the general uptake and elimination pathways of toxicants by organisms.

PAHs, being hydrophobic compounds, are readily absorbed into fatty tissues of aquatic organisms by dermal absorption. They are also taken up through gill ventilation, ingestion of contaminated sediment or suspended particles, and from consumption of other contaminated species (Patrolecco *et al*., 2010). The passive uptake of contaminants from the ambient environment via respiratory and/or dermal surface is specifically referred to as bioconcentration, while the exposure through combination of contaminated food uptake and bioconcentration is termed bioaccumulation (Mackay & Fraser, 2000; Hou *et al*., 2013). Bioaccumulation via contaminated food may result in biomagnification, a process in which pollutant concentration in an organism of higher trophic level exceeds that in organism of lower level at a steady state within a food chain (Hou *et al*., 2013). Hence, bioavailable PAHs could be bioaccumulated and biomagnified in aquatic organisms. They may also be bio-transformed into possibly more potent metabolites, leading to deleterious effects on the organisms.

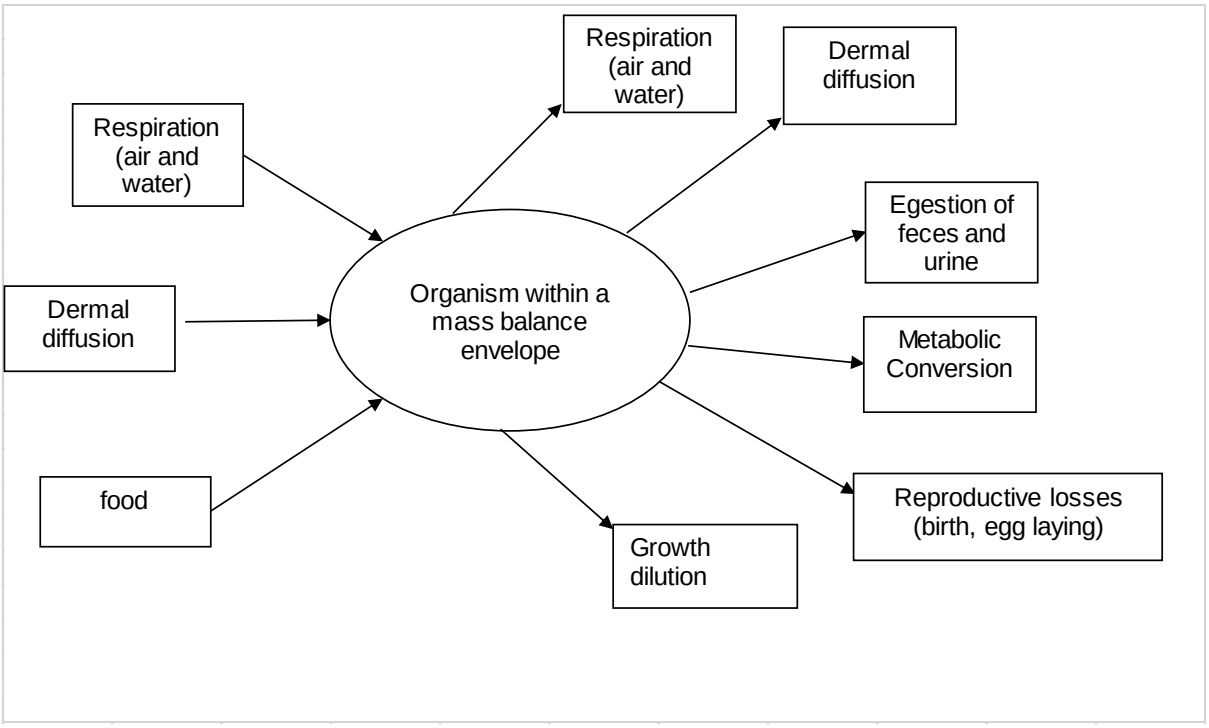

Figure 2.3: Uptake and elimination pathways of toxicant by organisms [Adapted from: Mackay & Fraser (2000)]

The potential of the PAHs to produce toxic symptoms and effects in organisms has been documented (Hatch & Burton, 1999; Incardona *et al*., 2006; Kim *et al*., 2007). The LMW PAHs are known to produce acute lethal toxicity, while some of the HMW PAHs have a higher potential for causing chronic toxicity to organisms (Eisler, 1987). Chronic exposure of organisms to the PAHs produces many different effects including cancer (of various tissues), induction of cardiovascular diseases, loss of fertility, immunosuppression, mutations and endocrine disruption (Boonyatumanond *et al*., 2007; Toyooka & Ibuki, 2007). The toxicity of PAHs to aquatic biota can be greatly enhanced by exposure to ultraviolet (UV) light and temperature increases (Hatch & Burton, 1999; Engraff *et al*., 2011). Increases in temperature and UV light intensity are capable of increasing the mobility of PAHs in aqueous solution, and conversion to more reactive and potent intermediates (Hatch & Burton, 1999; Toyooka & Ibuki, 2007; Engraff *et al*., 2011).

Photo-induced toxicity of PAHs to *Hyalella azteca* (lawn shrimp) and *Chironomus tentans* (midge) was reported by Hatch and Burton (1999). The study established that PAHs toxicity to these organisms was greatly enhanced when there was a simultaneous exposure to ultraviolet light (UV), and that species-specific behaviour also played a significant role in such toxicity. Photo-induced toxicity of anthracene and fluoranthene was reported to result from the sensitisation of PAHs occurring within the biological tissue.

Ruiz *et al.* (2011) linked neoplastic disorders (abnormal growths) observed in mussels (*Mytilus spp*) to the toxic effect of five- to six- ring PAHs congeners. This biotoxic effect was deduced from the correlations observed between mutagenic PAHs congener's accumulation and gonadic neoplastic disorder occurrences.

Pang *et al.* (2012) studied the effect of bioturbation by the oligochaete *Lumbriculus variegates* on the bioavailability of PAHs in electronic-waste contaminated sediment. Toxic effects of the PAHs on the oligochaete and the epi-benthic amphipod *Hyalella azteca* were also studied. Various bioturbation levels were achieved by employing *L. variegates* of different densities. *L. variegates* bioaccumulated up to 22.47±3.87 µg/g lipid of 28 different PAHs after 28 days of exposure to contaminated sediment. The highest bioturbation level achieved at highest density, gave the highest mortality of *H. azteca* and the lowest worm growth. PAH-bioaccumulation was also reported to be lowest at the highest bioturbation level. Sub-lethal toxicity caused by migration of PAH-contaminated sediment to the sediment surface and water column because of bioturbation (which is interrelated to density) was reported to be responsible for decrease in PAH-bioaccumulation and increase in mortality.

Fish embryos are popularly used for investigating the biotoxic effects of PAHs on aquatic organisms, because fish embryos and larvae are highly sensitive to PAH mixtures from different sources. Incardona *et al.* (2006) investigated the developmental toxicity of four types of PAHs on zebrafish embryos. The types of damage reported included liver abnormalities, pericardial oedema, dorsal curvature, cardiovascular defects, incomplete cardiac looping, reduced cardiac chambers, intracranial haemorrhage, yolk sac oedema and reduced body length. It was concluded that the modes of action leading to toxicity in aquatic species exposed to PAHs are either dioxin-like or nonpolar-narcosis-like. It was proposed that the PAHs are pharmacologically active compounds that have specific cellular targets. Zebrafish embryos exposed to Pyr, Chy and BaA experienced toxicity mediated by the activation of aryl hydrocarbon receptors (AHR). In addition, these PAHs agents induced cytochrome P4501A (CYP1A) enzymes in different tissues and organs. Dissolved PAHs are also known to induce cardio-toxicity in fish embryos (Carls *et al*., 2008). Abnormal cardiac looping, pericardial oedema and intracranial haemorrhaging were reported as the biotoxic effects observed in zebrafish embryos exposed to PAHs and effects increased as molecular size and alkyl substitution of dissolved PAHs increased (Carls *et al*., 2008).

Also, PAHs become oxidised during combustion (i.e. when pyrolysed) or when photo-oxidised, to generate oxygenated PAHs (OPAHs), that may be quite toxic. Knecht *et al.* (2013) used zebrafish embryos to examine malformations, gene expression changes and mitochondrial functions induced by a structurally diverse set of 38 different OPAHs. Of the 38 OPAHs investigated 1,4-naphthoquinone was the most toxic (producing 100% mortality 24 hours' post fertilisation in embryos exposed, at all tested concentrations). Apart from mortality, yolk sac oedema and body axis curvature were the most common morphological biotoxic effects reported, in which oxidative stress played a key role in causing toxicity.

2.4 Routes of exposure and toxicity of PAHs to humans

PAHs released from biological, petrogenic and pyrogenic sources contaminate air, food, soil, sediments, vegetation and water (Phillips, 1999; Srogi, 2007). Therefore, human intake of PAHs are via inhalation, dermal contact as well as dietary and accidental ingestion of these pollutants are of great concern (Moen *et al*., 1996; Singh *et al*., 2008; Xia *et al*., 2009). PAHs are adsorbed through the respiratory tract, skin and gastrointestinal tract into the bloodstream that distributes adsorbed PAHs and their consequent metabolites to other body tissues (Singh *et al*., 2008). Occupational, environmental and dietary sources could considerably increase PAHs burden in humans. Coke oven workers, auto-mechanics, spray painters and ship engine room workers expressed higher PAH burdens (enhanced by smoking) compared to the general population (VanRooij *et al*., 1993; Moen *et al*., 1996; Kamal *et al*., 2011). Dermal uptake has been shown to be the major route of PAH uptake, as compared to respiratory uptake in occupationally exposed humans (VanRooij *et al*., 1993; Boogaard & van Sittert, 1994).

Diet is also a significant PAH exposure route to humans, as certain foods have been reported to have high PAH content which could be enhanced by preparation methods (Buckley & Lioy, 1992; Olatunji *et al*., 2014). Foods with high PAH content and those with low PAH content are presented in Table 2.4, whereas, the detected levels of PAHs in various foods, with the impact of food preparation method on processed food PAH content are shown in Table 2.5. Also, increased PAH concentrations in higher trophic levels via food web transmission have been reported (Zhang *et al*., 2015).

To ascertain and assess occupational and dietary PAHs exposure in humans, the metabolite 1-hydroxypyrene in urine has been largely utilised as the biomarker (Buckley & Lioy, 1992; Moen *et al*., 1996), while parent PAHs are assessed in blood samples (Singh *et al*., 2008; Kamal *et al*., 2011). Therefore, unmetabolised PAHs and monohydroxyl PAH-metabolites can be utilised as biomarkers of PAH exposure in humans (Rossella *et al*., 2009).

Table 2.4: PAH Content in Food

Low PAH Content	High PAH Content
Cereal	Fried food
Oatmeal	Vegetable oils
Fruits: Tomatoes, Apples	Charcoal broiled/smoked meat and fish
Fluid milk	Potato chips
Alcoholic beverages	Green leafy vegetables
Cheese	Toasted bread
Fish/shellfish	Roasted coffee
	Mayonnaise
	Tea

Adapted from Buckley & Lioy (1992); Menzie *et al*. (1992).

Table 2.5: Detected levels of PAHs in different food samples

Food Sample	Detected level	Analytical technique	% Recovery	Reference
Meat and meat products	13.434 µg/kg (∑16 PAHs)	HPLC-FLD/UV	48 to 113 % (48 to 105 % for naphthalene and others 55 to 113%)	Falcó *et al*. (2003)
Fish and shellfish	7.894 µg/kg (∑16 PAHs)			
Vegetable	0.887 µg/kg (∑16 PAHs)			
Tubers	3.606 µg/kg (∑16 PAHs)			
Fruits	0.946 µg/kg (∑16 PAHs)			
Eggs	2.423 µg/kg (∑16 PAHs)			
Milk	1.532 µg/kg (∑16 PAHs)			
Dairy products	6.636 µg/kg (∑16 PAHs)			
Cereals	14.454 µg/kg (∑16 PAHs)			
Pulses	2.742 µg/kg (∑16 PAHs)			
0ils and fats	63.237 µg/kg (∑16 PAHs)			
Smoked meat	92.200 µg/kg (∑16 PAHs)	GC-MS	≥ 85%	Alomirah *et al*. (2011)
Smoked fish	259.000 µg/kg (∑16 PAHs)			
Grilled vegetables	111.000 µg/kg (∑16 PAHs)			
Charcoal-barbecued chicken	9.460 µg/kg (∑7 PAHs)	HPLC-FLD	70 to 116%	Chung *et al*. (2011)
Wood-barbecued chicken	1.870 µg/kg (∑7 PAHs)			
Raw chicken	ND			
Kitchen range hood oil	122.980 µg/kg (∑16 PAHs)	GC-MS	70 to 128%	Wu & Yu (2012)
Fried food stall oil	58.320 µg/kg (∑16 PAHs)			
Olive oil	827.270 µg/kg (∑16 PAHs)			
Peanut oil	41.470 µg/kg (∑16 PAHs)			
Pepper oil	3.000 µg/kg (Benzo[a]pyrene)	GC-MS	78 to 85%	Wang & Guo (2010)

Food Sample	Detected level	Analytical technique	% Recovery	Reference
Smoked bread	3.500 µg/kg (∑10 PAHs)	HPLC-FLD	66 to 107%	Fasano *et al*. (2016)
Smoked Paprika	9937.000 µg/kg (∑10 PAHs)			
Smoked meat sausage	1779 µg/kg (∑10 PAHs)			
Smoked cheese	88 µg/kg (∑10 PAHs)			
Raw beef	ND	GC-FID	84 to 94%	Olatunji *et al*. (2014)
Smoked beef	14.430 µg/kg (∑4PAHs)			
Grilled beef	6.720 µg/kg (∑4PAHs)			
Boiled beef	3.320 µg/kg (∑4PAHs)			
Raw pork	ND			
Smoked pork	10.630 µg/kg (∑4PAHs)			
Grilled pork	8.970 µg/kg (∑4PAHs)			
Boiled pork	4.610 µg/kg (∑4PAHs)			
Raw chicken	ND			
Smoked chicken	10.520 µg/kg (∑4PAHs)			
Grilled chicken	5.060 µg/kg (∑4PAHs)			
Boiled chicken	2.690 µg/kg (∑4PAHs)			

16 PAHs: 16 US EPA priority PAHs
10 PAHs: fluoranthene, pyrene, benzo [a] anthracene, Chrysene, Benzo [b] fluoranthene, Benzo [k] fluoranthene, Benzo [a] pyrene, Dibenzo [a, h] pyrene, Benzo [g, h, i] perylene, Indeno [1,2,3-cd] pyrene.
7 PAHs: Chrysene, Benzo [b] fluoranthene, Benzo [k] fluoranthene, Benzo [a] pyrene, Benzo [g, h, i] perylene, Indeno [1, 2, 3-cd] pyrene and Dibenzo [a, h] anthracene.
4 PAHs: Benzo [k] fluoranthene, Benzo [a] pyrene, Indeno [1, 2, 3-cd] pyrene and Benzo [g, h, i] perylene.
ND: Not detected

Exposure to PAHs, make humans susceptible to the toxic effects of PAHs (WHO, 1998b). The exposure of ancient populations to PAHs from cultural use of natural bitumen (chewing like gum, body application for rituals, cast for broken bones, basket or tomol canoe making) and consumption of PAH-contaminated water and marine food have been linked to prehistoric health decline as expressed in; reduced cranial size and stature, periosteal lesions, cribra orbitalia and tooth enamel hypoplasia (Warmlander *et al*., 2011). More recently, PAHs have been implicated to cause oxidative stress, induce immunological alteration and consequently lipid peroxidation in blood plasma of coke oven workers that were occupationally exposed to chronic PAHs levels (Jeng *et al*., 2011). Human exposure to PAHs was also linked to cases of oesophageal cancer, which is the 8th most common cancer and 6th most frequent cause of cancer death in the world (Roshandel *et al*., 2012). Also linked to PAHs exposure was the reduction of blood mitochondrial DNA content, a condition associated with type II diabetes, soft cell sarcoma, ovarian cancer, breast cancer, gastric cancer, hepatocellular carcinoma as well as renal cell carcinoma (Pieters *et al*., 2013). The activation/metabolism of PAHs taken up in humans by cytochrome P450 enzymes is one of the principal pathways proposed for PAHs toxicity (Toyooka & Ibuki, 2007).

However, apart from PAH-activation by the cytochrome P450 enzymes to produce ultimate potent PAH mutagens in humans, it has also been reported that the human colon microbiota are also capable of PAH-activation to estrogenic metabolites (1-hydroxypyrene and 7-hydroxyBaP) with increased toxicity (Wiele *et al*., 2005; Spink *et al*., 2008). Ajayi *et al*.(2016) also reported colonic toxicity in mice exposed to PAH. They reported that BaP induced oxidative and nitrosative stress, which resulted in colon injury. Mice have been largely utilised to explore the deleterious effects that could be caused by xenobiotics and other substances in humans (Belles *et al*., 2016; Costa *et al*., 2016; Oliveira *et al*., 2016).

The implication of PAH-exposure on pregnancy and female reproductive system was investigated by Zhao *et al.* (2014a), utilising pregnant mice. They demonstrated that BaP is an endocrine disruptive toxicant capable of causing endometrium morphology impairment, reduction in the number of implantation sites and oestrogen and progesterone imbalance. Furthermore, BaP was reported to induce the phosphorylation of H2AX (linked to double-strand DNA breaks), cause plasma membrane remodelling (remodelled both lipid and protein content) and expression of P2X7 receptor in modelled placenta (Wakx *et al*., 2016). Hence, exposure to PAHs could result in their infertility and may effect developmental toxicity to foetuses during pregnancy.

Kim *et al*. (2007) however, examined the mode of PAH-toxicity as expressed by various stress genes of *Escherichia coli*. These authors investigated the ability of selected PAHs to effect DNA damage, oxidative stress, membrane and protein damage utilising stress response genes in *Escherichia coli*. The stress responsive genes utilised were those capable of responding specifically to DNA damage, oxidative damage, and membrane and protein damage. Benzo [a] pyrene and naphthalene were reported to effect DNA damage and as such may be classified as genotoxic.

Furthermore, enhanced toxic effect has been reported for co-exposure of PAHs with other toxicants or even binary PAH-mixtures and complex PAH-mixtures. For instance, the capability of PAH-exposure to enhance atherosclerosis was demonstrated in mice fed with atherogenic diet. BaP incorporated diet was shown to cause increased levels of reactive oxygen species and inflammatory biomarkers (Uno *et al*., 2014). BaP was therefore implicated in enhanced aorta toxicity because it was linked to the development of lesions in the organ. The co-exposure of BaP and sulphur dioxide was reported to have led to enhanced cell morphology alterations, protein expression changes and apoptosis in the liver of mice (Qin *et al*., 2015).

Also, the binary mixture of benzo [a] pyrene (BaP) and dibenzo [a, l] pyrene and a complex mixture of PAHs in urban air particulate matter extracts have caused more than an additive response, in inducing cytochrome P450 enzymes and activating DNA-damage signalling. PAHs toxicity are linked mainly to the larger PAHs (>3 aromatic rings). The PAHs having ≥5 aromatic rings are likely to pose a larger risk to human health, and these are classified as being either probable or actual carcinogens in humans (Jarvis *et al*., 2013).

2.5 Occurrence and distribution of PAHs in aquatic environments

The levels of contaminants in an aquatic environment may vary with seasons (temporal distribution), spatially and also within various media in the aquatic environment such as vegetation, sediment and water (Wang *et al*., 2012b; Li *et al*., 2017). Data on pollution trends are of great importance to increase understanding in cause-effect relationships, agent identification, source identification as well as developing appropriate strategies for adequate and effective control of contaminants, all essential for environmental management and protection (Gómez-Gutiérrez *et al*., 2007; Campillo *et al*., 2017).

Liu *et al*. (2016b) reported significant temporal variation in levels of PAHs in water sampled from the urban river networks of Shanghai (China). Average detected level of total dissolved 16 PAHs in water samples in winter was 183.54 ng/L (levels ranged from 71.92 to 460.53 ng/L) and in summer was 106.67 ng/L (levels ranged from 46.53 to 221.54 ng/L). They attributed the consequent variation to mobility and dilution effect. The study stations were reported to have shallow-water level and slow flowing water velocity in winter that resulted in poor scour and dilution ability of the rivers, hence the higher PAHs levels in winter. The average detected level of the 16 PAHs in sediment samples from the study in winter was 4944.97 ng/g (ranged from 352.37 to 36198.23 ng/g) and in summer was 2336.63 ng/g (ranged from 456.11 to 14948.40 ng/g). The significant seasonal variation in sediment samples was attributed to flooding in summer, possibly causing dilution effect on PAHs, coupled with accelerated microbial degradation of PAHs resulting from the elevated temperatures in summer.

Natural occurrences and anthropogenic activities have also been reported to cause seasonal variations in PAHs levels particularly in developing countries (Wang *et al*., 2017a). In winter, there is serious pollution from huge levels of uncontrolled or poorly controlled coal combustion and biomass burning used for warmth and daily cooking, resulting in elevated levels of PAHs in winter as compared to summer (Wang *et al*., 2017a).

The effect of different climatic regimes could be easily inferred from temporal distribution data, while site characteristics is easily inferred from spatial distribution data with pollution point sources being easily identified (Liu *et al*., 2016a). Spatial distribution will be more defined in an environment with poor dilution effect and low mobility of pollutants (Liu *et al*., 2016b). Anthropogenic activities have been identified as the predominant sources of PAHs in the environment with industrial activities and urbanisation being of major concern. This is because elevated PAHs levels have been reported for sites at close proximity to these activities (Liu *et al*., 2016a; Busso *et al*., 2018).

The mean total of 16 US EPA PAHs detected in *Ligustrum lucidum* leaves obtained from Cordoba City, Argentina at industrial, urban and peri-urban areas were 168.04 ng/g, 112.62 ng/g and 94.87 ng/g, respectively (Busso *et al*., 2018). The PAHs levels reported for the industrial areas were higher than those reported for the urban areas and almost doubled those reported for the peri-urban areas. Thus, the release of PAHs into the environment from industrial sources must be regularly assessed. The report also highlighted that PAHs bioaccumulate in plant tissues and could serve as effective biomarker for PAHs contamination.

Various processes and exchange take place between the compartments of the aquatic systems, which are either abiotic (air, water and solid materials) or biotic (flora and fauna) (Duursma & Carroll, 1996). The distribution of contaminants between the compartments is determined by their chemical-physical affinity for the compartment matrix or matrices and the transfer parameters regulating apparent equilibria (Duursma & Carroll, 1996). Compartmental distribution of contaminants should be monitored, to generate data that could assist in understanding and predicting contaminant transfer between compartments, as well as accumulation and loss of contaminants in abiotic and biotic systems. How contaminants interact with certain matrix or matrices could also suggest the time of pollution and help in identifying the suitable marker for further monitoring regime (Duursma & Carroll, 1996).

The distribution of PAHs in water, pore water, sediment, soil and vegetables was reported by Zhang *et al*. (2004a). The order of PAHs mean concentrations in the samples were as follows: levels in vegetable (48300 ng/g) > sediment (433 ng/g) > soil (313 ng/g) > pore water (140 µg/L) > water (72.4 µg/L). A clear indication that PAHs prefer to affiliate and adhere to organic environments due to their particular properties, including hydrophobicity, low volatility and high octanol-water partition coefficient (K_{ow}) (Gharibzadeh *et al*., 2016). The magnitude of detected levels in vegetables was a clear indication of PAH bioaccumulation by plants and the ease of PAHs entering the food chain (Yang *et al*., 2017).

The distribution of PAHs in different plant tissues has also been studied by researchers (Wang *et al*., 2008; Wang *et al*., 2012b; Wang *et al*., 2017b). The levels of ∑PAHs reported for different tissues of *Phragmites australis* (tissues mean was higher than level in sediment) were 170.1 ng/g (leaves), 75.2 ng/g (stem) and 79.1 ng/g (root) (Wang *et al*., 2012b). The higher PAHs levels in leaves relative to those in roots was attributed to dry and wet atmospheric deposition of PAHs on leaves in addition to the translocated PAHs from sediments through root uptake. It was also found that the lower molecular weight PAHs (phenanthrene and fluoranthene) were more abundant in

leaves compared to roots, validating the fact that uptake of PAHs from the atmosphere is an important pathway in the bioaccumulation of PAHs in plants.

Therefore, leafy vegetables could be a major exposure route of humans to PAHs. Irrigation of these vegetables with PAHs contaminated freshwater especially around informal settlements could further increase their PAHs burden. Also, the use of contaminated waters in aquaculture is concerning.

Plants are therefore relevant biomonitoring agent in assessing anthropogenic contaminants in the environment based on their ability to uptake and bioaccumulate these contaminants (Agunbiade *et al*., 2009; Sojinu *et al*., 2010; Wang *et al*., 2012b). Plant's density, wide spread, immobility and continuous exposure to contaminants, are also some of the features that made them to have been successfully utilised as biomonitoring agents in aquatic environments (Esmaeilzadeh *et al*., 2017). Amongst the plants that have been successfully utilised as biomonitoring agents in aquatic environment are *Phramites australis* and *Eichornia crassipes* (Agunbiade *et al*., 2009; Wang *et al*., 2012b). The *P. australis* (common reed) is a macrophyte plant found widely distributed in temperate and tropical regions of the world. It is a perennial reed grass with cane-like stems that develop from an extensive creeping rhizome system, the stems can grow up to 6 m in height, leaves are between 20 to 70 cm long and 1 to 5 cm broad (Mal & Narine, 2004). The *E. crassipes* (water hyacinth) is a member of the pickerelweed family (*Pontederiaceae*), that originated in the tropical South America (Agunbiade *et al*., 2009). *Eichornia crassipes* is invasive and one of the most notorious and lethal floating aquatic weed that grows up to 2 m above and 1 m below water surface (Thamaga & Dube, 2018). The wide spread of these plants had been reported to be as a result of anthropogenic activities (Thamaga & Dube, 2018), making them ideal as biomonitoring agents in environmental assessment

2.6 Extraction of PAHs from environmental matrices

As far back as 1974, scientists have seen the need to develop rapid analytical methods for the analysis of PAHs and their metabolites (Salmon *et al*., 1974). However, most analytical instruments lack the capability to identify and/or quantify analytes of interest directly in matrices and analytes may also occur at ultra-trace levels. Extraction of analytes from complex matrices (effluent, sludge, surface water and sediment amongst others) therefore becomes highly important in analytical processes. Hence, prior to instrumental analysis, PAHs are extracted, pre-concentrated and cleaned to remove interfering substances in a process called sample enrichment. Sample enrichment allows for the monitoring and quantification of PAHs at trace/ultra-trace levels in the environment. A wide range of extraction techniques including conventional techniques (liquid-liquid extraction (LLE), solid-liquid extraction (SLE) and soxhlet extraction) and non-conventional (newer and more sophisticated) techniques [microwave-assisted solvent extraction (MASE), ultrasound-assisted extraction (UAE), accelerated solvent extraction (ASE), liquid-phase micro-extraction (LPME), Solid-phase extraction (SPE), solid-phase micro-extraction (SPME), stir bar sorptive extraction (SBSE), supported-liquid membrane extraction (SLME), extracting-syringe technique (ESy), supercritical fluid extraction (SFE) and single-drop micro-extraction (SDME)] were developed to achieve less solvent consumption, improved extraction throughput, higher recoveries, better reproducibility, higher efficiency, improved quality and sensitivity, cost effectiveness and greener techniques (Marcé & Borrull, 2000; Lambropoulou & Albanis, 2007; Ramos, 2012; Sanchez-Prado *et al*., 2015).

Krüger *et al*. (2011) described SPE, SPME and SBSE as acceptable and better alternatives to LLE methods as they are based on equilibrium extraction and reported higher PAH level of up to 288% with SBSE than with LLE. Equilibrium extraction methods are fast and allow for parallel analyses of samples. However, equilibrium extraction methods are generally relatively expensive. Thus, researchers continue to search for extraction and pre-concentration techniques that are both experimentally effective and economically feasible.

2.6.1 Extraction of PAHs from water samples

Extraction of PAHs in water is achieved quite easily with organic solvents using the conventional LLE technique as PAHs have poor solubility in water and have high solubility in organic solvents (Hexane, DCM, cyclohexane, acetone, carbon disulphide, diethyl ether and chloroform) (O'Neil, 2001; NCBI, 2004). However, to address the shortcomings of the conventional LLE technique (high cost and toxicity of organic solvents), modernised techniques like Dispersive liquid-liquid

micro-extraction (DLLME), which is rapid, simple and relatively cheap has been developed for the determination of PAHs in water. Rezaee *et al*. (2006) studied parameters that could affect the performance of DLLME for the extraction of PAHs from water samples. Under optimised conditions, the method achieved PAH recoveries of between 82.0-111.0% for spiked (5.0 µg/L) samples. A linear range of 0.02-200 µg/L and 0.007 – 0.030 µg/L detection limit were reported for most PAHs analysed. The comparison of DLLME to other modernised techniques (LPME and SPME), confirmed DLLME to be a fast (few seconds), simple, inexpensive and effective extraction technique (Rezaee *et al*., 2006).

Cloud point extraction (CPE) is a surfactant-based separation phenomenon that has been applied for extracting/pre-concentrating organic contaminants in water samples prior to gas chromatography (GC) or high pressure liquid chromatography (HPLC) analyses (Bingjia *et al*., 2007; Ling *et al*., 2007). In contrast to LLE, CPE does not utilise toxic or expensive organic solvents, making it more economical and environmentally friendly. Bingjia *et al*. (2007) utilised silicon surfactants, rather than anionic-cationic ones in a CPE process for extracting PAHs from water, because most anionic and cationic surfactants require high acid or salt concentrations that may damage chromatographic columns. Moreover, utilising common surfactants requires a clean-up step prior to HPLC analysis, because most surfactants retain an organic moiety that produces fluorescence signals that masks PAH detection (Ferrer *et al*., 1996).

The stir bar sorptive extraction (SBSE) technique is also utilised for PAHs analysing in water samples (García-Falcón *et al*., 2004). The enrichment of volatile and semi-volatile analytes is achieved by SBSE technique by sorbing analytes into a polydimethylsiloxane (PDMS) layer that is coated onto a stir bar, after which the adsorbed analytes are thermally desorbed. The efficacy of SBSE is attributed to the fact that sorption onto the PDMS layer is a weaker process than adsorption onto conventional adsorbents such as silica and alumina. The weaker interaction process allows analytes to be desorbed at lower temperatures, which minimises the loss of thermolabile solutes and unstable analytes tend not to degrade (Baltussen *et al*., 1999). The SBSE method produces results that have good linearity, precision, sensitivity, high analyte enrichment and also avoids using toxic/expensive solvents. García-Falcón *et al*. (2004) assessed the use of SBSE/HPLC-fluorescence detector (FLD) for determining eight PAHs in water samples and achieved a relative recovery of about 100%.

Ozcan *et al*. (2010) on the other hand, compared the ultrasound-assisted emulsification-micro-extraction (USAEME) technique to the LLE and SPE techniques for the extraction of 16 US EPA priority PAHs. Chloroform was selected as the extracting solvent for the USAEME method, and

recoveries from water samples were ≥90 %. The recovery efficiency was comparable to that of LLE. USAEME was demonstrated to be robust, viable, rapid and an easy method for extracting PAHs from water samples.

Oliferova *et al*. (2005) and Liang *et al*. (2006) used an automated one-step on-line technique, that combined pre-concentration and analysis of PAHs in water samples. This technique utilised an SPE approach that has been reported to be fast and reliable in performing trace analysis (Hennio, 1999). The SPE is a practical extraction method that is suitable for automation, because it does not require sophisticated equipment and provides high pre-concentration efficiency (Oliferova *et al*., 2005). LLE coupled with the SPE step have been widely accepted for the extraction and enrichment of PAHs from aqueous media. LLE is still one of the most commonly employed extraction techniques because of its simplicity, robustness, ease of application, efficiency, wealth of available analytical data and wide acceptance in most standard methods (Lambropoulou & Albanis, 2007). Various extraction methods that have been applied for the extraction of PAHs in water samples are presented in Table 2.6.

Table 2.6: A summary of methods used to analyse PAHs in water samples

Sample	Sampling area	Extraction method/Analytical technique	Detection limit	% Recovery	Reference
Urban road runoff	Beijing, China	SPE/GC-MS	0.7 - 2.8 ng/L	41 - 117 %	Zhang *et al*. (2008a)
Surface water	Yellow River, China	SPE/GC-MS	0.13 - 0.92 ng/L	35 - 95 %	Sun *et al*. (2009)
River water	Hyogo, Japan	SPE/HPLC-ESI-MS (ESI-electrospray ionisation)	0.001 – 0.03 ng/mL	88 – 97%	Takino *et al*. (2001)
River water	Xinyang, China	SPE/HPLC-FLD	0.10 - 0.25 ng/L	80 - 120%	Liu *et al*. (2016a)
Produced water	Sergipe, Brazil	LLE/GC-MS	5 - 15 µg/L	62 - 114 %, except for Phe.	Dorea *et al*. (2007)
Surface water	Vhembe District, South Africa	LLE-SPE/GC-TOF-MS (TOF-time of flight)	NR	96 – 149%	Edokpayi *et al*. (2016)
Surface runoff	Limpopo Province, South Africa	LLE/GC-FID	44 – 4290 µg/L	67 – 102%	Nekhavhambe *et al*. (2014)
Groundwater	Salvador City, Bahia, Brazil	SDME/GC-MS	0.01 – 0.03 µg/L	36 -152%	Santos *et al*. (2017)
Surface water	Johannesburg City, South Africa	SPMD/GC-MS	NR	55 - 115%	Amdany *et al*. (2014)
River, well, and surface water	Tehran, Iran	DLLME/GC-FID	0.007-.030 µg/L	82 - 111%	Rezaee *et al*. (2006)
Surface river water	Pontelandolfo, Italy	DLLME/GC-IT-MS (IT-ion trap)	0.001 -0.009 µg/L	97 -108%	Avino *et al*. (2017)

NR: not recorded

2.6.2 Extraction of PAHs from solid matrices

Classical organic solvent extraction of analytes from solid matrices are based mostly on the correct choice of solvent coupled with the use of heat and/or agitation (Picó, 2013). However, these techniques generally take hours or days to implement, which has necessitated the development of modern methods that miniaturised the implementation of the classical ones for PAH-extraction from solid matrices. The use of optimised Accelerated Solvent Extraction (ASE) was reported to give higher extraction efficiency compared to classical soxhlet method for PAHs extraction from plant samples. The range of 53 -117% recovery of matrix spiked standards obtained with ASE were said to meet the EPA 8270 method requirements (Yin *et al*., 2011). A consistent extraction efficiency was obtained in 50 min with ASE in contrast to 36 h for the classic soxhlet method.

In order to overcome the limitation with soxhlet extraction method, the use of microwave heating instead of electrical heating has also been utilised, termed Microwave-Assisted Solvent Extraction (MASE) method (Luque de Castro & Priego-Capote, 2012). Apart from heating, microwave energy also promotes the partitioning of analytes from sample matrix into the extractant (Sanchez-Prado *et al*., 2015). However, MASE application is limited to extracting solvents that absorb microwave energy and safety concerns due to the high pressure and temperature involved (Sun *et al*., 1998; Sanchez-Prado *et al*., 2015).

Ultrasonic extraction (UE) is another technique, being utilised as an alternative to conventional techniques. It gives equivalent or better recoveries, requires lower volume of toxic extractants and does not require sophisticated and highly expensive instrumentation (Sun *et al*., 1998; Kayali-Sayadi *et al*., 2000).

2.6.2.1 Extraction of PAHs from sediment samples

To assess the pristine state of aquatic ecosystems, it is of utmost necessity to assess sediments, as they serve as effective sinks for pollutants such as PAHs and could also act as or constitute secondary source of pollutants in aquatic ecosystems (Gu *et al*., 2017). As a result, the integrity of assessment data for aquatic ecosystems will depend largely on the extraction procedure adopted for sediment matrices. The health risks posed by pollutants via dermal adsorption can also be estimated from the levels of pollutants detected in sediment samples (Duodu *et al*., 2017).

Soxhlet extraction, ultrasonic agitation/sonication, mechanical agitation, accelerated solvent extraction (ASE)/pressurised liquid extraction (PLE), supercritical fluid extraction (SFE), subcritical fluid extraction, microwave-assisted extraction (MAE), solid phase micro-extraction (SPME),

magnetic solid phase extraction (MSPE), fluidised-bed extraction, thermal desorption as well as pyrolysis (Py) or high temperature distillation (HTD) extraction are some of the extraction techniques that have been adopted for the extraction of PAHs from sediment and soil samples (Banjoo & Nelson, 2005; Lau *et al*., 2010). Factors like temperature, extracting solvent type, moisture content and other characteristics of the media (carbon content, clay content and particle size) influences the efficiency of these extraction techniques (Lau *et al*., 2010). Mixture content for instance has been reported to reduce extraction efficiency of organic solvents like hexane and dichloromethane, in extracting PAHs from sediment (Song *et al*., 2002; Banjoo & Nelson, 2005). The choice of extracting solvent thus becomes critical in solving the challenge pose by moisture. The use of acetone-hexane/dichloromethane mixture in such situation has been reported to preventing clumping of wet sediment and also improves the extraction efficiency (Song *et al*., 2002; Banjoo & Nelson, 2005).

Comparable or even better recoveries are achievable with ultrasonic agitation in less time as compared to soxhlet traditional method in the extraction of PAHs from sediment samples (Marvin *et al*., 1992; Banjoo & Nelson, 2005). Banjoo and Nelson (2005) reported that for most analytes, recoveries of over 90% were achieved in 30 min with ultrasonication as compared to 3 h with KOH reflux method for the extraction of PAHs from sediments. Ultrasonication was described as having excellent extraction efficiency, precision and recovery for PAHs with little sample preparation, low set-up cost and high sample throughput. The integration of extraction and clean-up steps, in a one-step/on-line approach is also attractive, as the advantages of modern extraction techniques (low time, low solvent as well as high sample throughput) are further improved as shown by (Choi *et al*., 2014). They reported that a one-step integrated PLE and clean-up method for the analysis of 34 PAHs (parent and alkylated) in sediments achieved over 50% reduction in time and solvent requirements relative to unintegrated PLE methods previously utilised. The method was also described to be accurate and adequate for the analysis of PAHs, with mean recoveries of 92% and 94% reported for low and high PAHs concentrations spiked-matrix respectively and a mean recovery of 86% for certified reference material concentrations. The thermal desorption technique is another attractive technique, as it does not require solvents or high pressure extraction instruments and allows for direct analysis of solid samples by GC (Banerjee & Gray, 1997). Some extraction methods that have been utilised for the extraction of PAHs from different sediment samples and their respective percentage recoveries achieved are presented in Table 2.7.

Table 2.7: A summary of methods used to analyse PAHs in sediment samples

Sample	Sampling area	Extraction method/Analytical technique	Detection limit	% Recovery	Reference
Surface sediments	Queensland, Australia	ASE/GC-MS	0.19 - 0.35 ng/g	81 - 103%	Duodu *et al*. (2017)
Core sediments	Heilongjiang Province, China	ASE/GC-MS	1 -16 ng/g	45 – 104%	Sun and Zang (2013)
Sediments	Beijing, China	UE/GC-MS	0.02 - 0.38 ng/g	62 - 101%	Zhang *et al.* (2004b)
Surface sediments	Yunnan Province, China	UE/GC-MS	0.2 - 2 ng/g	82 - 105%	Gu *et al*. (2017)
Sediments	Edo State, Nigeria	UE/GC-FID	0.001 - 0.003 µg/kg	78 - 102%	Tongo *et al*. (2017)
Core sediments	Shandong Province, China	Soxhlet/GC-IT-MS	NR	85 – 99%	Zhang *et al.* (2016)
Sediments	Ohio, USA	Soxhlet/GC-MS	NR	78% on average	Gu *et al*. (2003)
Sediments	Finland	Soxhlet/GC-FID	0.5 ng/g	NR	Hyötyläinen and Olkari (1999)
Sediments	Bayelsa State, Nigeria	Soxhlet/GC-FID	NR	NR	Okafor and Opuene (2007)
Reclaimed mudflat sediments	Mumbai, India	SLP/GC-MS	0.09 – 0.52 ng/g	80 – 120%	Basavaiah *et al*. (2017)
Sediment	Johannesburg, South Africa	MAE/HPLC-FLD	NR	61 – 93%	Sibiya *et al*. (2013)

ASE: accelerated solvent extraction. GC-MS: gas chromatography mass spectrophotometer. UE: ultrasonic extraction. SLP: solid-liquid-partitioning. NR: not recorded

2.6.2.2 Extraction of PAHs from plant samples

Pollutants in plants are easily transferred into the food chain, resulting in biomagnification over two or more trophic levels (Meodor *et al*., 1995), thus posing a direct health risk to humans as humans occupy a high trophic level and depend largely on plants and herbivores for food. Although, the biomagnification of PAHs in humans is not expected (PAHs are actively bio-transformed by vertebrates), PAHs metabolites have been reported to be more potent than parent PAHs in causing estrogenic effects (Wiele *et al*., 2005). Plants serve as good indicators for use in environmental monitoring programs (Wang *et al*., 2012b), as pollutants in sediments, water and the atmosphere bioaccumulate in plants through absorption (by root, stem and leaf tissues), atmospheric deposition on leaves and gas phase uptake via stomata (Kargar *et al*., 2017). These multiple pathways by which plants could uptake PAHs, have often resulted in elevated PAH levels in plant samples relative to other media (water, soil as well as sediment) (Li *et al*., 2010a). To have a robust and satisfactory data for ecosystem management purposes, efficient extraction methods are therefore needed for accurate analyses of pollutants in plants. Various organic solvents which include methanol, acetone, toluene, chloroform, dichloromethane, n-hexane as well as cyclohexane have been widely applied in different extraction methods (ASE, PLE, soxhlet, ultrasonic and MAE amongst others), for the extraction of PAHs from plant samples (Pavelkajr *et al*., 1998; Sushkova *et al*., 2014). Ultrasonic agitation/sonication is a preferred method to soxhlet which requires high energy coupled with other drawbacks (Pavelkajr *et al*., 1998). The MAE method, in which temperature and pressure could be optimised for PAHs extraction from plant samples, represents a very attractive technique, even with high set-up cost relative to sonication method (Pavelkajr *et al*., 1998).

The coextraction of hydrophobic plant pigments (chlorophylls and carotene) by extraction methods necessitated a clean-up step, which could be achieved through gel permeation chromatography or SPE (Dugay *et al*., 2002). A selective ultrasonic extraction coupled with a SPE step was described by Dugay *et al*. (2002) for the extraction of PAHs from plants. The procedure achieved an average recovery of 70, 74, 79 and 89% for naphthalene, acenaphthylene, acenaphthene and chrysene, while over 94% mean recoveries were reported for the rest of the 16 US EPA priority PAHs. Some reported extraction methods for the extraction of PAHs in plant samples are presented in Table 2.8.

Table 2.8: A summary of methods used to analyse PAHs in plant samples

Sample	Sampling area	Extraction method/Analytical technique	Detection limit	% Recovery	Reference
Tissues of wetland plants	Shanghai, China	ASE/GC-MS	NR	79 – 102%	Wang *et al*. (2012b)
Pine leaves	Izmir, Turkey	UE/GC-FID	NR	NR	Kargar *et al*. (2017)
Moringa Herbal Tea	Nigeria	UE/GC-FID	0.30 µg/kg	90 – 109%	Benson *et al*. (2017)
Tree leaves	Beijing, China	SLE-ASE/GC-MS	NR	72 -105%	Wang *et al*. (2008)
Vegetables	Tianjin, China	ASE/GC-MS	NR	49 – 92%	Tao *et al*. (2004)
Gingko leave	Tokyo	PFE, PE/GC-MS (PFE- Pressurised fluid extraction, PE-Polytron extraction)	NR	> 65%	Murakami *et al*. (2012)
Holm oak leaves	Campania and Tuscany, Italy	UE/GC-HRMS	0.001 – 0.003 µg/mL (Instrument)	≤ 70%	De Nicola *et al*. (2015)
Vegetables	Thessaloniki, Greece	Soxhlet/HPLC-FLD	NR	71 -92%	Kipopoulou *et al*. (1999)
Wild plants, vegetables and rice stalks	Guangdong Province, China	Soxhlet/GC-MS	NR	69 – 95%	Wang *et al*. (2012a)

NR: not recorded

2.7 Analysis of PAHs

Sample clean-up is often required to ensure data integrity prior to the instrumental analysis of PAHs, as analyte signals could be largely obscured/masked by the presence of other interfering entities (elemental sulphur, surfactant and humic materials) (Ferrer *et al*., 1996; Pietzsch *et al*., 2010). To achieve effective determination of PAHs from environmental matrices, column chromatography (automated in some instances with the use of prepacked SPE cartridges with varieties of stationary phases) has been widely utilised for clean-up (Okuda *et al*., 2010; Nekhavhambe *et al*., 2014; Thea *et al*., 2016). Silica gel, polystyrene-divinylbenzene SPE, and gel permeation chromatography are popular clean-up methods to ensure data integrity (Wang & Guo, 2010).

To separate, identify and quantify PAHs after the extraction and clean-up protocols, GC rather than LC is often preferred, mainly because GC methods generally provide greater selectivity, resolution and sensitivity (Poster *et al*., 2006). Some PAHs also have poor solubility in mobile phase solvents popular with LC (methanol and acetonitrile) (IARC, 1983), which may result in poor elution of target compounds. Generally, GC are more often fitted with flame ionisation detectors (FIDs) than any other detector and have been in use since 1958 (Holm, 1999). Gas chromatography coupled with flame ionisation detectors (GC-FID) have been used to analyse PAHs in environmental samples (Moreda *et al*., 1998; Zhou *et al*., 2000; Li *et al*., 2011). Zhou *et al*. (2000) quantified the levels of the 16 US EPA priority PAHs in water (106 - 945 ng/L), pore water (1 - 3548 ng/L) and sediment (247 – 480 ng/g), with the mean recovery range of 66 to 96%. Flame ionisation detectors is universally used to analyse trace levels of organic compounds, due to its high sensitivity, wide linear range, detection of most organics and non-detection of most inert gases, other than methane (Wang *et al*., 2010b). It is also a detector that is insensitive to modest changes in operating parameters such as fuel and oxidant gas flow, environmental air pressure and temperature (Kuipers & Müller, 2010).

The Minjiang River Estuary in Southeast China was monitored for the16 US EPA priority PAHs in water, pore water, sediment, soil and vegetable samples using GC-FID. Prior to GC analysis, the PAHs in water samples were extracted and cleaned-up using SPE, while ultra-sonication was used to extract PAHs from sediment, soil and vegetation samples (Zhang *et al*., 2004a). Recoveries ranged from 79 to 111%, 85 to 101% and 63 to 81% in water, sediment and vegetable samples, respectively. The limit of detection for water samples ranged from 0.07 to 1.10 ng/L and the values were from 3.3 to 53.0 pg/g for sediment, soil and vegetable samples. The mean of each

detected PAHs ranged from 0.44 to 18.2 µg/L (water), 0.93 to 23.00 µg/L (pore water), 4.2 to 70.2 ng/g (sediment), 2.2 to 55.5 ng/g (soil) and 9.3 to 24600 ng/g (vegetables).

The GC-FID was also utilised for the determination of 16 priority PAHs in coastal sediment of Lebanon (Manneh *et al*., 2016) after Soxhlet extraction was performed for PAHs extraction. Recoveries ranged between 80 and 120%, detection limits ranged from 0.20 to 2.10 ng/g and the concentration of ∑16 PAHs at studied sites ranged from 1.22 to 731.90 µg/kg. Therefore, GC-FID is sufficiently adoptable for the analysis of PAHs in environmental samples. Tables 2.6 to 2.8 shows further instances where GC-FID has efficiently been utilised for PAH analysis

Mass spectrophotometer (MS) is another detector that is often coupled with GC and commonly utilised for PAHs analysis (Gu *et al*., 2003; Kannan & Perrotta, 2008; Santos *et al*., 2017). In MS, ions are produced and measured and eventually gives mass spectrum, showing fragmentation patterns and accurate mass for effective identification of substances. Variation in MS comes from the differences in its main components, including the ion source [electron impact (EI), chemical ionisation (CI), field ionisation (FI) and atmospheric pressure ionisation (API) (Mendham *et al*., 2000)], mass analyser and detector [magnetic sector analyser, quadrupole mass filter, ion trap detector and time-of-flight analyser are the different types of mass analysers, while photographic plates, Faraday cup, electron multipliers, channel electron multiplier and scintillation detectors are the different types of detectors utilised in mass spectrometry (Mendham *et al*., 2000)]. The recovery of 82 to 117% and 0.40 to 263 ng/L limit of detection were obtained on GC coupled with quadrupole MS, utilising SPE [oasis HLB (hydrophilic-lipophilic balance)] for analyte enrichment in the determination of 16 US EPA PAHs in wastewater (Sánchez-Avila *et al*., 2009). The levels of detected PAHs ranged from 0.009 to 5.050 µg/L, showing the high sensitivity of GC-MS in determining trace levels of PAHs. See Tables 2.6 to 2.8 for more evidence on the high sensitivity of GC-MS.

Unlike FID, MS can be coupled with LC in hyphenated LC-MS techniques which are applicable in the analyses of PAHs in environmental matrices with the development of efficient interfaces (Takino *et al*., 2001). The different ion sources in MS spectrometry for liquid phase input include; field desorption (FD), desorption chemical ionisation (DCI), fast atom bombardment (FAB), plasma desorption (PD), laser desorption, Secondary Ion mass spectrometry (SIMS), atmospheric pressure ionisation (API), thermospray (TSP), plasmaspray (PS), electrospray ionisation (ESI) and particle beam interface (PBI) (Mendham *et al*., 2000). Titato and Lancas (2006) compared a hyphenated mass spectrometric protocol, that has atmospheric pressure chemical ionisation (APCI) interface (HPLC-APCI-MS) with HPLC-UV- diode-array detection (DAD) protocol (HPLC-

UV-DAD), for the determination of selected PAHs in water samples. Detection- and quantification limits obtained ranged from 0.05 to 0.12 µg/mL and 0.165 to 0.396 µg/mL, respectively for the HPLC-APCI-MS protocol. The detection- and quantification limits obtained ranged from 0.0010 to 0.0300 µg/mL and 0.0033 to 0.0999 µg/mL, respectively for the HPLC-UV-DAD technique. They reported that, structural information obtainable from HPLC-APCI-MS makes the technique valuable, even though the HPLC-UV-DAD technique has higher sensitivity for the determination of PAHs in water samples based on better detection limit and quantification limit values obtained. A highly sensitive HPLC-MS hyphenated protocol, has however been reported for the determination of PAHs in water by Takino *et al.* (2001). The protocol utilised SPE (using blue-chitin cartridges) coupled with HPLC-ESI-MS with silver nitrate as post column reagent. The 10 PAHs analysed were separated by reversed-phase LC with analytes forming complexes with Ag^+ on mixing with the $AgNO_3$ solution. The molecular ions of the PAHs were then transferred by the complexes through charge transfer, using in-source collision induced dissociation. The detection limit of the method; ranged from 1 to 30 pg/mL, the recovery ranged from 88 to 97% and the levels of the10 PAHs analysed in river water; ranged from 6 to 12 pg/mL. Hence, the HPLC-ESI-MS protocol described above is powerful in the determination of trace levels of PAHs in water due to enhanced selective enrichment by the SPE (blue-chitin cartridges), efficiency in separation by reversed-phase LC and the high sensitivity of the ESI-MS.

Liquid chromatographic (LC) methods, including HPLC coupled with a fluorescence detector (HPLC-FLD) have also been employed for PAHs analyses (Williamson *et al*., 2002; Pietzsch *et al*., 2010). HPLC does not require a high-pressure cylinder of carrier gas, it is easier to maintain than GC as the detector does not come into contact with the sample solution and the analysis technique is non-destructive (Okuda *et al*., 2006). The downside is that there is the likelihood that co-extractives will have chemical properties that are similar to some PAH isomers and may therefore exhibit similar fluorescence properties. Co-extractives are not always removed when conventional silica-gel column clean-up methods are used, possibly negatively affecting the precision and accuracy of PAHs analysis when using HPLC-FLD (Okuda *et al*., 2006). A rapid HPLC fluorimetric detection which does not require a clean-up step was developed for the determination of PAHs (Kayali-Sayadi *et al*., 2000). The method employed a low solvent solid-liquid extraction by means of ultrasonic agitation and hypersil green PAH column. Recoveries reported for the method ranged from 70 to 98% for most of the PAHs and detection limits ranged from 0.100 to 0.448 µg/L. The use of HPLC-FLD technique for PAH analysis is limited to PAHs that have fluorescence, however the technique could be interfaced with MS to give a powerful identification and quantification tool.

Enzyme-linked immuno-sorbent assay (ELISA) and immuno-polymerase chain reaction (IPCR) are biotic techniques that have been applied to analyse PAHs (Barceló *et al*., 1998; Ye *et al*., 2009). Immuno-PCR detection method was developed by combining polymerase chain reaction (PCR) with ELISA through a chimeric protein, a molecule capable of linking DNA and antibodies (Ye *et al*., 2009). The ELISA involves an antigen-antibody interaction with the analyte, in which the antibodies or antigens are immobilised on a solid phase (Hennion & Barcelo, 1998). A real time fluorescent quantitative IPCR assay was carried out by Ye *et al*. (2010), for the determination of fluoranthene in environmental water samples. They reported a method recovery range of 90 to 116%, detection limit of o.6 fg/mL and that the analyte can be quantified in the concentration range of 1 fg/mL to 100 ng/mL. This technique is promising because it is highly sensitive, cheap and it can be carried out rapidly in real time [through automation] (Oubina *et al*., 1997; Ye *et al*., 2009).

2.8 Evidence and monitoring of PAHS in South African environment

South Africa, being a developing country and one of the largest economies in Africa, has witnessed a surge in urbanisation and industrialisation over the past decades. Increased levels of contaminants in the environment are often linked to rapid urbanisation and industrialisation (Mcmichael, 2000). As a result, there has been an increase in the need to assess the presence and levels of contaminants like PAHs in our environment, so as to guide policy makers in making policies for sustainable growth, that will ensure water, food and energy security (Amdany *et al*., 2014; Nekhavhambe *et al*., 2014; Geldenhuys *et al*., 2015).

Nieuwoudt *et al.* (2011) reported that, they carried out the initial assessment of PAHs in soils and sediments, focusing on industrial, residential and agricultural areas of central South Africa. The assessment conducted covered mainly the Free State and Gauteng provinces. They reported that the levels of total PAHs monitored ranged between 44 and 39,000 ng/g and that of carcinogenic PAHs ranged between 19 and 19,000 ng/g. The authors recommended that there is an ever-increasing need for regular PAHs assessment in industrial and residential areas that should include more environmental matrices.

Okedeyi *et al*. (2013) focused on the levels of 15 PAHs in soils at the vicinity of three coal-fired power plants in South Africa. The plants selected for the study are situated in Mpumalanga, Free State and Gauteng provinces. The levels of total PAHs monitored ranged between 9.73 and 61.24 µg/g and those of carcinogenic PAHs ranged between 4.03 to 34.78 µg/g. Soils from sites close

to coal-fired plants (power stations) were significantly contaminated by PAHs with high carcinogenic burden.

Amdany *et al*. (2014) assessed the levels of freely dissolved PAHs in water samples of selected water bodies around Johannesburg (South Africa). The total concentrations of the 16 US EPA priority PAHs ranged from 33.49 to 126.78 ng/L. The concentrations of the freely dissolved PAHs were reported to be at least one or two orders of magnitude higher than levels of freely dissolved-organochlorine pesticides (OCPs) [ranged from 0.146 to 36.937 ng/L], polychlorinated biphenyls (PCBs) [ranged from 0.021 to 0.121 ng/L] and dichlorodiphenyltrichloroethane (DDT) with its metabolites (ranged from 0.03 to 0.55 ng/L) at the selected sites. Thus, PAHs are ubiquitous in South African environmental media at higher concentrations compared to other persistent organic pollutants (POPs).

The levels of PAHs in water and sediment samples of rivers and surface run-off of Limpopo province was reported by Nekhavhambe *et al*. (2014). Only six PAHs were identified and quantified by the study, with total PAHs levels in water samples from both rivers and surface run-off ranging between 29.2 and 3,064.8 µg/L, while higher levels were reported for sediment samples (111.6 to 61,764 µg/kg). High PAH-toxicity burden above acceptable levels were envisaged from the data obtained from the six PAHs of even low toxicity quantified.

2.9 Remediation of PAHs

PAHs do not degrade easily under natural environmental conditions, therefore, different methods are often needed to accelerate the degradation and/or removal of PAHs from contaminated environmental matrices (Haritash & Kaushik, 2009). Some conventional remediation methods that have been used include soil washing, solidification and stabilisation, incineration, thermal treatment, as well as advanced oxidation. Summary of conventional remediation approaches that have been utilised for PAH-degradation is presented in Table 2.9. Physicochemical methods such as adsorption, volatilisation, photolysis amongst others, have also been used for PAH remediation (Miller & Olejnik, 2001; Gong *et al*., 2007; Megharaj *et al*., 2011).

2.9.1 Conventional remediation methods for PAHs

Soil Washing*:* Soil washing allows for the desorption of PAHs that have been strongly adsorbed by soil or sediment due to PAHs hydrophobicity, low volatility, and high octanol-water partition coefficient (K_{ow}) (Gharibzadeh *et al*., 2016). Solvents (water, organics, and vegetable oil), supercritical fluids, subcritical fluids and cyclodextrins were reported to have been utilised for soil washing (Gan *et al*., 2009). The use of surfactants, which are amphiphilic compounds have been largely shown to enhance the desorption of PAHs from soil or sediment during soil washing (Ahn *et al*., 2008; López-Vizcaíno *et al*., 2012). Due to the unique structure of surfactants, they enhance the solubility of PAHs significantly by partitioning PAHs into the hydrophobic cores of surfactant micelles and promote mass transfer of PAHs from soil or sediment into an aqueous phase (by micelles that decreases the interfacial tension between the PAHs and water) (Ahn *et al*., 2008). Hence, soil washing aided by surfactants allows for rapid reclamation of soil or sediment that has been impacted with PAHs that would have required a continuing bioremediation process.

López-Vizcaíno *et al.* (2012) described the use of surfactant aided soil washing for PAH remediation. They employed anionic, cationic and non-ionic surfactants and utilised metallic salts ($AlCl_3.6H_2O$ and $FeCl_3$) as coagulants in the study. The anionic surfactant yielded the highest removal efficiency for the PAHs, with over 90% contaminant removal recorded. In contrast, the cationic surfactant had a removal efficiency of 30%. Aluminium and iron salts were reported to be the most commonly used coagulants for the treatment of wastewater generated from surfactant aided soil washing.

Table 2.9: Summary of conventional remediation approaches utilised for PAH-degradation

PAHs remediated	PAH –matrix	Approach used	Reagent/condition used	Primary mechanism	Removal efficiency	Reference
16 US EPA PAHs	Contaminated soil	Soil washing	Sunflower oil (solvent) and active carbon for recycling	Dissolution and mass transfer	81.0-100.0%	Gong *et al*. (2005)
3- ringed PAHs	Soil	Soil washing	Soybean oil (solvent) and tea saponin (surfactant)	Dissolution and mass transfer	Up to 98.2% (after two consecutive washing cycle)	Ye *et al.* (2017)
Nap and Phe	contaminated soil	Soil washing	Cyclodextrin enhanced	Solubilisation and desorption	80% (Nap) 64% (Phe)	Badr *et al.* (2004)
Acy	Contaminated water	Chemical oxidation	Ozone	Ozonation and disintegration	95 – 100%	Rivas *et al.* (2000)
16 US EPA PAHs	Aged contaminated sediment	Chemical oxidation	hydrogen peroxide, modified Fenton's reagent, activated sodium persulfate, and potassium permanganate	Oxidation and disintegration	Up to 98.0% (with modified Fenton's reagent)	Ferrarese *et al*. (2008)
16 US EPA PAHs	Contaminated soil	Chemical oxidation	Fenton-like reagent (magnetite as catalyst)	Oxidation and disintegration	> 90%	Usman *et al.* (2012)
Phe	subcritical water (< 374^{o}C and < 221 bar)	Thermal treatment and chemical oxidation	Deionised water and hydrogen peroxide	Degradation and oxidation	Up to 100%	Yang and Hildebrand (2006)
Flu	Soil	Thermal treatment	Microwave heating	Thermal desorption and degradation	100%	Falciglia *et al.* (2016)

3-ringed PAHs: Acenaphthylene, Acenaphthene, Fluorene, Phenanthrene and Anthracene. Nap: Naphthalene. Phe: Phenanthrene. Acy: Acenaphthylene. Flu: Fluorene

The treatment of generated wastewater from PAHs remediation by surfactant aided soil washing have also attracted research interests (Ahn *et al*., 2008; Gharibzadeh *et al*., 2016).The use of bioremediation approach for soil washing effluent treatment and the possible reusability of the biologically recycled surfactant solution was reported by Gharibzadeh *et al.* (2016). This approach requires the use of surfactants that are not toxic to microorganisms to allow for pollutant biodegradation. The method achieved complete biodegradation of pollutant in effluent within seven days of enriched bacterial consortium inoculation and after seven consecutive washing cycles with the recycled surfactant solution >99% PAHs removal efficiency was achieved, which stood at 74.4% with the first washing. Hence, no need for large volume of water and huge quantity of expensive surfactants.

Furthermore, the use of tea saponin (a biological amphipathic compound) to aid soil washing by soybean oil-water solvent was reported (Ye *et al*., 2017). The washing method achieved up to 96% PAHs removal after two consecutive washing cycles and It was reported that the bio-accessibility of the residual PAHs in the soil were extremely low. Hence, the residual PAHs posed limited risk to human and ecological health. The reusability of the saponin aided soil washing effluent was made possible by PAH-degrading strain of *Sphingobium sp*, which achieved 93 to 98% mineralisation of the PAHs that were made bioavailable by the tea saponin soybean oil-water solvent. The solvent utilised for washing was made up of 15.0 mL/L soybean oil and 7.5 g/L tea saponin.

In another study, Li *et al.* (2014) reported the use of biochar from wheat straw for selective removal of PAHs from soil washing effluent. The method achieved 72 to 99% selective PAHs removal efficiency and >87% surfactant recovery, being that the biochar micropores were not accessible for the surfactant employed. Remediation of soil or sediment impacted with PAHs by soil washing seems promising, but requires excavation, high volume of solvent and expensive or fine surfactants, making the approach non-economical.

Solidification/Stabilisation (S/S): This approach involves the use of cementing agents such as portland cement, blast furnace slag, flay ash, natural or modified clay, waste/by-product with cementitious properties, proprietary additives and quicklime to immobilise contaminants within a given media, rendering the contaminants passive with extremely low or no bioavailability (Ma *et al*., 2018; Antemir *et al*., 2010). Solidification is the physical inclusion of contaminants into solid mass with lower permeability and stabilisation is the conversion of contaminants into less soluble forms (Antemir *et al*., 2010). The S/S remediation approach is quite attractive, because it does not

require high energy input, causes less atmospheric emissions, lifecycle secondary environmental impact is minimised and in some cases can be incorporated with concrete works (Ma *et al*., 2018).

Karamalidis and Voudrias (2007) demonstrated that PAHs in oil refinery sludge could be stabilised in a cement-based solidification process. The effectiveness of two types of cements (portland and blended cement) for stabilising and solidifying PAH-contaminated sludge was studied. Results showed that portland cement was more effective than blended cement for immobilising acenaphthylene, acenaphthene, fluorene, Pyrene, benzo[a]anthracene, Chrysene, benzo[b]fluoranthene, benzo[a]pyrene and indeno[1,2,3-cd]pyrene. The study showed that 12 of 16 higher PAHs were leached from the oil sludge that had been stabilised by blended cement (the four PAHs that remained stable were naphthalene, phenanthrene, benzo[k]fluoranthene, and dibenzo[a, h]anthracene). The use of only hydraulic binders like cements is insufficient for chemical immobilisation of PAHs, as PAH-molecules cannot be incorporated into the cement matrix (Mulder *et al*., 2001). Additives, such as clay modifiers and adsorbents, [capable of forming physico-chemical bond with PAHs and binders (organic matter, chloride salts and sulphates)] have been studied for being capable of improving compactness and strength when used in chemical immobilisation approach, even in the presence of secondary impurities. Ma *et al*. (2018) employed portland cement, activated carbon and sulfonated oil for the treatment of PAH-contaminated soil. The sulfonated oil significantly improved the unconfined compressive strength of the treated soil, resulting in improved resistance to disintegration and reduction in leaching.

Thermal Treatment: This approach has been reported to be effective in the remediation of PAHs from contaminated soil through PAHs volatilisation or destruction under high temperatures (Kuppusamy *et al*., 2017; Falciglia *et al*., 2016). The incineration of contaminated soil at elevated temperatures (870 to 1200^{o}C) was reported to effectively destroy PAHs (Gan *et al*., 2009). However, the drawbacks of the technology include the need for moisture removal, high energy demand, excavation, generation of toxic off-gases (hydrogen chloride, sulphur oxides, nitrogen oxide, dioxins and furans) and emission of metals, necessitated the development of other thermal treatment approaches such as *in-situ* thermal desorption (ISTD) (Hosseini, 2006) and microwave thermal treatment (Falciglia *et al*., 2018). The ISTD approach does not require excavation as the name implies. The treatment is carried out on site and the emission of toxic off-gases into the environment were prevented with the incorporation of carrier gas or vacuum system that sweeps volatilised products into the gas treatment unit for secondary treatment or off-site disposal (Kuppusamy *et al*., 2017). The microwave thermal treatment approach on the other hand, does not rely on heat transfer but utilises electromagnetic radiation that allows for uniform, selective and rapid heating and have high flexibility for application without excavation or disturbance of

contaminated media (Chien, 2012). Microwave thermal treatment of PAHs to achieve remediation was studied by Robinson *et al.* (2009). More than 95% of the PAHs in light- and heavy-contaminated soils were removed, which demonstrated the remediation efficacy of microwave energy.

Chemical Oxidation: This approach is described as one of the *in-situ* technologies that have the efficacy to degrade both LMW and HMW PAHs in contaminated media through oxidants injection (Lemaire *et al*., 2013). The technique gained popularity, because it is rapid and aggressive in the remediation of PAH impacted media as compared to biological techniques that are sensitive to contaminant type and concentration (Ferrarese *et al*., 2008). Ozone, permanganate, fenton's reagents, percarbonate and activated persulfate are the common oxidants that have been utilised in the remediation of contaminated media (Lemaire *et al*., 2013). Fenton's reagent, activated persulfate and perozone are the most common oxidants with advanced oxidation processes (AOPs), which utilises various reactant combinations to enhance the production of highly reactive radicals that are capable of degrading most recalcitrant compounds (Ferrarese *et al*., 2008). O'Mahony *et al*. (2006) demonstrated the potential of chemical oxidation for PAH removal by using ozone to degrade phenanthrene in different soil samples. The study showed higher removal efficiency of Phe from sandy soil in contrast to clayey soil. They also reported that water content of soil reduced the potency of ozone treatment, due to the negative correlation that existed between the two parameters.

A major drawback in the application of chemical oxidation technique, is the determination of optimal doses of the oxidising solution for field application, an overdose may negatively affects soil microbial communities and alters soil organic matter (Chen *et al*., 2009; Ranc *et al*., 2016).

2.9.2 Remediation of PAHs using nanoparticles

Nanotechnology has received lots of attention from scientists in the remediation of recalcitrant contaminants in the environment, based on the fact that nanomaterials have unique physical and chemical properties (Rizwan *et al*., 2014). Chang *et al*. (2005) reported the use of nanoscale zero-valent iron (nZVI) for the removal of pyrene from contaminated soil. The massive specific area of the nanoparticles was credited for pyrene removal efficiency and they reported a 72% pyrene removal in an optimal time of 60 min at 150 rpm agitation speed with 0.1 g/g dosage of nZVI. The incorporation of nanoparticles with other remediation approaches was reported by Chen *et al*. (2015). They utilised $Na_2S_2O_3$ for the remediation of 16 PAHs in sediments via chemical oxidation, that was simultaneously activated by temperature and nZVI. The PAH removal efficiency of $Na_2S_2O_3$ (10.7 to 39.1%) was increased to up to 90% by the addition of nZVI (0.01 g/L) at 70^0C. The removal of acenaphthene in aqueous solution utilising magnetic nanoparticles was also reported by Huang *et al*. (2016b). They reported acenaphthene removal of above 85% and up to 2250 mg/Kg sorption capacity for the adsorbents. Nanotechnology has thus been efficiently applied for the remediation of PAHs in different environmental matrices. However, nanotoxicology has received lots of attention in recent years due to safety concerns about nanoparticles (by scientists and the general public) and their potential impact on the environment and biota (Nowack, 2008).

2.9.3 Bioremediation of PAHs

Bioremediation utilises biological organisms/materials to mineralise/immobilise contaminants. Examples of techniques used include bioventing, bioleaching, land farming, composting, bioaugmentation, Rhizofiltration, biostimulation and biosorption. Bioremediation is a cost-effective and environmentally friendly means of remediation, as treatment efficacy does not adversely affect site material or its indigenous flora and fauna (Ang *et al*., 2005; Haritash & Kaushik, 2009; Megharaj *et al*., 2011). Microorganisms degrade PAHs in tandem with their natural potential to utilise hydrocarbons as an energy source (Larsen *et al*., 2009). Hence, PAHs are biodegraded or biotransformed into less complex metabolites, and are eventually mineralised by aerobic or anaerobic processes into more basic chemical entities such as H_2O, CO_2 or CH_4 (Haritash & Kaushik, 2009). Megharaj *et al*. (2011) showed that bioremediation is a promising treatment approach for PAH-remediation in the environment.

2.9.3.1 Phytoremediation/phytobial remediation of PAHs

Phytoremediation is an attractive technique for the clean-up of contaminated sites and can be defined as the proficient use of plants to remove, detoxify or immobilise environmental contaminants in a growth matrix (soil, water or sediments) through natural-, biological-, chemical- or physical activities and processes of the plant (Ciura *et al*., 2005). It is an emerging technology which deserves to be considered for remediating contaminated sites, because it is cost-effectiveness, aesthetic advantages and long term applicability (Su & Wong, 2004; Agunbiade *et al*., 2009). Phytoremediation approaches that have been utilised for PAH-degradation are presented in Table 2.10.

Table 2.10: Phytoremediation approaches for PAH-degradation

PAHs Investigated	PAH–matrix	Plant and material(s) used	PAH-removal pathway(s)	Result/Removal efficiency	Reference
Phe and Pyr	Contaminated soil	Maize (*Zea mays* L.) and surfactants	Bioaccumulation, abiotic and microbial dissipation	Negligible plant PAH-uptake with higher PAH-level in leaf (66.8 ng/g) compared to root (58.2 ng/g). Surfactants have no significant effect on PAH-uptake by maize plant but enhanced PAHs desorption in soil (up to 89% for Pyr).	Liao *et al.* (2015)
Pyr	Contaminated soil	*Medicago sativa, Brassica napus* and *Lolium perenne*	Microbial dissipation	Up to 32%.	D'Orazio *et al.* (2013)
Phe and Pyr	Aqueous solution	Red clover (*Trifolium pretense* L.) and nonionic surfactant	Plant uptake and bioaccumulation	Significant PAH-accumulation in root and shoot were recorded without surfactant and uptake increased with duration from 0 to 228 h. The level of PAHs in plant increased with Tween 80 (surfactant) soil treatment from 0 to 6.6 mg/L with 18 to 155% increase in plant PAH-uptake. However, higher surfactant levels inhibited plant PAH-uptake. PAHs levels in root were higher in root as compared to shoot.	Gao *et al.* (2008)
16 US EPA PAHs	Oil treated soil	Mangrove *Bruguiera gymnorrhiza*	Plant uptake and bioaccumulation	99% of accumulated PAHs were in root and 1% in leaf. Two to three ringed PAHs were mainly accumulated by the plant. Only 2 to 3-ringed PAHs (Phe is the only 3-ringed PAH) were accumulated in leaf, whereby root accumulated 2-,3-,4- and 5-ringed PAHs (BaP is the only 5-ringed PAH) but no uptake of 6-ringed PAHs.	Naidoo and Naidoo (2016)
Phe and Pyr	Aged soil	*Cucurbita pepo* (Gold rush) and purine alkaloid (caffeine)	Plant uptake and bioaccumulation	PAHs water solubility increased with caffeine concentration. Caffeine enhanced PAHs uptake by the plant. The shoot level of Phe increased from 0.09 to 0.13 µg/g with caffeine treatment while Pyr level increased from 0.17 to 0.47 µg/g. The root level of Phe increased from 1.5 to 6.3 µg/g with caffeine treatment, while the Pyr level increased from 3.0 to 10.6 µg/g.	Navarro *et al*. (2009)
Phe and Pyr	spiked soils	Tall fescue, ryegrass, alfalfa and rape seed	Plant uptake and bioaccumulation	Combined plants cultivation gave 98.3 to 99.2 % Phe removal and 79.8 to 86.0 % Pyr removal.	Cheema *et al*. (2010)

Phe = Phenanthrene. Pyr =Pyrene

.

Some phytoremediation processes that have been effectively applied include:

1. Phytoextraction: This is also known as phytoaccummulation, and refers to the process by which plant roots take up contaminants from soil and translocate them to above ground plant parts (shoot and leaves) (Garbisu & Alkorta, 2001).
2. Rhizofiltration: This is similar in concept to phytoextraction, but it is process by which plant uptake contaminants from water rather than contaminated soils (Anderson *et al*., 1993).
3. Phytostabilisation: This is a process in which certain plant species are used to immobilise soil and water contaminants. Contaminants are absorbed and adsorbed by plant roots or are precipitated in the rhizosphere. Such action prevents the mobility of contaminants in soil, water and air, and reduces bioavailability of the contaminants, thereby preventing their spread through the food chain (Anderson *et al*., 1993).
4. Phytostimulation: This is a process in which microbial degradation of contaminants are stimulated in the plant root zone; it is also called plant-assisted bioremediation (Khan *et al*., 2004).
5. Phytotransformation: This is the degradation of contaminants via plant metabolism to non-toxic metabolites or end products (Khan *et al*., 2004).

There are at least four pathways by which phytoremediation achieve reduced contaminant loads, including (i). abiotic losses, (ii). indigenous microbial degradation, (iii). root tissue-enhanced dissipation as well as (iv). root exudate-enhanced biodegradation (Sun *et al*., 2010). Additionally, the rhizosphere of plants used for bioremediation is exceedingly important in contributing to the dissipation of contaminants (Ma *et al*., 2010). Eelgrass (*Zostera marina*) is a plant that has been studied for its capability to remove PAHs from contaminated sediments (Huesemann *et al*., 2009). Eelgrass was reported to translocate PAHs (irrespective of the number of aromatic rings) from a contaminated substrate into its component body parts, with bioaccumulation factors that amounted to approximately 3 and 1 in roots and shoots respectively. They reported 73% total PAHs removal from sediments, whereby only 25% dissipation occurred in controls (without eelgrass). Eelgrass stimulated microbial biodegradation of PAHs was however proposed to be the main PAHs remediation pathway after eliminating possible losses to the water column or absorption and PAHs transformation by the plant. Elsewhere, a similar potential of various plant species for phytoremediation of persistent organic pollutants (POPs) from contaminated sites have been reported (Tesar *et al*., 2002; Euliss *et al*., 2008; Lin and Mendelssohn, 2009).

The concept of phytobial remediation takes advantage of the synergistic relationship that may exist between microbes and plants (Sun *et al*., 2010). This concept explores the ability of plants to enhance the microbial degradation of contaminants. Yu *et al*. (2011) reported that ryegrass enhanced the growth of *Acinetobacter sp.*, linking this phenomenon to specific circumstances that occur in the rhizosphere of ryegrass root. Plants secrete photosynthate in root exudates, which supports the growth and metabolic activities of diverse fungal and bacterial communities in the rhizosphere (Alkorta & Garbisu, 2001).

The phytoremediation capabilities of plants have been enhanced by inoculating them with microorganisms (arbuscular mycorrhizal fungus) to enhance PAH degradation. Gao *et al*. (2011) enhanced phytoremediation of PAHs by inoculating alfalfa (*Medicago sativa L.*) with *Glomus mosseae* and *Glomus etunicatum*. After 70 days of the arbuscular mycorrhizal phytoremediation (AMPR) experiments in greenhouse pots, more than 98.6% and 88.1% PAHs (phenanthrene and pyrene) were dissipated in soils by *G. mosseae* and *G. etunicatum* respectively, whereby insignificant dissipation (< 3.24%) was attributed to plant uptake.

These remediation processes may be carried out either *in-situ* or *ex-situ*, using bioaugmentation and/or biostimulation enhancement. The *in-situ* approach involves treating contaminated material on-site. Conversely, the *ex-situ* approach involves the physical removal of contaminated material via excavation or pumping prior to treatment (Boopathy, 2000; Farhadian *et al*., 2008).

Since PAHs are known toxicants, the effects on plants utilised for phytoremediation have been explored. Zhang *et al.* (2010) studied the effect of PAHs on plant growth in constructed wetlands. The study showed that different plant species interact differently with PAHs. They reported that the growth of *Baumea juncea* and *Schoenoplectus validus* increased with increasing naphthalene concentration while the growth of *Juncus subsecundus* decreased at high naphthalene levels in a hydroponic system. The authors concluded that PAHs affect wetland plant growth in a species-specific manner, and the effect is independent of PAH type and media.

2.9.3.2 Bioremediation Systems for PAHs Degradation

A bioremediation system mainly utilises microbial degradation processes in a technical and controlled treatment system to metabolise organic contaminants to inorganic materials such as carbon dioxide, water, inorganic salts and perhaps methane (Langwaldt & Puhakka, 2000; Farhadian *et al*., 2008). Bioremediation systems are employed to treat wastewater and runoff prior to discharge into aquatic systems. Remediation processes are carried out either in aerobic or anaerobic conditions (Gan *et al*., 2009). Anaerobic bioremediation processes have received increased attention in wastewater treatment due to advantages such as low energy consumption, low quantity of sludge generation and biogas recovery (Wen *et al*., 1999). A bioremediation system can be formed either with a bioreactor or in a constructed wetland. A bioreactor is a contained vessel, in which biological treatment takes place, while a constructed wetland utilises inherent natural geochemical and biological processes extant in a wetland ecosystem to accumulate and remove contaminants from influent waters (Van Stempvoort & Biggar, 2008).

2.9.3.2.1 Bioreactors

A bioreactor is highly effective at increasing bioavailability of poorly soluble compounds in the aqueous phase, and some of the bioreactors that have been utilised for PAH-biodegradation include fluidised-bed bioreactor (FBB), membrane bioreactor (MBR) as well as two-phase partitioning bioreactor (TPPB) [Kuyukina *et al*., 2009; Mozo *et al*., 2011]. Kuyukina *et al*. (2009) employed a FBB with immobilised *Rhodococcus* cells to treat petroleum-contaminated water. The advantages of FBB are based on its hydrodynamic and mass transfer phenomena. *Rhodococcus* cells were used because the *Rhodococcus* genus has diverse metabolic activities that enhance the degradation of petroleum hydrocarbons in the environment. Sawdust, polyvinyl alcohol cryogel and polyacrylamide cryogel were the hydrophobic carriers examined to immobilise *Rhodococcus* cells. The highest cell immobilisation yield and stable metabolic activity was reported for a hydrophobised sawdust-supported biocatalyst and was utilised in the FBB. A 46 - 70% removal of two to three ring PAHs was achieved for the contaminated water. Sawdust was therefore established as a non-toxic, economically viable, biodegradable and effective immobiliser in the FBB system for the treatment of PAH contaminated water.

Membrane bioreactors operates as biological reactors to which a filtration module is added for the removal of contaminants (Wisniewski & Grasmick, 1998). Mozo *et al*. (2011) reported the use of membrane bioreactors for PAHs degradation. The authors examined PAH-degradation rates in two membrane bioreactor types; a cross-flow membrane bioreactor (which generates high shear

stress) and a semi dead-end membrane bioreactor (generates a low shear stress). The semi dead-end membrane bioreactor removed PAHs more efficiently and non-biotic (sorption and volatilisation) processes contributed more to removal of PAHs. However, higher degradation rates were reported for the cross-flow membrane bioreactor relative to the semi dead-end membrane bioreactor. Shear stress was found to be a predominant factor that influenced PAH-removal. High shear stress dispersed bacteria and generated copious quantities of dissolved and colloidal matter, thus increasing PAHs bio-availability.

Two-phase partitioning bioreactors have also been applied to achieve PAH-degradation (Guieysse & Viklund, 2005; MacLeod & Daugulis, 2005). The concept of TPPB is based on using water immiscible and biocompatible organic solvent that is allowed to float on the surface of a cell-containing aqueous phase (Daugulis, 2001). This arrangement allows for optimal substrate delivery to microbes in the bioreactor. MacLeod and Daugulis (2005) noted that the pathways for microbial substrate uptake in TPPBs were predominantly, uptake of dissolved substrates in aqueous phase, biosurfactant-enhanced uptake of hydrophobic substrates, and substrate uptake when in direct contact with the organic phase. Mahanty *et al*. (2008) utilised silicone oil as non-aqueous phase liquid and *Mycobacterium frederiksbergense* for biodegradation of pyrene in a TPPB. Results also showed that complete biodegradation of pyrene was achieved and thus TPPBs were efficient in enhancing the microbial biodegradation of the PAHs.

Elsewhere, a roller bioreactor was also designed and tested for PAH-degradation. Purwaningsih *et al*. (2004) inoculated a roller bioreactor with *Pseudomonas putida* to degrade naphthalene. Such roller bioreactors are regarded to be ideal for bioremediation studies because they limit stripping losses of analytes better than traditional continuous stirred-tank reactors (CSTR). Table 2.11 shows more evidence of studies where bioreactors have been employed in remediating PAHs.

Table 2.11: Bioreactors utilised for PAH-degradation

PAHs remediated	PAH –matrix	Bioreactor/material	Organism used	Primary mechanism	Removal efficiency	Reference
BaA and BaP	Water	Mini-bioreactors (batch continuous stirred tank reactor (CSTR) and tubular semi-continuous reactor) packed with alginate beads	*Selenastrum capricornutum* and *Scenedesmus acutus*	Biodegradation, sorption and photooxidation	At 6 h up to 78% BaA removal and 66% for BaP, while at 15 h up to 90% BaA removal and 85% BaP removal for both organisms during basic bioassay with 90 beads. Up to 92% PAH- removal in CSTR and 85% in semi-continuous reactor	García de Llasera *et al*. (2018)
Pyr	Aqueous and Organic phases	Two-phase partitioning bioreactor (TPPB)	*Mycobacterium frederiksbergense*	Biodegradation	Up to 100.0 %	Mahanty *et al*. (2008)
Nap, Flu, Phe, Ant, Flt, Pyr, BaA, BbF, BaP and DBA	Aqueous and Organic phases	Two-liquid-phase bioreactor (TLPB)	Contaminated soil and agricultural soil as inocula	Biodegradation	Complete degradation of Nap, Flu, Phe, Ant, Flt and Pyr were achieved within 4 to 50 days for both inocula. Other PAHs were degraded to varying extent at the end of 170 days except for DBA. Higher PAH degradation was achieved with contaminated soil inocula as compared to that from unpolluted agricultural soil	Wang *et al.* (2010a)
Phe, Ant, Flt, Pyr, BaA, Chy, BbF, BkF, BaP, DBA, BgP, and IcP	Manufactured gas plant soil	Mushroom compost	NR	Biodegradation	Up to 98.0%	Sasek *et al*. (2003)

PAHs remediated	PAH –matrix	Bioreactor/material	Organism used	Primary mechanism	Removal efficiency	Reference
Nap, Acy, Can, Flu, Phe, Ant, Flt, Pyr, BaA, Chy, BbF, BkF, BaP, DBA, BgP, and IcP	coal-tar contaminated soil	laboratory-scale in-vessel composting reactors	NR	Biodegradation	Up to 90.0%	Antizar-Ladislao *et al*. (2005)
Nap	soil model systems	NR	*Pseudomonas* sp. HOB1	Biodegradation	97.0 % of 2000 ppm of Nap degraded in 24 hours and culture showed potential to tolerate Nap concentration of up to 60000 ppm.	Pathak *et al*. (2009)
Nap, Phe, BaP, and BgP	Spiked garden soil	spent mushroom compost	fungi, bacteria and enzymes	Biodegradation and Sorption	Over 90.0%	Lau *et al*. (2003)

Nap: Naphthalene. Pyr: Pyrene. Phe: Phenanthrene. BaP: Benzo [a] pyrene. BgP: Benzo [g, h, i] perylene. Ant: Anthracene. Flt: Fluoranthene. BaA: Benzo [a] anthracene. Chy: Chrysene. BbF: Benzo [b] fluoranthene. BkF: Benzo [k] fluoranthene. DBA: Dibenzo [a, h] anthracene. IcP: Indeno [1,2,3-cd] pyrene. Acy: Acenaphthylene. Can: Acenaphthene. Flu: Fluorene.

2.9.3.2.2 Constructed Wetlands

Wetlands serve as natural water purification ecosystems, in part, because the microphyte and microbial organisms that inhabit them can biotransform contaminants into products that are not harmful to the ecosystems (Yao *et al*., 2017; Sabia *et al*., 2018). Wetland microorganisms have been shown to induce enzymes for organic compounds assimilation, for use as substrates for cell growth and energy sources (Tran *et al*., 2013). Constructed wetlands are engineered to mimic natural wetlands, in the form of plants, soil and microorganisms that are associated with natural water purification in natural wetlands and are employed to remove contaminants from wastewater effluents (Kivaisi, 2001). The potential that constructed wetlands have for removing pollutants can be maximised if components that contribute to pollutant removal are selected carefully (Dordio & Carvalho, 2013). Much research has been dedicated to selecting the proper macrophytic plant species for PAH degradation in constructed wetlands (Zhang *et al*., 2008b). The main mechanisms by which contaminants are reduced in wetland ecosystems include sedimentation, filtration, chemical precipitation, adsorption, microbial interaction as well as plant uptake (Kivaisi, 2001). Constructed wetlands are successful because they are easy to use, require low maintenance, have low construction costs and have high remediation efficiency (Cottin & Merlin, 2008). Different types of constructed wetlands have been successfully designed and used for treating wastewater from various anthropogenic sources (Vymazal, 2009). Tromp *et al*. (2012) investigated the efficiency of a vertical-flow constructed wetland for removing eight PAHs from road runoff. More than 80% PAH-removal was achieved for most of the 11 PAHs (anthracene, phenanthrene, fluoranthene, pyrene, benzo[a]anthracene, chrysene, benzo[b]fluoranthene, benzo[a]pyrene, benzo[k]fluoranthene, dibenzo[a, h]anthracene and benzo[g, h, i]perylene), all amongst the 16 US EPA priority PAHs. The highest % removal was 94, reported for fluoranthene-, benzo[a]anthracene- and benzo[a]pyrene removal and the authors indicated that sedimentation played a very important role in PAH retention/removal.

Giraud *et al*. (2001) studied the biodegradation of anthracene and fluoranthene in a constructed wetland system, and the role of fungi present within the system. This study demonstrated that constructed wetlands may serve as a media appropriate for isolating fungi capable of degrading PAHs. A total of 40 fungal species were isolated and assayed for capacity to degrade anthracene and fluoranthene from a liquid medium. *Absidia cyclindrospora* was the species most capable of degrading both compounds, with over 80% removal efficiencies. The workers also reported that fluoranthene was more susceptible to fungal depletion than was anthracene. The targeted contaminants in constructed wetlands were more easily degraded by strains that had previously been exposed to soils that were contaminated rather than to non-contaminated ones. Moreover,

the number of fungal colonies increased in soils that were contaminated with fluoranthene, which suggested that some fungal species might fluoranthene as a nutrient source. Fluoranthene was efficiently degraded by 33 species of fungi that had been isolated from contaminated wetlands, while only two species achieved >70% anthracene degradation. Giraud *et al*. (2001) suggested that microbial (especially fungal) biotransformation contributed greatly to PAH-biodegradation in the wetland system.

Fountoulakis *et al*. (2009) studied the removal of PAHs from domestic wastewater in pilot scale constructed subsurface flow (SSF) and free-water surface (FWS) constructed wetlands. Average PAH removal efficiencies of 79.2% and 68.2% for SFF and FWS respectively were reported. Settling and sedimentation were suggested as the most likely removal processes in SSF, because PAH mean removal efficiencies correlated well with total suspended solid (TSS) removal efficiencies. The correlation for the mean PAHs removal rate in the FWS system was much lower, suggesting that photo-degradation could have been the main PAH removal process from this system.

2.9.3.3 Biosorption

Different biomass types have been used in both industrial and environmental applications; in biofuel production and the manufacture of renewable adsorbents for contaminants amongst others. Biomass have several attributes that makes them ideal in remediation approaches which include availability, low cost, high contaminant removal efficiency and environmental friendliness (Demirbaş, 2001; Opeolu *et al*., 2011). Agricultural wastes are such biomass, which contains hemicellulose, lignin, extractives, lipids, proteins, simple sugars, hydrocarbon forms, and starch [with functional groups that facilitate adsorption] (Dordio & Carvalho, 2013). Lignin in agricultural biomass is thought to be a major component that adsorbs organic pollutants like PAHs (Ho *et al*., 2005).

The non-polar nature of PAHs, limits their bioavailability and biodegradation rates which makes them subject to biosorption (adsorption by biomass), previously described by Chen *et al*. (2011) as being amongst the most economical and effective techniques for removing organic pollutants at low concentrations. Biosorption is defined as a physico-chemical process for sorbing chemicals in/on biological matrices/surfaces (Chen *et al*., 2010). Biosorption avoids the generation of toxic sludge and can be used under a broad range of operating conditions such as pH, adsorbate concentration and temperature, amongst others (Wang & Qin, 2005). Biosorption studies have

been performed on heavy metals, dyes, pesticides and on other organic pollutants (Aksu, 2005; Garg *et al*., 2007; Opeolu *et al*., 2011).

Biosorption approaches have also been integrated with other remediation approaches to effectively remediate impacted media, such as in biomass recycling of effluent during soil washing (Li *et al*., 2014) and in the inoculation of biomass with microorganisms to enhance contaminant biodegradation (Xiong *et al*., 2017). Some biosorption approaches for PAHs remediation are presented in Table 2.12.

Plant residues (dead biomass generally from crops) have also attracted research interest for their biosorption application as it has been shown that they have high sorption affinity for POPs and are easy to modify (Chen *et al*., 2011). Plant residues are often preferred over living biomass, because they are not affected by toxic wastes, do not require nutrients, and can often be regenerated and reused for many treatment cycles. Dead biomass may also be used or stored for extended periods at room temperature without putrefaction occurring (Aksu, 2005). Plant residues, wood chips, ryegrass root, orange peels, bamboo leaves and pine needles were studied by Chen *et al*. (2011) for their capacity to adsorb PAHs in batch biosorption experiments. Phenanthrene sorption coefficients reported, ranged from 2484 to 5306 L/kg and the lowest was for wood chips, which has low vibration band intensity for lignin and high sugar content (60.6%). The results showed that plant residues with high lignin content have enormous potential for removing PAHs and suggested that lowering the polar components (mainly sugar) of plant derived biosorbents could enhance sorption capability. Modified pine bark (through acid hydrolysis) with increased lignin content has also been reported to display enhanced phenanthrene-sorption (from 62.91% to up to 91.16% PAH-removal) compared to the raw pine bark that has low lignin content (Li *et al*., 2010b). Lignin was assumed to be the main sorption medium in pine bark for organic pollutants due to its hydrophobic nature.

Biomass from grape have also been studied for their adsorption potential; grape peel for dye-sorption (Saeed *et al*., 2010) and grape waste from wine production for Cr (VI)-sorption (Chand *et al*., 2009). Chand *et al*. (2009) reported that Cr (VI) was selectively adsorbed over other metal ions tested by cross-linked grape waste gel. The adsorption of Cr (VI) was highly dependent on pH, with maximum adsorption (1.91 mol/Kg) at pH 4.These studies established the potential of grape waste as an effective adsorbent. Saeed *et al*. (2010) reported the sorption of crystal violet dye by grape fruit peel. The studies demonstrated that grape fruit peel could be used as a cost-effective adsorbent for the removal of crystal violet dye from aqueous solution. Crystal violet removal was reported to be dependent upon process parameters such as pH, sorbate and sorbent

concentration, and contact time as shown by batch adsorption studies. The adsorption of diuron (3-(3,4-dichlorophenyl)-1,1-dimethylurea) an organic herbicide from water onto chemically activated carbons produced from grape seeds has also been studied (Al-Bahri *et al*., 2012). They reported that, the best adsorbent produced, had a surface area and mesopore volume of 1139 m^2/g and 0.24 cm^3/g respectively. The uptake of diuron by the adsorbent was time dependent and it was reported that most uptake occurred in the first 8 h. The quantity adsorbed at 8 h, initial diuron concentration (C_0) of 65.7 µmol/L, adsorbent dosage of 50 mg was 61.2 µmol/g at 25^{o}C. Varied temperatures [15 to 45^{o}C at initial diuron concentration of 65.7 µmol/L] and initial concentrations (24.2 to 141.7 µmol/g at 25^{o}C) led to increase in amount of diuron adsorbed, from 59.3 to 63.5 µmol/g and 20.5 to 129.1 µmol/g respectively. They concluded that waste agricultural biomass from grape can serve as a precursor for adsorbents that could be favourably applied for the adsorption of organic contaminants from aqueous solutions. High removal efficiencies (88 - 95%) were reported by Fagbayigbo *et al*. (2017) for the removal of perfluorooctane sulfonate (PFOS) and perfluorooctanoic acid (PFOA) from aqueous solution onto activated carbons produced from grape leaf litter. They also reported maximum adsorption capacity of 75.13 and 78.90 mg/g for PFOS and PFOA respectively.

Table 2.12: Biosorption approaches for PAHs remediation

PAHs	PAH-Matrix	Biomass	Biomass modification	Carbon content (C) and surface area (SA) of Adsorbent		Percentage removal	Reference
16 US EPA PAHs	Contaminated soil	Dried willow (DW) (*Salix viminalis*) and wheat straw (WS)	Pyrolysed at 600 – 700^{o}C	C were 52.20% and 53.87%, while BET SA were 5.3 m^2/g and 26.3 m^2/g for biochars from dried willow and wheat straw respectively.		Biochars reduction of bioaccessible PAHs in soil were 29.3% and 38.0% for DW and WS biochars respectively.	Oleszczuk *et al*. (2017)
16 US EPA PAHs	Polluted soil	Sawdust and wheat straw	Pyrolysed at 300^{o}C and 500^{o}C	**Biochar at 300^{o}C**	**Biochar at 500^{o}C**	Wheat straw biochar gave relatively higher efficiency and the one produced at 500^{o}C enhanced the degradation of 3-,4-,5- and 6-ringed PAHs by 69.95%, 45.96%, 37.92% and 30.66% respectively.	Kong *et al*. (2018)
				C: 51.59% and 63.94% BET SA: 4.78 m^2/g and 5.96 m^2/g for biochars from sawdust and wheat straw respectively.	C: 81.29% and 88.10%. BET SA: 28.46 m^2/g and 33.46 m^2/g for biochars from sawdust and wheat straw respectively.		
Pyr and **BaP**	Simulated wastewater	*Enteromorpha prolifera*	Pyrolysed at temperature range of 200 to 600^{o}C, 20g each was then activated with mixture of 1M HCl (180 mL) and conc. HF (20 mL)	**Biochar at 500^{o}C**	**Activated biochar at 500^{o}C**	Biochar produced at 500^{o}C gave the highest efficiency with 59.8% and 48.1% removal of Pyr and BaP respectively. Higher removal was achieved with the biochar after acid treatment with 92.5% and 85.2% Pyr and BaP removal respectively.	Qiao *et al*. (2018)
				C: 22.81% BET SA: 7.33 m^2/g	C: 38.27% BET SA: 205.32 m^2/g		
BaA, BbF, BkF, BaP and DBA	Water	Coconut waste (CW) and Orange waste (OW)	Pyrolysed at 350^{o}C to give biochars (BCW and BOW	**Raw (CW & OW)**	**Biochar (BCW & BOW)**	PAHs adsorption capacity of adsorbents were in the ranges of 34 to 87%(CW), 23 to 64% (OW), 41 to 86% (BCW) and 23 to 88% (BOW). No significant difference in PAHs adsorption by raw CW and the resulting biochar.	de Jesus *et al*. (2017)
				C: 43.31% and 40.52% BET SA: 118.612 m^2/g and 109.971 m^2/g	C: 61.04% and 59.98% BET SA: 233.869 m^2/g and 261.233 m^2/g		

PAHs	PAH-Matrix	Biomass	Biomass modification	Carbon content (C) and surface area (SA) of Adsorbent		Percentage removal	Reference
				Pyrolysed biomass	**Activated biochar**		
Phe	Aqueous solution	Debarked loblolly pine (*Pinus taeda*)	Pyrolysed at different temperatures (300,350,500 and 700^{o}C), then activated with NaOH i.e. 3g of pyrolysed biomass was treated with 40 mL of 4 M NaOH.	C obtained were 23.6, 56.3, 79.4 and 87.1%, while BET SA were 1.41,7.37,239 and 321 m^2/g for biochars obtained at 300, 350,500 and 700^{o}C respectively. (Raw biomass: 11.0% C and 0.38 m^2/g BET)	C obtained were 79.7, 77.4, 86.5 and 83.8%, while BET SA were 1250, 702, 346 and 57.0 m^2/g for activated carbon obtained from biochar produced at 300, 350,500 and 700^{o}C respectively.	Activation of biochars with NaOH greatly enhanced their PAH sorption ability, especially those obtained from low temperature pyrolysis (300 and 350^{o}C), with that obtained at 300^{o}C exhibiting good initial sorption efficiency (156 mg/g) after 30 min and higher adsorbed PAH concentration at equilibrium, while that produced at 700^{o}C binds the PAH more strongly.	Park *et al.* (2013)

Pyr: Pyrene. Bap: Benzo[a]pyrene. Phe: Phenanthrene. BaA: Benzo[a]anthracene. BbF: Benzo[b]fluoranthene. BkF: Benzo[k]fluoranthene. DBA: Dibenzo[a, h]anthracene.

Application of pyrolytically modified biomass (biochar) with improved biosorption efficiency in remediation approaches have been widely successful (Li *et al*., 2014; Xiong *et al*., 2017). Biochars are produced through carbonisation, a thermochemical process, called slow pyrolysis which converts biomass into solid char. This solid char is a residue with higher fixed carbon that results from the cracking of the weakest oxygenated bonds in the biomass. Char, pyrolysis vapours and gases are the main products of carbonisation. This process is carried out in an inert atmosphere (Peláez-Samaniego *et al*., 2008; Ioannidou & Zabaniotou, 2007). Pyrolysis of biomass can be classified as a heterogeneous chemical reaction. The reaction involves the breakage and redistribution of chemical bonds, changing reaction geometry and the interfacial diffusion of reactants and products (White *et al*., 2011). The solid char (biochar) shows different properties than the parent biomass materials. The remarkable differences are mainly in porosity, surface area, pore structure (micropores and macropores) and physicochemical properties such as composition, elemental constituent and ash content. Also, the biochar has variable charges and functional groups which enhances its adsorption and cation exchange capacity (Anawar *et al*., 2015). This is as a result of thermal treatment, which removes the moisture and the volatile matter content of biomass (Ioannidou & Zabaniotou, 2007).

Li *et al*. (2014) produced biochars from wheat straw through pyrolysis at 400^{o}C, 600^{o}C and 800^{o}C, which were utilised to selectively adsorb PAHs from soil washing effluents. The produced biochars were characterised and it was reported that the characteristics were highly dependent on pyrolytic temperature. Biochar carbon content increased with pyrolytic temperature, while oxygen, hydrogen and sulphur contents decreased. Hence, biochar produced at elevated temperature exhibited high aromaticity. The biochar surface area and total pore volume also increased with increase in pyrolytic temperature, whereas the pore width decreased. The biochar produced at 800^{o}C yielded the highest PAH removal efficiency (95.8 – 98.6%), followed by the biochar produced at 600^{o}C (82.4 – 93.4%) and lastly the biochar produced at 400^{o}C (71.8 – 88.1%). Hydrogen bonding, hydrophobic and π – π interaction; electrostatic attraction/repulsion and micropore filling were the mechanisms highlighted to be responsible for biochar-organic pollutant interactions.

Xiong *et al.* (2017) inoculated biochar produced from rice straw with PAH-degrading *Mycobacterium gilvum* for enhanced PAH-biodegradation. Biochars were also produced from sewage sludge and pig manure (all pyrolysed at 500^{o}C under limited oxygen atmosphere). Results showed that the biochar from plant origin (rice straw) showed the largest specific surface area (68.1 m^2/g), pore volume (0.17 cm^3/g) and surface basic groups (0.172 mmol/g), and was selected

as the inoculum immobiliser/carrier for the batch biodegradation study. The biochar-microbe composite was reported to show superior phenanthrene, fluoranthene and pyrene degradation in historically contaminated soil with degradation improvement of 15.5% for phenanthrene, 45.55% for fluoranthene and 42.6% for pyrene relative to *M. gilvum* cells alone after 18 days incubation. This was attributed to biochar improved PAHs mass transfer from the soil to the biochar-composite, where subsequent PAHs degradation took place.

The capability of six biochars produced from varied materials (maize stover residues, pine wood, switchgrass, food waste, digested dairy manure and paper mill waste) in the stabilisation of sewage sludge to reduce freely dissolved PAHs (dominated by Phe (46%), Flu (19%) and Pyr 12%)) content was investigated by Oleszczuk *et al.* (2014). Biochars capability significantly increased with increases in biochar-dose from 2% to 5%. Biochar feedstock was also shown to play a significant role in biochar-organic pollutant affinity, with biochar having lower polarity index (O/C), being more effective in the reduction of PAHs. Biochar obtained from switchgrass gave the highest effectiveness in PAH reduction, while biochar from pinewood showed relatively large freely dissolved PAH reduction. However, the poorest PAH reduction was reported for biochar obtained from the nonplant origin (digested dairy manure). The obtained reduction of PAHs ranged from 17.4 to 58.0% while the reduction of freely dissolved PAHs ranged from 38.3 to 69.0%.

Biochar can also be converted into activated carbon through either chemical activation or physical activation (Mohan *et al*., 2006). Activated carbon is a crude form of graphite with random or amorphous structure, which is highly porous, exhibiting a broad range of pore sizes from visible cracks, crevices to slits of molecular dimensions (Mohan *et al*., 2006). Activated carbon is used extensively in industrial purification and chemical recovery operations. They are particularly advantageous because of their high internal surface area and active surface. In general, higher surface area results in higher adsorption capacity (Williams & Reed, 2006).

Chemical activation is a single step method for preparation of activated carbon in the presence of chemical agents. Physical activation involves carbonisation of carbonaceous materials followed by activation of the resulting char in the presence of activating agents such as CO_2 or steam. The chemical activation usually takes place at a temperature lower than that used in physical activation, therefore a higher carbon yield, as a result of lower burn-off and improvement in pore structure development due to chemical effects (Sudaryanto *et al*., 2006). Various dehydrating reagents and oxidants have been used for the activation of char from different biomass; H_3PO_4 for tobacco stems (Li *et al*., 2008) and KOH for cassava peels (Sudaryanto *et al*., 2006). Other reagents that have been used include zinc(II)chloride, ammonium salts, borates, calcium oxide,

ferric and ferrous compounds, nickel salts, hydrochloric acid, nitric acid and sulfuric acid (Mohan *et al*., 2006).

Gustafsson *et al*. (2017) reported the use of activated carbon from softwood kraft lignin in an *in-situ* remediation approach for PAHs impacted sediments. The PAH-sorption test conducted on softwood and hardwood kraft lignin showed that without chemical modifications, they are both poor sorbents. However, when the softwood lignin was activated by KOH (lignin: KOH, 1:3) and carbonised at 700^{o}C, the resultant activated carbon had sorption capability in water and contaminated sediments comparable to those of commercially available activated carbons. The amendment of the contaminated sediment to have 1% composition of activated carbon, resulted in 80% PAHs concentration reduction in pore water and reduced the bioavailability of larger PAHs by 54% on average in sediments. Up to 90% reduction in pore water desorption and bioavailability of contaminants in sediments was achieved. Furthermore, the high affinity of activated carbons for pollutants was shown by the study conducted by Oleszczuk *et al*. (2012). They investigated the utilisation of activated carbons and biochar in the amendment of sewage sludge in order to decrease pore water concentrations of PAHs. The polarity index (O/C) of the utilised adsorbents showed that activated carbons (O/C of 0.08 to 0.10) had fewer surface polar functional groups, hence higher aromaticity as compared to biochar (O/C of 0.19 to 1.12) and similar trend is true for adsorbents from plant origin as compared to other feedstocks. Carbon contents were observed to be higher in activated carbons (81.1 to 91.78%) compared to biochar (19.22 to 41.57%). Also from the study by Oleszczuk *et al*. (2012), activated carbons were reported to have exhibited higher influence on freely dissolved PAHs as compared to biochars. Addition of 5% dose of activated carbons to sewage sludge achieved up to 95% reduction in freely dissolved PAHs concentration, whereby biochars at 10% dose only achieved up to 57.7% reduction. Thus, chemical activation is effective in promoting sorption capabilities of biochars.

2.10 Adsorption remediation technology

A wide range of treatment technologies such as precipitation, coagulation-flocculation, sedimentation, flotation, filtration, membrane processes, electrochemical techniques, biological processes, chemical reactions, adsorption and ion exchange have been developed for the purification of wastewaters (Foo & Hameed, 2010; Munir *et al*., 2017; Sarasidis *et al*., 2017). Adsorption treatment technology is a surface phenomenon, it is efficient, promising and a broadly used essential approach in wastewater treatment processes, due to its simplicity, economic viability, technical feasibility and environmental friendliness (Foo & Hameed, 2010). Adsorption is the adhesion of atoms, ions, biomolecules or molecules of gas, liquid or dissolved solids to a surface via chemical and physical bonds. It involves separation of a substance or adsorbate from one phase, followed by its accumulation onto the surface of the adsorbent (Abdullah *et al*., 2009). The process creates a film on the surface of the adsorbent, when the adsorbate is transferred onto the surface of the adsorbent until equilibrium has been reached (Gökmen & Serpen, 2002).

The optimum removal efficiency of an adsorbent for a given adsorbate can be determined, which involves the investigation of a range of factors that may influence sorption. These include pH, contact time, weight of adsorbent, initial concentration of adsorbate, temperature, agitation speed and/or time, and particle size, amongst others.

2.10.1 Adsorption isotherm models

Adsorption equilibria information is the most important piece of information in understanding an adsorption process. No matter how many components are present in the system, the adsorption equilibria of pure components are the essential ingredient for the understanding of how much those components can be accommodated by a solid adsorbent (Hamdaoui & Naffrechoux, 2007). Adsorption isotherms are therefore used to describe the equilibrium of an adsorption process, which is the equilibrium relationship between the concentration in the fluid phase and concentration in the adsorbent particles at a given temperature (Gökmen & Serpen, 2002). In modelling adsorption data, more than one candidate model is often fitted to the experimental data with the aim of studying the closeness of experimental data to the theoretical (model) data obtained from known isotherm models with known background theories (Akpa & Unuabonah, 2011). The two commonly used isotherms are Langmuir and Freundlich, while others include Temkin, Dubinin-Radushkevich and Redlich-Peterson isotherm models (Qu *et al*., 2009; Dada *et al*., 2012).

2.10.1.1 Langmuir isotherm model

The Langmuir model has been described as the simplest theoretical model, valid for monolayer sorption onto a surface with a finite number of identical adsorption sites (Abdullah *et al*., 2009; Liu *et al*., 2010). The model gives a quantitative description of adsorbate-monolayer formation on the outer surface of an adsorbent, besides which no further adsorption takes place. The model therefore represents the distribution of adsorbates between the adsorbent and the liquid phase (Dada *et al*., 2012). The Langmuir model assumes the following:

1. That a fixed number of adsorbate molecules are adsorbed onto well-defined localised sites of the adsorbent;
2. That all adsorption sites have uniform energies;
3. That each site holds one adsorbate molecule;
4. That there is no transmigration of adsorbate in the plane of the adsorbent surface i.e. adsorbate molecules in neighbouring sites do not interact (Abdullah *et al*., 2009).

The nonlinear Langmuir isotherm is represented as follows:

$$\boldsymbol{q_e = \frac{QK_LC_e}{1+(a_LC_e)}} \qquad \textbf{Equation 2.1}$$

where q_e (mg/g) represents solid phase equilibrium concentration, C_e (mg/dm^3) represents liquid phase equilibrium concentration, Q an energy term which is equal to unity in most cases and K_L (dm^3/g) and a_L (dm^3/g) are the Langmuir constants (El Qada *et al*., 2006).

2.10.1.2 Freundlich isotherm model

The Freundlich model is an empirical equation usually employed to interpret non-ideal sorption on heterogenous surface as well as multilayer sorption or surfaces supporting sites of varied adsorptive energies (Qu *et al*., 2009; Liu *et al*., 2010; Abdullah *et al*., 2009). The model assumes that the stronger binding sites are preferentially occupied and that binding strength decreases with increasing degree in site occupation (Qu *et al*., 2009). Also, that the adsorption sites are non-identical and are not always available (El Qada *et al*., 2006). the model is characterised by the heterogeneity factor '*1/n*' mathematically (El Qada *et al*., 2006).

The nonlinear Freundlich isotherm is represented as follows:

$$\boldsymbol{q_e = K_F C_e^{\frac{1}{n}}} \qquad \textbf{Equation 2.2}$$

where q_e (mg/g) is the amount of solute adsorbed, C_e (mg/dm^3) is solute concentration in equilibrium solution, K_F ((mg/g)/(dm^3/g)^n) is Freundlich isotherm constant and *n* is the heterogeneity factor. The K_F value relates adsorption capacity and 1/*n* is the constant that relates to adsorption intensity (El Qada *et al*., 2006).

2.10.1.3 Temkin isotherm model

Temkin isotherm model contains a factor that explicitly takes into account the adsorbent-adsorbate interaction (Qu *et al*., 2009; Foo & Hameed, 2010). The model assumes that the decrease in the heat of sorption of all molecules in the layer is linear rather than logarithmic with coverage due to adsorbent-adsorbate interaction (Qu *et al*., 2009; Foo & Hameed, 2010). Extremely low and high concentration values are ignored in the model and its derivation is characterised by a uniform distribution of binding energies (Foo & Hameed, 2010).

The nonlinear Temkin isotherm model is represented as follows:

$$\boldsymbol{q_e = \frac{RT}{b_T}\, ln(K_T C_e)} \qquad \textbf{Equation 2.3}$$

where q_e is the amount of solute adsorbed, K_T represent Temkin isotherm equilibrium binding constant (L/g), C_e is solute concentration in equilibrium solution, b_T is the Temkin isotherm constant, R is the universal gas constant (8.314 J/mol K), T is the absolute temperature (K) and $RT/b_T = B$ (J/mol), which is the Temkin constant related to heat of sorption (Qu *et al*., 2009).

2.10.1.4 Dubinin-Radushkevich model

The Dubinin-Radushkevich model is an empirical equation developed originally to describe the adsorption pathway of subcritical vapours onto microporous solids such as activated carbons and zeolites (Nguyen & Do, 2001). It is however, applicable in describing the sorption nature of the sorbate onto sorbent heterogenous surface and in examining the characteristics, the mean free energy and the porosity of adsorbents (Akar *et al*., 2010). The model has been successfully applied to distinguish between the physical and chemical adsorption of solutes, having the mean free energy per adsorbate molecule (E) expressed as follows:

$$\boldsymbol{E = \left[\frac{1}{\sqrt{2B_{DR}}}\right]} \qquad \textbf{Equation 2.4}$$

where B_{DR} is the Dubinin-Radushkevich isotherm constant (Foo & Hameed, 2010).

2.10.1.5 Redlich-Peterson model

The Redlich-Peterson Model is a hybrid isotherm usually employed as a compromise between Langmuir and Freundlich isotherms, and the model incorporates three parameters into an empirical expression (Foo & Hameed, 2010). The model has the advantageous significance of both Langmuir and Freundlich models, making it versatile and applicable in either homogeneous or heterogeneous systems (Qu *et al*., 2009; Foo & Hameed, 2010).

The Redlich-Peterson model is represented as follows:

$$q_e = \frac{K_{RP} C_e}{1 + (\propto C_e)^{\beta}} \qquad \textbf{Equation 2.5}$$

where K_{RP} (L/g) and $(\alpha C_e)^{\beta}$ are Redlich-Peterson isotherm constants and β ranges between 0 and 1 (Qu *et al*., 2009).

2.10.2 Adsorption kinetic models

Adsorption kinetic information is necessary for the design of sorption systems. Kinetic models help in investigating sorption mechanisms and the potential rate controlling steps like mass transfer and chemical reaction processes (Ho & McKay, 1998). While chemical kinetics explains the rate of chemical reactions and the factors affecting the reaction rate, measurement of sorption rate constants could evaluate the basic qualities of a good sorbent such as the contaminant removal efficiency of the sorbent. Pseudo-first order and Pseudo-second order models are the most commonly used models to explain adsorption kinetics (Abdullah *et al*. 2009). The Elovich model and Weber Morris intraparticle diffusion model have both been employed too (Wu *et al*., 2009).

2.10.2.1 Pseudo-first order model

The pseudo-first order model was first used to describe the kinetics of sorption onto solid surface in a liquid-solid phase system around 1898 by Lagergren, who studied the sorption of oxalic acid and malonic acid onto charcoal (Ho & McKay, 1998). This kinetic model has since been employed by numerous scientists to describe the sorption of different solutes onto solid surfaces: sorption of Cu (II) from aqueous solution onto fly ash (Panday *et al*., 1985); sorption of phenol, m-cresol, o-cresol and p-cresol from aqueous solution onto fly ash and impregnated fly ash (Singh & Rawat, 1994); sorption of tannic acid, humic acid and dyes (reactive red RR222 and methylene blue) from water onto activated clay (Chang & Juang, 2004). In first order mechanism, the film diffusion is an

important rate controlling-step and the initial rate of solute sorption can be characterised by mass transfer (Aksu, 2005).

The pseudo-first order equation is generally represented as follows:

$$\frac{dq_t}{dt} = k_1(q_e - q_t) \qquad \textbf{Equation 2.6}$$

where q_e and q_t are the sorption capacity (mg/g) at equilibrium and at time t (min) respectively and k_1 is the model sorption rate constant (1/min) (Abdullah *et al*., 2009).

Integrating the pseudo-first order rate expression above gives:

$$log(q_e - q_t) = logq_e - \frac{k_1}{2.303}t \qquad \textbf{Equation 2.7}$$

2.10.2.2 Pseudo-second Order Model

The pseudo-second order mathematical rate expression was first presented by Blanchard and co-workers in 1984, to predict the removal rate of heavy metals from water by means of natural zeolites (Plazinski *et al*., 2013). Blanchard and co-workers assumed that the metallic concentration varies very slightly during the first hours and that the kinetic order is two with respect to the number (n_0 - n) of available sites for the exchange of NH_4^+ ions fixed on zeolites by divalent metallic ions (M^{2+}) in solution, which they gave the differential and integrated equations respectively as follows:

$$-\frac{d_n}{d_t} = K(n_0 - n)^2 \qquad \textbf{Equation 2. 8}$$

$$\frac{1}{(n_0 - n)} - \alpha = Kt \qquad \textbf{Equation 2. 9}$$

Where n is the amount of M^{2+} removed/fixed or the amount of NH_4^+ released at each instant, n_0 is the exchange capacity and K is the rate constant (Blanchard *et al*., 1984; Ho, 2006).
In more recent time however, pseudo-second order rate expression based on adsorbent capacity has been presented for adsorption kinetics as follows:

$$\frac{dq_t}{dt} = k_2 (q_e - q)^2 \qquad \textbf{Equation 2.10}$$

Integrating the pseudo-second order rate expression above gives:

$$\frac{t}{q_t} = \frac{1}{(k_2 q_e)^2} + \frac{t}{q_e}$$ **Equation 2.11**

where k_2 (g/ (mg min)) = pseudo-second order model rate constant (Qu *et al*., 2009).

Experimental data obtained from adsorption experiments of PAHs onto activated carbons, have been reported to be well fitted by pseudo-second order kinetic model (Shi *et al*., 2013; Rad *et al*., 2014; Lamichhane *et al*., 2016). Shi *et al*. (2013) reported a correlation coefficient (R^2) of 0.9991 and adsorption rate of 31.95 mg/(g. min) at 0.08 g/L activated carbon dosage, when experimental data obtained from naphthalene adsorption onto high surface area activated carbon were fitted by pseudo-second order kinetic model.

2.10.2.3 Elovich Model

The Elovich model which describes chemical adsorption mechanism in nature, was originally presented in 1939 and has been reported to fit satisfactorily to a number of chemisorption processes, a wide array of slow adsorption rates and valid for adsorption on heterogenous surfaces (Wu *et al*., 2009; Aljeboree *et al*., 2017). The adsorption of metals, dyes, humic acid, phenols as well as PAHs onto varied adsorbents have been reported to follow Elovich kinetic model (Wu *et al*., 2009; Demirbas *et al*., 2004; Olu-owolabi *et al*., 2014; Lamichhane *et al*., 2016).

The Elovich model expression is represented as follows:

$$\frac{dq_t}{dt} = \alpha\, exp(-\beta q_t)$$ **Equation 2.12**

Where α and β are constants during an experiment.

α (mg/ (g. min)) = initial adsorption rate

β (g/mg) = Elovich desorption constant (Wu *et al*., 2009)

2.10.2.4 Weber Morris Intraparticle Diffusion Model

The Weber Morris intraparticle diffusion model was developed by Weber and Morris and can be utilised when intraparticle diffusion is involved in a sorption process, to establish the region where intraparticle diffusion is the rate-limiting step and also to determine the intraparticle diffusion rate in such system (Aksu, 2005). If a plot of quantity of solute sorbed versus the square root of the

contact time result in a linear relationship with the straight line passing through the origin, intraparticle diffusion is the rate limiting step in such sorption system (Weber & Morris, 1963).

The rate expression for intraparticle diffusion can be represented as follows:

$$q_t = f\left(\frac{Dt}{r_p^2}\right)^{1/2} = K\left(t^{1/2}\right) \qquad \textbf{Equation 2.13}$$

where r_p is the radius of adsorbing particle, D is the effective diffusivity of solute within the particle and K is the intraparticular diffusion rate (Aksu, 2005).

2.11 Diep River

The Diep River rises from the Riebeek-Kasteel Mountains and flows south-westerly through Malmesbury, Table View and Milnerton, to drain into Milnerton Lagoon. The river is about 65 km long and forms an extensive vlei (wetland) at the Table Bay coastline, known as Rietvlei, which is largely utilised for recreational activities. Hence, the tidal inlet at the Milnerton lagoon and the wetland system (Rietvlei) constitute the important features of the Diep River (Mafejane *et al*., 2002; Jackson *et al*., 2009).

The Diep River catchment has industrial areas, agricultural areas, formal and informal settlements and wastewater treatment works with a total area of 1495 km^2. The catchment is low and flat (making it ideal for crop cultivation) but has isolated mountains (the Perdeberg, Kasteelberg and Paarlberg mountains) on its eastern boundary. The Diep River catchment is bound by the following towns: Riebeek-West (to the north), Paarl (to the east), Atlantis (to the west) and Milnerton (to the south) (Mafejane *et al*., 2002).

The Messelbark River is the major tributary of the Diep River, while the Riebeek River, Klein River, Swart River, Platklip River and the Sout River are the others. The Diep River and its tributaries experience high water level in winter due to rainfall, but low water level and even dries up at certain locations in summer due to high evaporation regimes (Mafejane *et al*., 2002). Also, due to extensive siltation over the years as a result of catchment erosion, the Diep Rietvlei system serves as storage area of sediment-rich water during river floods and after the flood there is reduction in water level (Paulse *et al*. 2009).

2.12 Plankenburg River

The Plankenburg River rises from the mountains of the Boland region, Western Cape, South Africa. It is about 10 km long and flows through Stellenbosch (known for winery) and Kayamandi township (informal residence) (Jackson *et al*., 2009). The Plankenburg River is the major tributary of the Eerste River in the Stellenbosch area, with the Kromme and the Jonkershoek Rivers being the other tributaries of the Eerste River in this area. The Plankenburg River flows south-easterly and joins the Eerste River at the Adam Tas bridge, that ultimately opens into the ocean at Macassar beach. The Plankenburg River services various industrial and agricultural activities, which includes irrigation of edible crops. Some of the establishments on the Plankenburg River catchment includes: clothing factory, cheese factory, spray painting, mechanical workshops, wineries and dairy factories (Nleya, 2005; Paulse *et al*., 2009).

CHAPTER 3
METHODOLOGY

3.1 Method of analysis

3.1.1 Chemicals

The 16 US EPA PAHs (naphthalene, acenaphthylene, acenaphthene, fluorene, phenanthrene, anthracene, fluoranthene, pyrene, chrysene, benzo[a]anthracene, benzo[b]fluoranthene, benzo[k]fluoranthene, benzo[a]pyrene, dibenzo[a, h]anthracene, Benzo[g, h, i]perylene and Indeno[1,2,3-cd]pyrene) standards were purchased from Supelco, Bellefonte, PA, USA. Dichloromethane (DCM), n-hexane, other solvents and chemicals were obtained from Sigma-Aldrich (South Africa).

3.1.2 Method development on GC-FID

A SPE-GC-FID method was developed for the simultaneous determination of the 16 US EPA priority PAHs.

3.1.2.1 Standards and calibration solutions

Stock solutions (1000 µg/mL) of the 16 PAHs were prepared in dichloromethane by dissolving 0.01 g of each PAH with dichloromethane (DCM) in 10 mL standard flask. A working mixture (cocktail), containing each of the 16 PAHs at 1000 µg/mL was also prepared. The stock solutions were subsequently transferred into amber vials and kept refrigerated at 4^{o}C. Calibration standards (1 µg/mL, 2 µg/mL, 5 µg/mL, 10 µg/mL and 50 µg/mL) were serially prepared from the stock solution by diluting with appropriate volume of dichloromethane and stored at 4^{o}C prior to GC-FID analysis.

3.1.2.2 GC-FID instrumentation and analytical conditions

Chromatographic analysis was performed on Agilent 7890A GC-FID system equipped with an auto sampler and Agilent Chemstation software. An Agilent DB-EUPAH column (20 m x 0.18mm I.D) with 0.14 µm film thickness was utilised for the separation. The GC-FID parameters [injector temperature, injection type (split/splitless), oven temperature programming, carrier gas flow and detector temperature] were optimised for the simultaneous detection and quantification of the 16 US EPA priority PAHs in a cocktail. Nitrogen gas was used as carrier gas at a constant flow of 1.2591 mL/min. Split injection (3:1) was used with injection volume of 1 µl. Hydrogen (32 mL/min),

air (380 mL/min) and nitrogen (28 mL/min) were used as auxiliary gases for the flame ionisation detector. A summary of the GC-FID operating parameters utilised is presented in Table 3.1.

Table 3.1: Specifications and the operating conditions of the GC-FID

Parameters	Specification/Operating Condition
Instrument	Agilent 7890A GC-FID equipped with auto sampler
Column	DB-EUPAH column (20 m, 0.18mm I.D, 0.14 µm film thickness)
Injector temperature	250^{o}C
Injection volume	1 µL
Injection mode	Split (3:1)
Carrier gas	Nitrogen
Column flow rate	1.2591 mL/min.
Oven temperature programming	100^{o}C (1 min hold), ramped at 5^{o}C/min to 200^{o}C (1 min hold), ramped at 10^{o}C/min to 250^{o}C (5 min hold), ramped at 5^{o}C/min to 300^{o}C (3 min hold).
Detector temperature	320^{o}C

3.1.2.3 Analyte identification and calibration

After the GC-FID conditions have been optimised for the detection of 16 PAHs in a cocktail, each of the standard solutions of the 16 PAHs were individually injected for GC-FID analysis to determine its average retention time, as well as to identify each analyte. This was performed ten times for each standard solution. The identified average retention time for each analyte was subsequently used to set up a calibration method with the Chemstation software on the GC-FID with the calibration standards (1 µg/mL, 2 µg/mL, 5 µg/mL, 10 µg/mL and 50 µg/mL).

3.1.3 Extraction and SPE clean-up of PAHs from samples

The clean-up of PAHs in water, sediment and plant samples were carried out with C18 solid phase extraction tubes (Supelclean ENVI -18 SPE tubes 6mL), purchased from Supelco, Bellefonte, USA.

3.1.3.1 PAHs extraction and SPE clean-up from water samples

The extraction of PAHs from water samples were carried out with n-hexane in five extraction sequences (25, 20, 15, 10 and 10 mL) and utilised 250 mL of milli-Q water as matrix for the recovery procedure. Clean-up was done on SPE tubes that have been preconditioned with n-hexane and DCM (3 mL each of DCM, n-hexane and DCM/hexane (1:1) sequentially).

The extraction was carried out by placing 250 mL water sample into a precleaned 500-mL separating funnel, then the required volume of the extracting solvent was added, and the funnel corked. The content of the funnel was thoroughly mixed for 1 min, then allowed to stand for 2 h for the separation of the organic phase from the polar phase. The organic phase was then carefully collected, by first letting out the heavier polar phase from the funnel. The combined organic phase from 5 extractions was then cleaned up as described below.

3.1.3.2 PAHs extraction and SPE clean-up from sediment samples

Stones and sewage were carefully removed from air dried sediment samples, before they were sieved through a 250 µm aperture. Analytes from 2 g, of sieved sediment samples were extracted with n-hexane and DCM in three extraction sequences using ultrasonic agitation at 30^{o}C in a total time of 30 min i.e. extraction with 20 mL n-hexane for 20 min, extraction with 10 mL DCM/n-hexane (1:3) for 10 min and lastly with 10 mL n-hexane for 10 min.

The extraction was carried out by placing the prepared sediment sample (2 g) into 50-mL amber bottle. Thereafter, the extracting solvent was added, the bottle was then covered with aluminium foil and carefully swirled before placing it into the sonicator that had been allowed to reach the required temperature (30^{o}C), then sonicated for the required time for each extraction sequence. The extract was then carefully decanted into a clean amber bottle. The extracts from the three extraction sequences were combined and cleaned up as described below. Sediment cleaned with n-hexane and DCM by means of ultrasonic agitation, was used for the recovery study.

3.1.3.3 PAHs extraction and SPE clean-up from plant samples

Plant samples were washed with milli-Q water, air dried, milled and sieved through a 250 µm aperture, after which analytes from 2 g of plant samples were extracted with n-hexane and DCM in three extraction sequences as described for sediment samples. Plant cleaned with n-hexane and DCM by means of ultrasonic agitation, was used for the recovery procedure.

The clean-up of extracts from matrices were carried out using solid phase extraction (SPE) tubes, fitted onto a vacuum manifold with the vacuum regulated to give a flow rate of 4 - 5 mL/min. About 1 g Na_2SO_3 was placed in each tube to remove water residue in extracts. Extracts were then passed through preconditioned SPE tubes and 3 mL DCM was used to release any analytes trapped by the solid phase. The 3 mL DCM washing was repeated thrice. The resulting eluents were reduced to less than 1 mL by a rotary evaporator at 100 rpm and 30^{o}C water bath temperature. These were then placed in a 1 mL standard flask and made up to mark with DCM. The extracts were then transferred into amber vials and analysed using GC-FID. The extraction methods described above are based on the methods described by Manoli and Samara (1999), Zhou *et al*. (2000) and Chen *et al*. (2007).

3.1.4 Method validation

The optimised analytical method obtained from series of experimental runs, was validated by the established International Conference on Harmonisation (ICH) parameters such as linearity range, detection limit, quantification limit, precision, accuracy and recovery (ICH, 2005).

3.1.4.1 Linearity, detection limit and quantification limit

The linearity of method response to analyte's quantification was obtained from the plot of peak areas against calibration standards of analytes obtained through the Chemstation software (Appendix A), while the detection limits (DL) and quantification limits (QL) were obtained from the

standard deviation of the analyte's blank (s) and slope of the calibration curve (b) using the formulae below:

$$\boldsymbol{DL = \frac{3s}{b}}$$ **Equation 3.1**

$$\boldsymbol{QL = \frac{10s}{b}}$$ **Equation 3.2**

3.1.4.2 Precision

The precision of the GC-FID for simultaneous analysis of the 16 US EPA priority PAHs in DCM was evaluated from the relative standard deviation (RSD) of repeatability (within-run precision) and reproducibility (between-run precision) data, obtained from six runs. The repeatability was evaluated in one day, while reproducibility was evaluated over six days.

3.1.4.3 Accuracy

The accuracy of the method was evaluated by recovery of analytes (16 US EPA PAHs) from spiked matrices (mill-Q water, hexane/DCM cleaned plant and sediment samples), which was carried out in triplicate. Analytes from spiked matrices were extracted and cleaned up as described for each matrix, while unspiked matrices were utilised as blanks. Analytes recovered from spiked matrices were analysed through external standard calibration method as described by Zakeri-Milani *et al*. (2005) to validate the method.

3.2 Study area

This study focused on two rivers in the Western Cape, South Africa; the Diep and Plankenburg Rivers. They were selected for this study, because there are various anthropogenic activities such as industrial, domestic and agricultural activities along their banks that may contribute to PAH burden of both rivers. Also, due to the importance of the Diep River as a freshwater ecosystem in the Western Cape Province (having a natural wetland system and its utilisation for human activities and landuse practices). The anthropogenic source(s) contribution to PAH burden of these rivers were therefore investigated in 2015, over a 12-month period at seven identified sites to determine both the seasonal and spatial variations in PAHs concentrations.

3.2.1 The Diep River sites

Studies have shown that the Diep River, an important freshwater ecosystem (utilised for irrigation and recreation) in the Western Cape, South Africa have been impacted as a result of anthropogenic activities (Jackson *et al*., 2009; Shuping *et al*., 2011; Daso *et al*., 2016). Wastewater effluents from residential and industrial areas have been reported as priority point sources of contaminants to the Diep River (Paulse *et al*. 2009). The 16 US EPA priority PAHs from anthropogenic sources to this important freshwater ecosystem were therefore investigated. Description of the three sampling sites (DA, DB and DC) in the Diep River is presented in Table 3.2 and shown in Figure 3.1.

Table 3.2: Description of sampling sites of the Diep River

Site symbol	Site vicinity	Longitude	Latitude
DA	Nature reserve and boating club (Table Bay Nature Reserve)	-33.837625 S	18.519621 E
DB	Residential and industrial (Channel at Theo Marais sports club)	-33.859170 S	18.499011 E
DC	Residential and recreational (Milnerton Woodbridge)	-33.881853 S	18.489755 E

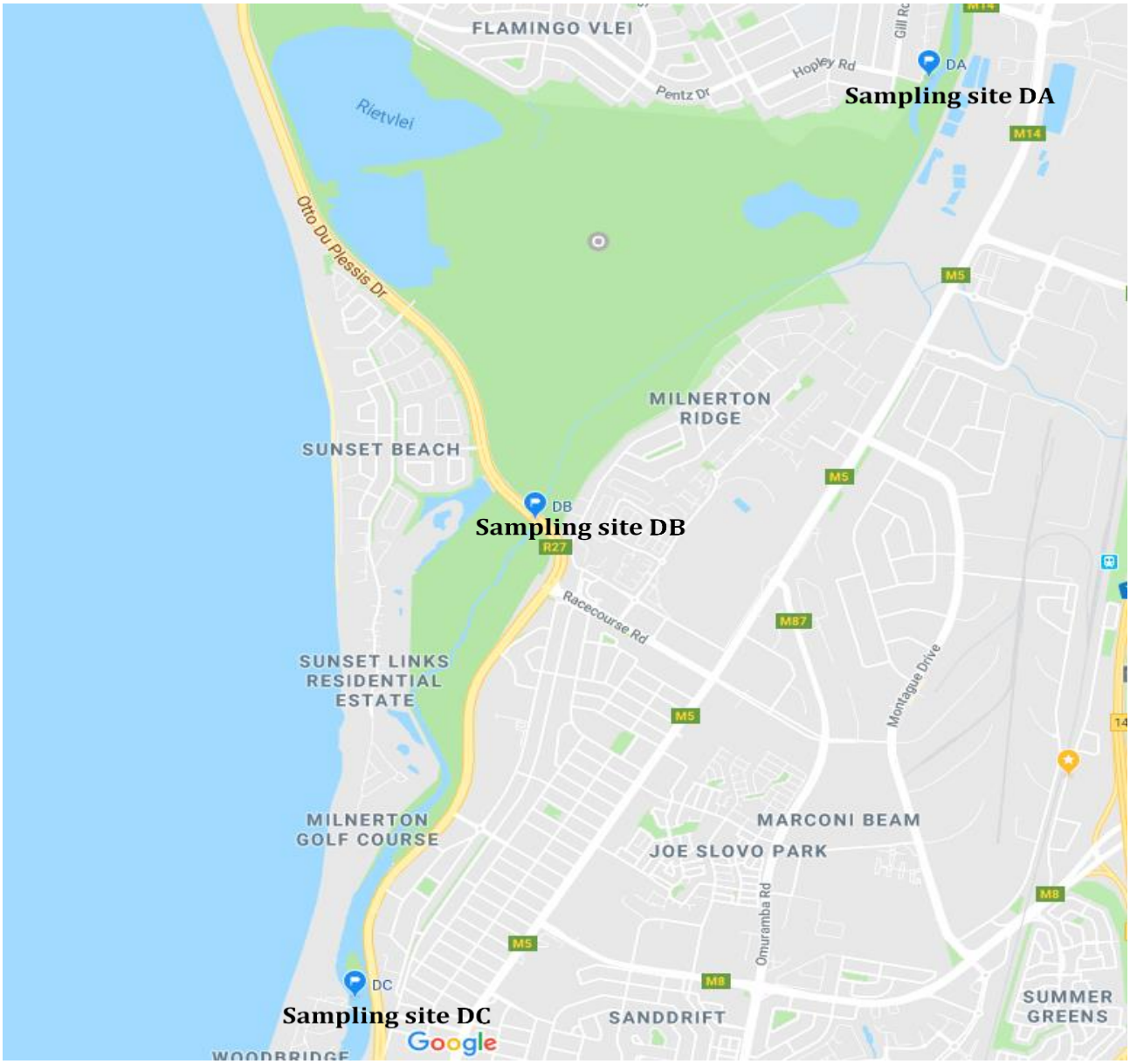

Figure 3.1: Map showing the sampling sites at the Diep River

3.2.2 The Plankenburg River sites

The Plankenburg River has been said to be heavily polluted as it receives sewage from Kayamandi, effluent from wineries and other industries and agricultural activities in its upper catchment (Nleya, 2005). Continuous monitoring of the impacts of these anthropogenic activities on the River is needed. This will enable pollution control and clean-up strategies of this important freshwater ecosystem. Four sampling sites were therefore identified in the Plankenburg River for this study. The sites PA, PB, PC and PD are described in Table 3.3 and presented in Figure 3.2.

Table 3.3: Description of sampling sites of the Plankenburg River

Site symbol	Site vicinity	Longitude	Latitude
PA	Agricultural and residential	-33.906662 S	18.8463319 E
PB	Informal settlement of Kayamandi	-33.919695 S	18.852591 E
PC	Industrial area	-33.925036 S	18.851910 E
PD	Industrial area of Adam Tas bridge	-33.930769 S	18.851696 E

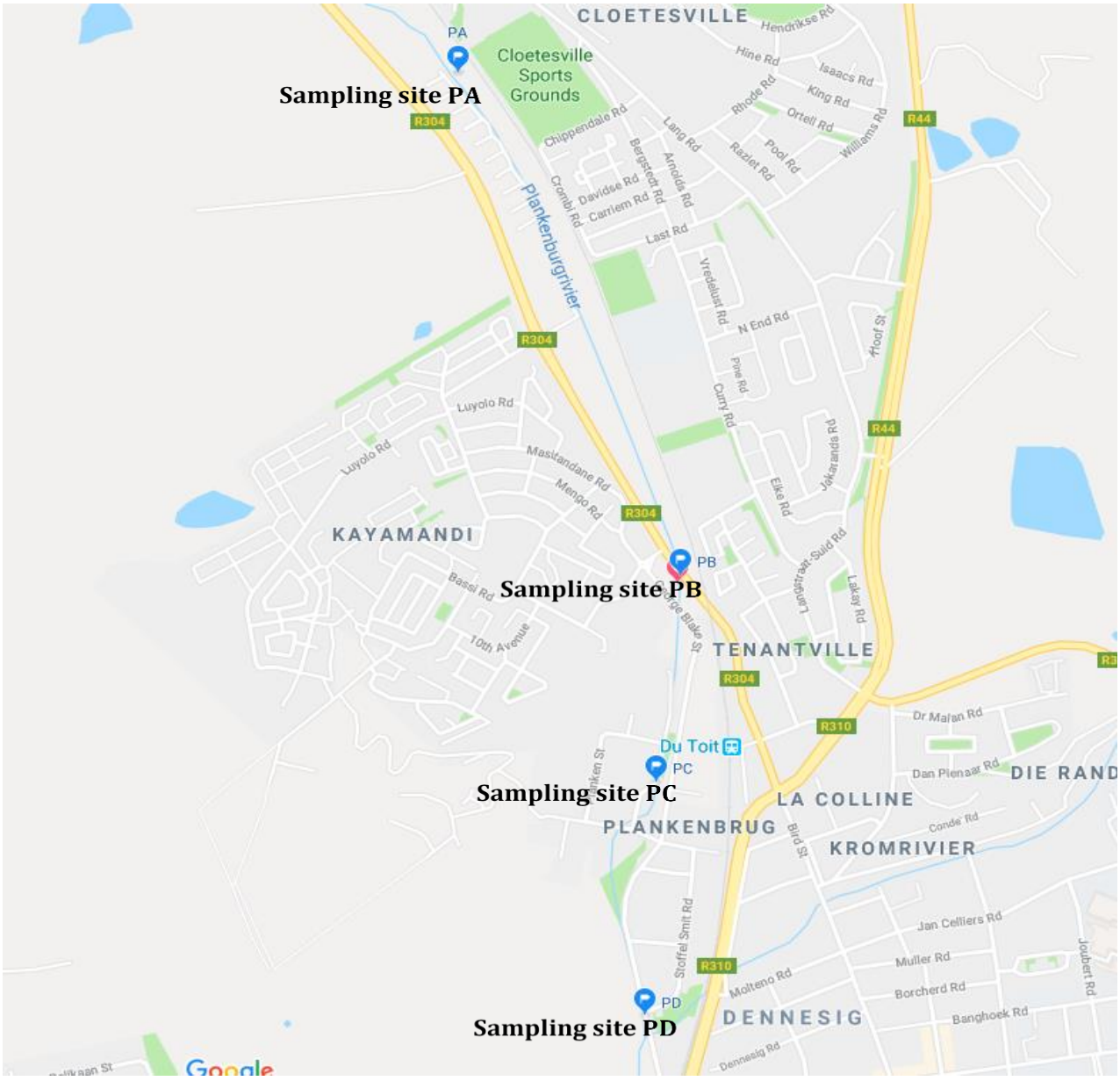

Figure 3.2: Map showing the sampling sites at the Plankenburg River

3.3 Sampling and sample pre-treatment

Surface water, sediment and plant samples were collected from selected sites for this study. The choice of sampling bottles, sample preservation method, holding time and analytical method were carried out based on established procedures (Hildebrandt *et al*., 2006). All sampling tools were washed with phosphate-free detergent (contrad concentrate) and rinsed with tap water. The tools were subsequently soaked in 0.1 M HNO_3 for 24 h, rinsed in milli-Q water and again soaked in acetone for 30 min, rinsed with DCM and dried. Amber bottles with Teflon-lined lids were utilised for water sampling.

3.3.1 Sampling and pre-treatment of water

Water samples in triplicate were collected once a month, consistently for a year at the selected sites. The sampling regime was grouped into summer (Jan, Feb and Dec), autumn (March, April and May), winter (June, July and August) and spring (Sept, Oct and Nov). Water samples were collected in pre-cleaned 500 mL amber bottles in triplicates at each site, by carefully lowering the containers below the water surface and 1 mL of 100 mg/L NaN_3 added to inhibit bacteria growth during transportation. Samples were stored on ice at 4^{o}C and transported to the laboratory for subsequent analyses. Water samples were analysed from each triplicate sample bottle, to obtain triplicate analyses. The extraction, clean-up and GC-FID analyses were done within 24 h of sample collection. Physicochemical parameters [temperature, pH, total dissolved solids (TDS), salinity and conductivity] of water samples were determined on site using a PCS teslr 35 handheld multi-parameter gauge.

3.3.2 Sampling and pre-treatment of sediment

Surface sediment samples were collected once a month, consistently over a one-year period at the seven sites, covering summer (Jan, Feb and Dec), autumn (March, April and May), winter (June, July and August) and spring (Sept, Oct and Nov). Sampling of sediments was done after water sampling to avoid perturbation and resuspension of the sediment system into the water phase. Sediment samples were collected with the use of a stainless-steel grab sampler and the top 1 cm surface layer was carefully removed with a stainless-steel spoon. Five representatives of the 1 cm top sediment layer samples were collected at each point to obtain a composite sediment sample. The samples were wrapped in aluminium foil pre-treated with DCM and then transported to the laboratory in an ice chest at 4^{o}C (Guo *et al*., 2007). Samples were air dried prior

to further analysis. The nature of sediments at each site was investigated through the determination of fractional organic carbon, organic matter and particulate matter of sediment.

3.3.3 Sampling and pre-treatment of plant samples

The plant samples obtained at the Diep River were from the species of *Eichhornia crassipes* (water hyacinth) [at sites DA and DC] and *Phragmites australis* (common reed) [site DB]. At the Plankenburg River the plant used for biomonitoring was *Phragmites australis* (common reed). The choice of plant species obtained was based on plant prevalence at each sampling point. Photographs taken from sampling sites are presented in Appendix B. Representative plant samples were collected by complete uprooting/scooping; samples were wrapped in aluminium foil and transported to the laboratory in an ice chest at 4^{o}C. The represntive *P. australis* samples were pooled into roots, stems and leaves, after rising thoroughly with milli-Q water, while the representative *E. crassipes* samples were kept as a whole and rinsed (Wang *et al*., 2012b). Samples were air dried prior to further analysis. Plant samples assessed for possible PAH bioaccumulation were collected in August towards the end of the sampling regime.

3.4 Quality assurance and quality control steps

The following quality assurance steps were followed, to ensure high quality of data were obtained and used in this study:

1. Analytical grade reagents and milli-Q water were utilised, to prevent contamination of the analytical procedure from external contributions.
2. Procedural blanks were included in each batch of analysis to determine and correct any external contribution.
3. Samples were analysed in triplicates and standard deviation calculated to ascertain the reproducibility of analytical procedures.
4. Water samples were collected into amber glass bottles, covered with Teflon-lined lids and strict adherence to sampling procedure, handling and preservation steps were observed according to standard procedures.
5. Precision, accuracy, linearity, sensitivity and method recovery were determined to validate the analytical methods utilised.
6. Spiked water, sediment and plant samples were processed to determine percentage recoveries.
7. Instruments were calibrated prior to use as required and ensured no drift in instrumental readings.

3.5 Analysis of grape leaf litter

Dried grape leaf litter, an agricultural waste was collected by hand at a vineyard in Stellenbosch, Western Cape, South Africa, into a precleaned sack. It was transported to the laboratory and stored in a cool dry place until further processing.

The suitability of grape leaf litter as precursor for activated carbons was assessed by the determination of moisture, ash and crude fibre contents and elemental composition.

3.5.1 Determination of moisture content

About 5 g sample of pulverised grape leaf litter was placed into a clean and dry ceramic crucible and dried at 105^{o}C for 3 h in an oven. The crucible was then removed from the oven and placed in the desiccator to cool and its weight was determined. The sample was then further dried at 105^{o}C, the mass checked at 30 min intervals until a constant mass was obtained (Association of Official Analytical Chemists (AOAC), 1990). The experiment was carried out in triplicate. Moisture content was calculated using Equation 3.3.

$$\% \textit{ Moisture} = \frac{W_0 - W_1}{W_0} \; x \; 100\% \qquad \textbf{Equation 3.3}$$

W_1 = mass of the grape leaf litter at constant weight

W_0 = Initial weight of grape leaf litter before drying at 105^{o}C.

3.5.2 Determination of ash content

Grape leaf litter sample (2 g) of dried grape leaf litter was weighed into a clean, dry crucible and placed into a furnace at 550^{o}C for 2 h. After the 2 h, the furnace was switched off and allowed to cool to 200^{o}C, before the crucible and its contents were removed and placed in a desiccator for complete cooling. The mass of the resulting ash was then determined (Maynard, 1970). Ash content was calculated using Equation 3.4.

$$\% \textit{ Ash content} = \frac{W_1}{W_0} \; x \; 100\% \qquad \textbf{Equation 3.4}$$

W_1 = mass of ash

W_0 = initial mass of dried grape leaf litter.

3.5.3 Crude fibre content determination

Approximately 1 g of pulverised grape leaf litter was weighed into a 500-mL quick fit round bottom flask and 150 mL hot 0.128 M H_2SO_4 was added to the sample. In order to prevent foaming, n-octanol (two to four drops) was also added to the mixture in the flask. It was refluxed for 30 min at 98^{o}C. The refluxed mixture was then filtered hot under vacuum and washed thrice with hot milli-Q water using 30 mL each time and sucked dry. This was then transferred into the 500-mL flask and hot 150 mL 0.223 M KOH was added with a further addition of two to four drops of n-octanol and refluxed for another 30 min at 98^{o}C. It was then filtered hot under vacuum and washed with 30 mL hot deionised water thrice, then sucked dry under vacuum. The sample was then washed thrice using 25 mL acetone and filtered under vacuum each time, after which it was dried at 130^{o}C in an oven until a constant weight was obtained (AOAC, 1990). The resulting residue was ashed at 50^{o}C for 2 h in a furnace and the weight of the resulting ash determined. The crude fibre was calculated using Equation 3.5.

$$\textit{\% Crude fibre} = \frac{W'_2 - W'_3}{W'_1} X100\% \qquad \textbf{Equation 3.5}$$

W'_1 = Initial weight of grape leaf litter

W'_2 = weight of residue before ashing

W'_3 = weight of ash.

3.5.4 Elemental analysis

The elemental composition of the raw milled biomass was obtained through Energy-dispersive X-ray spectroscopy (EDS). The EDS protocol which is carried out in tandem with the SEM imaging, rapidly determined elemental contents of biomass except for elements such as hydrogen, helium, lithium and beryllium that are light in weight at an energy of 25 kV. The biomass is coated with gold prior to elemental analysis by EDS, because the protocol is carried out under high energy (Darmawan *et al*., 2016).

3.6 Production and characterisation of activated carbons

Activated carbons were produced from grape leaf litter using H_3PO_4 and $ZnCl_2$ as the activating agents.

3.6.1 Adsorbent preparation

The leaf litter was milled and sieved with a standard mesh to obtain a particle size of ≤ 25 mesh (≤ 707 microns). The sieved milled leaf litter was then impregnated with the activating agent at 5:2, 5:1 and 10:1 biomass to activating agent ratios, respectively. The slurry after impregnation was sonicated at 50^{o}C for 3 h before drying at 110^{o}C overnight. 20 g of the impregnated biomass was then carbonised at 600^{o}C for 1 h and N_2 flow of 150 mL/min. The furnace was then switched off and allowed to cool to 200^{o}C with the nitrogen gas still flowing. The gas supply was cut off at 200^{o}C, the produced activated carbon was obtained and placed in a desiccator to cool. The charred biomass was subsequently weighed and percentage yield and burn off calculated. The carbonised biomass was washed with hot 1 M HCl, followed by milli-Q water until all acid was removed, then dried at 50^{o}C for 5 h. The carbonisation method was based on that reported by Sudaryanto *et al*. (2006). The % yield, burn off and attrition were calculated using Equations 3.6 to 3.8.

$$\textit{\% Yield} = \frac{M_1}{M_2}\ x\ 100\% \qquad \textbf{Equation 3.6}$$

$$\textit{\% burn off = (100 - \% yield)} \qquad \textbf{Equation 3.7}$$

M_1 = mass of charred biomass

M_2 = mass of uncharred biomass

The % attrition was calculated using the equation below:

$$\textit{\% Attrition} = \frac{A-B}{A}\ x\ 100\% \qquad \textbf{Equation 3.8}$$

A = Initial weight of charred biomass before washing with hot 1 M HCl and milli-Q water.

B = Final weight of Charred biomass after washing with hot 1 M HCl and milli-Q water.

3.6.2 Adsorbent characterisation

3.6.2.1 Fourier transform infrared (FTIR) spectrometry

The FTIR spectra of the produced activated carbons and raw grape leaf litter (recorded over 4000 - 400 cm^{-1} range) were obtained on a Universal Attenuated Total Reflectance (UATR) Infrared spectrometer Perkin Elmer Spectrum 2 (UK). The crystal area of the instrument was cleaned prior to analysis and background correction made. The samples were placed directly on the crystal area of the universal diamond attenuated total reflectance (ATR) top-plate. The pressure arm was positioned over the crystal-sample area, then locked into a precise position above the diamond crystal and force applied to the sample, pushing it onto the diamond surface. The sample was then scanned to obtain the spectrum.

3.6.2.2 Scanning electron microscopic analysis (SEM)

The surface morphologies of prepared adsorbents were obtained, using scanning electron microscope (Nova Nano SEM 230, USA). A gold sputtering device (JOEL, JFC-1600) was utilised in coating samples with a fine layer of gold for clarity in obtained surface morphology. The elemental contents of activated carbons were also obtained by EDS (Darmawan *et al*., 2016).

3.6.2.3 Brunauer-Emmett-Teller (BET)

An Automatic Adsorption Instrument (Quanta chrome Corp. Nova-1000 g gas sorption, USA) was utilised in obtaining the textural properties of the produced activated carbons. The BET surface area, total pore volume, micropore area, micropore volume and pore size were obtained. Degassing of samples was carried out at 170^{o}C for 13 h, before the adsorption and desorption of liquid N_2 at 77 K. MicroActive 4.00 software (TriStar II 3020 version 2.00) was utilised to generate the BET surface area and the BJH (Barrett, Joyner and Helenda) pore distribution of the activated carbons.

3.7 Adsorption studies

Adsorption studies were carried out using phenanthrene as the adsorbate. Phenanthrene is one of the most abundant PAHs and an acceptable representative of semi volatile organic compounds (Rad *et al*., 2014; Gupta, 2015). Activated carbons produced from grape leaf litter were used as adsorbents for phenanthrene removal from aqueous solution in batch experiments. Parameters such as contact time, adsorbent load, pH and initial concentration were investigated to establish

the optimum values for adsorbents efficiencies. The obtained data was fitted into adsorption kinetic models and isotherms to evaluate the quality of produced adsorbents and to describe the mechanism of the sorption process.

3.7.1 Optimisation of parameters

Effect of parameters (pH, adsorbent dosage, initial concentration and contact time) on the adsorption of phenanthrene on activated carbons were investigated in batch experiments carried out in triplicates. Due to the poor solubility of phenanthrene in water, milli-Q water containing 30% acetonitrile was utilised for this study.

3.7.1.1 Effect of pH on the adsorption of phenanthrene

To investigate the effect of pH, 25 mL of 1 mg/L adsorbate solutions with varying pH values (3 - 12) and 0.1 g activated carbon was utilised. The desired pH of the 0.1 mg/L phenanthrene solution was prepared from 10 mg/L solution with the addition of either 0.1 M HCl or 0.1 M NaOH to adjust the pH as required for obtaining the pH values of 3, 6, 9 and 12 investigated. A 25 mL phenanthrene solution that has been adjusted to the required pH was then added to 0.1 g activated carbon in a 50-mL amber bottle and covered with Teflon-lined lid. This was thereafter placed into an orbital shaker at 298 K and allowed for 180 min at 100 revolutions per minute (rpm). After which 1 ml was filtered through a GHP acrodisc syringe filter (0.2 µm, 13 mm), prior to GC-FID analysis for the quantification of the residual phenanthrene.

3.7.1.2 Effect of adsorbent dosage on the adsorption of phenanthrene

The effect of adsorbent dosage was studied using 25 mL of 1 mg/L adsorbate solution at pH 3 with varying weights (0.01 – 0.1 g) of adsorbents. The investigated weights (0.01, 0.025, 0.050, 0.075 and 0.1 g) of adsorbents were carefully weighed into 50-mL amber bottles and 25 mL of phenanthrene solution added and covered with Teflon-lined lids. The bottles and their contents were then placed into the orbital shaker at 298 K and allowed for 180 min at 100 rpm. Thereafter, 1 mL solution from each of the bottles was filtered through GHP filter and the filtrates analysed with GC-FID for the residual phenanthrene.

3.7.1.3 Effect of initial phenanthrene concentrations on adsorption capacity

The effect of initial concentration was studied using 25 mL of adsorbate solution of varying concentrations. The concentrations investigated were 1, 2, 3, 4 and 5 mg/L that have been adjusted to pH 3. Aliquot 25 mL of the phenanthrene solutions were measured into 50-mL amber bottles containing 0.1 g of adsorbents. The experiments were carried out in an orbital shaker at 298 K, 100 rpm for 180 min and the GHP filtrates analysed.

3.7.1.4 Effect of contact time on phenanthrene adsorption

The effect of contact time on the adsorption of phenanthrene was also investigated by varying the time the mixture of adsorbent and phenanthrene solution used in the orbital shaker at 298 K. Phenanthrene concentration of 1 mg/L (25 mL) that have been adjusted to pH 3 and 0.1 g of adsorbents were utilised. The time intervals investigated were 10, 20, 40, 60, 80, 120, and 180 min respectively. Amber bottles with Teflon-lined lids were used and the GHP filtrates analysed.

The percentage of phenanthrene removal and the equilibrium adsorption capacity (q_e) were estimated using Equations 3.9 and 3.10 respectively.

$$\%\,\boldsymbol{Adsorbed} = \frac{\boldsymbol{C_0 - C_t}}{\boldsymbol{C_0}}\,\boldsymbol{X}\,\mathbf{100} \qquad \textbf{Equation 3. 9}$$

$$\boldsymbol{q_e} = \frac{\boldsymbol{V\,(C_0 - C_e)}}{\boldsymbol{m}} \qquad \textbf{Equation 3. 10}$$

Where C_0 (mg/L), C_e (mg/L) and C_t (mg/L) are initial, equilibrium and after time t concentration of adsorbate, respectively, V (L) is the volume of adsorbate solution, m (g) is the mass of adsorbent and q_e (mg/g) is the equilibrium adsorption capacity of adsorbent (Gupta, 2015).

3.7.2 Adsorption Isotherms

Adsorption isotherm models were used to describe adsorption behaviour of analytes onto the surface of adsorbents at equilibrium. The amount of phenanthrene adsorbed, and removal efficiency of adsorbents could be deduced from the adsorption isotherm models.

3.7.2.1 Langmuir isotherm

The sorption of phenanthrene onto single layer of selected activated carbons surface was studied with Langmuir isotherm model. Langmuir isotherm model postulates that, there is no transmigration of adsorbate in the plane of adsorbent surface for single layer adsorption onto a surface with a finite number of identical sites and uniform energies of adsorption (Tiwari *et al*., 2013). A linearised equation for Langmuir isotherm model is given in Equation 3.11

$$\frac{1}{q_e} = \frac{1}{q_m} + \frac{1}{q_m K_L C_e}$$ **Equation 3. 11**

Where q_e is the amount of adsorbate adsorbed per gram of the adsorbent at equilibrium (mg/g), q_m represent the maximum monolayer coverage capacity (mg/g), K_L is Langmuir isotherm constant (L/mg) and C_e is the equilibrium concentration of adsorbate (mg/L).

The separation factor or equilibrium parameter (R_L) which is the crucial feature of the Langmuir isotherm model (Weber & Chakravorti, 1974) is presented as:

$$R_L = \frac{1}{1+(1+K_L C_o)}$$ **Equation 3. 12**

Where, C_o is the initial adsorbate concentration (mg/L).

The nature of adsorption can be adjudged from the value of R_L; $R_L > 1$ unfavourable, $R_L = 1$ linear, $0 < R_L < 1$ favourable and $R_L = 0$ irreversible (El Qada *et al*., 2006).

3.7.2.2 Freundlich isotherm

The adsorption characteristic of phenanthrene onto heterogeneous surfaces of the produced activated carbons was investigated by Freundlich adsorption isotherm. This isotherm model, assumes that the adsorbent has a heterogenous surface with adsorption sites that have different energies of adsorption that are not always available (Walker & Weatherley, 2001).The linearised Freundlich adsorption isotherm equation is presented as:

$$\log q_e = \log K_f - \frac{1}{n} \log C_e$$ **Equation 3. 13**

Where;

q_e= amount of adsorbate adsorbed per gram of adsorbent at equilibrium (mg/g)

K_f= Freundlich isotherm constant (mg/g)

$\boldsymbol{n}$ = adsorption intensity

$\boldsymbol{C_e}$ = concentration of adsorbate at equilibrium (mg/L)

The Freundlich constant *n* gives an indication of adsorption intensity, while K_f gives an indication of adsorption capacity. The extent of non-linearity between solution concentration and adsorption depends on n. Linear adsorption, chemical adsorption and favourable physical adsorption processes are indicated by n = 1, n < 1, and n > 1 respectively (Aljeboree *et al*., 2017).

3.7.2.3 Temkin isotherm

Experimental data obtained were assessed with Temkin isotherm model. Indirect adsorbent/adsorbate interactions influence on adsorption isotherms could be evaluated (Rahim & Garba, 2016). The model ignores the extremely low and large adsorbate concentration values and assumes that the heat of adsorption of all of the molecules in the layer would decrease linearly instead of logarithmically with coverage due to adsorbate/adsorbent interactions (Aljeboree *et al*., 2017).The linear equation is expressed as:

$$\boldsymbol{q_e = B \ln K_T + B \ln C_e} \qquad \textbf{Equation 3. 14}$$

Where B (J/mol) and K_T are Temkin constants related to heat of sorption and maximum binding energy respectively, R is the gas constant (8.31 J/mol K), and T (K) is the absolute temperature.

3.7.2.4 Dubinin-Radushkevich isotherm

Experimental data obtained were also fitted into the Dubinin-Radushkevich isotherm model, which had been widely utilised to describe adsorption onto microporous materials of carbonaceous origin (Nguyen & Do, 2001; Dada *et al*., 2012; Sun *et al*., 2016). The linear equation is expressed as:

$$\boldsymbol{\ln q_e = \ln(q_{DRB}) - (K_{ad}\varepsilon^2)} \qquad \textbf{Equation 3. 15}$$

Where $\boldsymbol{q_e}$ is the amount of adsorbate adsorbed per gram of adsorbent at equilibrium (mg/g), q_{DRB} is the theoretical isotherm saturation capacity (mg/g), K_{ad} is the Dubinin-Radushkevich isotherm constant (mol^2/kJ^2) and ε is the Dubinin-Radushkevich isotherm constant (Dada *et al*., 2012).

3.7.3 Kinetic studies

To gain valuable information into the reaction pathways, the rate of adsorption and the mechanism of adsorption, adsorption kinetics study were carried out. These insights were needed to establish the efficiency of adsorbents and to determine the optimum operating conditions for the adsorption process (Ho & McKay, 1999). Experimental data obtained were subjected to four kinetic models (pseudo-first order kinetic, pseudo-second order kinetic, Elovich and intra-particle diffusion models).

3.8 Analysis of data

Statistical Package for the Social Science (SPSS) utility 24, was utilised to obtain the Pearson correlation and ANOVA multivariate test results of data obtained from environmental studies. The Microsoft EXCEL software was used for descriptive statistics. The Weibull probabilistic and percentile ranking methodologies were utilised to determine the exceedence of detected levels of PAHs in sediment and water samples relative to quality guidelines.

CHAPTER 4
RESULTS AND DISCUSSION

4.1 GC-FID method optimisation and validation

4.1.1 Chromatographic separation

The LLE-SPE-GC-FID chromatogram of the investigated 16 US EPA priority PAHs obtained from the optimised GC-FID operation conditions is presented in Figure 4.1. The optimised GC parameters were used for the separation of the compounds, with acceptable resolution, sharp peaks and adequate sensitivity for analytes. A constant carrier gas flow, rather than constant column pressure also resulted in high stability of the method.

4.1.2 Linearity, detection limit and quantification limit

The developed method was validated based on linearity range, detection limits, quantification limits, precision and accuracy (ICH, 2005). The calibration range, regression plot, retention time, goodness of fit (R^2), detection limit (DL) and quantification limit (QL) for each analyte are presented in Table 4.1. The detector response for all the analytes in the concentration range studied was linear. The method is suitable for the determination of the 16 PAHs, because the R^2 values obtained for the analytes were above 0.999 (Opeolu *et al*., 2010). The calibration plots obtained using the instrument software are presented in Appendix A.

The DL for the analytes were between 0.02 and 0.04 µg/mL while the QL were between 0.06 and 0.13 µg/mL. These results confirmed that this method sensitivity was adequate for the detection and quantification of trace levels of PAHs in environmental samples.

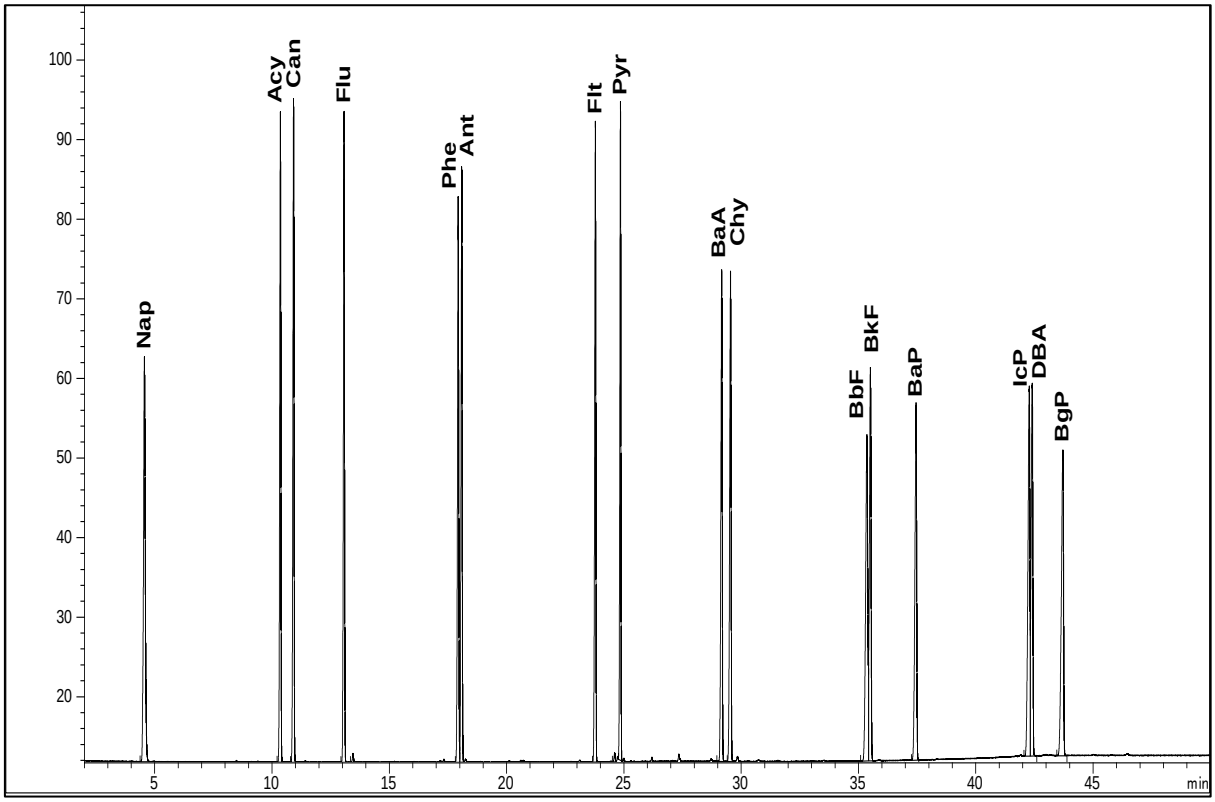

Figure 4.1: Chromatogram of the 16 US EPA priority PAHs

Nap: Naphthalene. Acy: Acenaphthylene. Can: Acenaphthene. Flu: Fluorene. Phe: Phenanthrene. Ant: Anthracene. Flt: Fluoranthene. Pyr: Pyrene. BaA: Benzo[a]anthracene. Chy: Chrysene. BbF: Benzo[b]fluoranthene. BkF: Benzo[k]fluoranthene. Bap: Benzo[a]pyrene. IcP: Indeno[1, 2, 3-cd]pyrene. DBA: Dibenzo[a, h]anthracene. BgP: Benzo[g, h, i]perylene.

Table 4.1: Calibration data and linearity for the 16 US EPA Priority PAHs

S/N	Analytes	Range (µg/mL)	Retention time (min)	Calibration Plot	DL (µg/mL)	QL (µg/mL)	R^2-value
1	Naphthalene	1-50	4.564	5.4075X + 2.1775	0.021699	0.07233	0.9998
2	Acenaphthylene	1-50	10.360	5.5171X + 2.1721	0.023226	0.07742	0.9998
3	Acenaphthene	1-50	10.921	5.6338X + 2.0741	0.022638	0.07546	0.9998
4	Fluorene	1-50	13.074	5.5333X + 2.6089	0.024982	0.08327	0.9998
5	Phenanthrene	1-50	17.941	5.2637X + 2.1914	0.026242	0.08747	0.9998
6	Anthracene	1-50	18.092	5.2186X + 1.9472	0.027505	0.09168	0.9997
7	Fluoranthene	1-50	23.787	5.5493X + 1.9110	0.026586	0.08862	0.9998
8	Pyrene	1-50	24.856	5.0500X + 3.2924	0.023940	0.07980	0.9998
9	Benzo[a]anthracene	1-50	29.171	4.9504X + 1.5474	0.027034	0.09011	0.9998
10	Chrysene	1-50	29.549	5.1841X + 1.7904	0.028507	0.09502	0.9997
11	Benzo[b]fluoranthene	1-50	35.364	4.9805X + 1.6059	0.024576	0.08192	0.9998
12	Benzo[k]fluoranthene	1-50	35.512	4.9533X + 1.8516	0.027695	0.09232	0.9997
13	Benzo[a]pyrene	1-50	37.447	4.6564X + 1.5607	0.027480	0.09160	0.9997
14	Indeno[1,2,3-cd]pyrene	1-50	42.272	5.3699X + 0.9102	0.017514	0.05838	0.9999
15	Dibenzo[a, h]anthracene	1-50	42.400	4.6555X + 2.7787	0.037713	0.12571	0.9995
16	Benzo[g, h, i]perylene	1-50	43.709	4.9071X + 1.8434	0.025306	0.08435	0.9998

4.1.3 Precision

The repeatability and reproducibility data obtained were used for precision measurement by calculating the relative standard deviation (RSD) [Table 4.2]. The % RSD for repeatability ranged between 1.2% and 2.0% and that for reproducibility ranged between 1.1% and 3.2%. Hence, the method had good precision and was robust like those previously utilised in chromatographical analyses (Zakeri-Milani *et al*., 2005; Wei and Jen, 2007; Opeolu *et al*., 2010). Zakeri-Milani *et al*. (2005) reported %RSD range of 0.48 to 5.30 and 0.22 to 1.33 for repeatability and reproducibility respectively. They developed HPLC mehtod for the simultaneous determination of naproxen, ketoprofen and phenol.

Table 4.2: Repeatability and reproducibility of GC-FID analysis of 16 US EPA priority PAHs

PAHs	Within-day (Repeatability) (n=6)			Between-day (Reproducibility) (n=6)		
	Initial conc. (µg/mL)	Mean Conc. (µg/mL)	%RSD	Initial Conc. (µg/mL)	Mean Conc. (µg/mL)	%RSD
Naphthalene	9.714	9.391 ± 0.191	2.036	9.303	9.240 ± 0.115	1.244
Acenaphthylene	6.866	6.679 ± 0.111	1.667	6.621	6.584 ± 0.084	1.272
Acenaphthene	9.172	8.911 ± 0.155	1.743	8.834	8.782 ± 0.116	1.317
Fluorene	10.309	10.029 ± 0.165	1.643	9.926	9.855 ± 0.109	1.110
Phenanthrene	8.092	7.933 ± 0.104	1.316	7.862	7.847 ± 0.131	1.673
Anthracene	9.918	9.713 ± 0.136	1.396	9.618	9.575 ± 0.136	1.418
Fluoranthene	9.619	9.447 ± 0.127	1.350	9.346	9.354 ± 0.190	2.026
Pyrene	10.694	10.516 ± 0.146	1.392	10.390	10.470 ± 0.337	3.217
Benzo[a]anthracene	10.969	10.784 ± 0.145	1.344	10.669	10.651 ± 0.197	1.851
Chrysene	10.142	9.977 ± 0.127	1.274	9.884	9.886 ± 0.175	1.774
Benzo[b]fluoranthene	9.803	9.668 ± 0.112	1.153	9.544	9.548 ± 0.131	1.374
Benzo[k]fluoranthene	11.826	11.575 ± 0.182	1.570	11.479	11.445 ± 0.210	1.836
Benzo[a]pyrene	10.447	10.261 ± 0.135	1.316	10.153	10.137 ± 0.160	1.579
Indeno[1,2,3-cd]pyrene	10.846	10.587 ± 0.148	1.394	10.528	10.491 ± 0.177	1.684
Dibenzo[a, h]anthracene	10.793	10.626 ± 0.184	1.729	10.408	10.448 ± 0.171	1.637
Benzo[g, h, i]perylene	11.269	11.037 ± 0.152	1.376	10.922	10.909 ± 0.171	1.571

4.1.4 Recovery of PAHs

The accuracy of analytical procedure was inferred from average percentage recovery obtained from triplicate analysis of PAHs extracted from spiked matrices. The recovery of PAHs from aqueous matrix is presented in Table 4.3. The lowest average percentage recovery of 60.05 ± 9.45% was obtained for naphthalene while average percentage recovery of over 80% (which ranged between 83.69 ± 1.47% and 96.44 ± 3.01%) were obtained for all other analytes in aqueous media. The high volatility of naphthalene was suspected to be responsible for its low recovery and high bias relative to other larger PAHs. A smaller recovery percentage (36.28%) was reported for naphthalene by Karyab *et al.*(2013).

The percentage recovery obtained for spiked plant samples ranged from 62.13 ± 3.77% to 100.83 ± 3.92%, while that of spiked sediment samples ranged from 47.98 ± 3.03% to 96.51 ± 5.02% (Table 4.4). The relatively high and acceptable recoveries obtained are consistent with those reported in literatures (Wei & Jen, 2007; Qiao *et al*., 2008; Liu *et al*., 2013; Ma *et al*., 2013). Qiao *et al*. (2008) reported recovery ranges of 62.1 to 106.5% and 58.7 to 96.3% for the US EPA individual PAHs in water and sediment samples respetively. The recovery ranges for four surrogate standards (naphthalene-d8, phenanthrene-d10, fluororene-d10 and perylene-d12) in water and sediment samples reported by Liu *et al*. (2013) were 51.5 to 97.8% and 60.2 to 99.8% respectively. The described methods are therefore suitable for the analysis of the 16 priority US EPA PAHs in water, sediment and plant samples.

Table 4.3: Average percentage recovery of the 16 US EPA priority PAHs from milli-Q water

PAHs	Reference (µg/mL)	$\bar{x}$ (µg/mL) n=3	% Recovery
Naphthalene	1.3937	0.8369 ± 0.271	60.05 ± 9.45
Acenaphthylene	1.0248	0.8747 ± 0.061	85.36 ± 5.99
Acenaphthene	1.3534	1.1330 ± 0.020	83.69 ± 1.47
Fluorene	1.4596	1.3480 ± 0.037	92.36 ± 2.53
Phenanthrene	1.1725	1.0740 ± 0.015	91.62 ± 1.28
Anthracene	1.3915	1.2720 ± 0.017	91.39 ± 1.19
Fluoranthene	1.3596	1.2930 ± 0.020	95.07 ± 1.46
Pyrene	1.4462	1.3670 ± 0.032	94.50 ± 2.24
Benzo[a]anthracene	1.5057	1.4170 ± 0.024	94.14 ± 1.60
Chrysene	1.4179	1.3410 ± 0.025	94.60 ± 1.78
Benzo[b]fluoranthene	1.4020	1.3180 ± 0.023	94.00 ± 1.64
Benzo[k]fluoranthene	1.5836	1.4970 ± 0.026	94.54 ± 1.66
Benzo[a]pyrene	1.4564	1.3440 ± 0.023	92.25 ± 1.55
Indeno[1,2,3-cd]pyrene	1.5148	1.4070 ± 0.027	92.92 ± 1.81
Dibenzo[a, h]anthracene	1.4703	1.4180 ± 0.440	96.44 ± 3.01
Benzo[g, h, i]perylene	1.5570	1.4640 ± 0.027	94.02 ± 1.76

Table 4.4: Percentage recovery of PAHs in plant and sediment samples (n = 3)

PAHs	Reference (µg/g)	Plant $\bar{x}$ (µg/g)	% Recovery in plant	Sediment $\bar{x}$ (µg/g)	% Recovery in sediment
Naphthalene	1.103	0.685 ± 0.04	62.13 ± 3.77	0.529 ± 0.03	47.98 ± 3.03
Acenaphthylene	0.791	0.605 ± 0.01	76.51 ± 1.83	0.556 ± 0.04	70.35 ± 5.04
Acenaphthene	1.056	0.829 ± 0.02	78.50 ± 1.63	0.788 ± 0.05	74.60 ± 4.73
Fluorene	1.108	0.774 ± 0.02	80.95 ± 1.67	0.876 ± 0.05	79.04 ± 4.72
Phenanthrene	0.827	0.744 ± 0.02	89.92 ± 2.47	0.725 ± 0.04	87.70 ± 5.00
Anthracene	0.927	0.825 ± 0.02	89.00 ± 2.58	0.806 ± 0.05	86.88 ± 5.05
Fluoranthene	0.963	0.887 ± 0.02	92.09 ± 2.37	0.863 ± 0.06	89.59 ± 5.91
Pyrene	1.031	0.927 ± 0.04	89.95 ± 3.86	0.906 ± 0.05	87.88 ± 5.13
Benzo[a]anthracene	0.991	1.000 ± 0.04	100.83 ± 3.92	0.916 ± 0.07	92.39 ± 6.67
Chrysene	1.033	0.967 ± 0.03	93.59 ± 2.97	0.931 ± 0.05	90.10 ± 5.06
Benzo[b]fluoranthene	0.964	0.882 ± 0.03	91.51 ± 3.20	0.903 ± 0.05	93.65 ± 5.30
Benzo[k]fluoranthene	1.122	1.001 ± 0.04	89.26 ± 3.51	1.054 ± 0.06	93.99 ± 5.05
Benzo[a]pyrene	1.007	0.770 ± 0.04	90.98 ± 3.50	0.902 ± 0.05	89.57 ± 5.31
Indeno[1,2,3-cd]pyrene	1.180	1.104 ± 0.03	93.53 ± 3.95	1.049 ± 0.07	88.83 ± 5.92
Dibenzo[a, h]anthracene	0.926	0.877 ± 0.04	94.68 ± 2.76	0.894 ± 0.05	96.51 ± 5.02
Benzo[g, h, i]perylene	1.083	0.990 ± 0.04	91.43 ± 3.41	0.976 ± 0.07	90.12 ± 6.22

4.2 Water quality parameters of the Diep and Plankenburg Rivers water samples

4.2.1 Temperature

Anthropogenic activities (including land use, sewage and effluent discharges) and climate change have negatively impacted the quality of surface water globally. This has resulted in less productivity, resource potentials and environmental functions of these natural resources of socio-economic and environmental importance (Caissie, 2006; Sallam and Elsayed, 2015; Cui *et al*., 2017; Korkanç *et al*., 2017). The need for water quality assessment for informed resource management decisions, therefore becomes imperative (Korkanç *et al*., 2017). The quality of surface water depends on a combination of factors (temperature, pH, salinity, amongst others.) that may be classified mainly as physical, chemical and biological characteristics (Korkanç *et al*., 2017).

Temperature is one of the parameters that is widely assessed to determine the overall health of aquatic ecosystems. Aquatic biota are highly sensitive to fluctuations in temperature (thermal pollution); changes in temperature may cause death, algal blooms and introduction of alien species in certain instances (Caissie, 2006; de Vries *et al*., 2008; Hester and Doyle, 2011; Wolf *et al*., 2014). Also, many physical and chemical water characteristics such as; solubility of oxygen and other gases, chemical reaction rate and toxicity, and microbial activities are strongly influenced by temperature (Dallas, 2008). Hence, toxicity and bioavailability of PAHs in the aquatic environment can be influenced by temperature profiles of water bodies.

Heated discharges, flow modifications, riparian vegetation removal and global climate change are the causes of thermal regime changes in aquatic ecosystems (Dallas, 2008). Almost 90% of thermally impacted freshwaters globally, are long-range impacts and are caused mainly by once-through cooling systems from old power plants (Raptis *et al*., 2017). A temperature change of 1.5^{o}C and 3^{o}C in salmonid and cyprinid waters respectively, above the natural water temperature as a result of thermal pollution, are not allowed in several US states (Raptis *et al*., 2017). This highlights the sensitivity of aquatic lives to temperature changes and the importance of temperature in water quality assessment.

The average temperature of water samples collected at various seasons ranged between 12.40^{o}C and 24.17^{o}C at the sampling sites (Tables 4.5a and 4.5b). Seasonal total temperature average was highest in summer for both the Diep and Plankenburg River (23.17 and 19.60^{o}C respectively) and lowest in winter (15.22 and 12.62^{o}C respectively). This corresponds to variation in solar radiation. However, the highest temperature (24.17^{o}C) was recorded in autumn at site DB, in

proximity to a refinery, which may suggest anthropogenic impact. Although, the water temperature was below 25ºC (acceptable limit for no risk, as indicated by the South African water quality guidelines for aquatic ecosystems), at all the sites (Department of Water Affairs and Forestry (DWAF), 1996a).

Table 4.5a: Seasonal variation of temperature (ºC) in the Diep River water samples

	Summer (Dec, Jan & Feb)	Autumn (March to May)	Winter (June to August)	Spring (Sept to Nov)
Site DA	23.300 ± 0.707	21.900 ± 1.706	14.500 ± 0.700	17.750 ± 0.778
Site DB	23.900 ± 1.838	24.167 ± 0.961	17.133 ± 2.401	21.100 ± 1.697
Site DC	22.300 ± 1.131	20.933 ± 0.981	14.033 ± 0.681	18.150 ± 1.061
Average	23.167 ± 0.808	22.333 ± 1.660	15.222 ± 1.671	19.000 ± 1.830

Site DA: Nature reserve (upstream). Site DB: Theo Marais Sports Club – industrial and residential area. Site DC: Woodbridge (downstream).

Table 4.5b: Seasonal variation of temperature (ºC) in the Plankenburg River water samples

	Summer (Dec, Jan & Feb)	Autumn (March to May)	Winter (June to August)	Spring (Sept to Nov)
Site PA	19.990 ± 1.146	19.267 ± 1.662	12.400 ± 2.762	17.350 ± 0.071
Site PB	19.550 ± 0.212	19.200 ± 1.136	12.700 ± 2.402	17.000 ± 0.283
Site PC	19.800 ± 0.141	19.300 ± 1.418	12.733 ± 2.421	16.650 ± 0.495
Site PD	19.050 ± 0.778	19.233 ± 0.723	12.633 ± 2.290	16.000 ± 0.566
Average	19.598 ± 0.407	19.250 ± 0.043	12.617 ± 0.150	17.714 ± 0.576

Site PA: Agricultural and residential areas. Site PB: Informal settlement of Kayamandi. Site PC: Substation in industrial area. Site PD: Industrial area at Adam Tas bridge.

4.2.2 pH

The pH of surface water is an important factor, that could influence the availability of nutrients and toxins to plants and animals (Agunbiade *et al*., 2009; Sallam and Elsayed, 2015). Agunbiade *et al*. (2009), reported that metal contaminants are more bioavailable to plant between pH 5.5 and 6.5. Water pH could be electrometrically measured using a pH meter giving an indication of hydrogen ion (H^+) concentration of water (Wurts & Durborow, 1992; DWAF, 1996a). The pH of natural waters results from complex acid-base balance of different dissolved compounds especially carbon dioxide-bicarbonate-carbonate equilibrium system, that can also be influenced by temperature (DWAF, 1996b). Also, pH is influenced by other parameters such as carbon dioxide, alkalinity and hardness (Wurts & Durborow, 1992). Acidification and alkalinisation of natural water caused by conditions that favour H^+ production (lower pH) and neutralisation of H^+ (higher pH) respectively are the processes that occur, because of changes in pH regimes.

The average water pH values for selected sites of the Diep River ranged from 7.16 to 7.98; corresponding values for the Plankenburg River were 6.37 to 7.15 (Tables 4.6a and 4.6b respectively). The pH range recorded fell within the recommended levels set by the Department of Water and Sanitation of South Africa (6 - 9) for domestic, recreational and agricultural water use (DWAF, 1996b), but the summer average of two sites [PC (6.37) and PD (6.38)] fell outside the optimum levels set by World Health Organisation (6.5 to 9.5) for water meant for recreational activities (WHO, 2006). Therefore, water from these two sites may not be suitable for recreational activities in summer as effluents from industries seem to influence the water pH values at these sites.

The hydrolysis of released organic contaminants coupled with rivers' natural pH buffering mechanism could be responsible for pH values of over 7.50 recorded in most instances at the Diep River. High pH levels of up to 9.02 in water samples from Msunduzi River (South Africa), have been previously attributed to the hydrolysis of organic-derived wastes by Munyengabe *et al*. (2017). They reported pH values that ranged from 5.89 to 9.02 in surface water relative to the 6.0 to 7.5 range for natural surface water.

In the Plankenburg River, the low pH values recorded especially at sites PC and PD (industrial areas) could be as a result of acidic industrial effluents and emissions (Sallam and Elsayed, 2015). The pH of surface water had been reported to display random seasonal fluctuation (Cui *et al*., 2017). Azizi *et al.* (2018) reported average pH value of 8.4, across the four seasons of summer (8.27), autumn (8.35), winter (8.27) and spring (8.71). The average pH value (8.71) recorded in spring in their study, was significantly different from and higher than those of the three other seasons. Wang *et al.* (2018), on the other hand reported mean pH values in autumn (8.30) and winter (8.26) that were higher than those in spring (8.21) and summer (8.10). Seasonal random flunctuation in pH, was observed in this study. Summer average pH value was highest for the Diep River (7.82) , but lowest for the Plankenburg River (6.63). Catchment activities and sundry of environmental effects may therefore be responsible for variations in pH values recorded.

Table 4.6a: Seasonal variation of pH values in the Diep River water samples

	Summer (Dec, Jan & Feb)	Autumn (March to May)	Winter (June to August)	Spring (Sept to Nov)
Site DA	7.750 ± 0.537	7.610 ± 0.475	7.193 ± 0.157	7.160 ± 0.028
Site DB	7.895 ± 0.247	7.613 ± 0.415	7.330 ± 0.147	7.975 ± 0.530
Site DC	7.815 ± 1.124	7.860 ± 0.745	7.917 ± 0.385	7.920 ± 0.523
Average	7.820 ± 0.073	7.694 ± 0.143	7.480 ± 0.385	7.685 ± 0.455

Site DA: Nature reserve (upstream). Site DB: Theo Marais Sports Club – industrial and residential area. Site DC: Woodbridge (downstream).

Table 4.6b: Seasonal variation of pH values in the Plankenburg River water samples

	Summer (Dec, Jan & Feb)	Autumn (March to May)	Winter (June to August)	Spring (Sept to Nov)
Site PA	6.930 ± 0.127	7.107 ± 0.231	7.153 ± 0.127	7.130 ± 0.140
Site PB	6.845 ± 0.177	6.993 ± 0.253	7.153 ± 0.277	7.095 ± 0.163
Site PC	6.365 ± 0.219	6.717 ± 0.206	6.863 ± 0.061	6.930 ± 0.028
Site PD	6.380 ± 0.042	6.633 ± 0.195	6.880 ± 0.428	6.810 ± 0.141
Average	6.630 ± 0.299	6.863 ± 0.224	7.012 ± 0.163	6.991 ± 0.149

Site PA: Agricultural and residential areas. Site PB: Informal settlement of Kayamandi. Site PC: Substation in industrial area. Site PD: Industrial area at Adam Tas bridge.

4.2.3 Electrical conductivity (EC)

The EC of surface waters is said to be a function of the geology of an area. It suggests the presence of dissolved ions in water that could alter the taste and contribute to water hardness (Edokpayi *et al*., 2015). Discharges (agricultural, domestic and industrial sewage) and runoff wastewater into water resources can however result in conductivity increase, rendering the water inapt for irrigation and domestic use (Korkanç *et al*., 2017). Sea water intrusion into rivers is another way surface waters are impacted, changing the pH, EC, and the TDS regimes (Kumar *et al*., 2015; Sylus & Ramesh, 2015). The EC values at the selected sites ranged between 582 and 6340 µS/cm (Tables 4.7a and 4.7b). The total seasonal average EC values obtained in spring were the highest for both the Diep (3249 µS/cm) and the Plankenburg (842 µS/cm) Rivers. Electrical conductivity values above the permissible level (0 to 1500 µS/cm) by the Department of Water and Sanitation of South Africa (DWAF, 1996b) were mainly recorded in the Diep River water samples. Apart from wastewater runoff into the rivers, tidal waves and river flows which are influenced by sundry and dynamic environmental conditions, possibly contributed to the high EC values recorded. These effects are more pronounced in the site DC which can be regarded as the zone of dispersion based on its closeness to the sea, with an EC value of 6340 µS/cm in spring. The EC range from this study is higher than those observed by Kumar *et al*. (2015) [49.8 to 1926

µS/cm] and Sylus & Ramesh (2015) [10 to 2500 µS/cm], from their investigation of seawater intrusion into coastal aquifers. However, the EC range observed in this study is lower than that reported by Tauhid Ur Rahman *et al*. (2017) from their assessment of rivers, ponds and tube wells. They reported EC average value of up to 7186.7 µS/cm.

Table 4.7a: Seasonal variation of electrical conductivity (µS/cm) values in the Diep River water samples

	Summer (Dec, Jan & Feb)	Autumn (March to May)	Winter (June to August)	Spring (Sept to Nov)
Site DA	1182 ± 611	988 ± 302	1177 ± 288	1790 ± 215
Site DB	1145 ± 651	1120 ± 379	1218 ± 219	1616 ± 276
Site DC	2792 ± 2267	4990 ± 3298	4859 ± 3205	6340 ± 693
Average	1706 ± 940	2366 ± 2273	2418 ± 2114	3249 ± 2679

Site DA: Nature reserve (upstream). Site DB: Theo Marais Sports Club – industrial and residential area. Site DC: Woodbridge (downstream).

Table 4.7b: **Seasonal variation of electrical conductivity (µS/cm) values in the Plankenburg River water samples**

	Summer (Dec, Jan & Feb)	Autumn (March to May)	Winter (June to August)	Spring (Sept to Nov)
Site PA	675 ± 109	620 ± 020	644 ± 067	885 ± 114
Site PB	671 ± 101	585 ± 062	626 ± 078	852 ± 122
Site PC	708 ± 051	627 ± 041	582 ± 044	834 ± 132
Site PD	699 ± 129	605 ± 019	589 ± 039	798 ± 120
Average	688 ± 018	609 ± 019	610 ± 030	842 ± 036

Site PA: Agricultural and residential areas. Site PB: Informal settlement of Kayamandi. Site PC: Substation in industrial area. Site PD: Industrial area at Adam Tas bridge.

4.2.4 Total dissolved solids (TDS)

The TDS is a measure of various dissolved inorganic salts in water and has a direct relationship with EC. Various inorganic salts are present in water naturally because of dissolution of minerals in rocks, soils and decomposing vegetation. Hence, TDS levels in surface water is also a function of the geology of the area that the water had contact (DWAF, 1996b). However, undesirable elevated levels of TDS could arise from salt intrusion, mining, irrigation water, oil field refinery, and domestic wastewaters (Kent & Landon, 2013; Feng *et al*., 2014; Sharma *et al*., 2017). Elevated levels of TDS have been reported to impact water odour and colour, resulting in poor growth performance of animals and post egg fertilisation impairment in aquatic organisms (Brix *et al*., 2010; Sharma *et al*., 2017). Total dissolved solids are therefore used as an index of water quality,

permissible limits range between 600 to < 1000 mg/L (Kut *et al*., 2019). The TDS values obtained from selected sites at different seasons are presented in Tables 4.8a and 4.8b for the Diep and Plankenburg Rivers respectively. The observed trend was similar to those obtained for EC. The TDS range (415 to 4340 mg/L) recorded in this study, is higher than those observed by Kumar *et al*. (2015) [1.21 to 774 mg/L] and Sylus & Ramesh (2015) [25 to 1800 mg/L]. Higher TDS values were observed in winter and spring relative to summer and autumn in both rivers. This observation is consistent to that of Kut *et al*. (2019). They reported higher TDS range of 121 to 1924 mg/L in wet season relative to 121 to 1467 mg/L in dry season. Storm water during the wet season must have enhanced the TDS values during the wet periods.

Table 4.8a: Seasonal variation of TDS (mg/L) values in the Diep River water samples

	Summer (Dec, Jan & Feb)	**Autumn (March to May)**	**Winter (June to August)**	**Spring (Sept to Nov)**
Site DA	849 ± 426	705 ± 205	829 ± 199	1235 ± 191
Site DB	813 ± 463	795 ± 270	863 ± 156	1140 ± 184
Site DC	1937 ± 1561	3211 ± 2070	3325 ± 2152	4340 ± 594
Average	1200 ± 639	1570 ± 1422	1672 ± 1431	2238 ± 1821

Site DA: Nature reserve (upstream). Site DB: Theo Marais Sports Club – industrial and residential area. Site DC: Woodbridge (downstream).

Table 4.8b: Seasonal variation of TDS (mg/L) values in the Plankenburg River water samples

	Summer (Dec, Jan & Feb)	**Autumn (March to May)**	**Winter (June to August)**	**Spring (Sept to Nov)**
Site PA	479 ± 77	440 ± 14	449 ± 47	603 ± 113
Site PB	478 ± 76	428 ± 18	443 ± 52	584 ± 83
Site PC	507 ± 45	443 ± 28	415 ± 29	590 ± 95
Site PD	498 ± 86	432 ± 13	420 ± 28	564 ± 88
Average	491 ± 14	436 ± 07	432 ± 17	585 ± 16

Site PA: Agricultural and residential areas. Site PB: Informal settlement of Kayamandi. Site PC: Substation in industrial area. Site PD: Industrial area at Adam Tas bridge.

4.2.5 Salinity

The amount of dissolved salts (mainly NaCl, KCl and $MgCl_2$) in water is known as salinity (Hussain *et al*., 2017). Salinity is a very important parameter in aquatic systems as it controls physical attributes of surface waterbodies such as, density and heat capacity in conjunction with temperature and pressure. Salinity also influences the development and growth of aquatic organisms, and only a few species are said not to be affected by salinity changes (Bœuf & Payan, 2001). Salinity also poses serious problems in crop production; they include delayed germination, high seedling mortality, poor crop stand, stunted growth and reduced yields (Al-Dakheel *et al*., 2015). Hence, crop irrigation and aquaculture using high salinity water threatens food security.

The salinity values obtained for water samples of studied sites are presented in Tables 4.9a and 4.9b for the Diep and Plankenburg Rivers respectively. The observed salinity trend was similar to those of EC and TDS. The recorded seasonal salinity ranged from 915 to 5231 mg/L and 529 to 681 mg/L for the Diep and Plankenburg Rivers respectively. Most of the observed seasonal salinity values across the studied sites of the Diep River exceeded the permissible value (<1000 mg/L) recommended for the protection of freshwater life (Kaushal *et al*., 2005). However, salinity values observed for the Plankenburg River were well below 1000 mg/L. The higher salinity levels in the Diep River relative to the Plankenburg River could be attributed to seawater intrusion which is evident at site DC (zone of dispersion) having the highest salinity range of 2252 to 5231 mg/L. The changes in the seasonal salinity values may be attributed to wastewater/storm water runoff and oceanic water intrusion into the aquatic system. A lower average salinity values of up to 4236.4 mg/L was reported by Tauhid Ur Rahman *et al*. (2017). They reported that salinity intrusion was responsible for the high salinity levels measured and scarcity of safe drinking water in the coastal regions of Bangladesh. The heavy reliance on irrigation for crop production and rising groundwater tables, are also important causes of river salinisation (Cañedo-Argüelles *et al*.,2013). The high salinity recorded may therefore be as a result of unadsorbed salt from irrigation water, used in crop farming on the river catchments. Spring salinity values were generally higher relative to other seasons, this is contrast with the report of Ruiz *et al.* (2011). They reported that salinity values were stable, but only declined at the beginning of late winter-early spring due high rain fall. The washing of unadsorbed soil salt from irrigation water into the rivers may therefore be responsible for the high salinity values recorded in this study during spring, in contrast to that reported by Ruiz *et al.* (2011).

Table 4.9a: Seasonal variation of salinity (mg/L) in the Diep River water samples

	Summer (Dec, Jan & Feb)	Autumn (March to May)	Winter (June to August)	Spring (Sept to Nov)
Site DA	992 ± 384	981 ± 320	1165 ± 288	1414 ± 135
Site DB	915 ± 498	1096 ± 464	1225 ± 229	1280 ± 175
Site DC	2252 ± 1787	5231 ± 3690	5018 ± 3336	5195 ± 630
Average	1386 ± 751	2436 ± 2421	2469 ± 2207	2630 ± 2223

Site DA: Nature reserve (upstream). Site DB: Theo Marais Sports Club – industrial and residential area. Site DC: Woodbridge (downstream).

Table 4.9b: Seasonal variation of salinity (mg/L) in the Plankenburg River water samples

	Summer (Dec, Jan & Feb)	Autumn (March to May)	Winter (June to August)	Spring (Sept to Nov)
Site PA	531 ± 60	575 ± 75	616 ± 59	681 ± 72
Site PB	529 ± 61	561 ± 71	601 ± 70	645 ± 63
Site PC	559 ± 15	577 ± 27	559 ± 44	631 ± 75
Site PD	545 ± 66	562 ± 57	569 ± 35	611 ± 80
Average	541± 14	569 ± 08	586 ± 27	642 ± 30

Site PA: Agricultural and residential areas. Site PB: Informal settlement of Kayamandi. Site PC: Substation in industrial area. Site PD: Industrial area at Adam Tas bridge.

Correlation between the water quality parameters measured on site

Conductivity, TDS and salinity showed identical trends across the seasons with higher values in wet regime relative to dry regime as shown in (Table 4.7 to Table 4.9). The Pearson correlation obtained through SPSS, showed that strong positive correlation existed between these three parameters (conductivity, TDS and salinity) as shown in Table 4.10. A 99.9% correlation existed between conductivity and TDS, 98.7% correlation between conductivity and salinity and 98.2% correlation between TDS and salinity. Strong correlations between EC, TDS and salinity in water samples are because EC depends on dissolved salts in water (Priya & Arulraj, 2011). Conductivity, TDS and salinity also gave positive significant correlation with pH, at 65.0%, 65.5% and 64.3 % respectively.

Table 4.10: Correlation matrix of water quality parameters measured on site

		pH	Temperature	Conductivity	TDS	Salinity
pH	Pearson Correlation	1				
	Sig. (2-tailed)					
	N	28				
Temperature	Pearson Correlation	.345	1			
	Sig. (2-tailed)	.073				
	N	28	28			
Conductivity	Pearson Correlation	.650**	.073	1		
	Sig. (2-tailed)	.000	.712			
	N	28	28	28		
TDS	Pearson Correlation	.655**	.074	.999**	1	
	Sig. (2-tailed)	.000	.708	.000		
	N	28	28	28	28	
Salinity	Pearson Correlation	.643**	.044	.987**	.982**	1
	Sig. (2-tailed)	.000	.824	.000	.000	
	N	28	28	28	28	28

**. Correlation is significant at the 0.01 level (2-tailed).

4.3 Levels of PAHs in the Diep and Plankenburg Rivers

4.3.1 Levels of PAHs in surface water samples

4.3.1.1 Levels of PAHs in surface water samples of the Diep River

The seasonal average levels of 16 priority US EPA PAHs in water samples of the Diep River were assessed at studied sites. The summary of data obtained is presented in Appendices C1 and C2. The seasonal averages of individual PAH detected at the studied sites on the Diep River, ranged between 0.12 µg/L and 72.38 µg/L. This range was comparable to another study in South Africa by Nekhavhambe *et al*. (2014) who reported 0.1 µg/L to 137 µg/L range in river water samples. However, a lower range of 33.5 ng/L to 126.8 ng/L was reported in South Africa by Amdany *et al*. (2014) who studied the bioavailable fraction of POPs in surface water. Seasonal regimes influenced the detected levels of PAHs, with highest levels recorded in summer. The seasonal levels measured, were in the order of summer > autumn > winter > spring, except for site DA (Figure 4.2). In summer (with elevated temperature and low precipitation), water level became critically low and more pronounced downstream. This could be responsible for more concentrated levels of PAH contaminants. Liu *et al*. (2016a) also reported high PAHs concentrations during elevated temperature period and low PAHs concentrations during flood period.

The prevalence of carcinogenic PAHs (benzo[a]anthracene, chrysene, benzo[b]fluoranthene, benzo[k]fluoranthene, benzo[a]pyrene, indeno[1,2,3-cd]pyrene and dibenzo[a, h]anthracene) in water samples analysed is of major concern, representing up to 72.36 % of the PAHs in water samples at the studied sites of the Diep River (Appendices C1 and C2). This poses potential risk to aquatic lives and human health through possible exposures via food webs.

The site near a refinery (site DB) was the most contaminated site on the Diep River, with 16 US EPA priority PAHs annual average of 169.47 µg/L, followed by the downstream site (site DC) at 99.81 µg/L and the lowest level was recorded upstream, at the nature reserve (site DA) with annual average of 73.91 µg/L (Figure 4.2). This suggests that, detected levels of PAHs were also site-specific and dependent on anthropogenic activities near sampling sites. Prevalence of petrogenic (3-ringed) PAHs at site DB relative to other sites was observed.

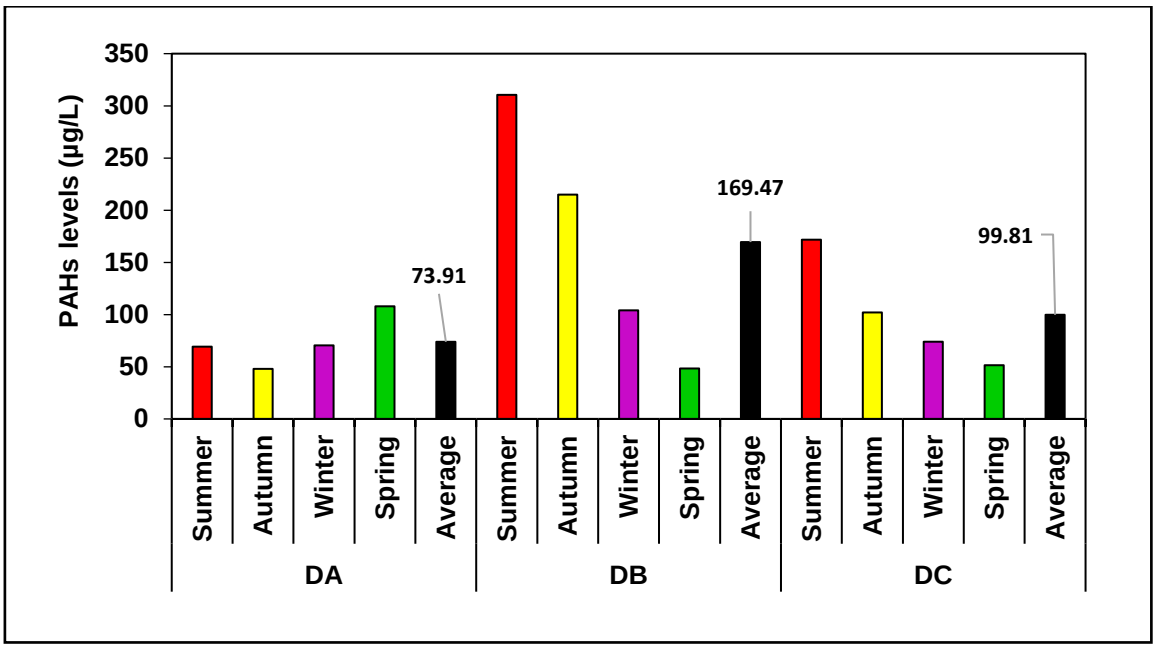

Figure 4.2: Seasonal variations and annual average levels of 16 US EPA priority PAHs in water samples of the Diep River

The influence of site's anthropogenic activities and seasons on detected levels of PAHs were examined statistically using two-way ANOVA multivariate test. The result showed that both sampling sites and seasonal regimes had significant effects on the levels of PAHs detected ($P<0.05$). However, sampling sites showed more significant effect on the detected levels of PAHs, based on the F-values of 14.787 and 4.268 obtained for sites and seasons respectively (Appendix D).

Acenaphthylene, acenaphthene, phenanthrene, anthracene, benzo[a]anthracene, chrysene, indeno[1, 2, 3-cd]pyrene, dibenzo[a, h]anthracene and benzo[g, h, i]perylene were found to be present in all the water samples analysed through the four seasons. The annual percentage distribution for each PAH in water samples from studied sites on the Diep River is shown in Figure 4.3, with chrysene as the highest contributor to the overall PAH-burden, followed by benzo [a] anthracene. The least contributors were benzo [a] pyrene, benzo [b] fluoranthene and benzo [k] fluoranthene with approximately 1% contribution each, to the overall water PAH-burden. The contribution of each PAH in water samples over a one-year period is in the order chrysene (20.51%) > benzo[a]anthracene (17.10%) > dibenzo[a, h]anthracene (9.24%) > indeno[1, 2, 3-cd]pyrene (9.03%) > phenanthrene (8.47%) > benzo[g, h, i]perylene (5.91%) > fluoranthene (5.85%) > anthracene (5.21%) > naphthalene (3.87%) > acenaphthylene (3.36%) >fluorene (2.88%) > pyrene (2.41%) > acenaphthene (2.13%) > benzo[k]fluoranthene (1.41%) > benzo[b]fluoranthene (1.34%) > benzo[a]pyrene (1.27%). The 4-ringed PAHs were the highest contributors (45.89%), followed by the high molecular weight (HMW) PAHs (5- and 6-ring) (28.20%) and the low molecular weight (LMW) PAHs (2 and 3-ring) were the lowest contributors (25.92%). This is an indication of pyrogenic sourced PAHs (Hong *et al*., 2016). Edokpayi *et al*. (2016), also reported that pyrogenic sources (i.e. combustion of bushes and other biomass) were the sources of PAHs detected in water samples from a South African River.

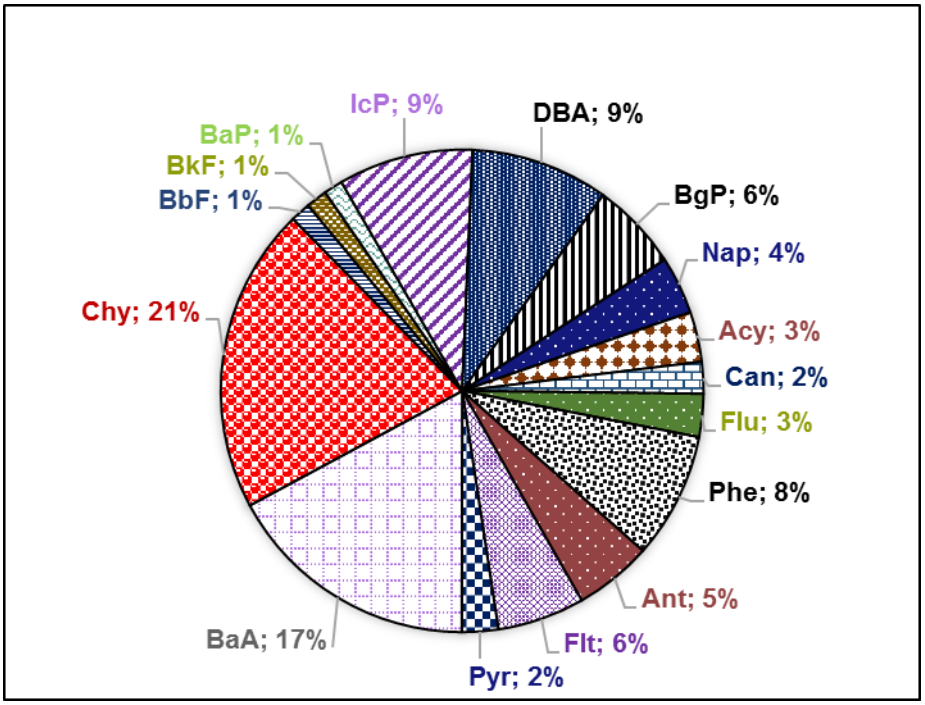

Figure 4.3: Annual distribution of 16 US EPA PAHs in water samples of the Diep River

The PAHs distribution in water samples from the studied sites were relatively comparable. The 4-ringed PAHs were the most abundant, followed by the 3-ringed congeners, except for site DC where there were more 5-ringed congeners relative to the 3-ringed congeners. The least abundant was the 2-ringed PAH as shown in Table 4.11 and Figure 4.4. The abundance of 4-ringed PAHs in water samples have been reported previously (Santos *et al*., 2018b). The dominance of the 4-ringed PAHs is obvious amongst the 16 US EPA PAHs, however the prevalence of the 3-ringed PAHs at site DB relative to sites DA and DC, suggest petrogenic contribution from anthropogenic activities near site DB. The 3-ringed PAHs are dominant in petroleum, their prevalence is usually linked to atmospheric deposition and petroleum contamination, while the prevalence of the 4-ringed PAHs at all the sampling sites suggested that PAHs contaminations were predominantly from pyrogenic sources. This observation is in line with that of Santos *et al*. (2018b), who assessed the distribution and seasonal variations of PAHs in a tropical estuarine system.

Table 4.11: Fractions of PAHs congeners in water samples of the Diep River

PAHs	**Site**		
	DA	**DB**	**DC**
% 2-ringed	4.46	3.13	4.65
% 3-ringed	17.70	28.32	14.63
% 4-ringed	50.14	42.06	49.23
% 5-ringed	13.24	11.74	15.85
% 6-ringed	14.46	14.75	15.65

Site DA: Nature reserve (upstream). Site DB: Theo Marais Sports Club – industrial and residential area. Site DC: Woodbridge (downstream).

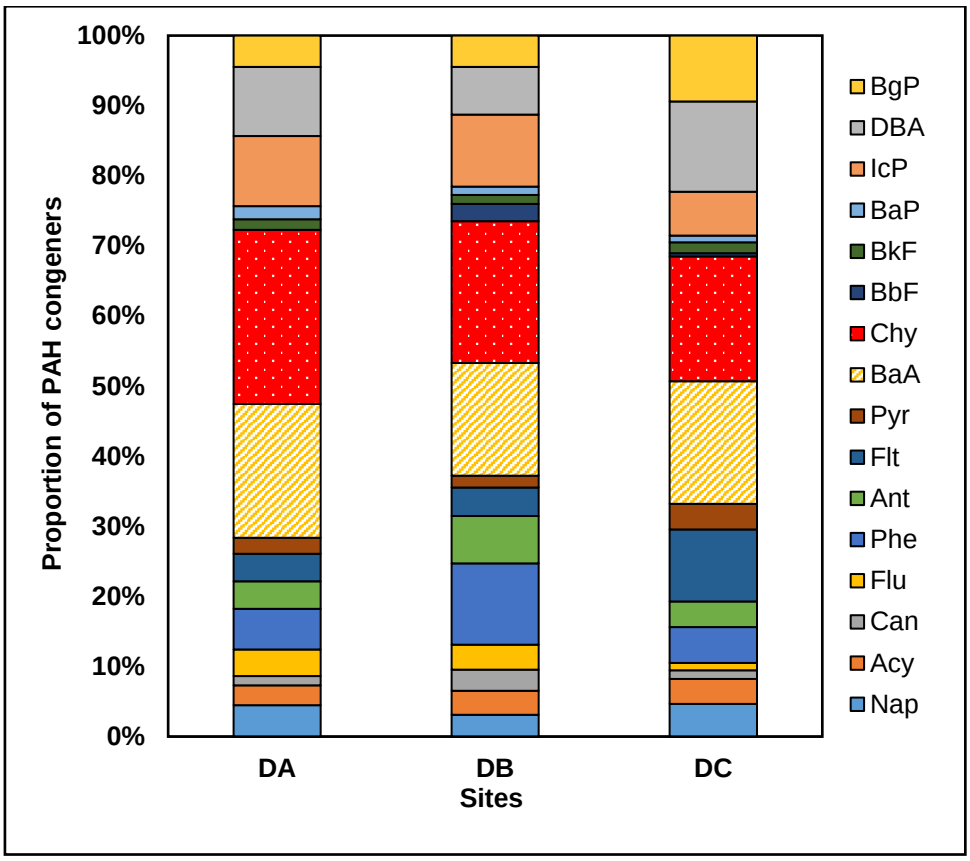

Figure 4.4: Fractions of PAHs in water samples of the Diep River

4.3.1.2 Levels of PAHs in surface water samples of the Plankenburg River

The spatial and temporal (seasonal) distribution of 16 US EPA priority PAHs were also assessed in water samples of the Plankenburg River. Results obtained from the assessment are presented in Appendices E1 and C2. The seasonal average of each detected PAH in water samples from the Plankenburg River at the studied sites ranged between 0.39 µg/L and 67.50 µg/L. Temporal variation was observed in PAHs levels at the studied sites, with the highest levels recorded in summer with the exception of site PC (Figure 4.5). Elevated levels of PAHs in summer months and prevalence of carcinogenic PAHs (which ranged between 39.36 to 87.17%) were also observed in water samples of the Plankenburg River similar to those of the Diep River.

Spatial variation was also observed in the annual average levels of the total 16 US EPA priority PAHs, with the highest level (187.11 µg/L) at the site located in an industrial area (site PC), followed by the site in an informal settlement (site PB) with a total PAHs value of 149.51µg/L (Figure 4.5). The upstream site of the river (site PA), which is in an agricultural area and the downstream site (site PD) close to its conflux, both had lower levels (119.06 µg/L and 119.57 µg/L respectively). High levels of PAHs in the industrial area and low levels upstream were also observed for the studied sites of the Diep River. Hence, anthropogenic activities around the sampling sites contributed to the occurrence of PAHs at both rivers. Numerous studies had observed similar trends, points associated with industrial activities often have higher levels of PAHs (Liu *et al*., 2016a; Ranjbar Jafarabadi *et al*., 2017; Cetin *et al*., 2017).

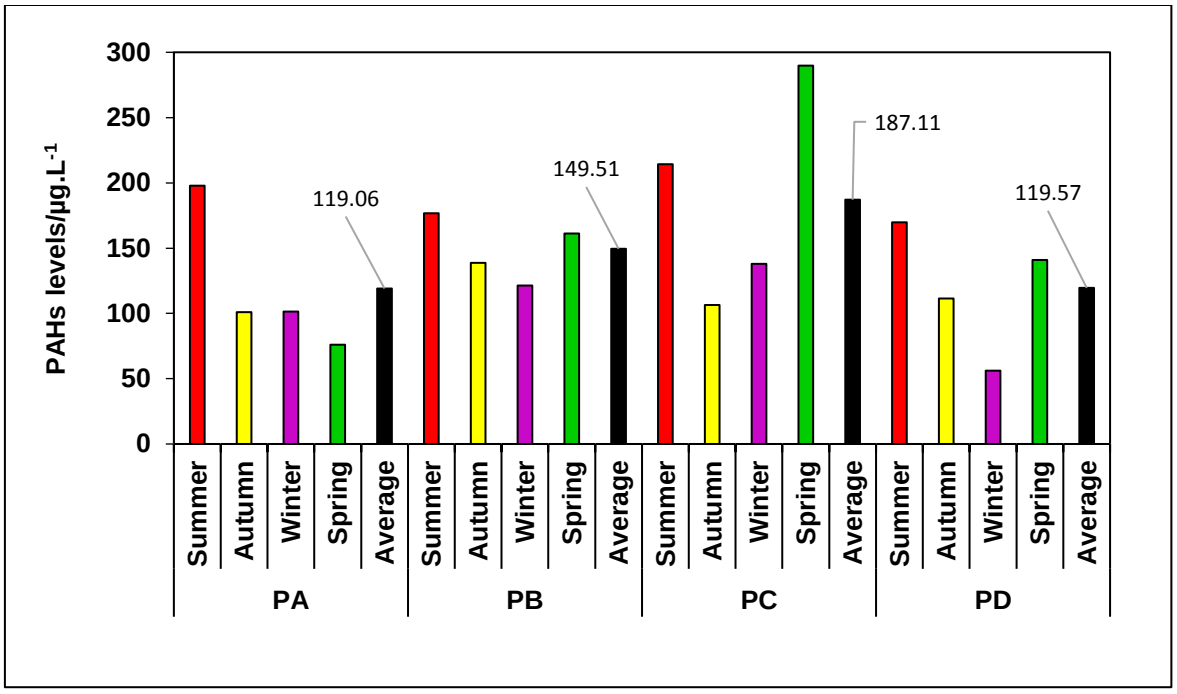

Figure 4.5: Seasonal variations and annual average levels of 16 US EPA priority PAHs in water samples of the Plankenburg River

Statistical analysis (two-way ANOVA, multivariate test) showed that sampling sites had significant effect on total concentrations of PAHs measured in water samples from the Plankenburg River ($P< 0.05$, $F= 9.223$), relative to seasonal variations ($P > 0.05$, $F=2.733$) as shown in Appendix F. Anthropogenic activities near sampling sites had been reported previously to significantly influence the total concentration of PAHs measured relative to seasonal variations (Ravindra *et al*., 2006). Ravindra *et al*. (2006) identified vehicular emission as an import anthropogenic source of PAHs. Chen *et al*. (2007) also reported that there were no obvious seasonal variations in PAHs concentrations in water samples during their study carried out over four seasons. They reported ∑15PAHs concentrations that ranged from 70.3 to 1844.4 ng/L.

Acenaphthylene, phenanthrene, anthracene, benzo[a]anthracene, chrysene, indeno[1, 2, 3-cd]pyrene, dibenzo[a, h]anthracene and benzo[g, h, i]perylene were frequently detected across the studied sites. The annual distribution pattern of the studied PAHs is shown in Figure 4.6. Occurrence was similar to that found in the Diep River; chrysene followed by benzo[a]anthracene were the highest contributors to the PAH-burden in water samples. The order is chrysene (20.92%) > benzo[a]anthracene (18.62%) > indeno[1, 2, 3-cd]pyrene (11.76%) > phenanthrene (8.32%) > dibenzo[a, h]anthracene (6.56%) > anthracene (5.17%) > benzo[b]fluoranthene (4.99%) > benzo[g, h, i]perylene (4.93%) > fluorene (4.10%) fluoranthene (3.42%) > benzo[k]fluoranthene (3.03%) > acenaphthylene (2.04%) > pyrene (2.00%) > naphthalene (1.80%) > benzo[a]pyrene (1.21%) > acenaphthene (1.11%). The 4-ringed PAHs were also the most abundant in water samples of the Plankenburg River, while the 2-ringed PAH was the least abundant (Table 4.12 and Figure 4.7).

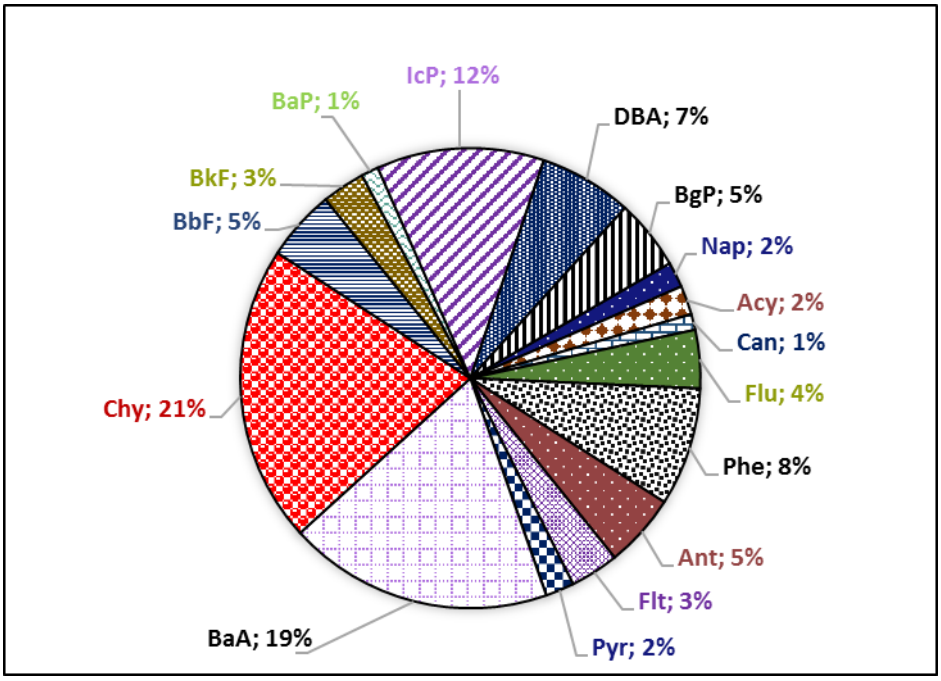

Figure 4.6: Annual distribution of 16 US EPA PAHs in water samples of the Plankenburg River

Table 4.12: Fractions of PAHs congeners in water samples of the Plankenburg River

PAHs	Site			
	PA	PB	PC	PD
% 2-ringed	1.60	2.01	1.44	2.34
% 3-ringed	17.04	28.31	15.76	22.54
% 4-ringed	50.21	37.35	45.03	49.17
% 5-ringed	13.35	15.60	18.11	15.03
% 6-ringed	17.80	16.73	19.66	10.93

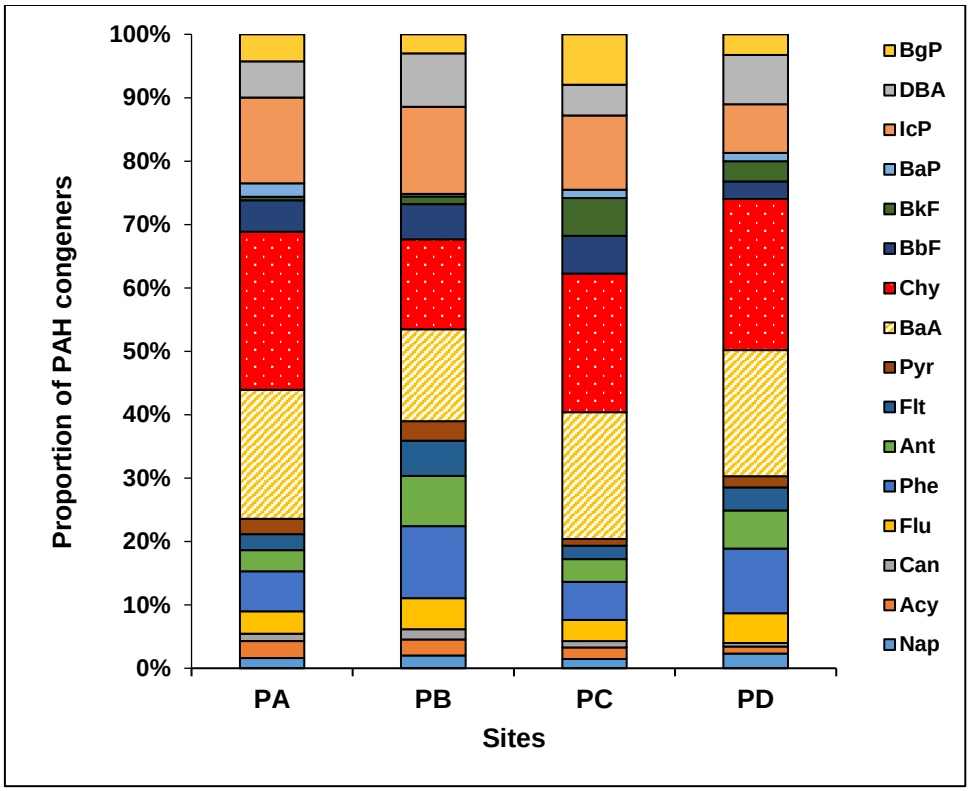

Figure 4.7: Fractions of PAHs in water samples of the Plankenburg River

The annual average of the 16 US EPA priority PAHs in water samples from the studied sites on the Diep and Plankenburg rivers ranged between 73.90 and 187.11µg/L; the concentrations of carcinogenic PAHs ranged between 49.56 and 133.95 µg/L. The site PC on the Plankenburg River (associated with industrial activities) had the highest annual average of PAHs measured (Figure 4.8). Generally, the distribution pattern of the PAHs was observed to be similar, with higher PAH levels detected at sites associated with industrial activities (petroleum refining and chemical production) i.e. sites DB and PC (Figure 4.8). The 4-ringed PAHs were detected as the most abundant in water samples of the two rivers (Figure 4.9). The prevalence of 4-ringed and heavier PAHs in aquatic systems have been attributed to biomass combustion and due to poor solubility of PAHs in water, the heavier PAHs are expected to settle into the sediment compartment (Guo *et al*., 2007; Chen & Chen, 2011; Santos *et al*., 2018b).

The annual average of each detected PAH in the investigated rivers, ranged between 0.45 and 40.87 µg/L (Table 4.13). The levels detected exceeded 0.015 to 5.800 µg/L range, the threshold of water quality guideline, recommended for the protection of aquatic life (Canadian Council of Ministers of the Environment (CCME), 1999; US EPA, 2006) (Table 4.14). Hence, water samples of the Diep and Plankenburg Rivers were highly polluted with PAHs and capable of impacting aquatic lives adversely.

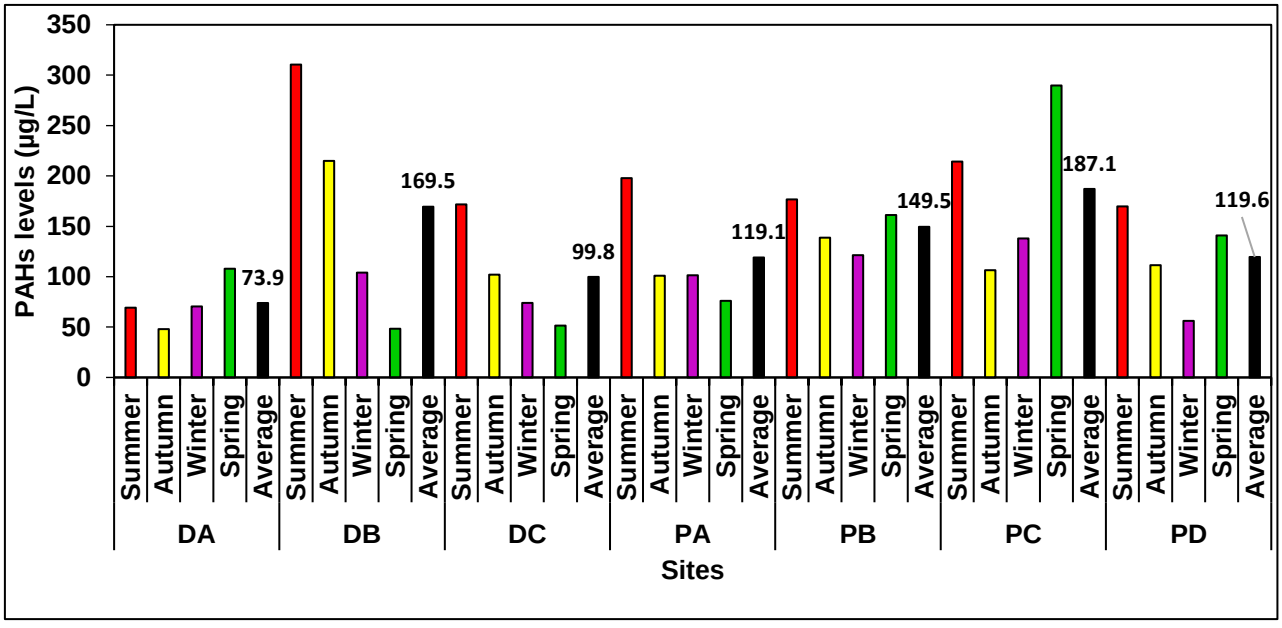

Figure 4.8: Seasonal variations and annual average levels of 16 US EPA priority PAHs in water samples of the Diep and Plankenburg Rivers

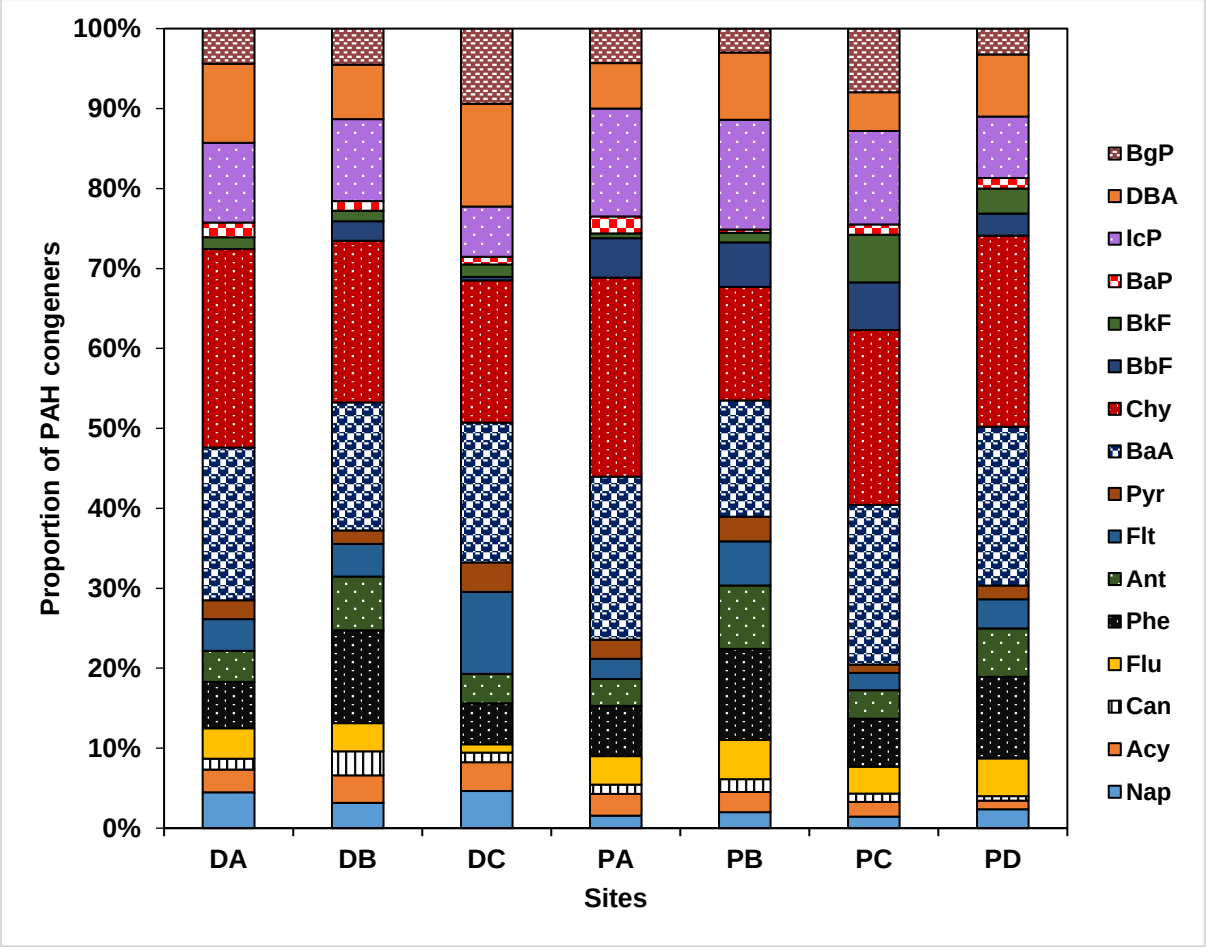

Figure 4.9: Fractions of PAHs in water samples of the Diep and Plankenburg Rivers

Table 4.13: Annual average concentrations of PAHs in water samples of the Diep and Plankenburg Rivers

Sites	PAHs concentrations (µg/L)																	
	Nap	Acy	Can	Flu	Phe	Ant	Flt	Pyr	BaA	Chy	BbF	BkF	BaP	IcP	DBA	BgP	∑16 PAHs	∑CPAHs
DA	3.31	2.10	1.01	2.82	4.28	2.88	2.94	1.75	14.09	18.37	nd	1.08	1.37	7.35	7.30	3.26	73.91	49.56
DB	5.34	5.83	5.09	6.01	19.66	11.37	6.91	2.86	27.16	34.26	4.15	2.22	2.02	17.39	11.53	7.64	169.47	98.73
DC	4.64	3.59	1.21	1.05	5.11	3.65	10.23	3.69	17.45	17.76	0.45	1.54	0.96	6.26	12.86	9.37	99.81	57.29
PA	1.87	3.24	1.37	4.24	7.50	3.98	3.00	2.90	24.25	29.66	5.87	0.71	2.50	16.05	6.80	5.13	119.06	85.84
PB	2.97	3.81	2.39	7.34	17.01	11.84	8.29	4.59	21.75	21.23	8.34	1.79	0.56	20.54	12.57	4.50	149.51	86.77
PC	2.70	3.41	1.94	6.34	11.20	6.72	4.01	1.97	37.36	40.87	11.21	11.17	2.36	21.87	9.10	14.86	187.11	133.95
PD	2.83	1.27	0.70	5.64	12.20	7.21	4.35	2.08	23.76	28.57	3.28	3.75	1.56	9.21	9.28	3.88	119.57	79.41

Nap: Naphthalene. Acy: Acenaphthylene. Can: Acenaphthene. Flu: Fluorene. Phe: Phenanthrene. Ant: Anthracene. Flt: Fluoranthene. Pyr: Pyrene. BaA: Benzo[a]anthracene. Chy: Chrysene. BbF: Benzo[b]fluoranthene. BkF: Benzo[k]fluoranthene. Bap: Benzo[a]pyrene. BgP: Benzo[g, h, i]perylene. IcP: Indeno[1, 2, 3-cd]pyrene. DBA: Dibenzo[a, h]anthracene. BgP: Benzo[g, h, i]perylene.

CPAHs: Carcinogenic PAHs (BaA, Chy, BbF, BkF, BaP IcP and DBA)

Table 4.14: Regulatory threshold limits of PAHs in sediment and water for the protection of aquatic life

PAHs	Carcinogenicity	Sediment µg/g			Water µg/L
		ISQG	PEL	FSSB	WQG
Naphthalene	NC	0.03460	0.39100	0.1760	1.10000
Acenaphthylene	NC	0.00587	0.12800	0.0059	-
Acenaphthene	NC	0.00671	0.08890	0.0067	5.80000
Fluorene	NC	0.02120	0.14400	0.0774	3.00000
Phenanthrene	NC	0.04190	0.51500	0.2040	0.40000
Anthracene	NC	0.04690	0.24500	0.0572	0.01200
Fluoranthene	WC	0.11100	2.35500	0.4230	0.04000
Pyrene	NC	0.05300	0.87500	0.1950	0.02500
Benzo [a] anthracene	C	0.03170	0.38500	0.1080	0.01800
Chrysene	C	0.05710	0.86200	0.1660	-
Benzo [b] fluoranthene	C	-	-	0.0272	-
Benzo [k] fluoranthene	C	-	-	0.2400	-
Benzo [a] pyrene	SC	0.03190	0.78200	0.1500	0.01500
Benzo [g, h, i] perylene	NC	-	-	0.1700	-
Indeno [1,2,3-cd] pyrene	C	-	-	0.0170	-
Dibenzo [a, h] anthracene	C	0.00622	0.13500	0.0330	-

Adapted from CCME 1999; US EPA 2006

NC: Non-Carcinogenic. C: Carcinogenic. WC: Weakly Carcinogenic. SC: Strongly Carcinogenic. ISQG: Interim Sediment Quality Guideline. PEL: Probable Effect Level. FSSB: Freshwater Sediment Screening Benchmarks. WQG: Water Quality Guideline.

4.3.2 Levels of PAHs in sediment samples

4.3.2.1 Levels of PAHs in sediment samples of the Diep River

Data obtained on the seasonal (temporal) levels of 16 priority US EPA PAHs in sediment samples of the Diep River is presented in Appendices G1 and G2. The seasonal detected levels of each PAH in the sediment samples ranged between 0.002 µg/g and 16.652 µg/g, the seasonal ∑16PAHs ranged between 2.867 µg/g and 70.706 µg/g, and proportion of carcinogenic PAHs obtained ranged between 25.16% and 77.44%. The PAH levels in sediment samples were higher than those measured in corresponding water samples. Higher levels of PAHs in sediment samples had been previously reported (Qiao *et al*., 2008; Ma *et al*., 2013; Hong *et al*., 2016); sediment serves as sink for PAHs and therefore accumulates PAHs. Detected levels in autumn were generally high and as observed with water samples, site DB, associated with industrial activity (oil refinery) was the most contaminated site with the 16 US EPA priority PAHs (annual average of 38.21 µg/g) and site DA a nature reserve, the least contaminated (annual average of 6.05 µg/g) (Figure 4.10).

The overall distribution of PAHs in sediments of the Diep River over a one-year sampling period is; phenanthrene (14.88%) > benzo[b]fluoranthene (14.62%) > benzo[k]fluoranthene (14.37%) > benzo[a]pyrene (9.77%) > fluoranthene (9.04%) > chrysene (5.96%) > naphthalene (5.19%) > benzo[a]anthracene (4.83%) > dibenzo[a, h]anthracene (4.59%) > indeno[1, 2, 3-cd]pyrene (4.52%) > benzo[g, h, i]perylene (3.20%) > pyrene (2.49%) > acenaphthene (2.05%) > anthracene (1.94%) > fluorene (1.61%) > acenaphthylene (0.94%) (Figure 4.11). The compositional pattern of PAHs in sediment samples, differed from that observed in corresponding water samples. The HMW PAHs (5- and 6- ring) had the highest proportion (51.07%), in contrast to the 4-ringed PAHs in water samples. The prevalence of HMW PAHs in sediment samples had been previously reported (Guo *et al*., 2007; Chen & Chen, 2011). This was attributed to pollution sources and the more recalcitrant nature of the compounds unlike the LMW PAHs. The HMW PAHs are less susceptible to biodegradation and photo-oxidation in water (Abdel-Shafy & Mansour, 2016).

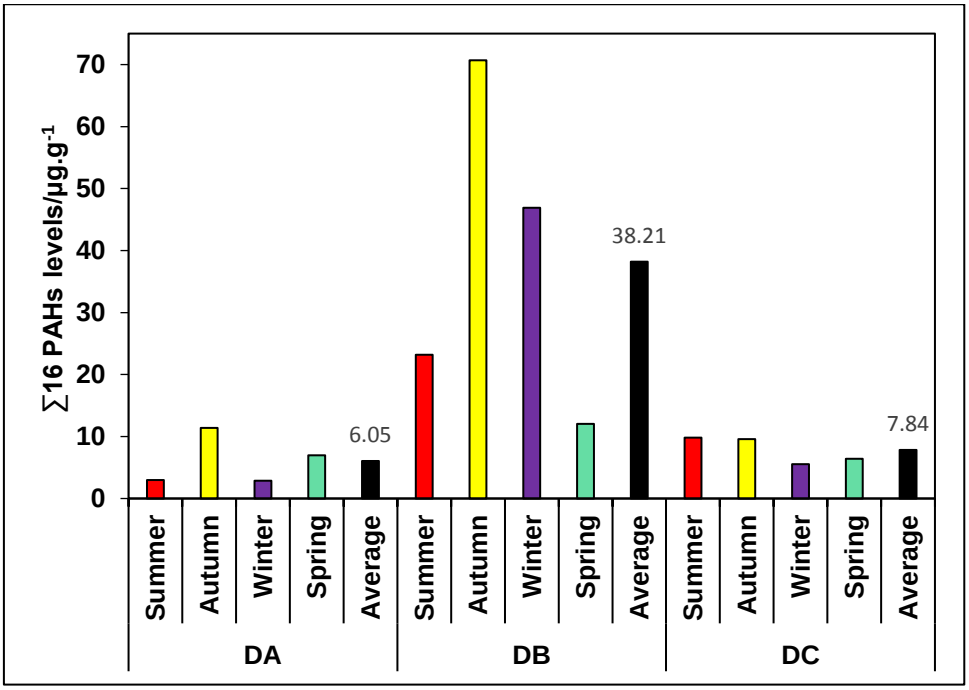

Figure 4.10: Seasonal variations and annual average levels of 16 US EPA PAHs in sediment samples of the Diep River

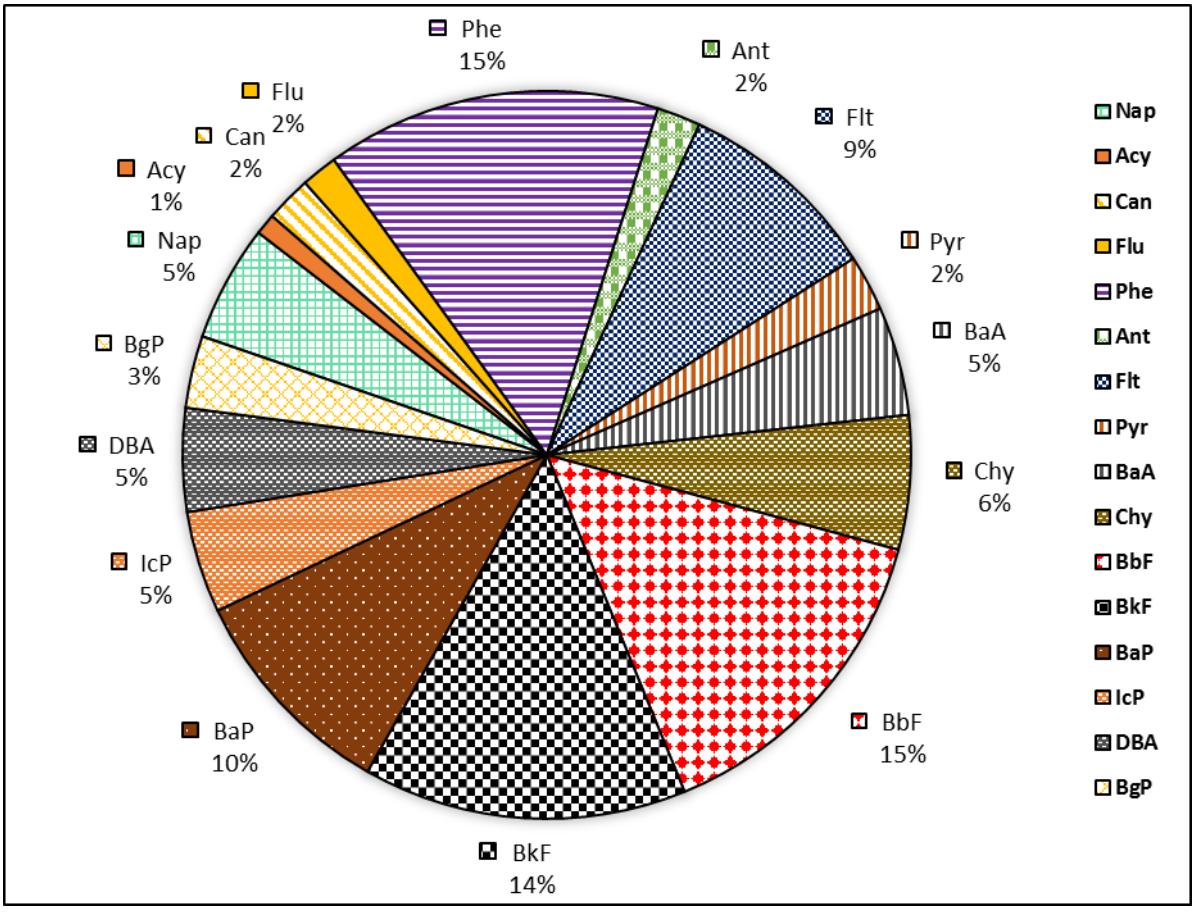

Figure 4.11: Annual distribution of 16 US EPA PAHs in sediment samples of the Diep River

The PAH distribution obtained in sediment samples from studied sites showed that the 5-ringed PAHs were the most abundant, followed by the 4-ringed PAHs (except at DB with higher 3-ringed PAHs) as shown in Figure 4.12 and Table 4.15. The site DB is associated with oil refining and the higher 3-ringed PAHs observed could be attributed to petroleum contamination from industrial effluent (Santos *et al*., 2018b). The predominance of HMW PAHs relative to LMW PAHs in sediment samples had been reported previously and attributed to pyrogenic PAHs from combustion of fossil fuels and vehicle exhausts (Nekhavhambe *et al*., 2014).

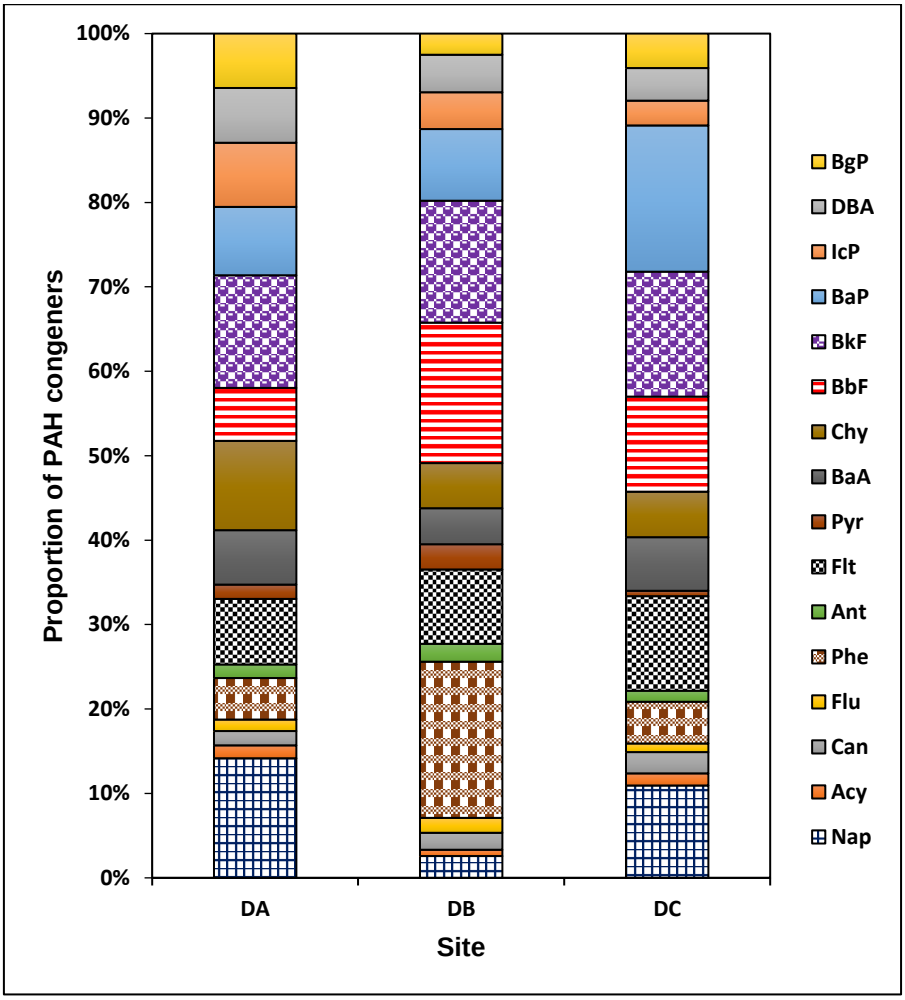

Figure 4.12: Fractions of PAHs in sediment samples of the Diep River

Table 4.15: Fractions of PAHs congeners in sediment samples of the Diep River

PAHs	Site		
	DA	DB	DC
% 2-ringed	14.19	2.58	10.97
% 3-ringed	11.16	25.14	11.16
% 4-ringed	26.41	21.40	23.57
% 5-ringed	35.31	43.93	46.36
% 6-ringed	12.93	6.95	7.95

4.3.2.2 Levels of PAHs in sediment samples of the Plankenburg River

All 16 priority US EPA PAHs were detected in sediment samples from studied sites on the Plankenburg River (Appendices H1 and H2). The seasonal levels of each PAH across the studied sites ranged between 0.006 µg/g and 27.869 µg/g (Figure 4.13). The annual average concentrations of the 16 US EPA priority PAHs measured, ranged between 21.783 µg/g and 39.656 µg/g. Higher prevalence of carcinogenic PAHs fractions (ranged between 48.81 and 91.84%) was observed in sediment samples compared to corresponding water samples (with values between 39.36 and 87.17%). This may be due to the fact that carcinogenic PAHs (consisting of 4- to 6-ringed PAHs) have low water solubility and become associated readily with sediment (Ma *et al*., 2013). Motor vehicles are regarded as a major source of carcinogenic PAHs especially in urban areas (Stogiannidis & Laane, 2015). The site PC, associated with industrial activities had the highest annual PAHs levels (39.66 µg/g). Unlike in water samples, the site prone to impact by agricultural activities (Site PA) had higher annual PAHs average (31.29 µg/g) relative to the point close to the informal settlement (Site PB) with an annual average of 21.79 µg/g. Anthropogenic PAHs contribution from agricultural activities could have preceded the contribution by activities at the informal settlement. The sediment compartment reveals the history of contamination in an aquatic environment, while contamination in water is more as a result of local pollution (Ma *et al*., 2013). Higher total PAHs concentrations (∑6PAHs) of up to 61.764 µg/g in sediment samples in Limpopo Province (South Africa) had been reported previously (Nekhavhambe *et al*., 2014). They attributed PAH levels measured to automobile exhausts, lubricating oil, atmospheric disposition, domestic heating and refuse burning. Edokpayi *et al*. (2016) reported total PAHs concentrations (∑10PAHs) range of 27.10 to 55.93 µg/g in sediment samples of Vhembe District Rivers (South Africa), which is comparable to the range measured in this study (Figure 4.13). They identified biomass combustion as the major possible source of PAHs.

The temporal variation showed higher PAHs concentrations during the dry season (summer and autumn) in general and the lowest PAHs levels in winter (Figure 4.13). This may be attributed to winter rain, causing a dilution effect due to the higher flow rate of the river. A high river flow rate can wash off surface sediment, leading to a reduction in total concentration of PAHs (Chen *et al*., 2007). However, the site PB associated with the informal settlement had its highest PAHs level in winter (35.33 µg/g); this could be as a result of uncontrolled residential heating in winter (Hong *et al*., 2016). The indiscriminate dumping of refuse into the river channel at site PB, could also have resulted in the accumulation of sediment washed down from upstream in winter, which led to the increase in PAHs levels. The overall maximum PAHs concentrations observed in the dry season

are consistent with the observations of Doong & Lin (2004) and Gdara *et al*. (2017) in sediment samples of the Gao-ping River (Taiwan) and Wadi El Bay Watershed (Tunisia) respectively.

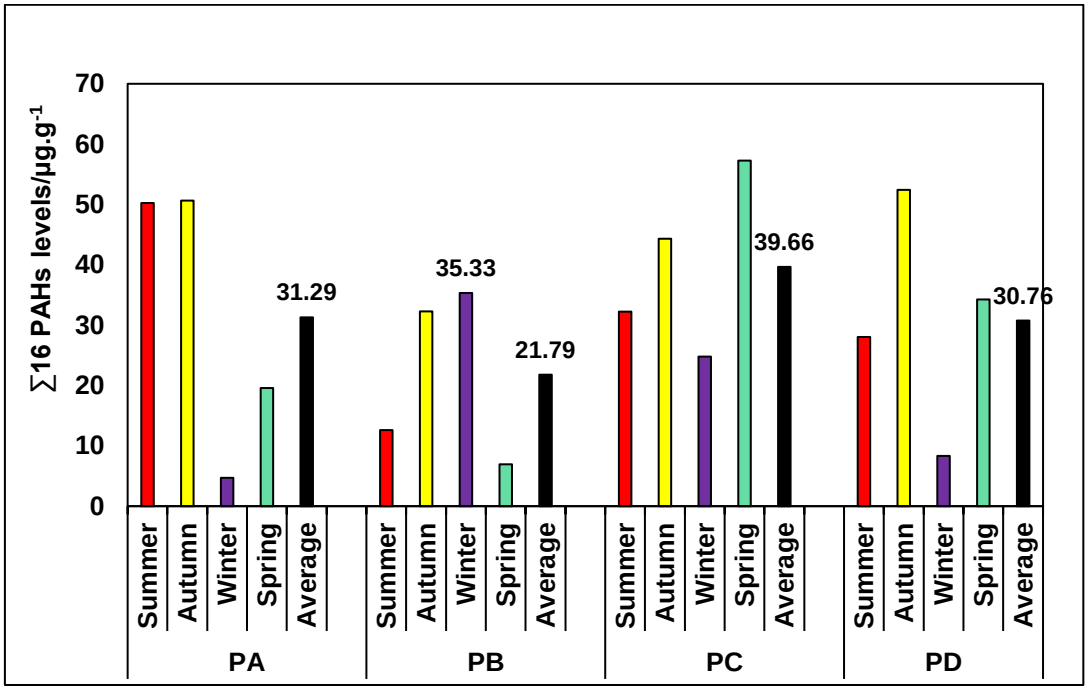

Figure 4.13: Seasonal variations and annual average levels of 16 US EPA priority PAHs in sediment samples of the Plankenburg River

The PAH distribution in sediment samples of the Plankenburg River was in the order benzo[b]fluoranthene > benzo[k]fluoranthene > phenanthrene > benzo[a]pyrene > naphthalene > fluoranthene > dibenzo[a, h]anthracene > chrysene > benzo[a]anthracene ≥ anthracene > indeno[1,2,3-cd]pyrene > benzo[g, h, i]perylene > pyrene > fluorene > acenaphthylene >acenaphthene (Figure 4.14). Occurrences of the different compounds was similar to those observed in sediment samples of the Diep River. The HMW PAHs (5- and 6-ring) occurred most in contrast to the abundance of 4-ringed PAHs in corresponding water samples.

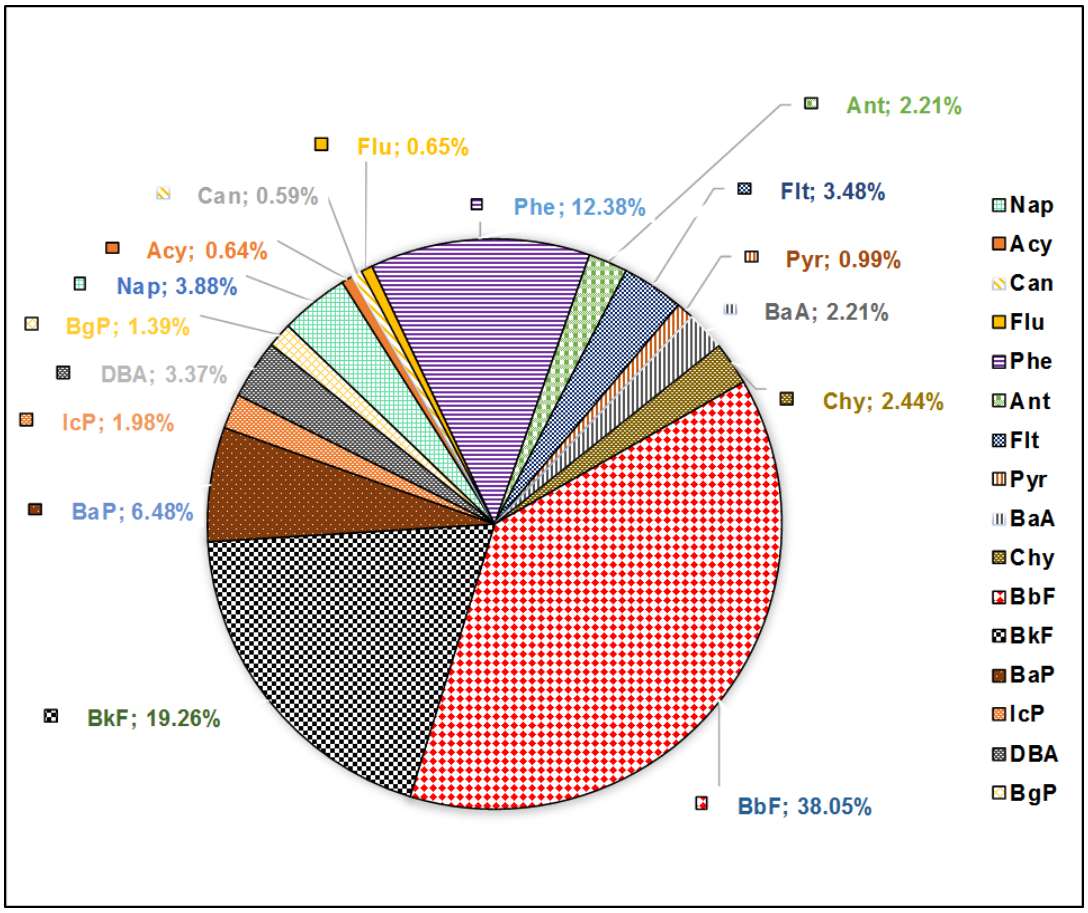

Figure 4.14: Annual distribution of 16 US EPA priority PAHs in sediment samples of the Plankenburg River

The 5-ringed PAHs were the dominant PAHs observed in sediment samples, contributing between 51.09% and 78.92% of the total 16 US EPA priority PAHs (Table 4.16). Figure 4.15 shows the annual distribution of PAHs in sediment samples of the Plankenburg River. Benzo[b]fluoranthene (19.46 to 77.39%), benzo[k]fluoranthene (12.89 to 40.52%) and phenanthrene (10.13 to 17.40%) were the major contributors to the PAH-burden in sediment of the studied sites. This indicates that, PAHs contributions were from both petrogenic (3-ring) and pyrolytic (above 4-ring) sources (Santos *et al*., 2018b). The abundance of benzo[b]fluoranthene relative to other PAHs in sediment samples of South Africa was previously reported by Edokpayi *et al*. (2016), which they attributed to biomass combustion.

Table 4.16: Fractions of PAHs congeners in sediment samples of the Plankenburg River

PAHs	Site			
	PA	PB	PC	PD
% 2-ringed	3.35	7.03	2.87	3.48
% 3-ringed	12.67	22.60	12.42	21.20
% 4-ringed	13.80	14.06	4.32	7.06
% 5-ringed	58.71	51.09	78.92	66.40
% 6-ringed	11.47	5.22	1.46	1.86

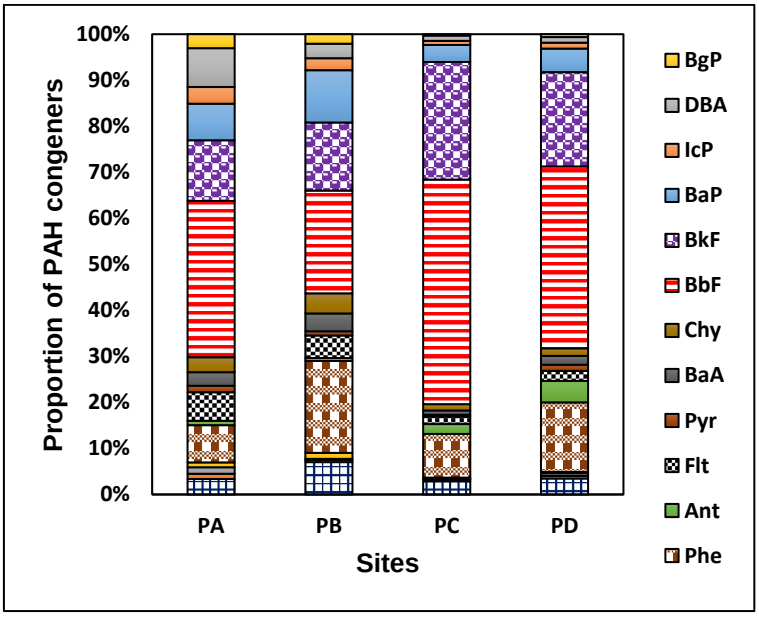

Figure 4.15: Fractions of PAHs in sediment samples of the Plankenburg River

The high portion of HMW PAHs in sediment samples of the Diep and Plankenburg Rivers, suggested that pyrogenic processes were the primary source of PAHs in these aquatic systems. The levels of PAHs detected varied with seasons, with the highest levels obtained in autumn for most sites and lowest in winter (Figure 4.16). The trend of values obtained were similar to those of water samples. The points associated with industrial activities were the most contaminated sites. Data from both the Diep and Plankenburg Rivers were subjected to two-way ANOVA multivariate analysis. The results obtained, showed that sampling sites ($P<0.05$, $F= 8.484$) rather than seasonal regimes ($P>0.05$, $F= 2.600$) had significant effects on measured levels of PAHs (Appendices I and J).

The annual average values of PAHs for sites PC and DB were 39.66 µg/g and 38.21 µg/g respectively. Carcinogenic PAHs' annual average in sediment samples ranged from 3.56 to 32.67 µg/g (Table 4.17); the results were similar to those observed in water samples with site PC having the highest level of carcinogenic PAHs. The lowest annual total and carcinogenic PAHs average (6.05 µg/g and 3.56 µg/g respectively) were recorded for the site DA at the nature reserve (Table 4.17).

Data obtained indicated that PAHs' levels in both rivers were largely influenced by localised anthropogenic activities. The nature of sediment samples (Appendix K) might have influenced the levels of PAHs detected in sediment samples. Total organic carbon, organic matter and particle size of sediment have been reported to influence sorption of PAHs (Ahangar, 2010; Olu-owolabi *et al*., 2014; Gu *et al*., 2016).

Comparison of the interim sediment quality guideline (ISQG) and the probable effect level (PEL) threshold limits of PAHs (Table 4.14) to the annual average measured in analysed sediment samples (Table 4.17) showed carcinogenic PAH pollution. The monitored aquatic systems were highly polluted with strongly carcinogenic PAH [benzo[a]pyrene (BaP)]. The annual average of BaP obtained ranged from 0.49 to 3.24 µg/ g (Table 4.17), which exceeded the ISQG (0.03190 µg/g) and the PEL (0.782 µg/g) for BaP (Table 4.14). The observed levels of BaP are therefore, detrimental to aquatic lives and capable of impacting human health adversely.

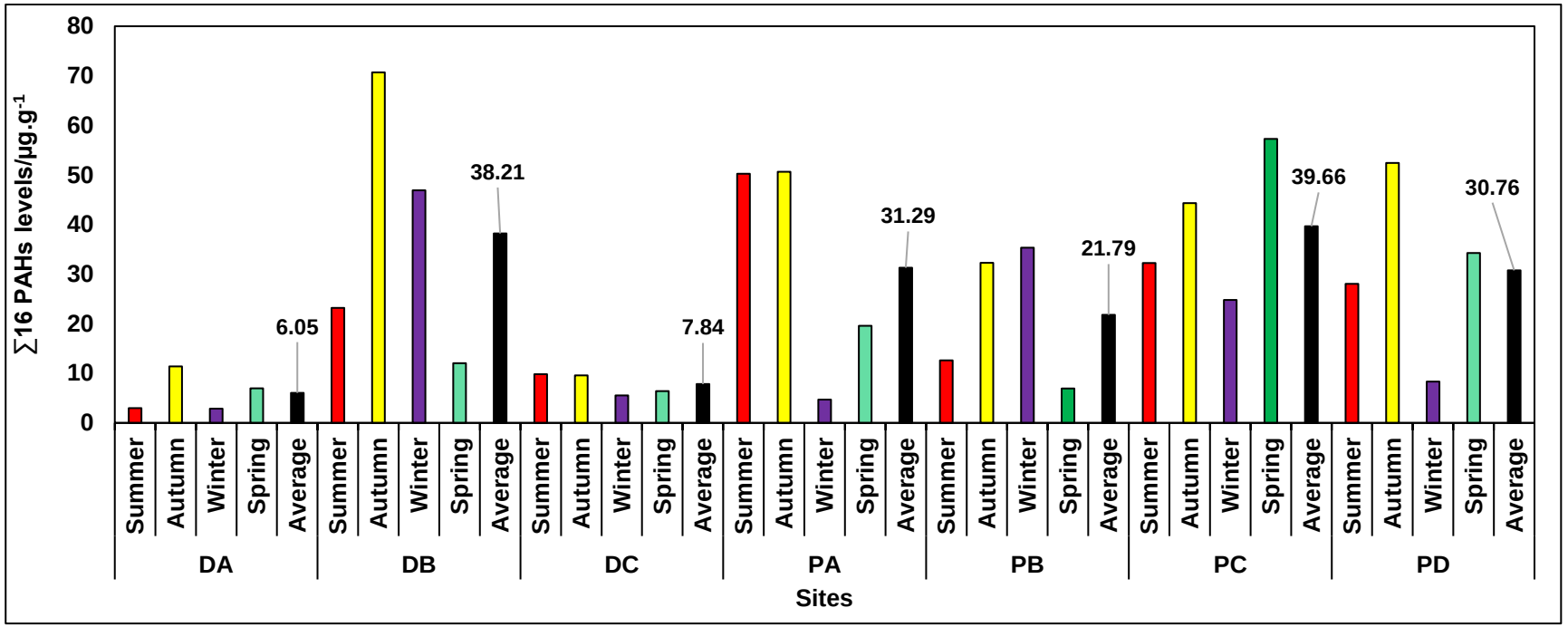

Figure 4.16: Seasonal variations and annual average levels of 16 US EPA priority PAHs in sediment samples of the Diep and Plankenburg Rivers

Table 4.17: Annual average concentrations of PAHs in sediment samples of the Diep and Plankenburg Rivers

Sites	PAHs levels (µg/g)																	
	Nap	**Acy**	**Can**	**Flu**	**Phe**	**Ant**	**Flt**	**Pyr**	**BaA**	**Chy**	**BbF**	**BkF**	**BaP**	**IcP**	**DBA**	**BgP**	**∑16 PAHs**	**∑C PAHs**
DA	0.859	0.093	0.101	0.082	0.299	0.101	0.469	0.100	0.387	0.641	0.378	0.807	0.491	0.459	0.394	0.389	6.049	3.557
DB	0.987	0.285	0.769	0.675	7.067	0.810	3.361	1.142	1.631	2.042	6.355	5.516	3.244	1.668	1.698	0.958	38.210	22.155
DC	0.859	0.112	0.198	0.077	0.386	0.101	0.876	0.051	0.495	0.424	0.883	1.159	1.359	0.231	0.303	0.321	7.833	4.853
PA	1.048	0.356	0.445	0.330	2.533	0.301	1.935	0.442	0.922	1.019	10.625	4.125	2.485	1.136	2.640	0.950	31.292	22.953
PB	1.532	0.106	0.047	0.282	4.349	0.138	1.068	0.196	0.846	0.952	4.867	3.220	2.474	0.569	0.684	0.453	21.783	13.612
PC	1.140	0.151	0.063	0.099	3.764	0.850	0.631	0.172	0.370	0.541	19.344	10.131	1.469	0.352	0.461	0.117	39.656	32.669
PD	1.070	0.170	0.179	0.091	4.645	1.437	0.664	0.412	0.592	0.504	12.157	6.305	1.574	0.393	0.378	0.195	30.763	21.902

4.3.3 Levels of PAHs in plant samples of the Diep and Plankenburg Rivers

The bioaccumulation potential of PAHs in plants was investigated in this study. Concentrations of PAHs in plant samples of the Diep and Plankenburg Rivers were quantified.

4.3.4.1 Levels of PAHs in plant samples (*E. crassipes* and *P. australis*) of the Diep River

Eichhornia crassipes (water hyacinth) samples were collected at sites DA and DC; *Phragmites australis* (common reed) was collected from site DB. The water hyacinth was analysed whole, while the common reed was divided into leaves, stems and roots. The total PAHs concentrations measured in *E. crassipes* samples of the Diep River were 169.26 µg/g and 72.08 µg/g for sites DA and DC respectively; the corresponding percentages of carcinogenic PAHs were 70.60 and 66.98 (Table 4.18a). The total PAHs average concentration of 226.72 µg/g and 61.91% carcinogenic PAHs were measured in *P. australis* of site DB (Table 4.18b). The levels of PAHs in plants were higher than those recorded for sediment samples. The observation was consistent with previous studies reported in the literature (O'Connor, 1996; Howsam *et al*., 2001; Huang *et al*., 2004; Sojinu *et al*., 2010). Sojinu *et al*. (2010) reported the sum of 28 target PAHs of 80 ng/g, 168 ng/g and 1430 µg/kg on average, in soil, sediment and plant samples respectively. The plant sample from site DB (proximal to oil refinery) had the highest PAH levels (∑PAHs plant average of 226.72 µg/g), and the distribution of PAHs in their tissues follows the order of leaves (∑PAHs of 411.64 µg/g) > stems (173.29 µg/g) > roots (∑PAHs of 95.24 µg/g) [Figure 4.17]. Higher PAHs concentrations in aerial part of plants relative to roots had been reported previously (Tao *et al*., 2004; Wang *et al*., 2012b). Tao *et al*. (2004) reported ∑16PAHs of up to 0.984 µg/g in the aerial part of vegetables relative to 0.201 µg/g in the roots. This was attributed to atmospheric uptake of PAHs by leaves (through cuticular waxes or by stomatal uptake) as the major pathway relative to absorbed PAHs from sediments.

Table 4.18a: Levels of PAHs (mean (n = 3) ± SD) in *E. crassipes* samples of the Diep River

PAHs (µg/ g)	Site DA	Site DC
Nap	nd	0.20 ± 0.14
Acy	2.59 ± 0.71	nd
Can	1.20 ± 0.94	0.70 ± 0.32
Flu	nd	3.83 ± 2.71
Phe	na	na
Ant	na	na
Flt	5.35 ± 0.48	1.87 ± 1.11
Pyr	7.78 ± 2.87	0.65 ± 0.11
BaA	23.22 ± 0.91	1.51 ± 1.23
Chy	47.84 ± 1.84	4.64 ± 5.25
BbF	nd	0.77 ± 0.05
BkF	23.30 ± 1.01	25.44 ± 2.54
BaP	12.06 ± 5.15	4.64 ± 2.60
IcP	3.84 ± 0.11	4.67 ± 1.84
DBA	9.23 ± 0.48	6.61 ± 2.32
BgP	32.83 ± 0.68	16.56 ± 14.50
∑ PAHs	169.26	72.08
∑C PAHs	119.49	48.28
% C PAHs	70.60	66.98

Site DA: Nature reserve (upstream). Site DC: Woodbridge (downstream). nd: not detected. na: not available. C PAHs: Carcinogenic PAHs

Table 4.18b: Levels of PAHs (mean (n = 3) ± SD) in *P. australis* tissues of the Diep River

PAHs (µg/g)	Site DB		
	leaves	**stems**	**roots**
Nap	8.81 ± 8.84	7.33 ± 9.41	10.43 ± 0.47
Acy	0.62 ± 0.44	0.82 ± 0.58	0.73 ± 0.09
Can	0.83 ± 0.59	1.40 ± 0.99	nd
Flu	6.94 ± 3.31	nd	nd
Phe	na	na	na
Ant	na	na	na
Flt	4.05 ± 0.27	4.25 ± 4.98	6.11 ± 5.03
Pyr	39.79 ± 12.85	44.14 ± 3.37	9.77 ± 3.19
BaA	41.25 ± 53.30	27.88 ± 11.90	6.15 ± 4.35
Chy	46.53 ± 40.98	6.51 ± 0.01	nd
BbF	15.66 ± 10.77	nd	nd
BkF	54.07 ± 65.82	5.89 ± 0.90	11.95 ± 0.24
BaP	29.77 ± 39.63	7.97 ± 0.23	16.05 ± 0.21
IcP	39.05 ± 1.12	9.57 ± 0.66	8.81 ± 2.62
DBA	55.34 ± 1.65	28.43 ± 1.58	10.18 ± 7.19
BgP	68.92 ± 23.13	29.08 ± 13.07	15.05 ± 18.79
∑PAHs	411.64	173.29	95.24
Plant ∑PAHs	226.72		
Plant ∑C PAHs	140.36		
%C PAHs	61.91		

Site DB: Theo Marais Sports Club – industrial and residential area. nd: not detected. na: not available. C PAHs: Carcinogenic PAHs

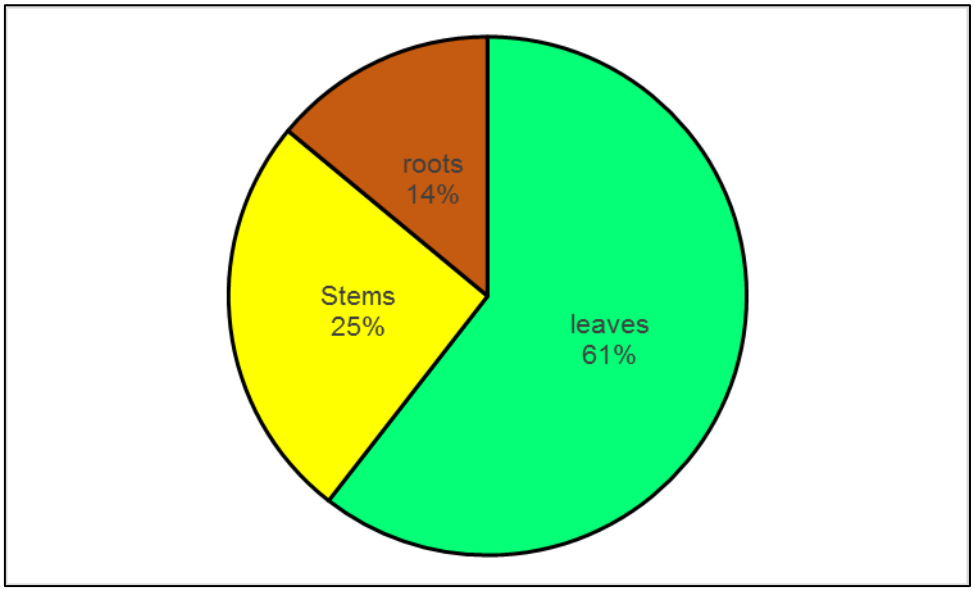

Figure 4.17: Occurrence of PAHs in *P. australis* tissues of the Diep River (site DB)

4.3.4.2 Levels of PAHs in *P. australis* of the Plankenburg River

Phragmites australis (common reed) were collected from all four selected sites (PA, PB, PC and PD) on the Plankenburg River. Levels of PAHs were determined in roots, stems and leaves of the plant. PAHs levels in plant samples were higher than levels of PAHs detected in sediment samples. The ∑PAHs in plant tissues ranged between 42.77 µg/g and 117.89 µg/g (Tables 4.19a and 4.19b). The distribution order of PAHs in plant tissues is ∑PAHs levels in root > leaves > stem, except for site PD with distribution order of stem > leaves > root (Figure 4.18). The exception in site PD could be attributed to atmospheric PAHs from heavy vehicular movement around the site, whereas adsorption from water and sediment could be the primary PAHs uptake for the other sites. Though, the mechanism of PAHs uptake by plant is not yet fully understood, some have argued that the potential of PAHs uptake and translocation by root is low (Duarte-Davidson & Jones, 1996), while Fismes *et al*. (2002) reported high soil to root PAHs transfer and translocation. The concentrations of each PAH measured in the *P. australis* tissues (leaves, stem and root) of site PA ranged between 0.26 and 38.67 µg/g. Chrysene level was the highest in leaves (12.04 µg/g), while Benzo[a]pyrene (BaP) was the highest in both stem (20.78 µg/g) and root (38.67 µg/g). Chrysene level was also the highest in leaves (21.15 µg/g) of *P. australis* collected from site PB, while BaP was the highest in stem (24.36 µg/g), benzo[g, h, i]perylene (48.82 µg/g) followed by BaP (29.60 µg/g) in root. Concentration range of 0.09 to 48.82 µg/g PAH was measured in plant tissues of site PB. The level of BaP was the highest in leaves (11.70 µg/g), stem (19.68 µg/g) and root (40.44 µg/g) of *P. australis* collected from site PC and the measured PAH concentrations ranged from 0.14 to 40.44 µg/g. The measured concentration of BaP in leaves (13.59 µg/g) was the second highest after that of Indeno[1,2,3-cd]pyrene (17.92 µg/g), while BaP was the highest is both stem (46.39 µg/g) and root (18.34 µg/g) of *P. australis* collected at site PD, the PAH concentrations measured ranged between 0.31 and 46.39 µg/g. This shows the prevalence of strongly carcinogenic BaP and other HMW PAHs in *P. australis* samples analysed. Howsam *et al*. (2000) had previously reported high proportion of HMW PAHs (4-, 5- and 6-ring) in hazel leaves. This was attributed to the adaxial (upper) and abaxial (lower) dense hair cover of the leaves, which made the trapping of HMW atmospheric PAHs effective and less susceptible to wash-off by aqueous solution. The *P. australis* is a densely hairy plant, this might have resulted in the trapping of HMW PAHs from the air, sediment and water of the aquatic environment.

Table 4.19a: Levels of PAHs (mean (n = 3) ± SD) in *P. australis* tissues of the Plankenburg River (sites PA and PB)

PAHs (µg/g)	Site PA			Site PB		
	leaves	stems	roots	leaves	stems	roots
Nap	nd	nd	nd	nd	0.09 ± 0.06	nd
Acy	nd	0.29 ± 0.03	0.26 ± 0.18	0.32 ± 0.13	0.69 ± 0.10	nd
Can	1.46 ± 0.10	0.43 ± 0.13	nd	1.38 ± 0.12	1.10 ± 0.17	0.50 ± 0.05
Flu	5.86 ± 0.16	2.62 ± 1.86	nd	5.94 ± 0.06	3.46 ± 0.75	nd
Phe	na	na	na	na	na	na
Ant	2.93 ± 2.55	0.51 ± 0.36	9.94 ± 7.03	3.78 ± 0.13	0.44 ± 0.03	3.91 ± 2.76
Flt	2.10 ± 1.76	1.12 ± 0.57	4.92 ± 3.48	1.53 ± 0.76	0.95 ± 0.06	6.52 ± 0.77
Pyr	2.55 ± 0.05	0.97 ± 0.02	0.52 ± 0.37	4.01 ± 0.07	1.92 ± 0.09	8.76 ± 11.94
BaA	3.63 ± 1.51	1.52 ± 0.32	1.43 ± 1.01	8.39 ± 3.05	4.01 ± 2.63	0.80 ± 0.01
Chy	12.04 ± 3.15	1.27 ± 0.13	nd	21.15 ± 0.63	4.34 ± 2.05	0.59 ± 0.42
BbF	2.32 ± 0.43	2.01 ± 0.59	1.34 ± 0.95	6.99 ± 0.66	3.70 ± 2.37	2.21 ± 0.01
BkF	4.28 ± 0.09	1.40 ± 0.07	3.70 ± 2.62	9.09 ± 1.27	5.68 ± 2.01	5.79 ± 2.53
BaP	8.78 ± 0.10	20.78 ± 0.22	38.67 ± 27.34	16.14 ± 0.06	24.36 ± 0.47	29.60 ± 0.60
IcP	8.86 ± 0.17	2.88 ± 0.57	5.09 ± 3.60	14.08 ± 2.66	6.68 ± 1.54	5.09 ± 0.01
DBA	4.20 ± 0.75	1.58 ± 0.13	4.02 ± 2.84	14.15 ± 2.85	2.54 ± 0.07	5.30 ± 0.15
BgP	3.00 ± 1.74	5.39 ± 0.48	11.67 ± 8.25	6.31 ± 2.03	6.51 ± 0.66	48.82 ± 0.98
∑PAHs	62.01	42.77	81.56	113.26	66.47	117.89
Plant ∑PAHs	62.11			99.21		
Plant ∑C PAHs	43.27			63.56		
% C PAHs	69.66			64.07		

Site PA: Agricultural and residential areas. Site PB: Informal settlement of Kayamandi. nd: Not detected. na: not available. C PAHs: Carcinogenic PAHs.

Table 4.19b: Levels of PAHs (mean (n = 3) ± SD) in *P. australis* tissues of the Plankenburg River (sites PC and PD)

PAHs (µg/g)	Site PC			Site PD		
	leaves	stems	roots	leaves	stems	roots
Nap	nd	0.14 ± 0.10	nd	nd	0.55 ± 0.13	nd
Acy	0.47 ± 0.08	nd	0.41 ± 0.29	0.38 ± 0.27	0.28 ± 0.11	0.37 ± 0.15
Can	0.83 ± 0.25	0.48 ± 0.24	0.64	0.81 ± 0.14	0.31 ± 0.20	0.35 ± 0.14
Flu	3.72 ± 2.63	4.52 ± 2.14	0.51 ± 0.36	3.28 ± 2.32	2.27 ± 0.09	nd
Phe	na	na	na	na	na	na
Ant	3.43 ± 0.20	0.66	3.30 ± 4.10	1.78 ± 0.81	na	3.96 ± 2.25
Flt	3.59 ± 0.22	10.35 ± 3.04	0.83 ± 0.03	1.08 ± 0.01	1.13 ± 0.32	3.10 ± 0.22
Pyr	3.71 ± 0.46	2.34 ± 0.03	1.05 ± 0.13	9.59 ± 0.08	3.86 ± 0.09	3.60 ± 3.83
BaA	8.45 ± 2.23	0.86 ± 0.04	0.99 ± 0.02	3.35 ± 0.24	6.55 ± 0.02	0.87 ± 0.37
Chy	9.75 ± 6.25	2.15 ± 0.20	1.52 ± 0.24	9.77 ± 1.84	8.47 ± 1.84	1.01 ± 0.71
BbF	2.82 ± 1.26	2.88 ± 1.13	2.81 ± 1.97	7.36 ± 0.96	5.61 ± 2.77	1.75 ± 0.04
BkF	4.71 ± 0.83	3.24 ± 0.15	6.05 ± 0.32	6.31 ± 5.58	8.44 ± 3.66	3.64 ± 1.37
BaP	11.70 ± 0.19	19.68 ± 0.74	40.44 ± 1.28	13.59 ± 0.09	46.39 ± 1.90	18.34 ± 0.12
IcP	6.70 ± 1.62	3.32 ± 0.06	1.80 ± 0.13	17.92 ± 5.73	6.64 ± 5.42	3.79 ± 1.62
DBA	2.82 ± 0.04	4.21 ± 0.87	2.54 ± 0.25	4.68 ± 0.19	4.43 ± 5.19	2.02 ± 1.80
BgP	4.27 ± 1.52	2.96 ± 0.09	17.52 ± 0.38	3.62 ± 1.29	2.22 ± 0.15	5.08 ± 0.10
∑PAHs	66.95	57.79	80.41	83.48	97.17	47.88
Plant ∑PAHs	68.39			76.18		
Plant ∑C PAHs	46.48			60.31		
% C PAHs	67.97			79.17		

Site PC: Substation in industrial area. Site PD: Industrial area at Adam Tas Bridge. nd: Not detected. na: not available. C PAHs: Carcinogenic PAHs.

.

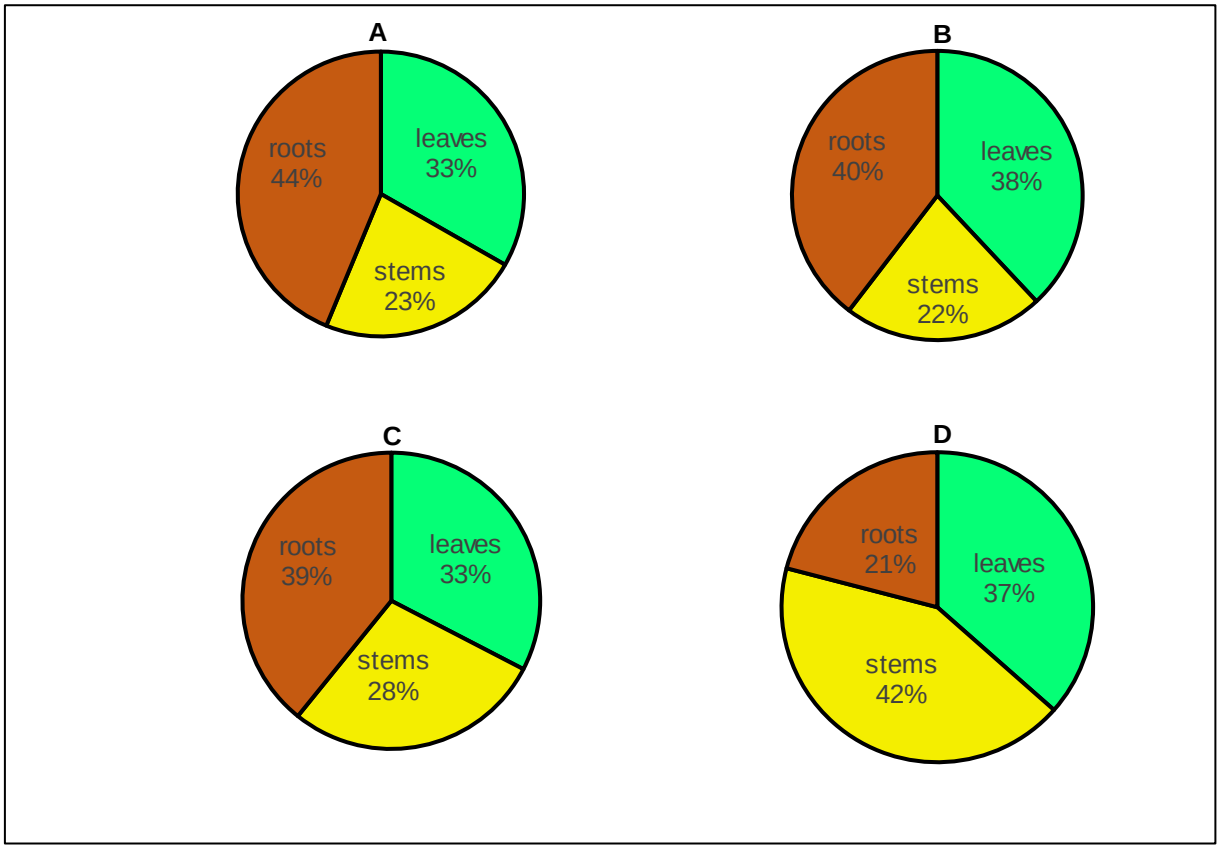

Figure 4.18: Occurrence of PAHs in *P. australis* tissues of the Plankenburg River

A: Site PA (Agricultural and residential areas). B: Site PB (Informal settlement of Kayamandi). C: Site PC (Substation in industrial area). D: Site PD (Industrial area at Adam Tas bridge).

The distribution of PAHs in plant samples had similar pattern along the two rivers that were studied. Generally, there was abundance of HMW PAHs (4-,5- and 6-ring) in plant samples from all the sites. The proportion of PAHs congeners' distribution in plants is given in Figure 4.19. However, elevated levels of benzo[a]pyrene (a strong carcinogen) were observed along the Plankenburg River relative to the Diep River.

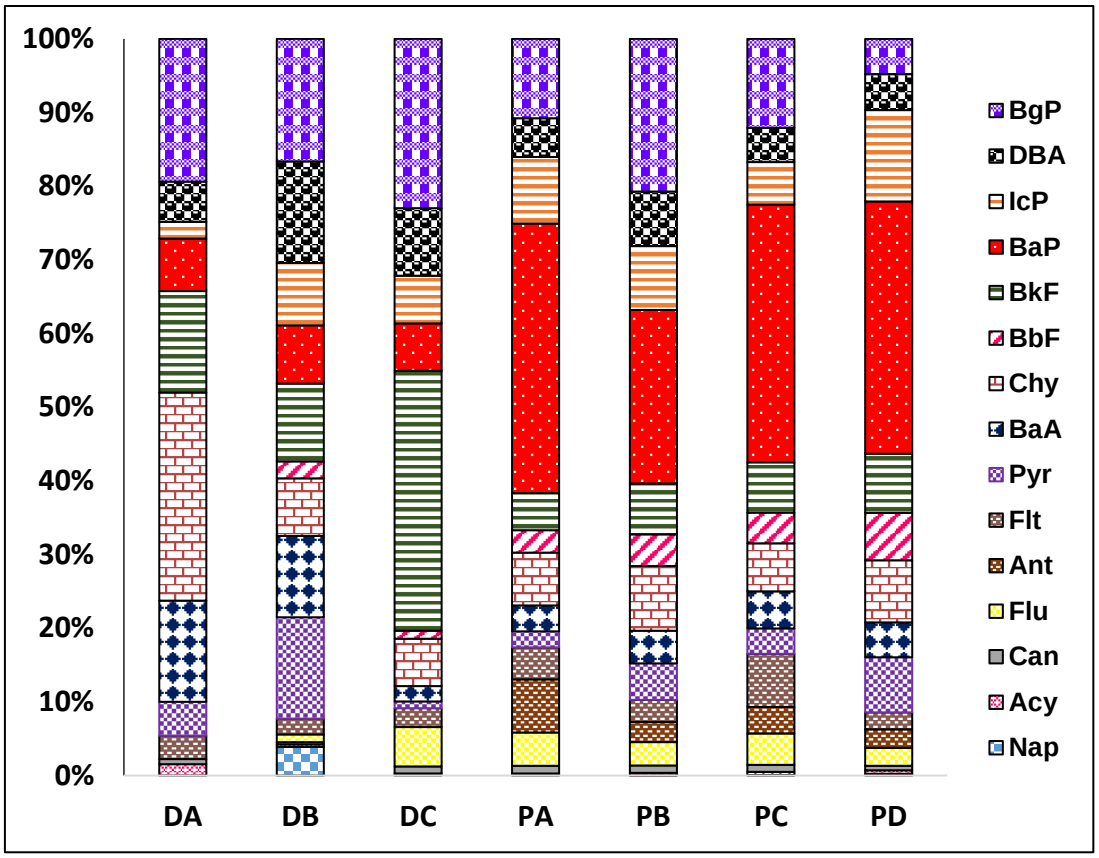

Figure 4.19: Fractions of PAHs in plant samples of the Diep and Plankenburg Rivers

4.3.4 Probabilistic risk assessment of PAHs in water and sediment samples

The levels of PAHs in water and sediment samples at the studied sites from the Diep and Plankenburg Rivers were evaluated through probabilistic methodologies to predict the exceedence of detected levels to available quality guidelines. The mean levels of PAHs detected over a one-year period were ranked, utilising Weibull probabilistic approach and percentile ranking (Berninger & Brooks, 2010; Corrales *et al*., 2015). The Weibull plots are presented in Appendices L and M.

4.3.4.1 Water sample probabilistic risk assessment

The environmental percentile distribution and percentage exceedence of the 16 US EPA priority PAHs in water samples from the Diep and Plankenburg Rivers are presented in Tables 4.20a and 4.20b respectively. The distribution of PAHs in surface water at 80^{th} centiles for the Diep River was estimated to range between 0.845 and 32.959 µg/L and between 2.264 and 45.556 µg/L for the Plankenburg River. This is an indication that the Plankenburg River had higher overall levels of PAHs contamination in surface water relative to the Diep River.

Over 40% exceedence was estimated for strongly carcinogenic benzo[a]pyrene (BaP), 100% exceedence for carcinogenic benzo[A]anthracene and over 95% exceedence for anthracene for both the Diep and Plankenburg Rivers, based on US EPA water quality guidelines (WQG) for PAHs. The average percentages exceedent for PAHs with available US EPA (WQG) were 63.26% and 42.81% for the Diep and Plankenburg Rivers respectively.

Table 4.20a: Summary of statistics of the tests of the Weibull distribution of the annual concentrations (µg/L) of PAHs in water samples of the Diep River

PAHs	Weibull plots				Centile values (%)				Exceedence values		
	n	R^2	a	b	20	40	60	80	US EPA (WQG)	CCME (WQG)	Average
Nap	36	0.5733	0.8002	-1.2880	0.000	1.020	2.500	10.660	19/36 (52.70%)	19/36 (52.70%)	63.26 %
Acy	36	0.7627	0.9277	-1.3980	0.590	2.030	3.650	5.960	-	-	
Can	36	0.5019	0.8888	-0.9050	0.480	0.790	1.156	2.765	5/36 (13.88%)	5/36 (13.88)	
Flu	36	0.6367	1.0350	-1.3780	0.000	1.099	2.823	5.131	13/36 (36.10%)	13/36 (36.10%)	
Phe	36	0.8396	0.8711	-1.8620	1.018	2.710	6.405	14.130	35/36 (97.22%)	35/36 (97.22%)	
Ant	36	0.8729	1.0211	-1.6890	1.287	1.966	3.145	6.718	36/36 (100.00%)	36/36 (100.00%)	
Flt	36	0.8829	1.2000	-2.3520	1.707	4.215	6.422	9.143	30/36 (83.33%)	30/36 (83.33%)	
Pyr	36	0.2148	0.3979	-0.6674	0.000	0.079	0.610	5.768	15/36 (41.66%)	15/36 (41.66%)	
BaA	36	0.9465	1.2338	-3.6958	7.260	8.507	16.494	32.468	36/36 (100.00%)	36/36 (100.00%)	
Chy	36	0.9562	1.1890	-3.7719	7.270	14.218	18.237	32.959	-	-	
BbF	36	0.2088	0.7777	-0.7492	0.000	0.000	0.000	0.888	-	-	
BkF	36	0.5912	1.4420	-1.3014	0.000	0.000	1.432	3.852	-	-	
BaP	36	0.3987	1.1690	-1.0205	0.000	0.000	0.473	0.845	16/36 (44.44%)	16/36 (44.44%)	
IcP	36	0.9260	1.2000	-2.7790	2.904	4.237	8.156	14.462	-	-	
DBA	36	0.9540	1.3250	-3.1802	3.789	5.907	9.256	14.434	-	-	
BgP	36	0.7910	1.0755	-1.9592	1.431	2.312	3.602	9.482	-	-	

n: no of compounds. a: slope. b: intercept. US EPA: United States Environmental Protection Agency. CCEM: Canadian Council of Ministers of the Environment. WQG: Water Quality Guideline.

Table 4.20b: Summary of statistics of the tests of the Weibull distribution of the annual concentrations (µg/L) of PAHs in water samples of the Plankenburg River

PAHs	Weibull plots				Centile values (%)				Exceedence values		
	n	R^2	a	b	20	40	60	80	US EPA (WQG)	CCME (WQG)	Average
Nap	48	0.6219	1.1756	-1.4155	0.000	1.383	2.501	5.429	20/48 (41.66%)	20/48 (41.66)	42.81%
Acy	48	0.5736	0.9315	-1.1377	0.000	1.169	2.399	5.212	-	-	
Can	48	0.5139	1.3510	-1.0473	0.000	0.948	1.664	2.264	2/48 (4.10%)	2/48 (4.10%)	
Flu	48	0.7582	0.9937	-1.9055	0.595	3.209	7.141	10.360	20/48 (41.66%)	20/48 (41.66)	
Phe	48	0.8695	0.9191	-2.3322	1.614	6.962	14.447	18.139	4/48 (8.33%)	4/48 (8.33%)	
Ant	48	0.8581	1.1150	-2.1998	1.604	2.839	6.656	10.811	47/48 (97.91%)	47/48 (97.91%)	
Flt	48	0.8702	1.3430	-2.2751	0.970	3.212	4.367	8.044	8/48 (16.67%)	8/48 (16.67%)	
Pyr	48	0.6452	1.1590	-1.4331	0.000	1.228	2.133	4.649	16/48 (33.33%)	16/48 (33.33%)	
BaA	48	0.9436	1.6499	-5.5707	10.693	18.790	24.567	38.962	48/48 (100.00%)	48/48 (100.00%)	
Chy	48	0.9899	1.3556	-4.7590	10.079	23.018	33.031	46.556	-	-	
BbF	48	0.7050	0.8543	-1.5820	0.000	1.645	3.866	12.097	-	-	
BkF	48	0.6962	1.0376	-1.5757	0.000	1.614	3.498	6.629	-	-	
BaP	48	0.5361	1.3147	-1.2048	0.000	0.583	1.804	3.008	20/48 (41.66%)	20/48 (41.66%)	
IcP	48	0.9689	1.2051	-3.4686	4.385	11.069	16.660	31.431	-	-	
DBA	48	0.9512	1.4329	-3.2776	2.955	5.470	8.125	13.666	-	-	
BgP	48	0.8867	1.2120	-2.3088	1.830	3.461	4.811	8.461	-	-	

n: no of compounds. a: slope. b: intercept. US EPA: United States Environmental Protection Agency. CCEM: Canadian Council of Ministers of the Environment. WQG: Water Quality Guideline.

4.3.4.2 Sediment sample probabilistic risk assessment

The environmental percentile distribution and percentage exceedence of the 16 US EPA priority PAHs in sediment samples of the Diep and Plankenburg Rivers are presented in Tables 4.21a and 4.21b respectively.

The distribution of PAHs in sediments at 80th centiles for the Diep River was estimated to range between 0.1613 and 2.5498 µg/g; corresponding values were 0.2325 and 21.307 µg/g for the Plankenburg River. These values were higher than those estimated for the corresponding water samples.

The percentage exceedence recorded for the strongly carcinogenic benzo [a] pyrene (BaP) in sediment were 80.55% and 87.20% for the Diep and Plankenburg Rivers respectively, based on US EPA freshwater sediment screening benchmarks (FSSB) for PAHs. These percentage exceedences were two-fold greater (44.44% and 41.66%) for BaP in the corresponding surface water of the Diep and Plankenburg Rivers respectively. This reaffirms the need for a holistic environmental assessment to estimate the health of the environment. A singular environmental medium assessment will not be sufficient in estimating the risk contaminants pose to humans. The estimated average US EPA FSSB exceedent percentages for the 16 priority PAHs in sediment samples were 63.71% and 77.20% for the Diep and Plankenburg Rivers respectively. This study showed that sediment samples had higher US EPA (FSSB) exceedent percentages for strongly carcinogenic benzo[a]pyrene compared to surface water and that the Plankenburg River was more contaminated than the Diep River with the 16 priority US EPA PAHs.

Table 4.21a: Summary of statistics of the tests of the Weibull distribution of the annual concentrations (µg/g) of PAHs in sediment samples of the Diep River

PAHs	Weibull plots				Centile values (%)				Exceedence values		
	n	R^2	a	b	20	40	60	80	US EPA (FSSB)	CCME (ISQG)	FSSB Average
Nap	36	0.8457	0.5560	-2.4532	0.0000	0.3672	1.0817	1.7719	8/36 (22.22%)	28/36 (77.77%)	63.71%
Acy	36	0.7502	0.6745	-1.7304	0.0000	0.0019	0.1006	0.2727	18/36 (50.00%)	18/36 (50.00%)	
Can	36	0.8949	0.7655	-2.4646	0.0353	0.0085	0.1511	0.6045	31/36 (86.11%)	31/36 (86.11%)	
Flu	36	0.7553	0.6151	-1.7357	0.0000	0.0289	0.1345	0.3347	20/36 (55.55%)	23/36 (63.88%)	
Phe	36	0.7559	0.4427	-1.8346	0.0251	0.0529	0.2004	2.5123	14/36 (38.88%)	25/36 (69.44%)	
Ant	36	0.7936	0.7293	-2.1123	0.0000	0.0766	0.1182	0.1613	24/36 (66.67%)	27/36 (75%)	
Flt	36	0.9625	0.7359	-3.4089	0.1348	0.4069	0.7300	2.0210	21/36 (58.33%)	30/36 (83.33%)	
Pyr	36	0.8290	0.6333	-2.0129	0.0146	0.0484	0.1361	0.4075	12/36 (33.33%)	21/36 (58.33%)	
BaA	36	0.9091	1.1550	-5.0445	0.2124	0.3398	0.5592	1.1697	34/36 (94.44%)	36/36 (100.00%)	
Chy	36	0.9492	0.7209	-3.1997	0.1010	0.2498	0.8118	2.1866	10/36 (27.77%)	32/36 (88.88%)	
BbF	36	0.9449	0.6310	-3.1278	0.1395	0.4322	0.9956	2.3319	33/36 (91.66%)	-	
BkF	36	0.8899	0.8221	-4.3132	0.2341	0.7637	1.5682	2.5498	28/36 (77.77%)	-	
BaP	36	0.9646	0.7058	-3.4844	0.1815	0.5997	1.0718	2.0597	29/36 (80.55%)	33/36 (91.66%)	
IcP	36	0.9189	0.6631	-2.7083	0.0858	0.1972	0.4835	1.1012	30/36 (83.33%)	-	
DBA	36	0.9447	0.7414	-3.0826	0.1253	0.2118	0.4825	1.1632	32/36 (88.88%)	32/36 (88.88%)	
BgP	36	0.9154	0.7103	-2.7016	0.0817	0.2367	0.2982	0.8435	23/36 (63.88%)	-	

n = number of compounds. a = slope. b = intercept. US EPA = United States Environmental Protection Agency. FSSB = Freshwater Sediment Screening Benchmarks. CCEM = Canadian Council of Ministers of the Environment. ISQG = Interim Sediment Quality Guideline

Table 4.21b: Summary of statistics of the tests of the Weibull distribution of the annual concentrations (µg/g) of PAHs in sediment samples of the Plankenburg River

PAHs	Weibull plots				Centile values (%)				Exceedence values		
	n	R^2	a	b	20	40	60	80	US EPA (FSSB)	CCME (ISQG)	FSSB Average
Nap	48	0.9080	0.7315	-3.5443	0.2848	0.5684	1.3433	2.1509	43/48 (89.58%)	43/48 (89.58%)	77.20%
Acy	48	0.8932	0.8434	-2.3953	0.0187	0.0680	0.1320	0.3168	40/48 (83.33%)	40/48 (83.33%)	
Can	48	0.7325	0.6690	-1.6743	0.0000	0.0248	0.0854	0.2325	30/48 (62.5%)	30/48 (62.5%)	
Flu	48	0.8747	0.8185	-2.2771	0.0450	0.0976	0.1393	0.3540	32/48 (66.67%)	38/48 (79.16%)	
Phe	48	0.7729	0.4506	-2.1850	0.0476	0.0674	0.3279	9.7475	22/48 (45.88%)	41/48 (85.41%)	
Ant	48	0.8729	0.7017	-2.6184	0.0963	0.1526	0.2700	0.5851	40/48 (83.33%)	40/48 (83.33%)	
Flt	48	0.9242	0.9878	-4.4746	0.2027	0.3720	0.7141	1.9084	27/48 (56.25%)	43/48 (89.58%)	
Pyr	48	0.7289	0.5547	-1.7394	0.0000	0.0310	0.2404	0.6203	20/48 (41.66%)	26/48 (54.16%)	
BaA	48	0.8847	1.3433	-5.7280	0.1869	0.3369	0.5762	0.9676	48/48 (100.00%)	48/48 (100.00%)	
Chy	48	0.9405	1.1965	-5.1596	0.1639	0.3442	0.5801	1.2636	38/48 (79.16%)	48/48 (100.00%)	
BbF	48	0.9796	1.0026	-7.1503	2.4547	7.1473	12.3900	21.3070	48/48 (100.00%)	-	
BkF	48	0.9832	1.1929	-7.6994	1.7206	4.2531	5.8422	8.3673	47/48 (97.91%)	-	
BaP	48	0.9821	0.8526	-4.4114	0.2475	0.7129	1.4994	2.6598	42/48 (87.20%)	47/48 (97.91%)	
IcP	48	0.9870	1.0976	-4.5286	0.1335	0.2917	0.6198	0.9806	47/48 (97.91%)	-	
DBA	48	0.9246	0.8257	-3.5784	0.1062	0.2305	0.6766	1.0627	48/48 (97.91%)	47/48 (97.91%)	
BgP	48	0.9005	0.7729	-2.6230	0.0475	0.0835	0.1830	0.5195	22/48 (45.83%)	-	

n = number of compounds. a = slope. b = intercept. US EPA = United States Environmental Protection Agency. FSSB = Freshwater Sediment Screening Benchmarks. CCEM = Canadian Council of Ministers of the Environment. ISQG = Interim Sediment Quality Guideline

.

4.4 Remediation of PAHs from aqueous solution

4.4.1 Characterisation of adsorbents produced from *V. vinifera* leaf litter

4.4.1.1 The ash, moisture, crude fibre and elemental composition of raw leaf litter

The ash, moisture, crude fibre and elemental composition of grape leaf litter are presented in Table 4.22. The ash, moisture and crude fibre content obtained were 7.22%, 8.19% and 13% respectively. The energy dispersion spectroscopic (EDS) analysis showed that the grape leaf litter contained 52.82% carbon, 46.05% oxygen, 0.41% calcium, 0.07% sulphur and 0.64% copper. These results make grape leaf litter a promising precursor for activated carbon. Precursors with high carbon content but with low ash and sulphur content results in high yield activated carbon with high adsorption capabilities and low/no emission of culprit sulphur oxides during the carbonisation process (Adebowale & Bayer, 2002; Rashidi *et al*., 2012). The results obtained from the analysis of the raw grape leaf litter, suggest that the material can be utilised as a cheap biomass in the production of activated carbons with great adsorption capabilities.

Table 4.22: Ash, moisture, crude fibre and atomic elements of raw grape leaf litter

Ash, moisture and crude fibre (Wt. %)	Ash content	7.22
	Moisture content	8.19
	Crude fibre content	13.00
Elemental Composition (Wt. %)	Carbon	52.82
	Oxygen	46.05
	Calcium	0.41
	Sulphur	0.07
	Copper	0.64

4.4.1.2 Physical properties and atomic elements of produced activated carbons

The yield, burn-off, attrition and elemental composition of charred products using two different activated agents are presented in Table 4.23. The yield obtained for chars were high (41.63% to 58.40%) with the exception of inactivated char (Nac) with 32.84% yield. Improved yield was obtained for biomass activated with H_3PO_4 and $ZnCl_2$. Yield was directly proportional to the concentration of the activating agent for the range studied. The more the activating agent the less the burn-off obtained (41.98% to 67.17%). The highest burn-off was obtained for inactivated char (Nac). Chemical agents have been reported to improve the yield and lower burn-off of conversion products at low concentrations. They act as catalysts to promote depolymerisation of cellulose, bond cleavage, hydrolysis, dehydration, condensation and cross-linkage with biopolymers (Molina-Sabio & Rodríguez-Reinoso, 2004; Sugumaran *et al*., 2012). At optimum level of activating agents, activated carbon with maximum uniform microporosity are formed (Molina-Sabio & Rodríguez-Reinoso, 2004; Sugumaran *et al*., 2012). The observed improved yields were higher than those reported by Adebowale & Bayer (2002). Attrition ranged from 9.24% to 42.86%, with Nac char having the lowest attrition and that activated with the highest proportion of $ZnCl_2$ (ZAac) had the highest attrition (Table 4.23). The percentage fixed carbon ranged from 51.37% to 67.38% and followed similar trend observed for percentage yield for each activating agent. Activation with $ZnCl_2$ gave higher fixed carbon in most instances relative to H_3PO_4 activation (Table 4.23).

The carbon matrix is not solely made-up of carbon atoms but consists of other atoms too. Oxygen, phosphorous, silicon, calcium, chlorine, sulphur, copper and zinc were atoms detected in produced activated carbons. These atoms are bonded to the edges of carbon layers and governs the surface chemistry of activated carbons (Prahas *et al*., 2008). Oxygen was detected in all produced chars and ranged from 30.87% to 45.17%. Phosphorous was detected in H_3PO_4 treated and untreated products and ranged from 0.01% to 1.64%. However, Zn was only detected in products treated with $ZnCl_2$ and ranged from 0.86% to 1.74% (Table 4.23).

Table 4.23: Yield, burn-off, attrition and elemental composition of the chars

ratio (biomass: chemical)/ chemical agent	Name	% yield	% burn-off	% Attrition	elemental composition (Wt. %)								
					C	O	P	Si	Ca	Cl	S	Cu	Zn
5:2/ H_3PO_4	PAac	58.40	41.98	36.75	60.04	37.64	1.04	0.14	0.51	0.04	0.03	0.56	-
5:1/ H_3PO_4	PBac	47.04	52.96	19.67	57.60	41.13	0.87	-	0.04	-	-	-	-
10:1/ H_3PO_4	PCac	41.63	58.37	16.21	57.58	40.23	0.01	0.37	0.53	0.69	-	0.58	-
5:2/ $ZnCl_2$	ZAac	47.08	52.92	42.86	67.21	30.87	-	0.00	-	0.43	0.00	1.48	-
5:1/ $ZnCl_2$	ZBac	45.54	54.46	22.67	62.38	32.16	-	0.13	0.77	2.66	0.16	-	1.74
10:1/ $ZnCl_2$	ZCac	44.65	55.36	16.00	52.21	42.86	-	0.72	0.72	1.82	0.14	0.47	0.88
No activation	Nac	32.84	67.16	9.24	51.37	45.17	1.64	0.72	0.93	0.18	-	-	-

The textural properties of produced activated carbons are presented in Table 4.24. The BET surface area of produced activated carbon ranged from 24.5399 m^2/g to 616.6038 m^2/g. Increase in concentration of activating agent led to increased surface area. The micropore area also increased with increasing concentration of activating agent with values between 17.5864 m^2/g and 462.5162 m^2/g. The micropore volume ranged between 0.0069 cm^3/g and 0.1843 cm^3/g while the single point adsorption total pore volume ranged between 0.021259 cm^3/g and 0.289066 cm^3/g. Similar trend was observed in all adsorbent properties, with the exception of pore size. The observed pore size ranged between 1.87521 nm and 4.05688 nm.

The surface area of 617 m^2/g and a pore volume of 0.3 cm^3/g showed the potential of grape leaf litter for activated carbon production. Commercially available activated carbons has surface area of about 1000 m^2/g and pore volume between 0.2 cm^3/g and 0.5 cm^3/g (Adebowale & Bayer, 2002). The results obtained from this study is comparable with that of Bagheri & Abedi (2009). They produced activated carbons with surface area ranging from 105 to 1320 m^2/g from corn cob activated with 1:2 corn/chemical ratio. They reported that biomass/chemical ratio and method of mixing i.e. mixing-filtration, solid-solid and impregnation were the most important parameters for obtaining optimal experimental conditions. The activated carbon with the highest BET surface area (1320 m^2/g) produced at the optimal experiment conditions was subsequently tested in a natural gas adsorption system. A 120 v/v natural gas adsorption capacity was reported. The importance of biomass/chemical ratio in improving the BET surface area of activated carbons can be seen clearly with the data obtained in this study (Table 4.24), increased from 10:1 to 5:2 biomass/chemical ratio led to increase in BET surface area of 24.54 to 616.60 m^2/g with $ZnCl_2$ activating agent.

The BET isotherms for nitrogen adsorption obtained with the produced activated carbons from this study, are presented in Figure 4.20. The activated carbon ZAac with the highest BET surface area (616.60 m^2/g) gave the highest nitrogen adsorption capacity of 8.37 mmol/g, while the activated carbon ZCac with the lowest BET surface area (24.54 m^2/g) gave the lowest nitrogen adsorption capacity of 0.64 mmol/g. Thus, BET surface area of activated carbons plays a crucial role in their adsorption capabilities.

Table 4.24: Textural properties of produced activated carbons

Activated Carbon	Surface Area (m^2/g)	Micropore area (m^2/g)	Micropore volume (cm^3/g)	Total pore volume (cm^3/g)	Pore size (nm)
PAac	295.4881	174.1876	0.0720	0.185445	2.51036
PBac	171.8277	104.7176	0.0423	0.141699	3.29863
PCac	109.9583	82.1013	0.0323	0.060340	2.19501
ZAac	616.6038	462.5162	0.1843	0.289066	1.87521
ZBac	120.8772	68.9333	0.0280	0.122596	4.05688
ZCac	24.5399	17.5864	0.0069	0.021259	3.46522

PAac: activated with H_3PO_4 at 5:2 biomass to H_3PO_4 ratio. PBac: activated with H_3PO_4 at 5:1 biomass to H_3PO_4 ratio. PCac: activated with H_3PO_4 at 10:1 biomass to H_3PO_4 ratio. ZAac: activated with $ZnCl_2$ at 5:2 biomass to $ZnCl_2$ ratio. ZBac: activated with $ZnCl_2$ at 5:1 biomass to $ZnCl_2$ ratio. ZCac: activated with $ZnCl_2$ at 10:1 biomass to $ZnCl_2$ ratio.

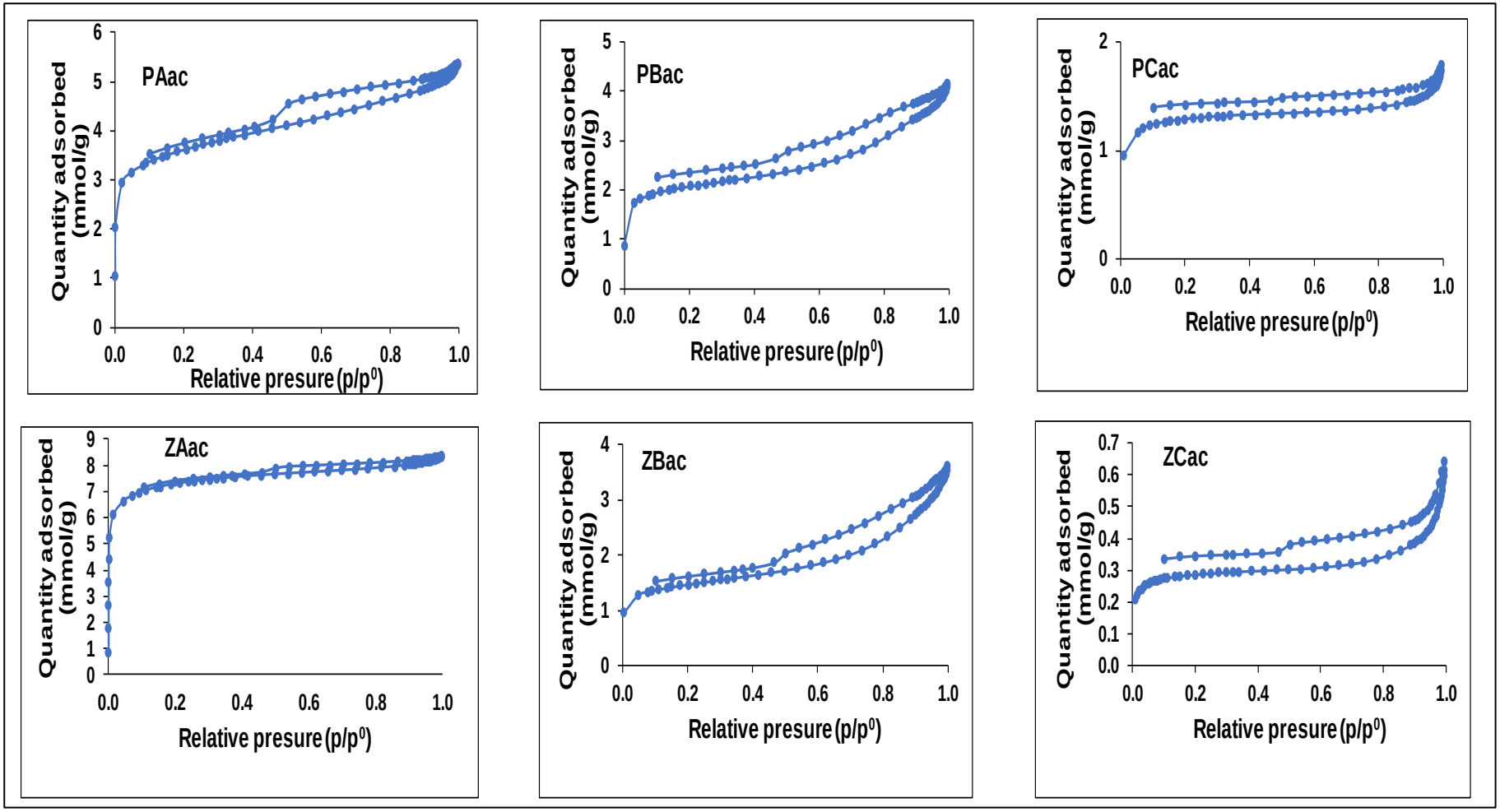

Figure 4.20: BET isotherm plots for nitrogen adsorption capacity of produced activated carbons

PAac: activated with H_3PO_4 at 5:2 biomass to H_3PO_4 ratio. PBac: activated with H_3PO_4 at 5:1 biomass to H_3PO_4 ratio. PCac: activated with H_3PO_4 at 10:1 biomass to H_3PO_4 ratio. ZAac: activated with $ZnCl_2$ at 5:2 biomass to $ZnCl_2$ ratio. ZBac: activated with $ZnCl_2$ at 5:1 biomass to $ZnCl_2$ ratio. ZCac: activated with $ZnCl_2$ at 10:1 biomass to $ZnCl_2$ ratio.

Chemical structure information of the biomass and charred products was obtained by infrared spectroscopy (Figure 4.21). Charred products were largely similar but differed from the precursor structurally. The asymmetrical stretching vibration of C – H bond at 2918 cm^{-1} and the symmetrical stretching vibration at 2851 cm^{-1} present in the precursor were obviously absent in charred products. The C – H bonds were probably broken during the thermal conversion process to form a more stable C = C bonds, that was observed at 1580 cm^{-1} for all the charred products. Also, the C = O stretching observed at 1734 cm^{-1} in the raw biomass was absent in charred products, as surface oxygenated groups were converted to CO and CO_2 during thermal conversion (Sun *et al*., 2016; Correa *et al*., 2017; Lawal *et al*., 2017; Dodevski *et al*., 2017). The bands at around 1580 cm^{-1} and 1070 cm^{-1} observed in all charred products are indicative of C = C bond stretching ascribed to aromatic compounds.

The scanning electron microscopy (SEM), a good tool for surface morphology characterisation of adsorbents (Aljeboree *et al*., 2017) was also utilised for characterising produced adsorbents. Figure 4.22 shows the SEM images of charred products and raw biomass. The SEM image of raw biomass is smooth with no evidence of porosity, while rough surfaces and evidence of porosity could be observed on the SEM images of charred products. The porosity of charred products was due to the decomposition of lignin, cellulose and hemicellulose during carbonisation, resulting in the formation of micropores and mesopores (Deng *et al*., 2016). There are tendencies of PAHs being trapped and adsorbed in the developed pores.

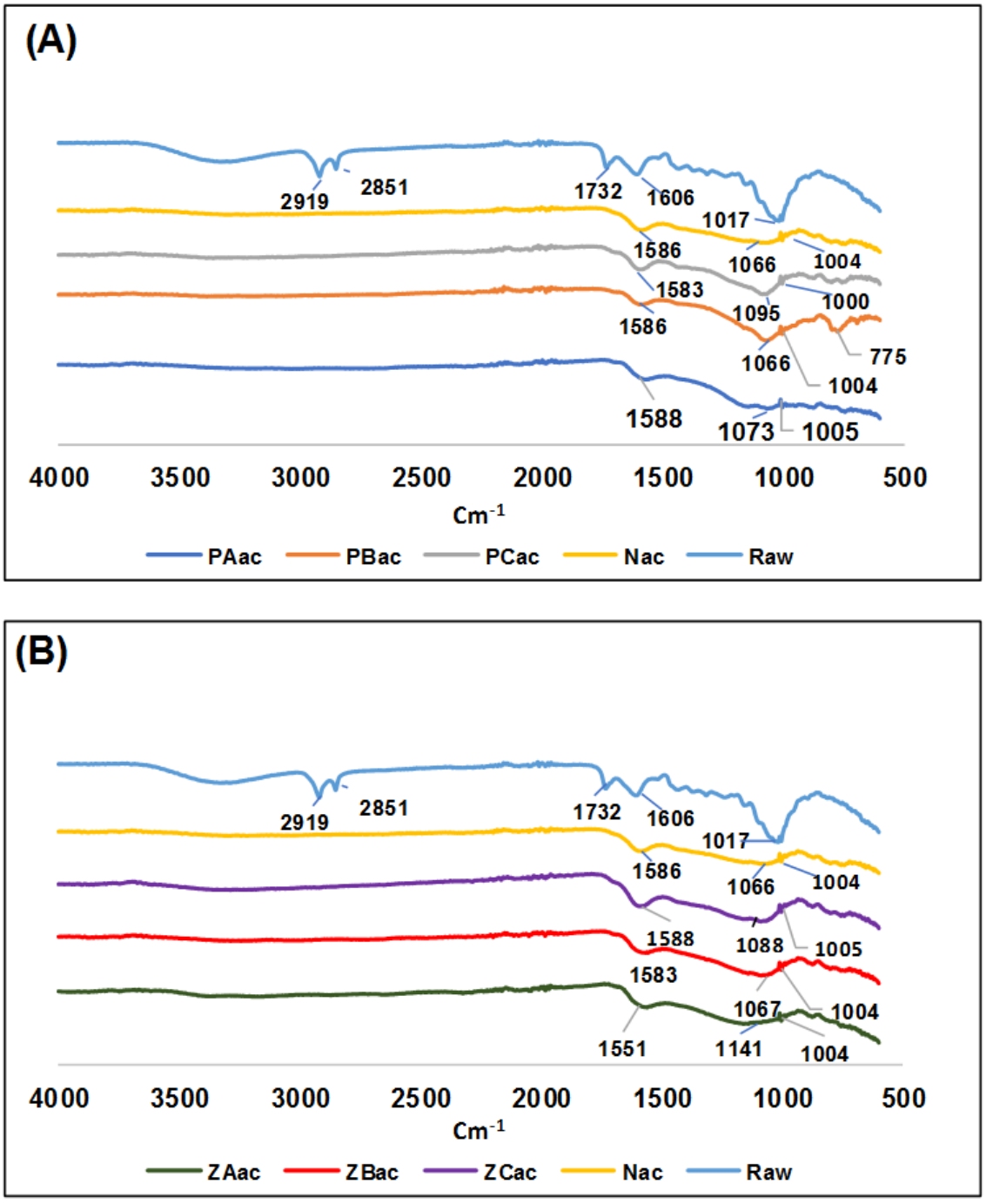

Figure 4.21: FTIR spectra of produced chars vs raw biomass

A: H_3PO_4 acid activated and inactivated chars versus raw biomass. B: $ZnCl_2$ activated and inactivated versus raw biomass. PAac: activated with H_3PO_4 at 5:2 biomass to H_3PO_4 ratio. PBac: activated with H_3PO_4 at 5:1 biomass to H_3PO_4 ratio. PCac: activated with H_3PO_4 at 10:1 biomass to H_3PO_4 ratio. Nac: charred with no activating agent. Raw: raw grape leaf litter. ZAac: activated with $ZnCl_2$ at 5:2 biomass to $ZnCl_2$ ratio. ZBac: activated with $ZnCl_2$ at 5:1 biomass to $ZnCl_2$ ratio. ZCac: activated with $ZnCl_2$ at 10:1 biomass to $ZnCl_2$ ratio.

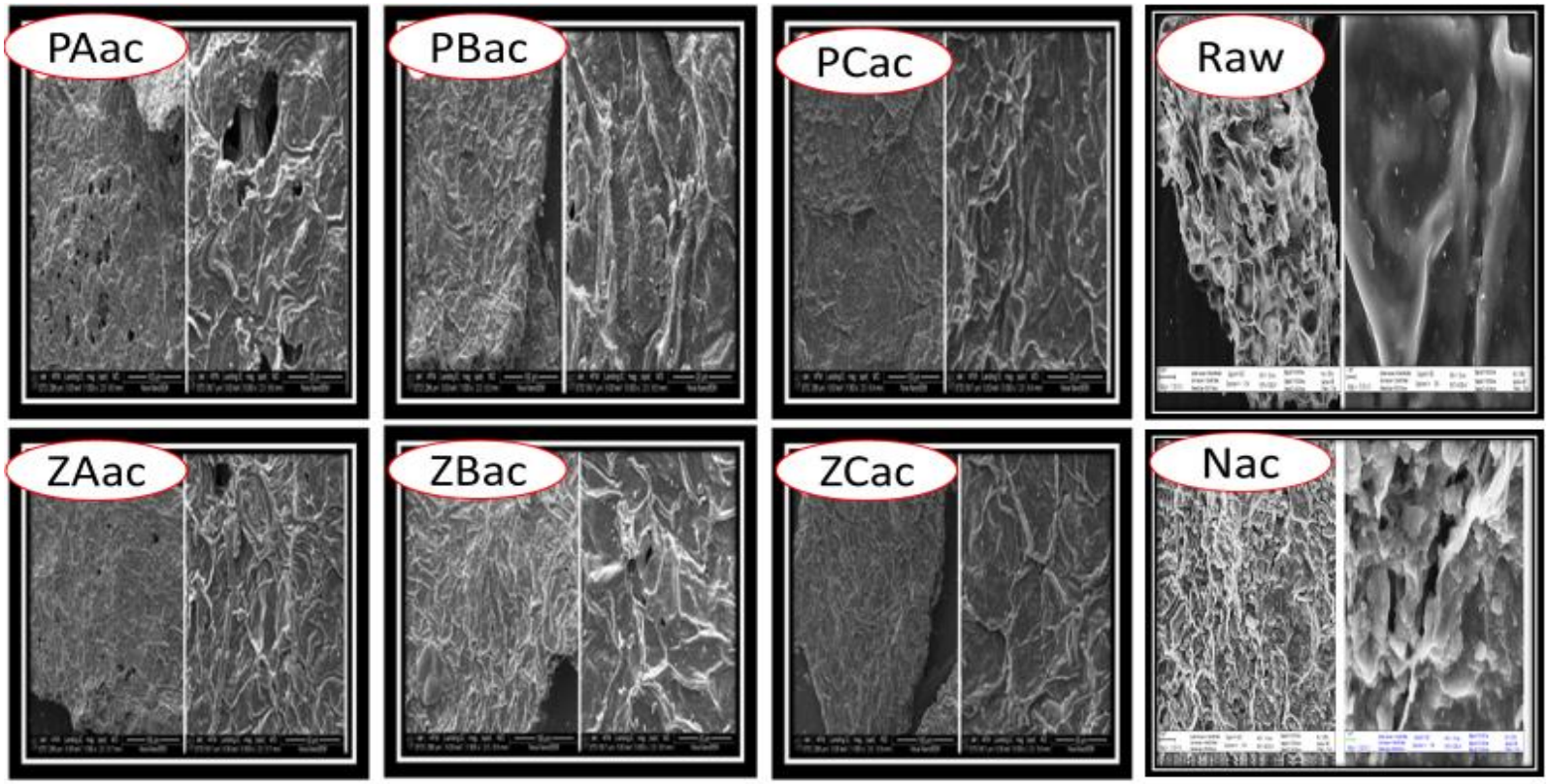

Figure 4.22: Scanning electron micrographs of produced activated carbons, charred and raw biomass (magnification: x1000 vs x5000)

PAac: activated with H_3PO_4 at 5:2 biomass to H_3PO_4 ratio. PBac: activated with H_3PO_4 at 5:1 biomass to H_3PO_4 ratio. PCac: activated with H_3PO_4 at 10:1 biomass to H_3PO_4 ratio. Raw: raw grape leaf litter. ZAac: activated with $ZnCl_2$ at 5:2 biomass to $ZnCl_2$ ratio. ZBac: activated with $ZnCl_2$ at 5:1 biomass to $ZnCl_2$ ratio. ZCac: activated with $ZnCl_2$ at 10:1 biomass to $ZnCl_2$ ratio. Nac: charred with no activating agent.

4.4.2 Adsorption of phenanthrene on obtained activated carbons

The adsorption of phenanthrene on produced activated carbons was studied to determine the potential of obtained charred products for remediation of PAHs contaminated water. Phenanthrene was selected being a suitable representative of semi-volatile organic compounds (Zhao *et al*., 2016).

4.4.2.1 Optimisation of experimental parameters for the adsorption processes

Effect of pH

The effect of pH on phenanthrene adsorption using produced activated carbons was investigated. A pH range of 3 to 12 was studied. The result obtained showed that adsorption of PAH was favourable in the acidic medium relative to alkaline conditions (Figure 4.23). This observation is consistent with that reported by Gupta (2015), who stated that the adsorption of phenanthrene on activated carbon derived from orange peel, was maximum at low pH values and least at high pH value. The increase in positive charge on the adsorbent surface at low pH led to higher interaction between the adsorbent surface and the PAH molecule (having π-electron cloud). At low pH, there will be availability of more protons to enhance electrostatic attraction between the adsorbent and adsorbate (Özcan *et al*., 2004). The higher adsorption observed at pH 3 relative to pH 12 was attributed to this. At high pH, the OH^- ions also competes with adsorbate molecules for adsorption active sites on the activated carbons (Gupta, 2015). Hence, the reduction of phenanthrene adsorption at high pH. The adsorption of dye onto modified biosorbent surface had also been reported to reduce as pH increased from 2 to 9 by Akar *et al*. (2010). They reported that the adsorbent was negatively charged above pH 3 and that the high positive charge on the biosorbent surface at pH 2 led to larger attraction forces between the anionic dye molecules and the biosorbent surface.

However, Huang *et al*. (2016b) reported increased simultaneous adsorption of acenaphthene and cadmium onto magnetic nanoparticle adsorbents at high pH, with significant increase in cadmium removal. Increased removal of Cd^{2+} was attributed to nanoparticle surface becoming more negatively charged at higher pH. Increased acenaphthene removal at higher pH was however attributed to hydrophobic interactions between acenaphthene and confined surfactant micelles in the nanoparticles and not the surface charge of adsorbents.

Adsorbent ZAac, performed most efficiently in the removal of phenanthrene from aqueous media comparatively to other adsorbents (Table 4.25). This could be attributed to the surface characteristics of the adsorbent and ionic activities on the sorbent during the adsorption process. Activated carbons with highly microporous structure and improved adsorption capacity were reported to be produced when optimum ratio of $ZnCl_2$ was utilised as activating agent of raw biomass carbonised in an inert atmosphere (Kim *et al*., 2001). This is because, $ZnCl_2$ is a strong dehydrator effective in the removal of hydrogen and oxygen from raw biomass (Kim *et al*., 2001).

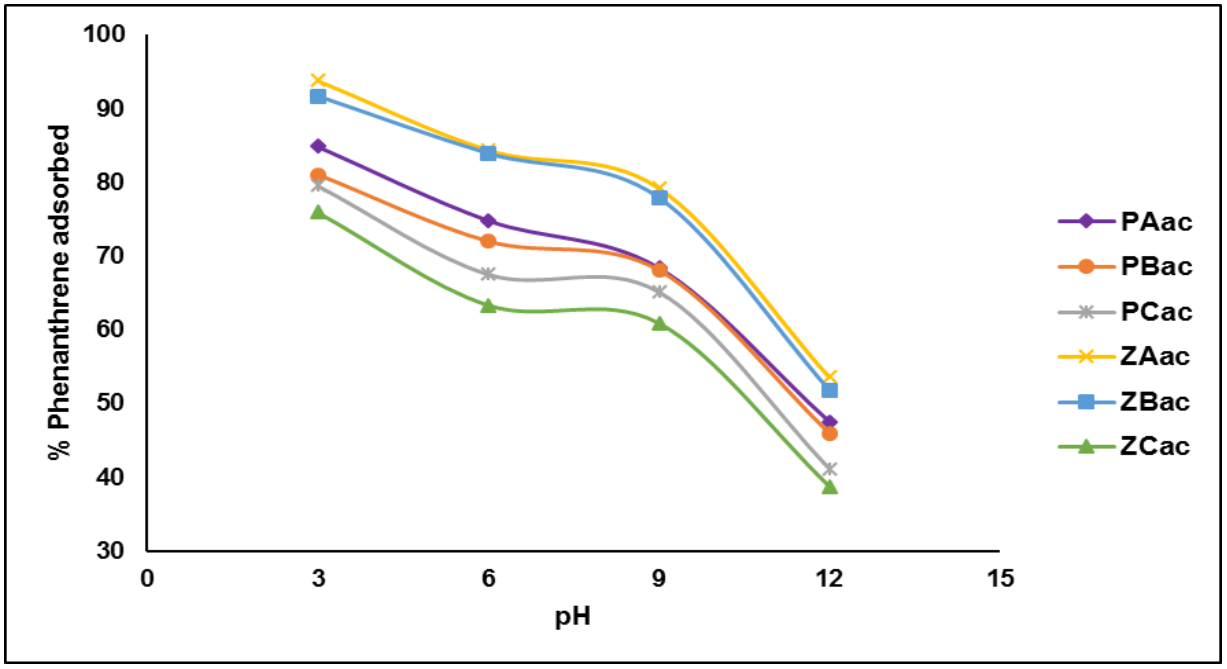

Figure 4.23: Effect of solution pH on phenanthrene adsorption using activated carbons

Table 4.25: Effect of aqueous solution pH on phenanthrene removal using activated carbons

Adsorbent	Amount adsorbed mg/L			
	pH 3	pH 6	pH 9	pH 12
PAac	0.8487	0.8109	0.7482	0.6839
PBac	0.8103	0.7898	0.7198	0.6808
PCac	0.7956	0.7394	0.6956	0.6517
ZAac	0.9384	0.8441	0.7411	0.6729
ZBac	0.9167	0.8389	0.7205	0.6491
ZCac	0.7592	0.7311	0.7033	0.6391

Other conditions observed: solution concentrations =1mg/L, solution volume = 25 mL, adsorbent dosage = 0.1g, temperature = 298 K, contact time =180 min and stirring agitation = 100 revolutions per minute (rpm)

Effect of Adsorbent Dosage

The effect of adsorbent dosage on the adsorption of phenanthrene onto produced activated carbons was determined using adsorbent weight range of 0.01 - 0.10 g (Figure 4.24). Results showed that phenanthrene adsorption increased rapidly with increased adsorbent dose from 0.01 to 0.05 g, with a gradual increase in adsorption when dose was increased to 0.075g, while a further increase to 0.1 g of adsorbent dose did not result in a significant increase in adsorption. This observation is consistent with that of Rad *et al*. (2014). They reported that phenanthrene adsorption increased with the dose of activated carbons until an optimum amount of 0.3 g/100 mL. Up to 8.34 mg/g phenanthrene removal on the activated carbons was achieved. The availability of more sorption active sites with increased adsorbent dose led to the increase in adsorbate removal efficiency at higher adsorbent dosage (Garg *et al*., 2003). The percentage adsorption increased from 59.6% to 99.8% with increased adsorbent dose of 0.2 to 1.0 g/100 mL. In this study, phenanthrene removal of > 90% was obtained with adsorbents PAac, ZAac and ZBac at increased adsorbent dosage.

The adsorption of dyes onto coconut shell activated carbon have also been reported to be a function of adsorbent dosage (Aljeboree *et al*., 2017). In the study, the amount of adsorbed dye increased apparently with increase in adsorbent dosage, but the amount adsorbed per unit mass decreased (adsorption density). The reduction in adsorption density with an increase adsorbent dosage was attributed to increased number of available sites that remained unsaturated during the adsorption process. Increased adsorbent dosage beyond the optimal level may also result in overcrowding of the adsorbent, causing adsorption sites to overlap, leading to reduction in the number of active sites available for adsorbate uptake (Padmavathy *et al*., 2016; Qiao *et al*., 2018). The reduction in adsorption density was also observed in this study, as shown in Table 4.26. Suggesting that lots of available active sites on the adsorbents were not utilised.

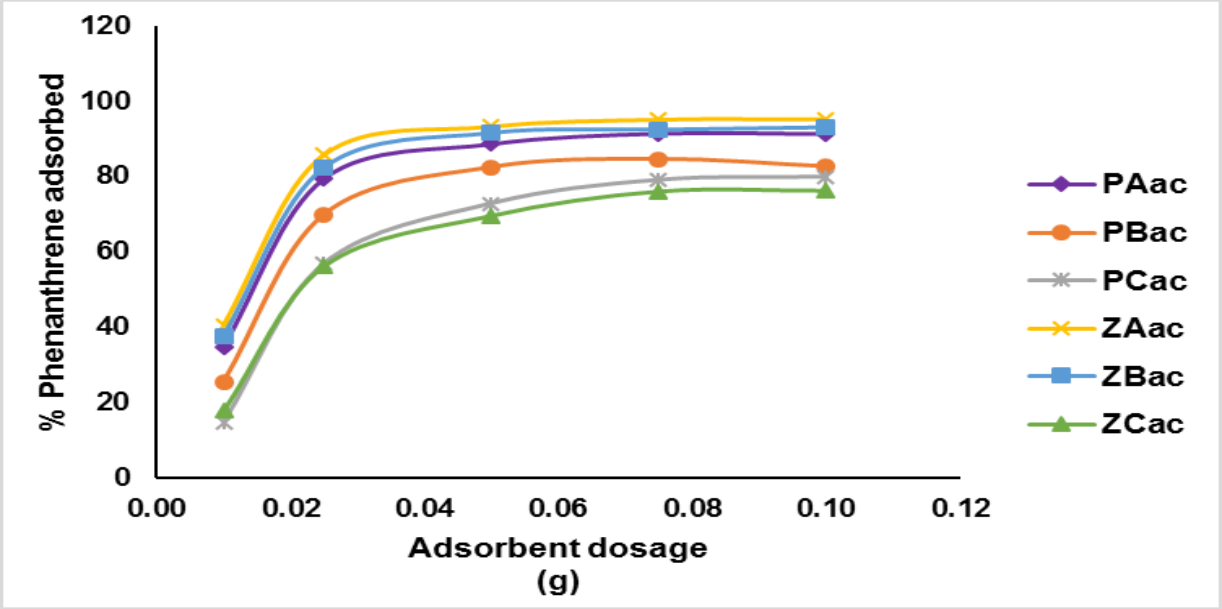

Figure 4.24: Effect of adsorbent dosage on phenanthrene removal using activated carbons

Table 4.26: Effect of adsorbent dosage on phenanthrene removal from solution using activated carbons

Adsorbent	0.010 g	0.025 g	0.050 g	0.075 g	0.100 g
	quantity adsorbed (mg/g)	quantity adsorbed (mg/g)	quantity adsorbed (mg/g)	quantity adsorbed (mg/g)	quantity adsorbed (mg/g)
PAac	0.88	0.79	0.45	0.30	0.23
PBac	0.65	0.70	0.41	0.28	0.21
PCac	0.38	0.57	0.37	0.26	0.20
ZAac	1.03	0.86	0.47	0.32	0.24
ZBac	0.95	0.82	0.46	0.31	0.23
ZCac	0.45	0.56	0.35	0.25	0.19

Other conditions observed: solution concentrations =1 mg/L, solution volume = 25 mL, pH = 3, temperature = 298 K, contact time = 180 min and stirring agitation =100 rpm.

PAac: activated with H_3PO_4 at 5:2 biomass to H_3PO_4 ratio. PBac: activated with H_3PO_4 at 5:1 biomass to H_3PO_4 ratio. PCac: activated with H_3PO_4 at 10:1 biomass to H_3PO_4 ratio. ZAac: activated with $ZnCl_2$ at 5:2 biomass to $ZnCl_2$ ratio. ZBac: activated with $ZnCl_2$ at 5:1 biomass to $ZnCl_2$ ratio. ZCac: activated with $ZnCl_2$ at 10:1 biomass to $ZnCl_2$ ratio

Effect of Initial concentration

Sorption of phenanthrene onto produced activated carbons at varying initial concentrations of phenanthrene (1 to 5 mg/L) in aqueous solution was studied. Initial phenanthrene concentration of 1 mg/L gave the highest removal efficiency of 92.13 % with ZAac (Figure 4.25). The percentage of phenanthrene adsorbed decreased with increase in initial adsorbate concentration, although, the actual amount of phenanthrene adsorbed increased with increase in initial concentration of phenanthrene (Table 4.27). This was due to the availability of more phenanthrene molecules to interact with the active sites of adsorbents. This however did not translate to increased percentage phenanthrene adsorbed, because there was also an increase in the amount of phenanthrene left in solution after the adsorption process. Saturation of adsorption sites on activated carbons surfaces maybe responsible for large percentage of unadsorbed adsorbate molecules (Qiao *et al*., 2018). The result obtained is consistent with other studies (Garg *et al*., 2003; Lamichhane *et al*., 2016). Garg *et al*. (2003) reported a reduction of 98.8 to 43.1% in percentage dye removal from aqueous solution onto formaldehyde treated sawdust when the initial concentration of adsorbate was increased from 50 to 250 mg/L in test carried out for 120 min. They also reported a slight decrease of 99.5 to 95.1% in dye removal, when sulphuric acid treated sawdust carbon was utilised under the same experimental conditions. The observation of Gupta (2015), who carried out batch experiments on the adsorption of phenanthrene in the initial concentration range of 10 to 50 mg/L using 10 mg of activated carbon, is also consistent with the result obtained in this study. Percentage phenanthrene removal from aqueous solution decreased with increase in initial adsorbate concentrations. Sartape *et al*. (2017) also reported that the percentage adsorption of dye onto low-cost adsorbent prepared, decreased with increased initial dye concentrations from 100 to 700 mg/L. Increased adsorption capacity of 12.35 to 80.65 mg/g was however reported, which was attributed to enhanced driving force to overcome resistance to mass transfer at higher dye initial concentrations coupled with enhanced interaction between dye and adsorbent. Initial concentration of adsorbate thus influences adsorption efficiency and capacity of adsorbents.

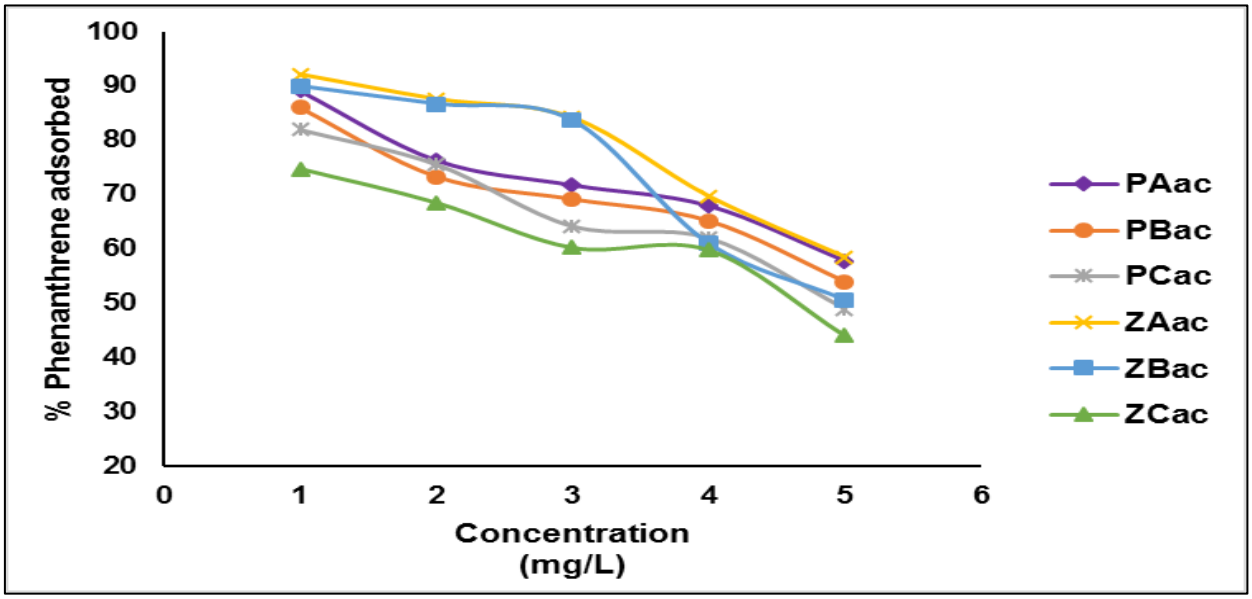

Figure 4.25: Effect of initial concentration of phenanthrene on activated carbons' efficiency

Table 4.27: Effect of initial concentration on phenanthrene removal from solution using activated carbons

Adsorbent	1 mg/L	2 mg/L	3 mg/L	4 mg/L	5 mg/L
	Amount adsorbed (mg/L)	Amount adsorbed (mg/L)	Amount adsorbed (mg/L)	Amount adsorbed (mg/L)	Amount adsorbed (mg/L)
PAac	0.89	1.53	2.15	2.72	2.89
PBac	0.86	1.47	2.07	2.61	2.70
PCac	0.82	1.51	1.92	2.48	2.45
ZAac	0.92	1.75	2.52	2.79	2.92
ZBac	0.90	1.73	2.51	2.44	2.53
ZCac	0.75	1.37	1.81	2.39	2.21

Other conditions observed: Adsorbent dosage = 0.1 g, solution volume = 25 mL, pH = 3, temperature = 298 K, contact time = 180 min and stirring agitation = 100 rpm.
PAac: activated with H_3PO_4 at 5:2 biomass to H_3PO_4 ratio. PBac: activated with H_3PO_4 at 5:1 biomass to H_3PO_4 ratio. PCac: activated with H_3PO_4 at 10:1 biomass to H_3PO_4 ratio. ZAac: activated with $ZnCl_2$ at 5:2 biomass to $ZnCl_2$ ratio. ZBac: activated with $ZnCl_2$ at 5:1 biomass to $ZnCl_2$ ratio. ZCac: activated with $ZnCl_2$ at 10:1 biomass to $ZnCl_2$ ratio

Adsorbents ZAac, ZBac and PAac were used for further studies, based on their efficiencies (> 90 %) for phenanthrene removal (Figure 4.25). The SEM images of these adsorbents before and after they were utilised for phenanthrene adsorption showed significant changes in surface texture (Figure 4.26). The SEM images of activated carbons after phenanthrene adsorption had significantly smoother surface morphology, which could be attributed to accumulation of phenanthrene onto the adsorbent's surfaces. The observed changes in morphology after the adsorption process is in agreement with that reported by Sartape *et al*. (2017). They utilised wood apple shell for the removal of malachite green dye from aqueous solution and observed changes in the SEM micrographs obtained for the adsorbent before and after adsorption. A rough surface morphology was reported before adsorption and a smoother surface morphology after adsorption. Aljeboree *et al*. (2017) also reported notable difference in surface morphologies of SEM characterised coconut shell before and after it was utilised as alternative adsorbent for the removal of hazardous dyes. After adsorption, the dyes were reported to have formed a void-free film, masking the porosity on the adsorbent and resulted in a smoother surface morphology.

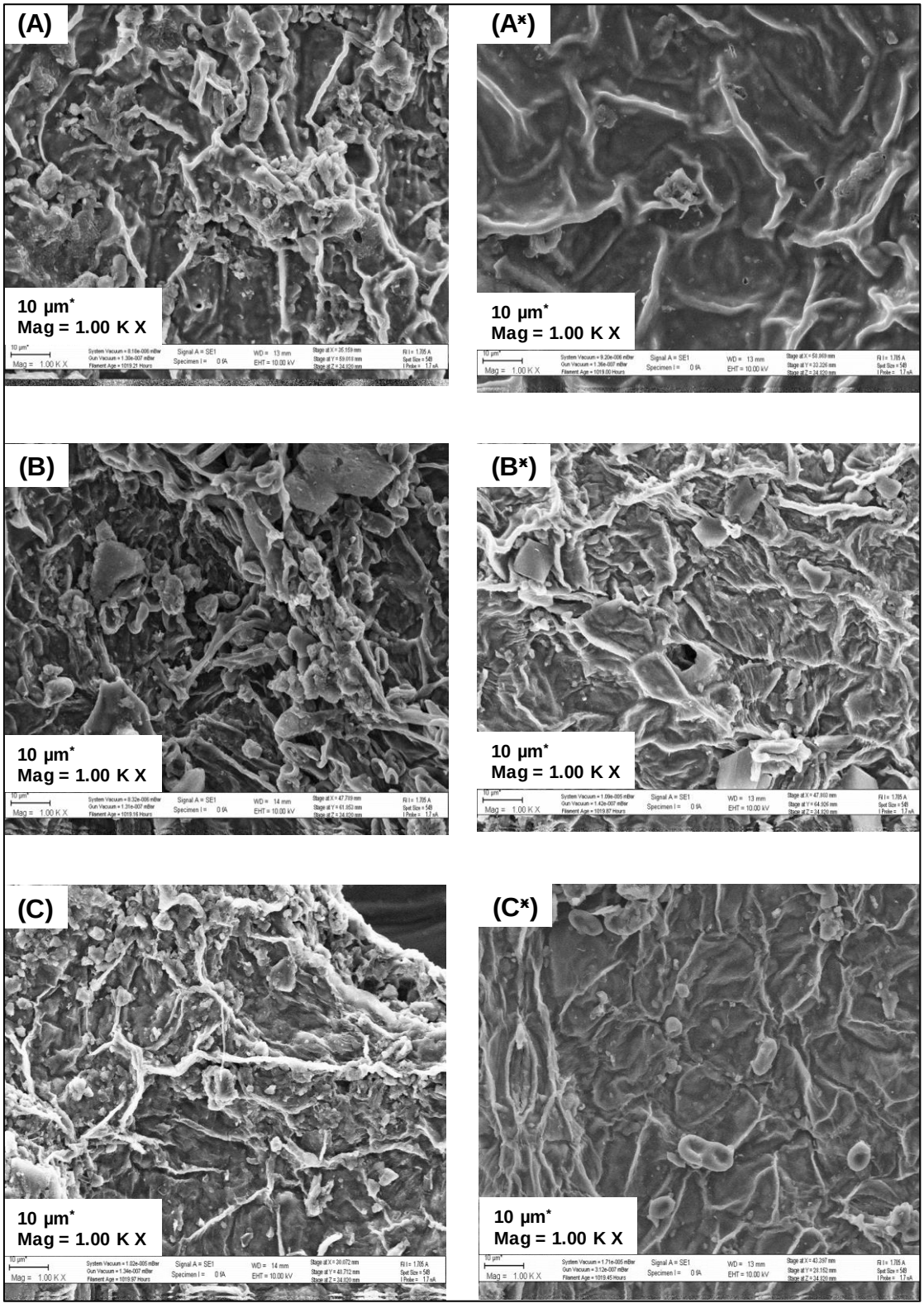

Figure 4.26: SEM images of activated carbons before and after adsorption of phenanthrene from aqueous solution

(A) ZAac (activated with $ZnCl_2$ at 5:2 biomass to $ZnCl_2$ ratio). (B) ZBac (activated with $ZnCl_2$ at 5:1 biomass to $ZnCl_2$ ratio). (C) PAac (activated with H_3PO_4 at 5:2 biomass to H_3PO_4 ratio).

4.4.2.2 Phenanthrene adsorption isotherms

Adsorption isotherms describe the partitioning of adsorbate molecules between the liquid phase and the solid phase at a given temperature and equilibrium state, during an adsorption process (Aljeboree *et al*., 2017). Experimental equilibrium data obtained from this study were subjected to four adsorption equilibrium isotherm models (Langmuir, Freundlich, Temkin and Dubinin-Radushkevich)

The Langmuir maximum monolayer coverage capacity (q_m) obtained for phenanthrene adsorption onto adsorbents ZAac, ZBac and PAac were 94.12 mg/g, 60.07 mg/g and 89.13 mg/g respectively and the corresponding Langmuir isotherm constants (K_L) of 0.48 L/mg, 0.19 L/mg and 0.39 L/mg were obtained respectively (Table 4.28). The separation factor R_L values obtained ranged from 0.83 to 0.98. A R_L value of less than one is an indication of favourable equilibrium sorption (El Qada *et al*., 2006). Hence, favourable equilibrium sorption of phenanthrene onto the activated carbons were achieved. Coefficient of determination value (R^2) ranged from 0.95 to 0.99 (Figure 4.27a), an indication that adsorption data fitted well into Langmuir isotherm model. The data obtained based on Langmuir adsorption isotherm is consistent with that reported by Gupta (2015). A 70.92 mg/g adsorption capacity (q_m) and R^2 value of 0.99 were reported for the adsorption of phenanthrene onto activated carbons produced from orange skin.

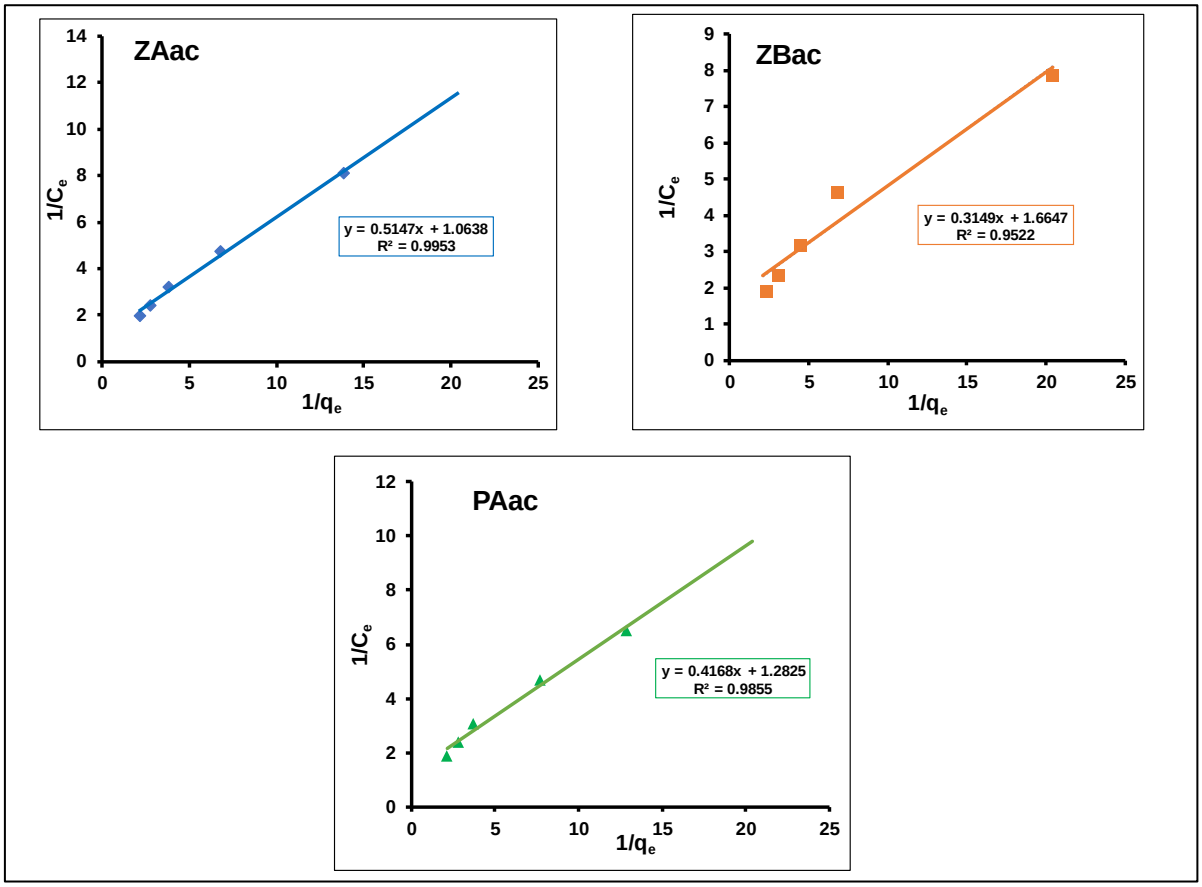

Figure 4.27a: Langmuir adsorption isotherm plots for phenanthrene removal using activated carbons (ZAac, ZBac and PAac)

ZAac (activated with $ZnCl_2$ at 5:2 biomass to $ZnCl_2$ ratio). ZBac (activated with $ZnCl_2$ at 5:1 biomass to $ZnCl_2$ ratio). PAac (activated with H_3PO_4 at 5:2 biomass to H_3PO_4 ratio

Data obtained from the Freundlich isotherm modelling i.e the plot of ln q_e against ln C_e (Figure 4.27b), showed that experimental data fitted into this isotherm model. The range of 0.97 to 0.99 for R^2 values and K_f range of 1.16 to 1.27 mg/g obtained (Table 4.28), indicated multilayer loading of phenanthrene on adsorbents. Also, the 1.33 to 1.52 values of n obtained suggested that the adsorption of phenanthrene onto the activated carbons were favourable, this because the values of n obtained were greater than one but less than ten i.e. $1 < n < 10$ (Sarada *et al*., 2014). The data obtained by Rad *et al*. (2014) from the adsorption of phenanthrene with varied initial concentrations (5 to 40 mg/L) using activated carbons (0.3 g to 100 mL) gave R^2 of 0.99, K_f of 2.71 and n of 1.73 based on Freundlich isotherm model. The results they reported were consistent with those obtained from this study. The R^2 values of experimental data obtained from the adsorption process with Freundlich isotherm signified adsorption onto heterogenous surfaces.

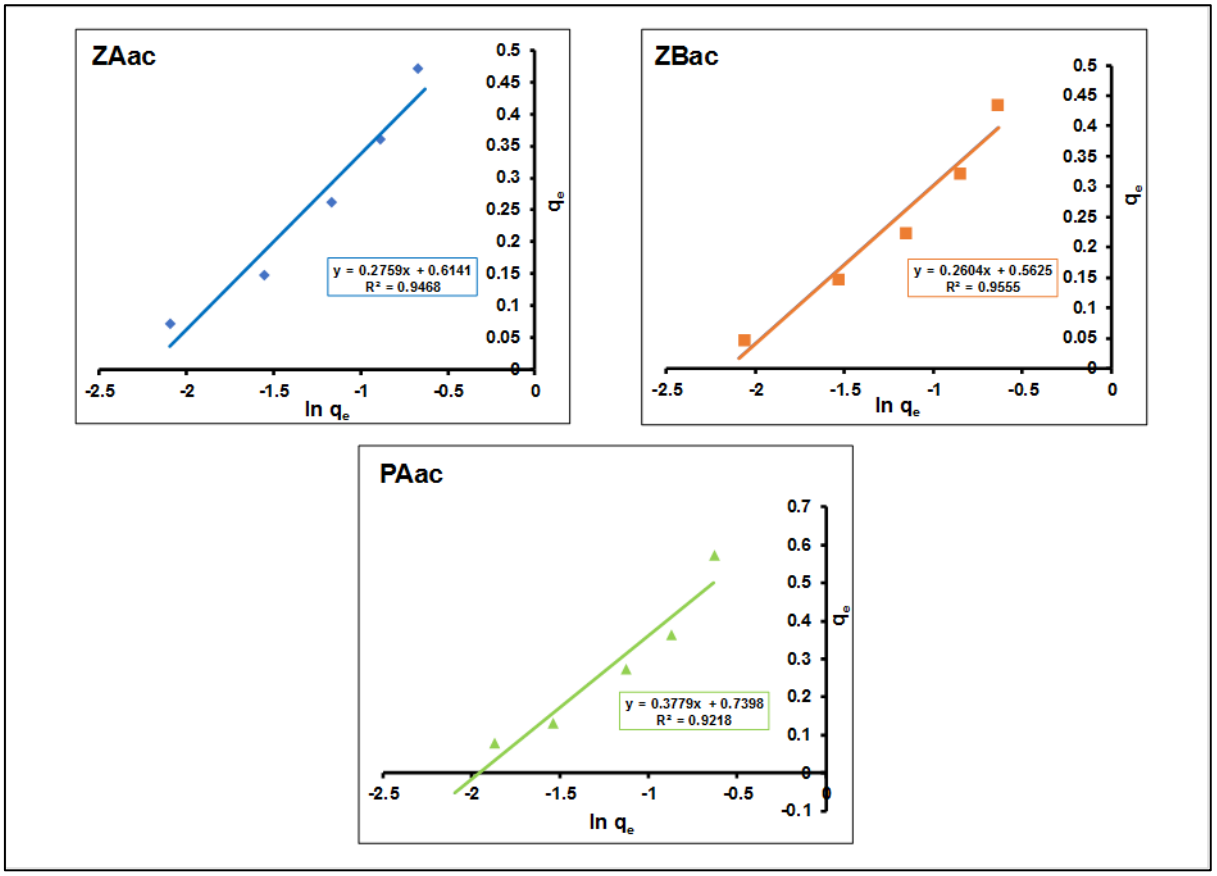

Figure 4.27b: Freudlich adsorption isotherm plots for phenanthrene removal using activated carbons (ZAac, ZBac and PAac)

ZAac (activated with $ZnCl_2$ at 5:2 biomass to $ZnCl_2$ ratio). ZBac (activated with $ZnCl_2$ at 5:1 biomass to $ZnCl_2$ ratio). PAac (activated with H_3PO_4 at 5:2 biomass to H_3PO_4 ratio

The R^2 value range (0.92 - 0.95) obtained from the Temkin isotherm modelling (Figure 4.27c), showed that experimental data fitted considerably well into the Temkin isotherm model, which is an expression of adsorbent-adsorbate interaction, ignoring extremely low and high analytes concentrations (Qu *et al*., 2009). The corresponding 0.26 to 0.38 L/mg and 3.34 to 4.40 kJ/mol ranges were obtained for Temkin isotherm constants K_T, which represents equilibrium binding constant and b_T, which is related to heat of sorption respectively (Table 4.28)

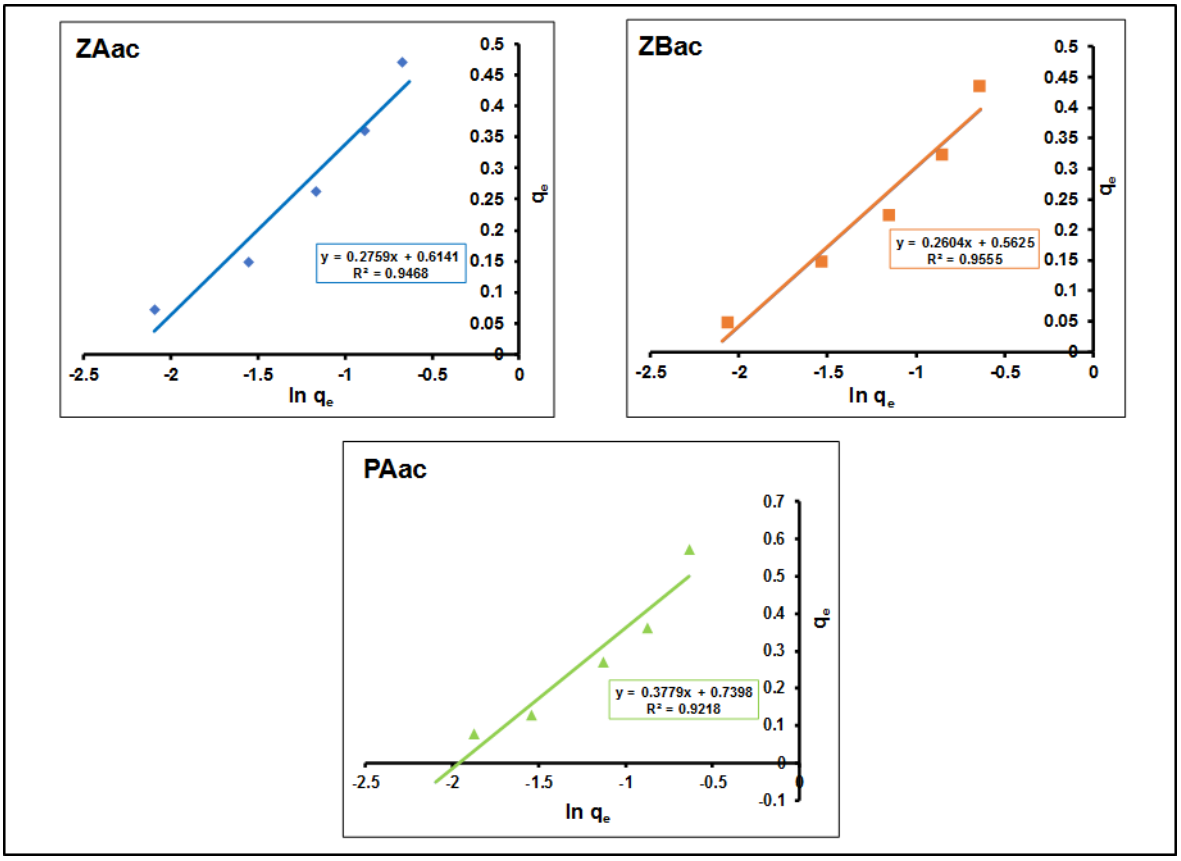

Figure 4.27c: Temkin adsorption isotherm plots for phenanthrene removal using activated carbons (ZAac, ZBac and PAac)

ZAac (activated with $ZnCl_2$ at 5:2 biomass to $ZnCl_2$ ratio). ZBac (activated with $ZnCl_2$ at 5:1 biomass to $ZnCl_2$ ratio). PAac (activated with H_3PO_4 at 5:2 biomass to H_3PO_4 ratio.

Table 4.28: Langmuir, Freundlich, Temkin and Dubinin-Radushkevich isotherm constants for the adsorption of phenanthrene onto activated carbons obtained from *V. vinifera*

Isotherm Models	Parameters	ZAac	ZBac	PAac
Langmuir	R^2	0.99	0.95	0.98
	q_m (mg/g)	94.12	60.07	89.13
	K_L (L/mg)	0.48	0.19	0.39
	R_L	0.94	0.98	0.83
Freundlich	R^2	0.99	0.97	0.99
	K_f	1.27	1.18	1.16
	1/n	0.75	0.66	0.68
	n	1.33	1.52	1.47
Temkin	R^2	0.94	0.95	0.92
	K_T (L/mg)	0.28	0.26	0.38
	b_T (kJ/mol)	4.03	4.40	3.34
Dubinin-Radushkevich	R^2	0.94	0.92	0.98
	q_{DRB}	2.80	1.13	1.06
	K_{ad} (mol^2/kJ^2)	3.00×10^{-8}	9.00×10^{-9}	4.0×10^{-9}
	E (kJ/mol)	4.08	7.45	11.18

The Dubinin-Radushkevich modelling gave R^2 value range of 0.92 to 0.98 9 (Figure 4.27d). The model was previously utilised to differentiate the physical and chemical adsorption of metal ions (Foo & Hameed, 2010). An adsorption mean free energy (E) of below 8 kJ/mol suggests occurrence of physical adsorption and E values between 8 and 16 kJ/mol suggests the dominance of chemical ion exchange (Akar *et al*., 2010). Hence, the adsorption of phenanthrene onto the $ZnCl_2$ activated carbons ZAac and ZBac with E values of 4.08 and 7.45 kJ/mol respectively may be considered as physical adsorption. However, the phenanthrene adsorption on the H_3PO_4 activated carbons PAac with E value of 11.18 kJ/mol may be considered to have followed a chemical ion exchange pathway.

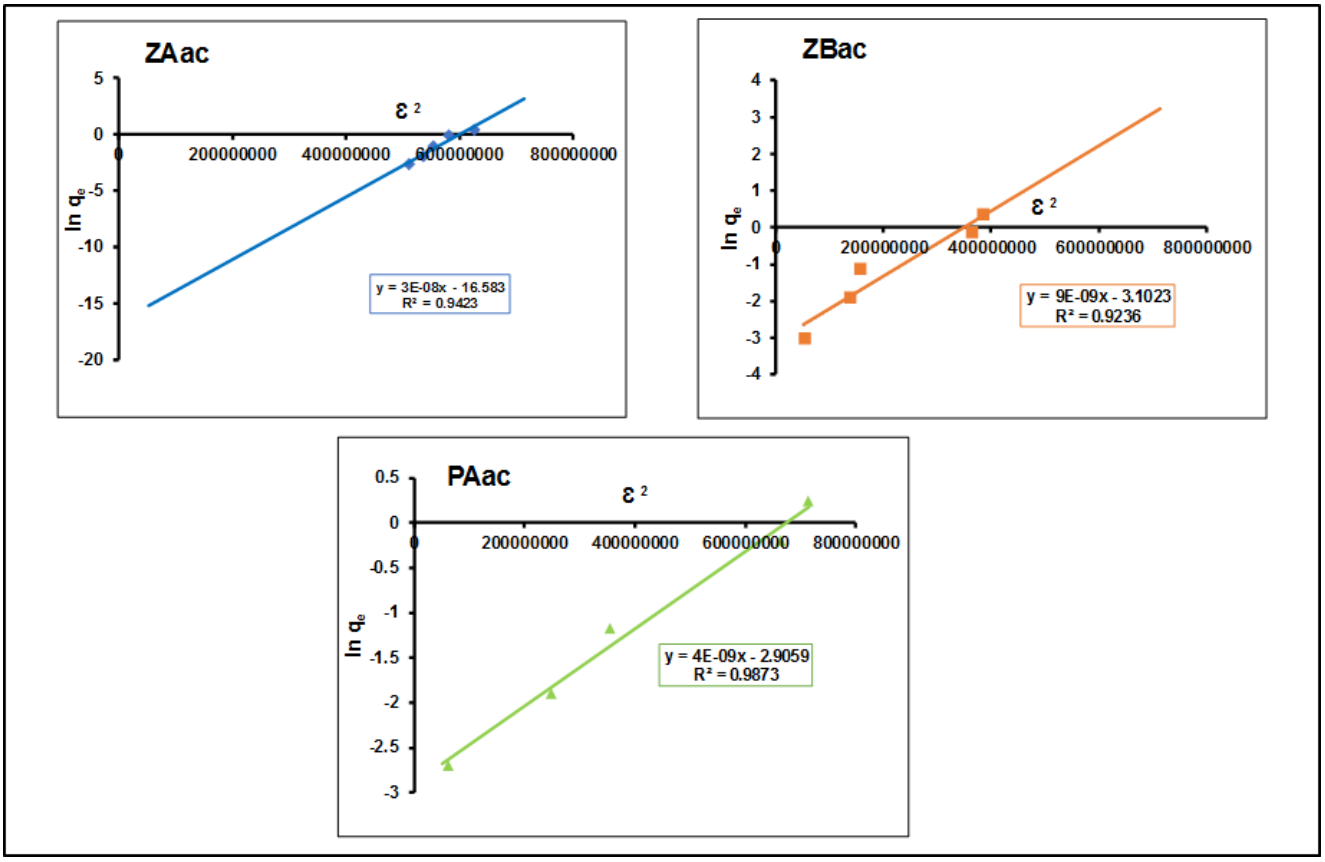

Figure 4.27d: Dubinin-Radushkevich adsorption isotherm plots for phenanthrene removal using activated carbons (ZAac, ZBac and PAac)

ZAac (activated with $ZnCl_2$ at 5:2 biomass to $ZnCl_2$ ratio). ZBac (activated with $ZnCl_2$ at 5:1 biomass to $ZnCl_2$ ratio). PAac (activated with H_3PO_4 at 5:2 biomass to H_3PO_4 ratio

The results obtained from isotherm models showed that the adsorption of phenanthrene from aqueous solution onto activated carbons (ZAac, ZBac and PAac), produced from grape leaf litter was favourable. The experimental data fitted best into the Freundlich isotherm model (R^2 of up to 0.999) of the four models employed, as shown in the adsorption isotherm plots (Figure 4.27a - Figure 4.27d). This is an indication that heterogenous and multilayer adsorption pathways are dominant in the adsorption of phenanthrene onto the produced activated carbons. Physical and chemical adsorption processes were responsible for phenanthrene removal. It can be concluded that the activated carbons from grape leaf litter have the potential to serve as biosorbents for the remediation of aqueous solutions and wastewaters contaminated with PAHs.

4.4.4.3 Adsorption kinetics

Adsorption kinetics study, is crucial in evaluating the efficiency of adsorbents and also in the determination of adsorption mechanism (Aljeboree *et al*., 2017). The effect of contact time on the adsorption of phenanthrene onto activated carbons was studied over time range of 0 to 180 min (Figure 4.28). The percentage phenanthrene adsorbed increased with contact time rapidly from 10 min to 80 min. After the 80 min contact time, no significant increase in phenanthrene adsorption was recorded, due to dynamic equilibrium being reached. This observation is consistent with that of Gupta (2015), who investigated the effect of contact time on phenanthrene adsorption in the time interval of 0 to 150 min. The study revealed that the amount of phenanthrene adsorbed from aqueous solution onto activated carbons, increased with contact time till 75 min and equilibrium was attained till 150 min. Aljeboree *et al*. (2017), reported a much faster adsorption rate for the uptake of dyes by coconut shell activated carbon compared to the rate observed in this study. They reported that most of the dye uptake took place within 10 min of the adsorption process.

The uptake of phenanthrene onto activated carbons as a function of time, was further analysed with pseudo-first order, pseudo-second order, Elovich and intra-particle diffusion kinetic models, in order to study the mechanism(s) of adsorption.

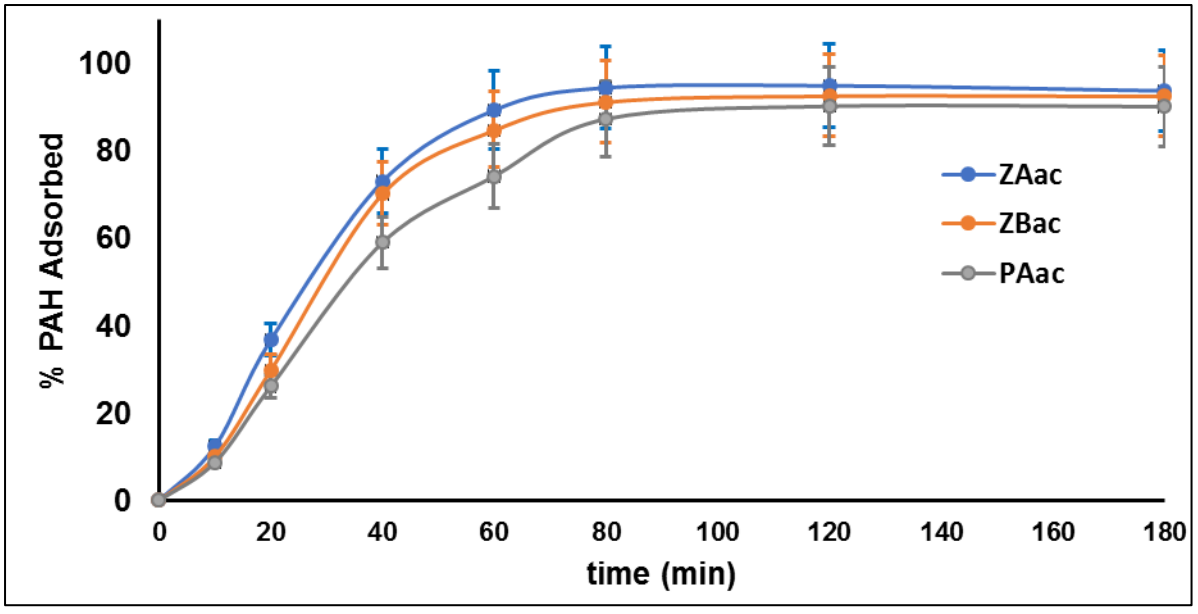

Figure 4.28: Effect of contact time on phenanthrene adsorption using activated carbons

Pseudo-first order kinetic model

The pseudo-first order kinetic model, also known as Lagergren kinetic, had its adsorption rate equation (for a liquid-solid system) derived, based on the adsorbent adsorption capacity. This adsorption rate equation is commonly used for solute adsorption from liquid matrix (Sarada *et al*., 2014)

The simplified pseudo first order kinetic equation can be expressed as:

$$\mathbf{In}(\boldsymbol{q_e} - \boldsymbol{q_t}) = \mathbf{In}\, \boldsymbol{q_e} - \boldsymbol{k_1}\, \boldsymbol{t} \qquad \textbf{Equation 4.1}$$

Where q_e and q_t are the amount of solute adsorbed per unit mass of adsorbent (mg/g) at equilibrium and at time t respectively and k_1 is the rate constant.

The value of $\boldsymbol{k_1}$ was obtained from the slope of the linear plot of $\mathbf{In}(\boldsymbol{q_e} - \boldsymbol{q_t})$ against 't'. The correlation coefficient (R^2) was also obtained from the linear plot (Figure 4.29a). The value of k_1 obtained for utilising adsorbents ZAac, ZBac and PAac for phenanthrene adsorption were 3.59 min^{-1}, 2.87 min^{-1}, and 2.34 min^{-1} respectively (Table 4.29). The q_e values obtained ranged from 0.46 to 0.73 mg/g and the R^2 value ranged from 0.533 to 0.829. The data therefore did not fit well into pseudo-first order model, since the R^2 values obtained were less than <0.9. The poor fitting of experimental data obtained from the adsorption of phenanthrene onto activated carbons, into pseudo first order kinetic model had been reported previously (Rad *et al*., 2014). They reported that phenanthrene adsorption showed a better fitting with the pseudo-second order kinetic model relative to the pseudo-first order kinetic model. They concluded that the adsorption mechanism of phenanthrene onto activated carbons was predominantly controlled by chemisorption.

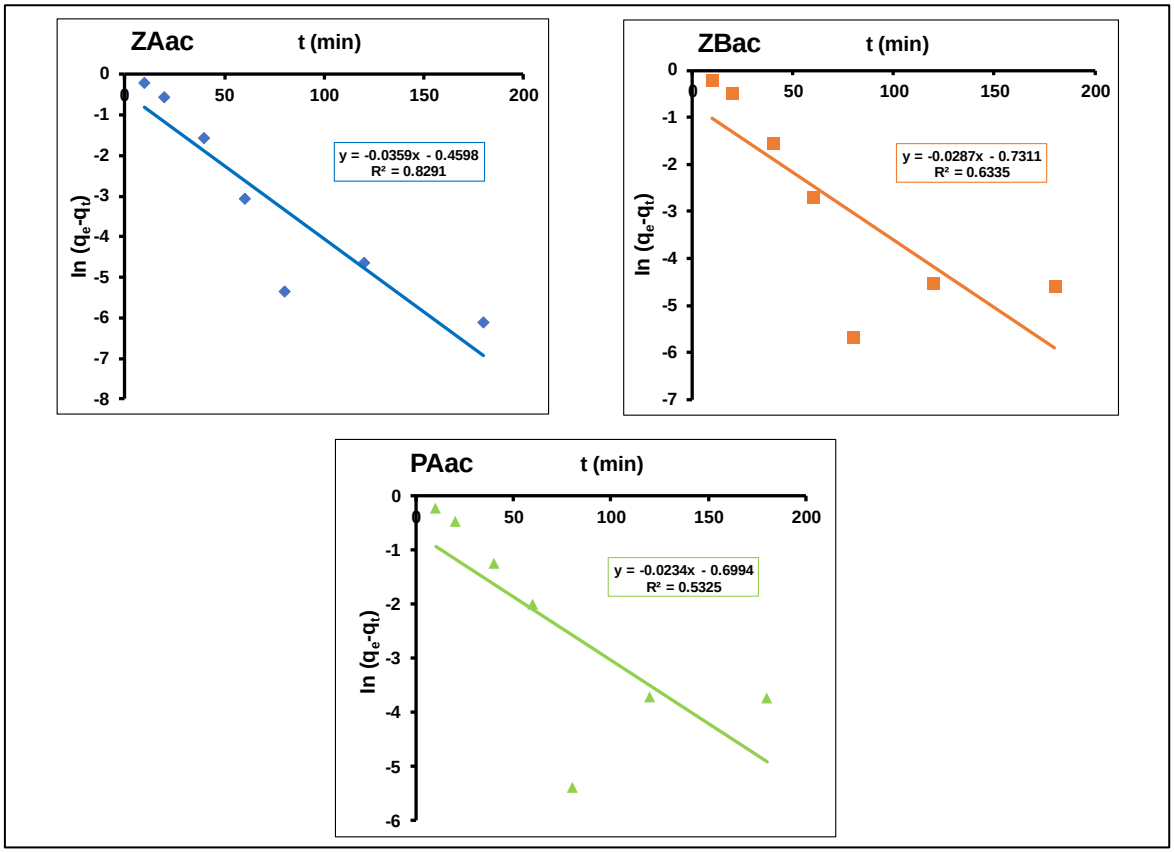

Figure 4.29a: Pseudo-first order adsorption kinetic plots for phenanthrene removal using activated carbons (ZAac, ZBac and PAac)

ZAac (activated with $ZnCl_2$ at 5:2 biomass to $ZnCl_2$ ratio). ZBac (activated with $ZnCl_2$ at 5:1 biomass to $ZnCl_2$ ratio). PAac (activated with H_3PO_4 at 5:2 biomass to H_3PO_4 ratio.

Pseudo-second order kinetic model

The pseudo-second order model is based on the sorption capacity of the solid phase which is associated with the number of available active sites. The linearised form of the kinetic model is expressed as Equation 4.2 (Ho & McKay, 1998).

$$\frac{t}{q_t} = \frac{1}{k_2 {q_e}^2} + \frac{1}{q_e}(t) \qquad \textbf{Equation 4.2}$$

This model is advantageous as it eliminates the problem of assigning q_e. The kinetics is presumed to proceed via chemisorption, being the rate determining step (Ho & McKay, 1998).

The plot of t/q_t against t gave a linear relationship (Figure 4.29b), from where q_e and k_2 were determined from the slope and intercept respectively. The value of k_2 [g (mg/min)] obtained for utilising ZAac, ZBac and PAac were 0.761, 0.692 and 0.637 respectively. The values q_e ranged from 38.78 to 62.58 mg/g with respective R^2 values of 0.696 to 0.8532 (Table 4.29). The data fitted

better into pseudo-second order model relative to pseudo-first order model (Table 4.29). This is consistent with the observation of Shi *et al*. (2013), who carried out kinetic studies on the adsorption of naphthalene onto activated carbons. They reported R^2 values of 0.9279 to 0.9514 for the pseudo-first order kinetic model and 0.9983 to 0.9991 for the pseudo-second order kinetic model. Rad *et al*. (2014), also reported that the adsorption of phenanthrene onto activated carbons fitted better with pseudo-second order model relative to pseudo-first order model, utilising phenanthrene initial concentration range of 5 to 40 ppm. They concluded that the adsorption mechanism of phenanthrene onto activated carbons was controlled predominantly by chemical bonding or chemisorption. The adsorption kinetics of various adsorbates onto activated carbons have also been reported to have followed the pseudo second-order rate equation better than that of the pseudo first-order; sorption of Chromium (IV) onto activated carbons produced from cornelian cherry, apricot stone and almond shell (Demirbas *et al*., 2004), sorption of ciprofloxacin onto activated carbons derived from *Arundo donax* Linn. and pomelo peel (Sun *et al*., 2016) and sorption of dyes onto activated carbons obtained from coconut shell (Aljeboree *et al*., 2017). Hence, chemisorption plays an important role in the adsorption of adsorbates onto activated carbons.

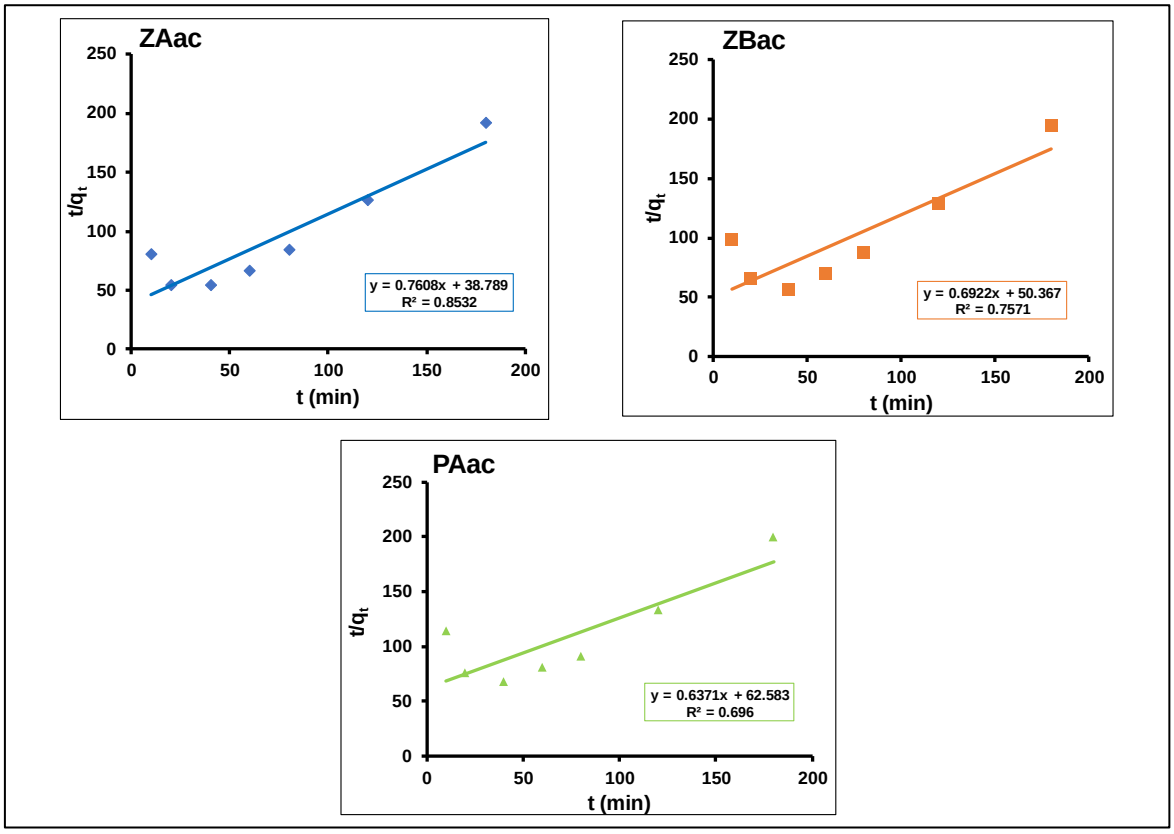

Figure 4.29b: Pseudo-second order adsorption kinetic plots for phenanthrene removal using activated carbons (ZAac, ZBac and PAac)

ZAac (activated with $ZnCl_2$ at 5:2 biomass to $ZnCl_2$ ratio). ZBac (activated with $ZnCl_2$ at 5:1 biomass to $ZnCl_2$ ratio). PAac (activated with H_3PO_4 at 5:2 biomass to H_3PO_4 ratio.

Elovich Kinetic model

The Elovich model has been widely utilised to describe chemical adsorption processes and it is applicable for systems with heterogenous adsorbing surfaces (Wu *et al*., 2009). Experimental data were subjected to Elovich model (Equation 4.3).

$$q_t = \left(\frac{1}{\beta}\right) ln\ (\alpha . \beta) + \left(\frac{1}{\beta}\right) ln\ (t)$$ **Equation 4.3**

q_t = sorption capacity at time t (mg/g)

α = initial sorption rate (mg/g min)

β = desorption constant (g/mg) during any one experiment (Ho & McKay, 1998)

A plot of q_t versus ln(t) gives a straight-line graph with a slope of (1/β) and intercept of (1/β) ln (αβ).

The Elovich kinetic model plots from this study are presented in Figure 4.29c. The α values obtained ranged from 0.04 to 0.06 mg/g min, while the β values ranged from 3.16 to 3.24 g/mg and the respective R^2 range of 0.88 to 0.94 was obtained (Table 4.29). A similar range of α values (0.04 to 0.18 mg/g min) was reported by Ramachandran *et al*. (2011). They studied the kinetics of reactive orange 16 dye removal from aqueous solution, utilising activated carbons produced from *Ananas comosus* leaves under varying adsorbate concentrations and temperatures. The range of β (g/mg) values (4.95 to 31.28) reported was however higher than that obtained in this study. Hence, phenanthrene adsorbed onto activated carbons in this study, appeared to be less susceptible to desorption relative to adsorbed dye onto activated carbons reported by Ramachandran *et al*. (2011) with higher desorption rates (β). However, a much lower β range (0.04 – 0.33 g/mg) was reported by Bedin *et al*. (2018) for the adsorption of methylene blue onto activated carbon. They reported that the adsorption of methylene blue onto the activated carbon appears to be irreversible, based on the low values of β obtained, that decreased as initial adsorbate concentration increases. Therefore, the range of β obtained in this study is an indication that the adsorbed phenanthrene molecules onto activated carbons were sufficiently held and may not be easily desorbed.

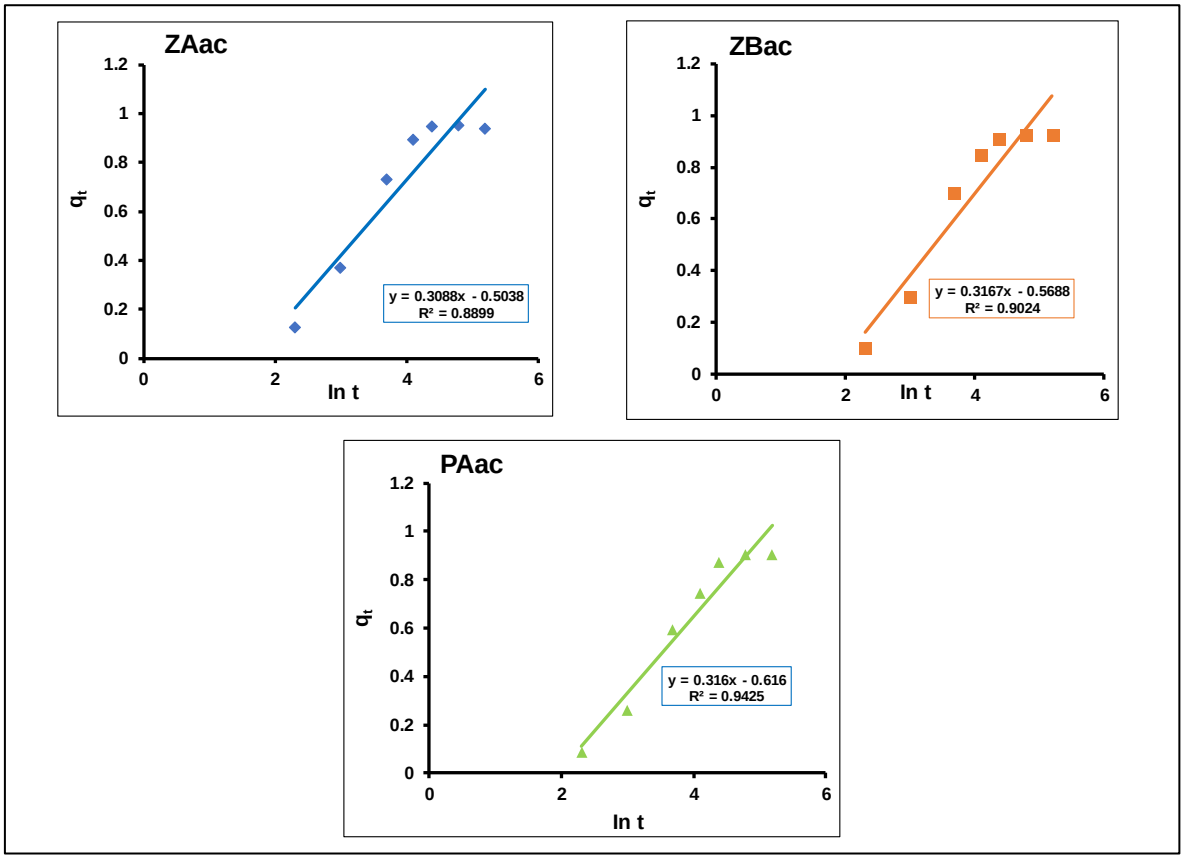

Figure 4.29c: Elovich adsorption kinetic plots for phenanthrene removal using activated carbons (ZAac, ZBac and PAac)

ZAac (activated with $ZnCl_2$ at 5:2 biomass to $ZnCl_2$ ratio). ZBac (activated with $ZnCl_2$ at 5:1 biomass to $ZnCl_2$ ratio). PAac (activated with H_3PO_4 at 5:2 biomass to H_3PO_4 ratio.

Table 4.29: Adsorption kinetics parameters for the removal of phenanthrene from aqueous solution using activated carbons obtained from *V. vinifera*

Models	Parameters	ZAac	ZBac	PAac
Pseudo first order kinetics	q_e	0.46	0.73	0.70
	K_1 (min^{-1}) X 10^{-2}	3.59	2.87	2.34
	R^2	0.82	0.63	0.53
Pseudo second order kinetics	q_e (mg/g)	38.78	50.37	62.58
	K_2 (g (mg min^{-1}))	0.76	0.69	0.64
	R^2	0.85	0.75	0.69
Elovich rate equation	α (mg/g min)	0.06	0.05	0.04
	β (g/mg)	3.24	3.16	3.16
	R^2	0.88	0.90	0.94
Intraparticle diffusion	K_{id}	0.09	0.03	0.03
	C	0.08	0.08	0.08
	R^2	0.73	0.75	0.82

Weber Morris intraparticle diffusion kinetic model

To describe the adsorption of phenanthrene onto produced activated carbons from a mechanistic point of view, the Weber Morris intraparticle diffusion model was used. This model is based on the hypothesis that the overall adsorption process maybe controlled either by one or combinations of more than one factors. These include film or external diffusion, pore diffusion, surface diffusion and adsorption onto the adsorbent pore surface (Fierro *et al*., 2008; Asuquo & Martin, 2016). The expression for the model is expressed as:

$$q_t = K_{id} \cdot t^{1/2} + C \qquad \textbf{Equation 4.4}$$

Where q_t is the amount of adsorbate adsorbed at time t (mg/g), K_{id} is the intraparticle diffusion rate constant (mg/g $min^{1/2}$) and C (mg/g) is the constant related to the thickness of the boundary layer (the higher the value of C, the greater the boundary layer effect) (Fierro *et al*., 2008).
The Weber Morris intraparticle diffusion kinetic model plots, from this study are presented in Figure 4.29d.

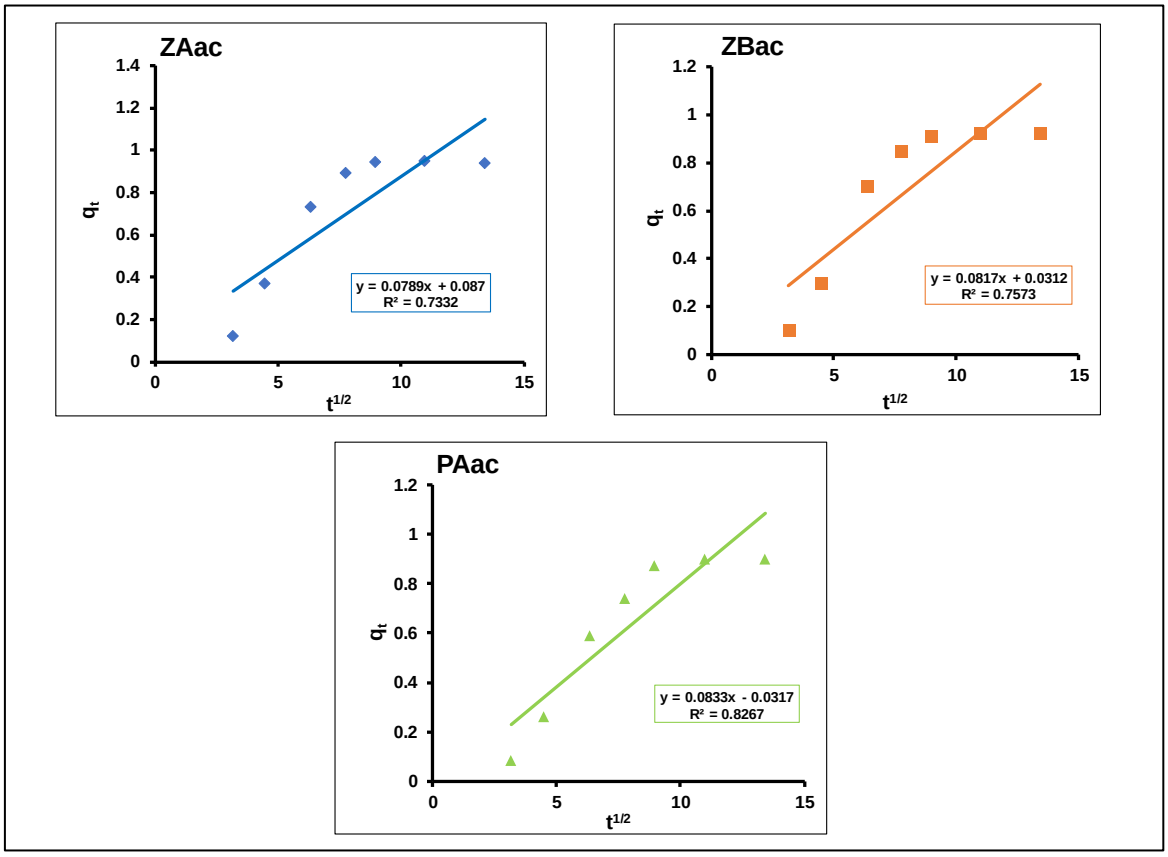

Figure 4.29d: Weber Morris intraparticle diffusion adsorption kinetic plots for phenanthrene removal using activated carbons (ZAac, ZBac and PAac)

A straight-line graph would be obtained from the plot of q_t vs $t^{1/2}$ when the sorption process is controlled by intraparticle diffusion only. However, if multi-linear plots were obtained, then it suggests that two or more steps (such as film diffusion and equilibrium adsorption) affected the sorption process (Fierro *et al*., 2008). The plots of q_t vs $t^{1/2}$ obtained from this study could be divided into two parts (a sharp rise and flat portion) as shown in Figure 4.30. Similar observations were reported by Liu *et al*. (2010), who studied the adsorption kinetics of phenols onto activated carbon fibres. Intraparticle film diffusion process was proposed as the dominant process at initial sharp rise portion and final equilibrium adsorption process for the flat portion (Liu *et al*., 2010). Hence, the sorption processes of phenanthrene onto activated carbons (ZAac, ZBac and PAac) were affected by two or more steps. The values of K_{id}, *C*, and R^2 Weber Morris intraparticle diffusion model parameters are presented in Table 4.29.

Based on the R^2 values obtained from the kinetic study, experimental data fitted best into the Elovich kinetic model relative to other kinetic models (Table 4.29). Hence, chemisorption was deduced as a major phenanthrene removal pathway from aqueous solution.

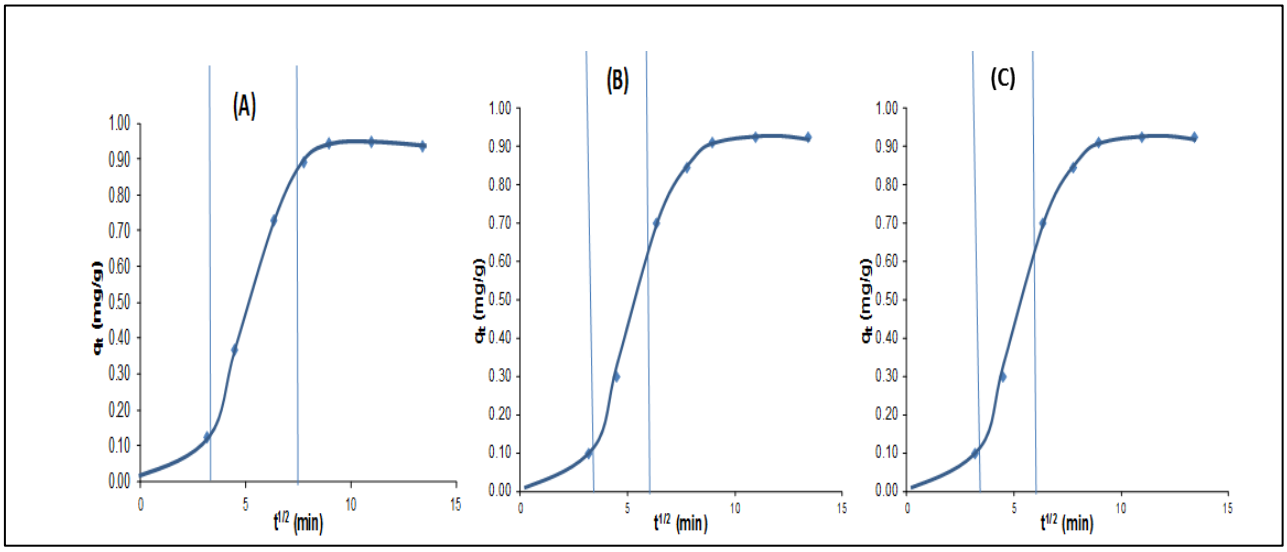

Figure 4.30: Intra particle diffusion kinetics for phenanthrene removal using activated carbons
(A) ZAac (activated with $ZnCl_2$ at 5:2 biomass to $ZnCl_2$ ratio). (B) ZBac (activated with $ZnCl_2$ at 5:1 biomass to $ZnCl_2$ ratio). (C) PAac (activated with H_3PO_4 at 5:2 biomass to H_3PO_4 ratio).

CHAPTER 5
CONCLUSIONS AND RECOMMENDATIONS

5.1 Conclusions

The US EPA PAHs were detected in water, sediment and plant samples collected from the Diep and Plankenburg Rivers. Industrial, domestic and agricultural activities were major sources of PAHs contamination of both rivers. The Diep River flows through different land-use areas; the upstream of the river is dominated by agricultural activities and formal and informal settlements as well as industrial establishments (oil refinery, chemical and clothing factories, as well as wastewater treatment plant) are the anthropogenic sources of PAHs downstream. The Plankenburg River also flows through similar land use areas; industrial area (clothing factory, dairy factory, spray painting and mechanical workshop), Kayamandi (an informal settlement) and through farmlands.

The spatial and temporal levels of PAHs in water and sediment samples from the Diep and Plankenburg Rivers showed seasonal variations. The annual average detected levels of Chrysene (Chy) and Benzo[a]anthracene (BaA) in water samples from all sampling sites were higher compared to other PAHs. Water samples from the Plankenburg River were more polluted with PAHs relative to those from the Diep River. In sediment samples however, Benzo[b]fluoranthene (BbF) was the compound with highest levels relative to other PAHs. The surface water and sediment samples of the Diep and Plankenburg Rivers were heavily contaminated with carcinogenic PAHs. The probabilistic risk assessment revealed that potential risks are associated with the compounds at the levels they occurred in both rivers.

The levels of PAHs detected in plant samples were of several magnitudes (up to x 10^3) higher than the detected levels in water samples and higher than levels detected in sediment samples (up to x 10^1). This suggests PAHs accumulation in plants. The leaf of *P. australis* had the highest levels of PAHs in all study sites. Results indicate the potential of the *P. australis* plant to translocate PAHs from water and/or sediment into its root and shoot. The plant may be further investigated for its phytoremediation potentials, especially for PAHs and other organic contaminants.

This study affirms the ubiquitous nature of PAHs in the environment. *Vitis vinifera* leaf litter served as a good precursor biomaterial for activated carbons. It may be substituted for the more expensive commercial activated carbons. The biomass is renewable and gave good yield of activated carbons with enormous potential for removal of organic contaminants from water and wastewater. Phenanthrene removal efficiency by produced activated carbons was enhanced at low pH values, high adsorbent dosage and low PAH initial concentration.

The study gave informative data on the levels of 16 US EPA priority PAHs in water, sediment and plant samples of fresh aquatic systems and demonstrated the potential of locally sourced agrowaste for the remediation of PAHs. Nevertheless, the levels of PAHs in air should be assessed, to further ascertain the contribution of atmospheric deposition from industrial and vehicular emissions on detected PAHs levels.

.

5.2 Recommendations

- There is need for continuous monitoring and identification of anthropogenic sources of PAHs into aquatic systems in South Africa for effective control and abatement of these toxic compounds.
- Further studies should asses the levels of PAHs in air to investigate atmospheric deposition pathway of PAHs into the aquatic systems.
- There is need to assess the levels of PAHs in vegetables and aquatic organisms to ensure food security.
- Industrial activities must be closely monitored to ensure adherence to global best practices; there is also need for more effective enforcement of environmental quality guidelines for emissions. Policy documents for PAHs threshold limits in emissions should also be formulated.
- The potential of *P. australis* for phytoremediation of PAHs and other organic contaminants may be further explored.
- Finally, there is need for the South Africa government to fund holistic environmental assessment that will ensure sustainable water and food security in the Republic. Water and food systems are impossible to separate, and Provinces in the Republic are facing acute water shortages. The security of these two essential systems are further threatened by contamination of the freshwater systems by PAHs and other carcinogenic chemicals.

REFERENCES

Abdel-Shafy, H.I. & Mansour, M.S.M. 2016. A review on polycyclic aromatic hydrocarbons: Source, environmental impact, effect on human health and remediation. *Egyptian Journal of Petroleum*, 25(1): 107–123.

Abdollahi, S., Raoufi, Z., Faghiri, I., Savari, A., Nikpour, Y. & Mansouri, A. 2013. Contamination levels and spatial distributions of heavy metals and PAHs in surface sediment of Imam Khomeini Port, Persian Gulf, Iran. *Marine Pollution Bulletin*, 71(1–2): 336–345.

Abdullah, M.A., Chiang, L. & Nadeem, M. 2009. Comparative evaluation of adsorption kinetics and isotherms of a natural product removal by Amberlite polymeric adsorbents. *Chemical Engineering Journal*, 146(3): 370–376.

Adebowale, K.O. & Bayer, E. 2002. Active carbons from low temperature conversion chars. https://inis.iaea.org/search/search.aspx?orig_q=RN:33050383 8 May 2017.

Agunbiade, F.O., Olu-Owolabi, B.I. & Adebowale, K.O. 2009. Phytoremediation potential of *Eichornia crassipes* in metal-contaminated coastal water. *Bioresource Technology*, 100: 4521-4526.

Ahangar, A.G. 2010. Sorption of PAHs in the soil environment with emphasis on the role of soil organic matter: A review. *World Applied Sciences Journal*, 11(7): 759–765.

Ahn, C.K., Kim, Y.M., Woo, S.H. & Park, J.M. 2008. Soil washing using various nonionic surfactants and their recovery by selective adsorption with activated carbon. *Journal of Hazardous Materials*, 154: 153–160.

Ahrens, M.J. & Depree, C. V. 2010. A source mixing model to apportion PAHs from coal tar and asphalt binders in street pavements and urban aquatic sediments. *Chemosphere*, 81(11): 1526–1535.

Ajayi, B.O., Adedara, I.A. & Farombi, E.O. 2016. Benzo[a]pyrene induces oxidative stress, pro-inflammatory cytokines, expression of nuclear factor-kappa B and deregulation of wnt/beta-catenin signaling in colons of BALB/c mice. *Food and Chemical Toxicology*, 95: 42–51.

Akar, T., Celik, S. & Akar, S.T. 2010. Biosorption performance of surface modified biomass obtained from *Pyracantha coccinea* for the decolourisation of dye contaminated solutions. *Chemical Engineering Journal*, 160(2): 466–472.

Akpa, O.M. & Unuabonah, E.I. 2011. Small-sample corrected Akaike information criterion: An appropriate statistical tool for ranking of adsorption isotherm models. *Desalination*, 272: 20–26.

Aksu, Z. 2005. Application of biosorption for the removal of organic pollutants: a review. *Process Biochemistry*, 40(3): 997–1026.

Al-Bahri, M. Al, Calvo, L., Gilarranz, M.A. & Rodriguez, J.J. 2012. Activated carbon from grape seeds upon chemical activation with phosphoric acid: Application to the adsorption of diuron from water. *Chemical Engineering Journal*, 203: 348–356.

Albinet, A., Leoz-Garziandia, E., Budzinski, H., Villenave, E. & Jaffrezo, J.L. 2008. Nitrated and oxygenated derivatives of polycyclic aromatic hydrocarbons in the ambient air of two French alpine valleys. Part 1: Concentrations, sources and gas/particle partitioning. *Atmospheric Environment*, 42: 43–54.

Al-Dakheel, A.J., Iftikhar Hussain, M. & Abdul Rahman, A.Q.M. 2015. Impact of irrigation water salinity on agronomical and quality attributes of *Cenchrus ciliaris* L. accessions. *Agricultural Water Management*, 159: 148–154.

Aldarondo-Torres, J.X., Samara, F., Mansilla-Rivera, I., Aga, D.S. & Rodríguez-Sierra, C.J. 2010. Trace metals, PAHs, and PCBs in sediments from the Jobos Bay area in Puerto Rico. *Marine*

Pollution Bulletin, 60(8): 1350–1358.

Aljeboree, A.M., Alshirifi, A.N. & Alkaim, A.F. 2017. Kinetics and equilibrium study for the adsorption of textile dyes on coconut shell activated carbon. *Arabian Journal of Chemistry*, 10: S3381–S3393.

Alkorta, I. & Garbisu, C. 2001. Phytoremediation of organic contaminants in soils. *Bioresource Technology*, 79: 273–276.

Alomirah, H., Al-Zenki, S., Al-Hooti, S., Zaghloul, S., Sawaya, W., Ahmed, N. & Kannan, K. 2011. Concentrations and dietary exposure to polycyclic aromatic hydrocarbons (PAHs) from grilled and smoked foods. *Food Control*, 22: 2028–2035.

Amador-Muñoz, O., Bazán-Torija, S., Villa-Ferreira, S.A., Villalobos-Pietrini, R., Bravo-Cabrera, J.L., Munive-Colín, Z., Hernández-Mena, L., Saldarriaga-Noreña, H. & Murillo-Tovar, M.A. 2013. Opposing seasonal trends for polycyclic aromatic hydrocarbons and PM10: Health risk and sources in southwest Mexico City. *Atmospheric Research*, 122: 199–212.

Amador-Muñoz, O., Villalobos-Pietrini, R., Miranda, J. & Vera-Avila, L.E. 2011. Organic compounds of PM2.5 in Mexico Valley: Spatial and temporal patterns, behavior and sources. *Science of The Total Environment*, 409(8): 1453–1465.

Amdany, R., Chimuka, L., Cukrowska, E., Kukučka, P., Kohoutek, J., Tölgyessy, P. & Vrana, B. 2014. Assessment of bioavailable fraction of POPS in surface water bodies in Johannesburg City, South Africa, using passive samplers: An initial assessment. *Environmental Monitoring and Assessment*, 186: 5639–5653.

Anawar, H.M., Akter, F., Solaiman, Z.M. & Strezov, V. 2015. Biochar: An emerging panacea for remediation of soil contaminants from mining, industry and sewage wastes. *Pedosphere*, 25: 654–665.

Anderson, T. A, Guthrie, E. A & Walton, B.T. 1993. Bioremediation. *Environmental Science and Technology*, 27(13): 2630–2636.

Ang, E.L., Zhao, H. & Obbard, J.P. 2005. Recent advances in the bioremediation of persistent organic pollutants via biomolecular engineering. *Enzyme and Microbial Technology*, 37(5): 487–496.

Antemir, A., Hills, C.D., Carey, P.J., Gardner, K.H., Bates, E.R. & Crumbie, A.K. 2010. Long-term performance of aged waste forms treated by stabilisation/solidification. *Journal of Hazardous Materials*, 181: 65–73.

Antizar-Ladislao, B., Lopez-Real, J. & Beck, A.J. 2005. Laboratory studies of the remediation of polycyclic aromatic hydrocarbon contaminated soil by in-vessel composting. *Waste Management*, 25(3): 281–289.

AOAC (Association of Official Analytical Chemists). 1990. *Official Methods of Analysis of the Association of Official Analytical Chemists*. 15th ed. Artington, Virgina: AOAC.

Asuquo, E.D. & Martin, A.D. 2016. Sorption of cadmium (II) ion from aqueous solution onto sweet potato (*Ipomoea batatas* L.) peel adsorbent: Characterisation, kinetic and isotherm studies. *Journal of Environmental Chemical Engineering*, 4(4): 4207–4228.

ATSDR (Agency for Toxic Substances and Disease Registry). 1995. Toxicological profile for polycyclic aromatic hydrocarbons: 1–487.

Avino, P., Notardonato, I., Perugini, L. & Russo, M.V. 2017. New protocol based on high-volume sampling followed by DLLME-GC-IT/MS for determining PAHs at ultra-trace levels in surface water samples. *Microchemical Journal*, 133: 251–257.

Azizi, G., Layachi, M., Akodad, M., Yáñez-Ruiz, D.R., Martín-García, A.I., Baghour, M., Mesfioui, A., Skalli, A. & Moumen, A. 2018. Seasonal variations of heavy metals content in mussels (*Mytilus galloprovincialis*) from Cala Iris offshore (Northern Morocco). *Marine Pollution*

Bulletin, 137: 688–694.

Badr, T., Hanna, K. & De Brauer, C. 2004. Enhanced solubilisation and removal of naphthalene and phenanthrene by cyclodextrins from two contaminated soils. *Journal of Hazardous Materials*, 112(3): 215–223.

Bagheri, N. & Abedi, J. 2009. Preparation of high surface area activated carbon from corn by chemical activation using potassium hydroxide. *Chemical Engineering Research and Design*, 87(8): 1059–1064.

Baltussen, E., Sandra, P., David, F. & Cramers, C. 1999. Stir bar sorptive extraction (SBSE), a novel extraction technique for aqueous samples: Theory and principles. *Journal of Microcolumn Separations*, 11(10): 737–747.

Banerjee, D.K. & Gray, M.R. 1997. Analysis of hydrocarbon-contaminated soil by thermal extraction−gas chromatography. *Environmental Science & Technology*, 31(3): 646–650.

Banjoo, D.R. & Nelson, P.K. 2005. Improved ultrasonic extraction procedure for the determination of polycyclic aromatic hydrocarbons in sediments. *Journal of Chromatography A*, 1066: 9–18.

Barakat, A.O., Mostafa, A., Wade, T.L., Sweet, S.T. & El Sayed, N.B. 2011. Distribution and characteristics of PAHs in sediments from the Mediterranean coastal environment of Egypt. *Marine Pollution Bulletin*, 62(9): 1969–1978.

Barceló, D., Oubiña, A., Salau, J.S. & Perez, S. 1998. Determination of PAHs in river water samples by ELISA. *Analytica Chimica Acta*, 376(1): 49–53.

Barron, M.G., Heintz, R. & Rice, S.D. 2004. Relative potency of PAHs and heterocycles as aryl hydrocarbon receptor agonists in fish. *Marine Environmental Research*, 58(2): 95–100.

Basavaiah, N., Mohite, R.D., Singare, P.U., Reddy, A.V.R., Singhal, R.K. & Blaha, U. 2017. Vertical distribution, composition profiles, sources and toxicity assessment of PAH residues in the reclaimed mudflat sediments from the adjacent Thane Creek of Mumbai. *Marine Pollution Bulletin*, 118: 112–124.

Baumard, P., Budzinski, H., Garrigues, P., Sorbe, J.C., Burgeot, T. & Bellocq, J. 1998. Concentrations of PAHs (polycyclic aromatic hydrocarbons) in various marine organisms in relation to those in sediments and to trophic level. *Marine Pollution Bulletin*, 36(12): 951–960.

Bedin, K.C., Souza, I.P.A.F., Cazetta, A.L., Spessato, L., Ronix, A. & Almeida, V.C. 2018. CO_2-spherical activated carbon as a new adsorbent for methylene blue removal: Kinetic, equilibrium and thermodynamic studies. *Journal of Molecular Liquids*, 269: 132–139.

Belles, M., Heredia, L., Serra, N., Domingo, L.J. & Linares, V. 2016. Exposure to low doses of 137 cesium and nicotine during postnatal development modifies anxiety levels, learning, and spatial memory performance in mice. *Food and Chemical Toxicology*, 97: 82–88.

Benson, N.U., Fred-Ahmadu, O.H., Olugbuyiro, J.A.O., Anake, W.U., Adedapo, A.E. & Olajire, A.A. 2017. Concentrations, sources and risk characterisation of polycyclic aromatic hydrocarbons (PAHs) in green, herbal and black tea products in Nigeria. *Journal of Food Composition and Analysis*, 66: 13-22.

Berninger, J.P. & Brooks, B.W. 2010. Leveraging mammalian pharmaceutical toxicology and pharmacology data to predict chronic fish responses to pharmaceuticals. *Toxicology Letters*, 193: 69–78.

Bingjia, Y., Li, Y., Qiong, H. & Akita, S. 2007. Cloud point extraction of polycyclic aromatic hydrocarbons in aqueous solution with silicone surfactants. *Chinese Journal of Chemical Engineering*, 15(4): 468–473.

Bixian, M., Jiamo, F., Gan, Z., Zheng, L., Yushun, M., Guoying, S. & Xingmin, W. 2001. Polycyclic aromatic hydrocarbons in sediments from the Pearl River and Estuary, China: Spatial and

temporal distribution and sources. *Applied Geochemistry*, 16(11–12): 1429–1445.

Blanchard, G., Maunaye, M. & Martin, G. 1984. Removal of heavy metals from waters by means of natural zeolites. *Water Research*, 18(12): 1501–1507.

Bœuf, G. & Payan, P. 2001. How should salinity influence fish growth? *Comparative Biochemistry and Physiology Part C*, 130: 411–423.

Boitsov, S., Jensen, H.K.B. & Klungsøyr, J. 2009. Natural background and anthropogenic inputs of polycyclic aromatic hydrocarbons (PAHs) in sediments of South-Western Barents Sea. *Marine Environmental Research*, 68(5): 236–245.

Bollmann, A.F., Seitz, W., Prasse, C., Lucke, T., Schulz, W. & Ternes, T. 2016. Occurrence and fate of amisulpride, sulpiride, and lamotrigine in municipal wastewater treatment plants with biological treatment and ozonation. *Journal of Hazardous Materials*, 320: 204–215.

Boogaard, P.J. & van Sittert, N.J. 1994. Exposure to polycyclic aromatic hydrocarbons in petrochemical industries by measurement of urinary 1-hydroxypyrene. *Occupational and Environmental Medicine*, 51(4): 250–258.

Boonyatumanond, R., Murakami, M., Wattayakorn, G., Togo, A. & Takada, H. 2007. Sources of polycyclic aromatic hydrocarbons (PAHs) in street dust in a tropical Asian mega-city, Bangkok, Thailand. *Science of The Total Environment*, 384(1): 420–432.

Boopathy, R. 2000. Factors limiting bioremediation technologies. *Bioresource Technology*, 74: 63–67.

Bouloubassi, I., Méjanelle, L., Pete, R., Fillaux, J., Lorre, A. & Point, V. 2006. PAH transport by sinking particles in the open Mediterranean Sea: A 1 year sediment trap study. *Marine Pollution Bulletin*, 52(5): 560–571.

Brix, K. V., Gerdes, R., Curry, N., Kasper, A. & Grosell, M. 2010. The effects of total dissolved solids on egg fertilisation and water hardening in two Salmonids-Arctic Grayling (*Thymallus arcticus*) and Dolly Varden (*Salvelinus malma*). *Aquatic Toxicology*, 97: 109–115.

Buckley, T.J. & Lioy, P.J. 1992. An examination of the time course from human dietary exposure to polycyclic aromatic hydrocarbons to urinary elimination of 1-hydroxypyrene. *British Journal of Industrial Medicine*, 49(2): 113–124.

Buening, M.K., Levin, W., Wood, A.W., Chang, R.L., Yagi, H., Kane, J.M., Jenina, D.M. & Conney, A.H. 1979. Tumorigenicity of the dihydrodiols of dibenzo[a , h]anthracene on mouse skin and in newborn mice. *Cancer Research*, 39: 1310–1314.

Busso, I.T., Tames, F., Silva, J.A., Ramos, S., Homem, V., Ratola, N. & Carreras, H. 2018. Biomonitoring levels and trends of PAHs and synthetic musks associated with land use in urban environments. *Science of the Total Environment*, 618: 93–100.

Caissie, D. 2006. The thermal regime of rivers: A review. *Freshwater Biology*, 51(8): 1389–1406.

Calheiros, C.S.C., Quitério, P.V.B., Silva, G., Crispim, L.F.C., Brix, H., Moura, S.C. & Castro, P.M.L. 2012. Use of constructed wetland systems with *Arundo* and *Sarcocornia* for polishing high salinity tannery wastewater. *Journal of Environmental Management*, 95: 66–71.

Campillo, J.A., Fernández, B., García, V., Benedicto, J. & León, V.M. 2017. Levels and temporal trends of organochlorine contaminants in mussels from Spanish Mediterranean waters. *Chemosphere*, 182: 584–594.

Cañedo-Argüelles, M., Kefford, B.J., Piscart, C., Prat, N., Schäfer, R.B. & Schulz, C.-J. 2013. Salinisation of rivers: An urgent ecological issue. *Environmental Pollution*, 173: 157–167

Cardellicchio, N., Buccolieri, A., Giandomenico, S., Lopez, L., Pizzulli, F. & Spada, L. 2007. Organic pollutants (PAHs, PCBs) in sediments from the Mar Piccolo in Taranto (Ionian Sea, Southern Italy). *Marine Pollution Bulletin*, 55(10): 451–458.

Carls, M., Holland, L., Larsen, M., Collier, T.K., Scholz, N.L. & Incardona, J.P. 2008. Fish embryos are damaged by dissolved PAHs, not oil particles. *Aquatic toxicology*, 88(2): 121–127.

CCME (Canadian Council of Ministers of the Environment). 1999. Canadian Water and Sediment Quality Guidelines for the Protection of Aquatic Life: Summary.

Cetin, B., Ozturk, F., Keles, M. & Yurdakul, S. 2017. PAHs and PCBs in an Eastern Mediterranean mega-city, Istanbul: Their spatial and temporal distributions, air-soil exchange and toxicological effects. *Environmental Pollution*, 220: 1322–1332.

Chakraborty, S., Biswas, S., Banerjee, K., Mitra, A., Lake, S., Bengal, W., Lake, S., Bengal, W. & Bengal, W. 2016. Concentration of Zn, Cu and Pb in muscle of two edible finfish species in and around Gangetic Delta Region. *International Journal of Life Science & Pharma Research*, 6(3): 14–22.

Chand, R., Narimura, K., Kawakita, H., Ohto, K., Watari, T. & Inoue, K. 2009. Grape waste as a biosorbent for removing Cr(VI) from aqueous solution. *Journal of Hazardous Materials*, 163(1): 245–250.

Chang, M.-C., Shu, H.-Y., Hsieh, W.-P. & Wang, M.-C. 2005. Using nanoscale zero-valent iron for the remediation of polycyclic aromatic hydrocarbons contaminated soil. *Journal of the Air & Waste Management Association*, 55(8): 1200–1207.

Chang, M.Y. & Juang, R.S. 2004. Adsorption of tannic acid, humic acid, and dyes from water using the composite of chitosan and activated clay. *Journal of Colloid and Interface Science*, 278: 18–25.

Cheema, S.A., Imran Khan, M., Shen, C., Tang, X., Farooq, M., Chen, L., Zhang, C. & Chen, Y. 2010. Degradation of phenanthrene and pyrene in spiked soils by single and combined plants cultivation. *Journal of hazardous materials*, 177: 384–389.

Chen, B., Wang, Y. & Hu, D. 2010. Biosorption and biodegradation of polycyclic aromatic hydrocarbons in aqueous solutions by a consortium of white-rot fungi. *Journal of Hazardous Materials*, 179(1): 845–851.

Chen, B., Yuan, M. & Liu, H. 2011. Removal of polycyclic aromatic hydrocarbons from aqueous solution using plant residue materials as a biosorbent. *Journal of Hazardous Materials*, 188: 436–442.

Chen, C.-F., Binh, N.T., Chen, C.-W. & Dong, C.-D. 2015. Removal of polycyclic aromatic hydrocarbons from sediments using sodium persulfate activated by temperature and nanoscale zero-valent iron. *Journal of the Air & Waste Management Association*, 65(4): 375–383.

Chen, C.-W. & Chen, C.-F. 2011. Distribution, origin, and potential toxicological significance of polycyclic aromatic hydrocarbons (PAHs) in sediments of Kaohsiung Harbor, Taiwan. *Marine Pollution Bulletin*, 63(5): 417–423.

Chen, W., Hou, L., Luo, X. & Zhu, L. 2009. Effects of chemical oxidation on sorption and desorption of PAHs in typical Chinese soils. *Environmental Pollution*, 157(6): 1894–1903.

Chen, Y., Zhu, L. & Zhou, R. 2007. Characterisation and distribution of polycyclic aromatic hydrocarbon in surface water and sediment from Qiantang River, China. *Journal of Hazardous Materials*, 141(1): 148–155.

Cherng, S.-H., Lin, P., Yang, J.-L., Hsu, S.-L. & Lee, H. 2001. Benzo[g,h,i]perylene synergistically transactivates benzo[a]pyrene-induced CYP1A1 gene expression by aryl hydrocarbon receptor pathway. *Toxicology and Applied Pharmacology*, 170(1): 63–68.

Cheruyiot, N.K., Lee, W.J., Mwangi, J.K., Wang, L.C., Lin, N.H., Lin, Y.C., Cao, J., Zhang, R. & Chang-Chien, G.P. 2015. An overview: Polycyclic aromatic hydrocarbon emissions from the stationary and mobile sources and in the ambient air. *Aerosol and Air Quality Research*,

15(7): 2730–2762.

Chevremont, A., Boudenne, J., Coulomb, B. & Farnet, A. 2013. Fate of carbamazepine and anthracene in soils watered with UV-LED treated wastewaters. *Water Research*, 47: 6574–6584.

Chien, Y.-C. 2012. Field study of *in situ* remediation of petroleum hydrocarbon contaminated soil on site using microwave energy. *Journal of Hazardous Materials*, 199–200: 457–461.

Choi, M., Kim, Y.-J., Lee, I.-S. & Choi, H.-G. 2014. Development of a one-step integrated pressurized liquid extraction and cleanup method for determining polycyclic aromatic hydrocarbons in marine sediments. *Journal of chromatography. A*, 1340: 8–14.

Choi, M.P.K., Kang, Y.H., Peng, X.L., Ng, K.W. & Wong, M.H. 2009. Stockholm Convention organochlorine pesticides and polycyclic aromatic hydrocarbons in Hong Kong air. *Chemosphere*, 77(6): 714–719.

Christensen, E.R. & Arora, S. 2007. Source apportionment of PAHs in sediments using factor analysis by time records: application to Lake Michigan, USA. *Water research*, 41(1): 168–76.

Christensen, E.R. & Bzdusek, P.A. 2005. PAHs in sediments of the Black River and the Ashtabula River, Ohio: source apportionment by factor analysis. *Water Research*, 39(4): 511–524.

Chung, S.Y., Yettella, R.R., Kim, J.S., Kwon, K., Kim, M.C. & Min, D.B. 2011. Effects of grilling and roasting on the levels of polycyclic aromatic hydrocarbons in beef and pork. *Food Chemistry*, 129(4): 1420–1426.

Ciura, J., Poniedzialek, M., Sekara, A. & Jedrszczyk, E. 2005. The possibility of using crops as metal phytoremediants. *Polish Journal of Environmental Studies*, 14(1): 17–22.

Corrales, J., Kristofco, L.A., Steele, W.B., Yates, B.S., Breed, C.S., Williams, E.S. & Brooks, B.W. 2015. Global assessment of bisphenol A in the environment: Review and analysis of its occurrence and bioaccumulation. *Dose-Response: An International Journal*, 13: 1–29.

Correa, R.C., Otto, T. & Kruse, A. 2017. Influence of the biomass components on the pore formation of activated carbon. *Biomass and Bioenergy*, 97: 53–64.

Costa, G. de A., Galvao, T.C., Bacchi, A.D., Moreira, E.G., Salles, M.J.S., Galvão, T.C., Bacchi, A.D., Moreira, E.G. & Salles, M.J.S. 2016. Investigation of possible teratogenic effects in the offspring of mice exposed to methylphenidate during pregnancy. *Reproductive BioMedicine Online*, 32(2): 170–177.

Cottin, N. & Merlin, G. 2008. Removal of PAHs from laboratory columns simulating the humus upper layer of vertical flow constructed wetlands. *Chemosphere*, 73(5): 711–716.

Cui, W., Fong, T. & Chui, M. 2017. Temporal variations in water quality in a brackish tidal pond : Implications for governing processes and management strategies. *Journal of Environmental Management*, 193: 108–117.

D'Orazio, V., Ghanem, A. & Senesi, N. 2013. Phytoremediation of pyrene contaminated soils by different plant species. *CLEAN – Soil, Air, Water*, 41(4): 377–382.

Dada, A., Olalekan, A., Olatunya, A. & Dada, O. 2012. Langmuir , Freundlich , Temkin and Dubinin–Radushkevich isotherms studies of equilibrium sorption of Zn^{2+} onto phosphoric acid modified rice husk. *IOSR Journal of Applied Chemistry*, 3(1): 38–45.

Dailianis, S., Tsarpali, V., Melas, K., Karapanagioti, H.K. & Manariotis, I.D. 2014. Aqueous phenanthrene toxicity after high-frequency ultrasound degradation. *Aquatic Toxicology*, 147: 32–40.

Dallas, H. 2008. Water temperature and riverine ecosystems: An overview of knowledge and approaches for assessing biotic responses, with special reference to South Africa. *Water SA*, 34(3): 393–404.

Darmawan, S., Wistara, N.J., Pari, G., Maddu, A. & Syafii, W. 2016. Characterisation of lignocellulosic biomass as raw material for the production of porous carbon-based materials. *BioResources*, 11(2): 3561–3574.

Daso, A.P., Fatoki, O.S. & Odendaal, J.P. 2016. Polybrominated diphenyl ethers (PBDEs) and hexabromobiphenyl in sediments of the Diep and Kuils Rivers in South Africa. *International Journal of Sediment Research*, 31(1): 61–70.

Daugulis, A.J. 2001. Two-phase partitioning bioreactors: A new technology platform for destroying xenobiotics. *Trends in Biotechnology*, 19(11): 457–462.

de Jesus, J.H.F., da, G., Cardoso, E.M.C., Mangrich, A.S. & Romão, L.P.C. 2017. Evaluation of waste biomasses and their biochars for removal of polycyclic aromatic hydrocarbons. *Journal of Environmental Management*, 200: 186–195.

De Nicola, F., Baldantoni, D., Sessa, L., Monaci, F., Bargagli, R. & Alfani, A. 2015. Distribution of heavy metals and polycyclic aromatic hydrocarbons in holm oak plant-soil system evaluated along urbanisation gradients. *Chemosphere*, 134: 91–97.

de Vries, P., Tamis, J.E., Murk, A.J. & Smit, M.G.D. 2008. Development and application of a species sensitivity distribution for temperature-induced mortality in the aquatic environment. *Environmental toxicology and chemistry/SETAC*, 27(12): 2591–2598.

DEAT (Department of Environmental Affairs and Tourism). 2006. *South Africa Environment Outlook: A report on the state of the environment. Executive summary and key findings*.

Degger, N., Wepener, V., Richardson, B.J. & Wu, R.S.S. 2011a. Brown mussels (*Perna perna*) and semi-permeable membrane devices (SPMDs) as indicators of organic pollutants in the South African marine environment. *Marine Pollution Bulletin*, 63: 91–97.

Degger, N., Wepener, V., Richardson, B.J. & Wu, R.S.S. 2011b. Application of artificial mussels (AMs) under South African marine conditions: A validation study. *Marine Pollution Bulletin*, 63(5): 108–118.

De-Gisi, S., Lofrano, G., Grassi, M. & Notarnicola, M. 2016. Characteristics and adsorption capacities of low-cost sorbents for wastewater treatment: A review. *Sustainable Materials and Technologies*, 9: 10–40.

Demirbaş, A. 2001. Biomass resource facilities and biomass conversion processing for fuels and chemicals. *Energy Conversion and Management*, 42(11): 1357–1378.

Demirbas, E., Kobya, M., Senturk, E. & Ozkan, T. 2004. Adsorption kinetics for the removal of chromium (VI) from aqueous solutions on the activated carbons prepared from agricultural wastes. *Water Sa*, 30: 533–539.

Deng, J., Xiong, T., Wang, H., Zheng, A. & Wang, Y. 2016. Effects of cellulose, hemicellulose, and lignin on the structure and morphology of porous carbons. *ACS Sustainable Chemistry and Engineering*, 4: 3750–3756.

Dodevski, V., Jankovi, B., Stojmenovi, M., Krsti´, S., Popovi´, J., Pagnacco, M.C. & Popovi, M. 2017. Plane tree seed biomass used for preparation of activated carbons (AC) derived from pyrolysis . Modeling the activation process. *Colloids and Surfaces A: Physicochemical and Engineering Aspects*, 522: 83–96.

Dong, T.T.T. & Lee, B.-K. 2009. Characteristics, toxicity, and source apportionment of polycylic aromatic hydrocarbons (PAHs) in road dust of Ulsan, Korea. *Chemosphere*, 74(9): 1245–1253.

Doong, R. & Lin, Y. 2004. Characterisation and distribution of polycyclic aromatic hydrocarbon contaminations in surface sediment and water from Gao-ping River , Taiwan. *Water research*, 38: 1733–1744.

Dordio, A.V. & Carvalho, A.J.P. 2013. Organic xenobiotics removal in constructed wetlands, with

emphasis on the importance of the support matrix. *Journal of Hazardous Materials*, 252–253: 272–292.

Dorea, H.S., Bispo, J.R.L., Aragao, K.A.S., Cunha, B.B., Navickiene, S., Alves, J.P.H., Romao, L.P.C. & Garcia, C. a B. 2007. Analysis of BTEX, PAHs and metals in the oilfield produced water in the State of Sergipe, Brazil. *Microchemical Journal*, 85(2): 234–238.

Duarte-Davidson, R. & Jones, K.C. 1996. Screening the environmental fate of organic contaminants in sewage sludge applied to agricultural soils: II. The potential for transfers to plants and grazing animals. *The Science of the Total Environment*, 185: 59–70.

Dugay, A., Herrenknecht, C., Czok, M., Guyon, F. & Pages, N. 2002. New procedure for selective extraction of polycyclic aromatic hydrocarbons in plants for gas chromatographic-mass spectrometric analysis. *Journal of Chromatography A*, 958: 1–7.

Duodu, G.O., Ogogo, K.N., Mummullage, S., Harden, F., Goonetilleke, A. & Ayoko, G.A. 2017. Source apportionment and risk assessment of PAHs in Brisbane River sediment, Australia. *Ecological Indicators*, 73: 784–799.

Duursma, E.K. & Carroll, J. 1996. *Environmental Compartments: Equilibria and Assessment of Processes Between Air, Water, Sediments and Biota*. 1st ed. New York, USA: Springer.

DWAF. 1996a. *South African Water Quality Guidelines. Volume 7: Aquatic ecosystems*.

DWAF. 1996b. *South African Water Quality Guidelines Volume 1: Domestic Water Use*.

Edokpayi, J.N., Odiyo, J.O., Msagati, T.A.M. & Potgieter, N. 2015. Temporal variations in physico-chemical and microbiological characteristics of Mvudi River, South Africa. *International Journal of Environmental Research and Public Health*, 12(4): 4128–4140.

Edokpayi, J.N., Odiyo, J.O., Popoola, O.E. & Msagati, T.A. 2016. Determination and distribution of polycyclic aromatic hydrocarbons in rivers, sediments and wastewater effluents in Vhembe District, South Africa. *International Journal of Environmental Research and Public Health*, 13(387): 1-12.

Eisler, R. 1987. Polycyclic aromatic hydrocarbon hazards to fish, wildlife, and invertebrates: a synoptic review. *U.S. Fish and Wildlife Service Biological Report*, 85(1.11): 1–55.

Ejiba, I. V, Onya, S.C. & Adams, O.K. 2016. Impact of Oil Pollution on Livelihood: Evidence from the Niger Delta Region of Nigeria. *Journal of Scientific Research & Reports Nigeria*, 12(523): 1–12.

El Qada, E.N., Allen, S.J. & Walker, G.M. 2006. Adsorption of Methylene Blue onto activated carbon produced from steam activated bituminous coal: A study of equilibrium adsorption isotherm. *Chemical Engineering Journal*, 124(1–3): 103–110.

Engraff, M., Solere, C., Smith, K.E.C., Mayer, P. & Dahllöf, I. 2011. Aquatic toxicity of PAHs and PAH mixtures at saturation to benthic amphipods: Linking toxic effects to chemical activity. *Aquatic Toxicology*, 102(3): 142–149.

Esmaeilzadeh, M., Karbassi, A. & Darvish, K. 2017. Antioxidant response to metal pollution in *Phragmites australis* from Anzali wetland. *Marine Pollution Bulletin*, 119: 376–380.

Euliss, K., Ho, C., Schwab, A.P., Rock, S. & Banks, M.K. 2008. Greenhouse and field assessment of phytoremediation for petroleum contaminants in a riparian zone. *Bioresource Technology*, 99: 1961–1971.

Fagbayigbo, B.O., Opeolu, B.O., Fatoki, O.S., Akenga, T.A. & Olatunji, O.S. 2017. Removal of PFOA and PFOS from aqueous solutions using activated carbon produced from *Vitis vinifera* leaf litter. *Environmental Science and Pollution Research*, 24(14): 13107–13120.

Falciglia, P.P., Catalfo, A., Finocchiaro, G., Vagliasindi, F.G.A., Romano, S. & De Guidi, G. 2018. Microwave heating coupled with UV-A irradiation for PAH removal from highly contaminated

marine sediments and subsequent photo-degradation of the generated vaporized organic compounds. *Chemical Engineering Journal*, 334: 172–183.

Falciglia, P.P., De Guidi, G., Catalfo, A. & Vagliasindi, F.G.A. 2016. Remediation of soils contaminated with PAHs and nitro-PAHs using microwave irradiation. *Chemical Engineering Journal*, 296: 162–172.

Falcó, G., Domingo, J.L., Llobet, J.M., Teixidó, A., Casas, C. & Müller, L. 2003. Polycyclic aromatic hydrocarbons in foods: Human exposure through the diet in Catalonia, Spain. *Journal of food protection*, 66(12): 2325–2331.

Fang, G.C., Chang, K.F., Lu, C. & Bai, H. 2004. Estimation of PAHs dry deposition and BaP toxic equivalency factors (TEFs) study at urban, industry park and rural sampling sites in central Taiwan, Taichung. *Chemosphere*, 55: 787–796.

Farhadian, M., Vachelard, C., Duchez, D. & Larroche, C. 2008. *In situ* bioremediation of monoaromatic pollutants in groundwater: A review. *Bioresource Technology*, 99: 5296–5308.

Fasano, E., Yebra-Pimentel, I., Martínez-Carballo, E. & Simal-Gándara, J. 2016. Profiling, distribution and levels of carcinogenic polycyclic aromatic hydrocarbons in traditional smoked plant and animal foods. *Food Control*, 59(1881): 581–590.

Feng, L., Zhang, W., Liang, D. & Lee, J. 2014. Total dissolved solids estimation with a fiber optic sensor of surface plasmon resonance. *Optik*, 125: 3337–3343.

Ferrarese, E., Andreottola, G. & Oprea, I.A. 2008. Remediation of PAH-contaminated sediments by chemical oxidation. *Journal of Hazardous Materials*, 152(1): 128–139.

Ferrer, R., Beltrán, J.L. & Guiteras, J. 1996. Use of cloud point extraction methodology for the determination of PAHs priority pollutants in water samples by high-performance liquid chromatography with fluorescence detection and wavelength programming. *Analytica Chimica Acta*, 330(2–3): 199–206.

Fierro, V., Torné-Fernández, V., Montané, D. & Celzard, A. 2008. Adsorption of phenol onto activated carbons having different textural and surface properties. *Microporous and Mesoporous Materials*, 111(1–3): 276–284.

Fismes, J., Perrin-Ganier, C., Empereur-Bissonnet, P. & Morel, J.L. 2002. Soil-to-root transfer and translocation of polycyclic aromatic hydrocarbons by vegetables grown on industrial contaminated soils. *Journal of Environmental Quality*, 31: 1649–1656.

Foo, K.Y. & Hameed, B.H. 2010. Insights into the modeling of adsorption isotherm systems. *Chemical Engineering Journal*, 156(1): 2–10.

Fountoulakis, M.S., Terzakis, S., Kalogerakis, N. & Manios, T. 2009. Removal of polycyclic aromatic hydrocarbons and linear alkylbenzene sulfonates from domestic wastewater in pilot constructed wetlands and a gravel filter. *Ecological Engineering*, 35(12): 1702–1709.

Gan, S., Lau, E.V.V. & Ng, H.K.K. 2009. Remediation of soils contaminated with polycyclic aromatic hydrocarbons (PAHs). *Journal of Hazardous Materials*, 172: 532–549.

Gao, Y., Li, Q., Ling, W. & Zhu, X. 2011. Arbuscular mycorrhizal phytoremediation of soils contaminated with phenanthrene and pyrene. *Journal of Hazardous Materials*, 185(2): 703–709.

Gao, Y., Shen, Q., Ling, W. & Ren, L. 2008. Uptake of polycyclic aromatic hydrocarbons by *Trifolium pretense* L. from water in the presence of a nonionic surfactant. *Chemosphere*, 72: 636–643.

Garbisu, C. & Alkorta, I. 2001. Phytoextraction: a cost-effective plant-based technology for the removal of metals from the environment. *Bioresource Technology*, 77: 229–236.

García de Llasera, M.P., León Santiago, M., Loera Flores, E.J., Bernal Toris, D.N. & Covarrubias

Herrera, M.R. 2018. Mini-bioreactors with immobilized microalgae for the removal of benzo[a]anthracene and benzo[a]pyrene from water. *Ecological Engineering*, 121: 89-98.

García-Falcón, M.S., Cancho-Grande, B. & Simal-Gándara, J. 2004. Stirring bar sorptive extraction in the determination of PAHs in drinking waters. *Water Research*, 38(7): 1679–1684.

Garg, U.K., Kaur, M.P., Garg, V.K. & Sud, D. 2007. Removal of hexavalent chromium from aqueous solution by agricultural waste biomass. *Journal of Hazardous Materials*, 140(1): 60–68.

Garg, V., Gupta, R., Bala Yadav, A. & Kumar, R. 2003. Dye removal from aqueous solution by adsorption on treated sawdust. *Bioresource Technology*, 89(2): 121–124.

Garrigues, P., Budzinski, H., Manitz, M.P. & Wise, S.A. 1995. Pyrolytic and petrogenic inputs in recent sediments: A definitive signature through phenanthrene and chrysene compound distribution. *Polycyclic Aromatic Compounds*, 7(4): 275–284.

Gdara, I., Zrafi, I., Balducci, C., Cecinato, A. & Ghrabi, A. 2017. Seasonal distribution, source identification , and toxicological risk assessment of polycyclic aromatic hydrocarbons (PAHs) in sediments from Wadi El Bey Watershed in Tunisia. *Archives of environmental contamination and toxicology*, 73: 488–510.

Geldenhuys, G., Rohwer, E.R., Naudé, Y. & Forbes, P.B.C. 2015. Monitoring of atmospheric gaseous and particulate polycyclic aromatic hydrocarbons in South African platinum mines utilising portable denuder sampling with analysis by thermal desorption-comprehensive gas chromatography-mass spectrometry. *Journal of Chromatography A*, 1380: 17–28.

Genies, C., Maître, A., Lefèbvre, E., Jullien, A., Lallier, M.C. & Douki, T. 2013. The extreme variety of genotoxic response to benzo[a]pyrene in three different human cell lines from three different organs. *PLOS ONE*, 8(11): 1–13.

Gervais, J., Luukinen, B., Buhl, K. & Stone, D. 2010. Naphthalene general fact sheet. *National Pesticide Information Center*: 1–3.

Gharibzadeh, F., Rezaei Kalantary, R., Nasseri, S., Esrafili, A. & Azari, A. 2016. Reuse of polycyclic aromatic hydrocarbons (PAHs) contaminated soil washing effluent by bioaugmentation/biostimulation process. *Separation and Purification Technology*, 168: 248–256.

Ghosh, A., Jose, D.A. & Kaushik, R. 2016. Anthraquinones as versatile colorimetric reagent for anions. *Sensors and Actuators B*, 229: 545–560.

Giraud, F., Guiraud, P., Kadri, M., Blake, G. & Steiman, R. 2001. Biodegradation of anthracene and fluoranthene by fungi isolated from an experimental constructed wetland for wastewater treatment. *Water Research*, 35(17): 4126–4136.

Gökmen, V. & Serpen, A. 2002. Equilibrium and kinetic studies on the adsorption of dark coloured compounds from apple juice using adsorbent resin. *Journal of Food Engineering*, 53(3): 221–227.

Gómez-Gutiérrez, A., Garnacho, E., Bayona, J.M. & Albaigés, J. 2007. Screening ecological risk assessment of persistent organic pollutants in Mediterranean Sea sediments. *Environment International*, 33: 867–876.

Gong, Z., Alef, K., Wilke, B.-M. & Li, P. 2007. Activated carbon adsorption of PAHs from vegetable oil used in soil remediation. *Journal of Hazardous Materials*, 143: 372–378.

Gong, Z., Alef, K., Wilke, B.-M. & Li, P. 2005. Dissolution and removal of PAHs from a contaminated soil using sunflower oil. *Chemosphere*, 58(3): 291–298.

Grubesic, T.H., Wei, R. & Nelson, J. 2017. Optimising oil spill cleanup efforts: A tactical approach and evaluation framework. *Marine Pollution Bulletin*, 125(1-2): 318-329.

Grueiro-Noche, G., Andrade, J.M., Muniategui-Lorenzo, S., López-Mahía, P. & Prada-Rodríguez, D. 2010. 3-Way pattern-recognition of PAHs from Galicia (NW Spain) seawater samples after the Prestige's wreck. *Environmental Pollution*, 158(1): 207–214.

Gu, S.-H., Kralovec, A.C., Christensen, E.R. & Van Camp, R.P. 2003. Source apportionment of PAHs in dated sediments from the Black River, Ohio. *Water research*, 37: 2149–2161.

Gu, Y.-G., Ke, C.-L., Liu, Q. & Lin, Q. 2016. Polycyclic aromatic hydrocarbons (PAHs) in sediments of Zhelin Bay, the largest mariculture base on the Eastern Guangdong coast, South China: Characterisation and risk implications. *Marine Pollution Bulletin*, 110: 603–608.

Gu, Y.G., Li, H.B. & Lu, H. Bin. 2017. Polycyclic aromatic hydrocarbons (PAHs) in surface sediments from the largest deep plateau lake in China: Occurrence, sources and biological risk. *Ecological Engineering*, 101: 179–184.

Guieysse, B. & Viklund, G. 2005. Sequential UV-biological degradation of polycyclic aromatic hydrocarbons in two-phases partitioning bioreactors. *Chemosphere*, 59: 369–376.

Guo, J.G., Cui, Y.M., Lin, H.X., Xie, X.Z. & Chen, H.F. 2011. New fluorene derivatives based on 3,9-dihydrofluoreno[3,2-d]imidazole (FI): Characterisation and influence of substituents on photoluminescence. *Journal of Photochemistry and Photobiology A: Chemistry*, 219(1): 42–49.

Guo, R., Pan, L., Lin, P. & Zheng, L. 2017. The detoxification responses, damage effects and bioaccumulation in the scallop *Chlamys farreri* exposed to single and mixtures of benzo[a]pyrene and chrysene. *Comparative Biochemistry and Physiology Part C: Toxicology & Pharmacology*, 191: 36–51.

Guo, W., He, M., Yang, Z., Lin, C., Quan, X. & Wang, H. 2007. Distribution of polycyclic aromatic hydrocarbons in water, suspended particulate matter and sediment from Daliao River watershed, China. *Chemosphere*, 68(1): 93–104.

Gupta, H. 2015. Removal of phenanthrene from water using activated carbon developed from orange rind. *International Journal of Science Research in Environmetal Sciences*, 3(7): 248–255.

Gustafsson, Å., Hale, S., Cornelissen, G., Sjöholm, E. & Gunnarsson, J.S. 2017. Activated carbon from kraft lignin: A sorbent for *in situ* remediation of contaminated sediments. *Environmental Technology & Innovation*, 7: 160–168.

Guzmán-Torres, D., Eiguren-Fernández, A., Cicero-Fernández, P., Maubert-Franco, M., Retama-Hernández, A., Ramos Villegas, R. & Miguel, A.H. 2009. Effects of meteorology on diurnal and nocturnal levels of priority polycyclic aromatic hydrocarbons and elemental and organic carbon in PM10 at a source and a receptor area in Mexico City. *Atmospheric Environment*, 43(17): 2693–2699.

Hamdaoui, O. & Naffrechoux, E. 2007. Modeling of adsorption isotherms of phenol and chlorophenols onto granular activated carbon: Part II. Models with more than two parameters. *Journal of Hazardous Materials*, 147(1): 401–411.

Haritash, A.K. & Kaushik, C.P. 2009. Biodegradation aspects of polycyclic aromatic hydrocarbons (PAHs): A review. *Journal of Hazardous Materials*, 169(1): 1–15.

Hatch, A.C. & Burton, G.A. 1999. Photo-induced toxicity of PAHs to *Hyalella azteca* and *Chironomus tentans*: effects of mixtures and behavior. *Environmental Pollution*, 106(2): 157–167.

Hawkins, W.E., Overstreet, R.M. & Walker, W.W. 1988. Carcinogenicity tests with small fish species. *Aquatic Toxicology*, 11(1–2): 113–128.

Hennio, M.-C. 1999. Solid-phase extraction: Method development, sorbents, and coupling with liquid chromatography. *Journal of Chromatography A*, 856: 3–54.

Hennion, M.C. & Barcelo, D. 1998. Strengths and limitations of immunoassays for effective and efficient use for pesticide analysis in water samples: A review. *Analytica Chimica Acta*, 362(1): 3–34.

Hester, E.T. & Doyle, M.W. 2011. Human impacts to river temperature and their effects on biological processes: A quantitative synthesis. *Journal of the American Water Resources Association*, 47(3): 571–587.

Hildebrandt, A., Lacorte, S. & Barceló, D. 2006. Sampling of water, soil and sediment to trace organic pollutants at a river-basin scale. *Analytical and Bioanalytical Chemistry*, 386(4): 1075–1088.

Ho, Y.-S., Chiang, T.-H. & Hsueh, Y.-M. 2005. Removal of basic dye from aqueous solution using tree fern as a biosorbent. *Process Biochemistry*, 40(1): 119–124.

Ho, Y.-S. 2006. Review of second-order models for adsorption systems. *Journal of Hazardous Materials*, 136: 681–689.

Ho, Y.S. & McKay, G. 1998. A comparison of chemisorption kinetic models applied to pollutant removal on various sorbents. *Process Safety and Environmental Protection*, 76(4): 332–340.

Ho, Y.S. & McKay, G. 1999. Pseudo-second order model for sorption processes. *Process Biochemistry*, 34(5): 451–465.

Holm, T. 1999. Aspects of the mechanism of the flame ionisation detector. *Journal of Chromatography A*, 842(1): 221–227.

Hong, W.-J., Jia, H., Li, Y.-F., Sun, Y., Liu, X. & Wang, L. 2016. Polycyclic aromatic hydrocarbons (PAHs) and alkylated PAHs in the coastal seawater, surface sediment and oyster from Dalian, Northeast China. *Ecotoxicology and Environmental Safety*, 128: 11–20.

Hosseini, M.S. 2006. *In situ thermal desorption of polycyclic aromatic hydrocarbons from lampblack impacted soils using natural gas combustion*. University of California, Los Angeles.

Hou, W.-C., Westerhoff, P. & Posner, J.D. 2013. Biological accumulation of engineered nanomaterials: A review of current knowledge. *Environmental Science: Processes Impacts*, 15(1): 103–122.

Howsam, M., Jones, K.C. & Ineson, P. 2000. PAHs associated with the leaves of three deciduous tree species. I - Concentrations and profiles. *Environmental Pollution*, 108: 413–424.

Howsam, M., Jones, K.C. & Ineson, P. 2001. PAHs associated with the leaves of three deciduous tree species. II: Uptake during a growing season. *Chemosphere*, 44(2): 155–164.

HSDB (Hazardous Substances Data Bank). 1983. PAHs. *National Library of Medicine's TOXNET System*.

Hu, G., Luo, X., Li, F., Dai, J., Guo, J., Chen, S., Hong, C., Mai, B. & Xu, M. 2010. Organochlorine compounds and polycyclic aromatic hydrocarbons in surface sediment from Baiyangdian Lake, North China: Concentrations, sources profiles and potential risk. *Journal of Environmental Sciences*, 22(2): 176–183.

Huang, J.L., Lu, H.H., Lu, Y.N., Hung, P.S., Lin, Y.J., Lin, C.C.C.S., Yang, C.C., Wong, T.Y., Lu, S.Y. & Lin, C.C.C.S. 2016a. Enhancement of the genotoxicity of benzo[a]pyrene by arecoline through suppression of DNA repair in HEp-2 cells. *Toxicology in Vitro*, 33: 80–87.

Huang, X.-D., El-Alawi, Y., Penrose, D.M., Glick, B.R. & Greenberg, B.M. 2004. A multi-process phytoremediation system for removal of polycyclic aromatic hydrocarbons from contaminated soils. *Environmental Pollution*, 130(3): 465–476.

Huang, Y., Fulton, A.N. & Keller, A.A. 2016b. Simultaneous removal of PAHs and metal contaminants from water using magnetic nanoparticle adsorbents. *Science of the Total Environment*, 571: 1029–1036.

Huesemann, M.H., Hausmann, T.S., Fortman, T.J., Thom, R.M. & Cullinan, V. 2009. *In situ* phytoremediation of PAH- and PCB-contaminated marine sediments with eelgrass (*Zostera marina*). *Ecological Engineering*, 35(10): 1395–1404.

Hussain, I., Das, M., Ahamad, K.U. & Nath, P. 2017. Water salinity detection using a smartphone. *Sensors and Actuators B*, 239: 1042–1050.

Hyötyläinen, T. & Olkari, A. 1999. The toxicity and concentrations of PAHs in creosote-contaminated lake sediment. *Chemosphere*, 38: 1135–1144.

IARC (International Agency for Research on Cancer). 1983. Polynuclear Aromatic Compounds PART 1, Chemical, environmental and experimental data. *IARC monographs on the evaluation of carcinogenic risks to humans*, 32.

IARC (International Agency for Research on Cancer). 2002. Some traditional herbal medicines, some mycotoxins, naphthalene and styrene. *IARC monographs on the evaluation of carcinogenic risks to humans*, 82: 1–556.

IARC (International Agency for Research on Cancer). 2016. Agents Classified by the IARC Monographs. *IARC Monographs*, 1–116: 1–25.

ICH (International Conference on Hormonisation). 2005. Validation of Analytical Procedures: Text and Methodology Q2(R1).

ICSC (International Chemical Safety Cards). 2006. Acenaphthene. *ICSC:1674*.

Incardona, J.P., Day, H.L., Collier, T.K. & Scholz, N.L. 2006. Developmental toxicity of 4-ring polycyclic aromatic hydrocarbons in zebrafish is differentially dependent on AH receptor isoforms and hepatic cytochrome P4501A metabolism. *Toxicology and applied pharmacology*, 217: 308–321.

Ioannidou, O. & Zabaniotou, A. 2007. Agricultural residues as precursors for activated carbon production: A review. *Renewable and Sustainable Energy Reviews*, 11(9): 1966–2005.

Jackson, V.A., Paulse, A.N., Odendaal, J.P. & Khan, W. 2009. Investigation into the metal contamination of the Plankenburg and Diep Rivers, Western Cape, South Africa. *Water SA*, 35(3): 289–300.

Jarvis, I.W.H., Bergvall, C., Bottai, M., Westerholm, R., Stenius, U. & Dreij, K. 2013. Persistent activation of DNA damage signaling in response to complex mixtures of PAHs in air particulate matter. *Toxicology and applied pharmacology*, 266: 408–418.

Jeng, A.H., Pan, C., Diawara, N., Chang-Chien, G.-P., Lin, W., Huang, C., Ho, C. & Wu, M. 2011. Polycyclic aromatic hydrocarbon-induced oxidative stress and lipid peroxidation in relation to immunological alteration. *Occupational and Environmental Medicine*, 68: 653–658.

Jiang, X., Qiu, L., Zhao, H., Song, Q., Zhou, H., Han, Q. & Diao, X. 2016. Transcriptomic responses of *Perna viridis* embryo to Benzo[a]pyrene exposure elucidated by RNA sequencing. *Chemosphere*, 163: 125–132.

Kamal, A., Qayyum, M., Cheema, I.U. & Rashid, A. 2011. Biological monitoring of blood naphthalene levels as a marker of occupational exposure to PAHs among auto-mechanics and spray painters in Rawalpindi. *BMC Public Health*, 11(467): 1-10.

Kannan, K. & Perrotta, E. 2008. Polycyclic aromatic hydrocarbons (PAHs) in livers of California sea otters. *Chemosphere*, 71: 649–655.

Karamalidis, A.K. & Voudrias, E. A. 2007. Cement-based stabilisation/solidification of oil refinery sludge: Leaching behavior of alkanes and PAHs. *Journal of Hazardous Materials*, 148(1–2): 122–35.

Kargar, N., Matin, G., Matin, A.A. & Buyukisik, H.B. 2017. Biomonitoring, status and source risk assessment of polycyclic aromatic hydrocarbons (PAHs) using honeybees, pine tree leaves,

and propolis. *Chemosphere*, 186: 140–150.

Karyab, H., Yunesian, M., Nasseri, S., Mahvi, A.H., Ahmadkhaniha, R., Rastkari, N. & Nabizadeh, R. 2013. Polycyclic aromatic hydrocarbons in drinking water of Tehran, Iran. *Journal of Environmental Health Science & Engineering*, 11(25): 1-7.

Kaushal, S.S., Groffman, P.M., Likens, G.E., Belt, K.T., Stack, W.P., Kelly, V.R., Band, L.E. & Fisher, G.T. 2005. Increased salinisation of fresh water in the northeastern United States. *Proceedings of the National Academy of Sciences*, 102(38): 13517–13520.

Kayali-Sayadi, M.N., Rubio, S. & Polo, L.M. 2000. Rapid determination of PAHs in soil samples by HPLC with fluorimetric detection following sonication extraction. *Fresenius Journal of Analytical Chemistry*, 368: 697–701.

Kazerouni, N., Sinha, R., Hsu, C., Greenberg, A. & Rothman, N. 2001. Analysis of 200 food items for benzo[a]pyrene and estimation of its intake in an epidemiologic study. *Food and Chemical Toxicology*, 39: 423–436.

Kent, R. & Landon, M.K. 2013. Trends in concentrations of nitrate and total dissolved solids in public supply wells of the Bunker Hill, Lytle, Rialto, and Colton groundwater subbasins, San Bernardino County, California: Influence of legacy land use. *Science of the Total Environment*, 452–453: 125–136.

Keshavarzifard, M., Zakaria, M.P., Shau Hwai, T., Mohamat Yusuff, F.F., Mustafa, S., Vaezzadeh, V., Magam, S.M., Masood, N., Alkhadher, S.A.A. & Abootalebi-Jahromi, F. 2014. Baseline distributions and sources of Polycyclic Aromatic Hydrocarbons (PAHs) in the surface sediments from the Prai and Malacca Rivers, Peninsular Malaysia. *Marine Pollution Bulletin*, 88(1–2): 366–372.

Khan, F.I., Husain, T. & Hejazi, R. 2004. An overview and analysis of site remediation technologies. *Journal of Environmental Management*, 71: 95–122.

Kim, A., Park, M., Yoon, T.K., Lee, W.S., Ko, J.-J., Lee, K. & Bae, J. 2011. Maternal exposure to benzo[b]fluoranthene disturbs reproductive performance in male offspring mice. *Toxicology Letters*, 203(1): 54–61.

Kim, A.W., Vane, C.H., Moss-Hayes, V., Engelhart, S.E. & Kemp, A.C. 2018. PAH, PCB, TPH and mercury in surface sediments of the Delaware River Estuary and Delmarva Peninsula, USA. *Marine Pollution Bulletin*, 129(2): 835–845.

Kim, H., Lim, Y.-W., Jeon, J.-M., Kim, T.-H., Lee, G., Lee, W.-S., Lim, J.-Y., Shin, D.-C. & Yang, J.-Y. 2013. Indoor exposure and health risk of polycyclic aromatic hydrocarbons (PAHs) in public facilities, Korea. *Asian Journal of Atmospheric Environment*, 7.2: 72–84.

Kim, J.W., Sohn, M.H., Kim, D.S., Sohn, S.M. & Kwon, Y.S. 2001. Production of granular activated carbon from waste walnut shell and its adsorption characteristics for Cu^{2+} ion. *Journal of Hazardous Materials*, 85(3): 301–315.

Kim, Y.S., Min, J., Hong, H.N., Park, J.H., Park, K.S. & Gu, M.B. 2007. Gene expression analysis and classification of mode of toxicity of polycyclic aromatic hydrocarbons (PAHs) in *Escherichia coli*. *Chemosphere*, 66(7): 1243–8.

Kipopoulou, A.M., Manoli, E. & Samara, C. 1999. Bioconcentration of polycyclic aromatic hydrocarbons in vegetables grown in an industrial area. *Environmental Pollution*, 106: 369–380.

Kivaisi, A.K. 2001. The potential for constructed wetlands for wastewater treatment and reuse in developing countries: A review. *Ecological Engineering*, 16(4): 545–560.

Knecht, A.L., Goodale, B.C., Truong, L., Simonich, M.T., Swanson, A.J., Matzke, M.M., Anderson, K.A., Waters, K.M. & Tanguay, R.L. 2013. Comparative developmental toxicity of environmentally relevant oxygenated PAHs. *Toxicology and Applied Pharmacology*, 271(2):

266–275.

Kong, L., Gao, Y., Zhou, Q., Zhao, X. & Sun, Z. 2018. Biochar accelerates PAHs biodegradation in petroleum-polluted soil by biostimulation strategy. *Journal of Hazardous Materials*, 343: 276–284.

Korkanç, S.Y., Kayıkçı, S. & Korkanç, M. 2017. Evaluation of spatial and temporal water quality in the Akkaya Dam watershed (Niğde, Turkey) and management implications. *Journal of African Earth Sciences*, 129: 481–491.

Krüger, O., Christoph, G., Kalbe, U. & Berger, W. 2011. Comparison of stir bar sorptive extraction (SBSE) and liquid-liquid extraction (LLE) for the analysis of polycyclic aromatic hydrocarbons (PAHs) in complex aqueous matrices. *Talanta*, 85: 1428–1434.

Kuipers, W. & Müller, J. 2010. Sensitivity of a planar micro-flame ionisation detector. *Talanta*, 82(5): 1674–1679.

Kumar, K.S.A., Priju, C.P. & Prasad, N.B.N. 2015. Study on saline water intrusion into the shallow coastal aquifers of Periyar River basin, Kerala using hydrochemical and electrical resistivity methods. *Aquatic Procedia*, 4: 32–40.

Kuppusamy, S., Thavamani, P. & Venkateswarlu, K. 2017. Remediation approaches for polycyclic aromatic hydrocarbons (PAHs) contaminated soils: Technological constraints, emerging trends and future directions. *Chemosphere*, 168: 944–968.

Kut, K.M.K., Sarswat, A., Bundschuh, J. & Mohan, D. 2019. Water as key to the sustainable development goals of South Sudan – A water quality assessment of Eastern Equatoria State. *Groundwater for Sustainable Development*, 8: 255–270.

Kuyukina, M.S., Ivshina, I.B., Serebrennikova, M.K., Krivorutchko, A.B., Podorozhko, E.A., Ivanov, R. V. & Lozinsky, V.I. 2009. Petroleum-contaminated water treatment in a fluidized-bed bioreactor with immobilized *Rhodococcus* cells. *International Biodeterioration and Biodegradation*, 63: 427–432.

Lafka, T.-I., Sinanoglou, V. & Lazos, E.S. 2007. On the extraction and antioxidant activity of phenolic compounds from winery wastes. *Food Chemistry*, 104(3): 1206–1214.

Lambropoulou, D.A. & Albanis, T.A. 2007. Liquid-phase micro-extraction techniques in pesticide residue analysis. *Journal of Biochemical and Biophysical Methods*, 70(2): 195–228.

Lamichhane, S., Bal Krishna, K.C. & Sarukkalige, R. 2016. Polycyclic aromatic hydrocarbons (PAHs) removal by sorption: A review. *Chemosphere*, 148: 336–353.

Langdon-jones, E.E. & Pope, S.J.A. 2014. The coordination chemistry of substituted anthraquinones : Developments and applications. *Coordination Chemistry Reviews*, 269: 32–53.

Langwaldt, J.H. & Puhakka, J.A. 2000. On-site biological remediation of contaminated groundwater: A review. *Environmental Pollution*, 107(2): 187–197.

Larsen, S.B., Karakashev, D., Angelidaki, I. & Schmidt, J.E. 2009. *Ex-situ* bioremediation of polycyclic aromatic hydrocarbons in sewage sludge. *Journal of Hazadous Materials*, 164: 1568-1572.

Lau, E. V., Gan, S. & Ng, H.K. 2010. Extraction techniques for polycyclic aromatic hydrocarbons in soils. *International Journal of Analytical Chemistry*, 2010: 1–9.

Lau, K.L., Tsang, Y.Y. & Chiu, S.W. 2003. Use of spent mushroom compost to bioremediate PAH-contaminated samples. *Chemosphere*, 52: 1539–1546.

Lawal, I.A., Chetty, D., Akpotu, S.O. & Moodley, B. 2017. Sorption of Congo red and reactive blue on biomass and activated carbon derived from biomass modified by ionic liquid. *Environmental Nanotechnology, Monitoring & Management*, 8: 83–91.

Le Bihanic, F., Sommard, V., Perrine, de L., Pichon, A., Grasset, J., Berrada, S., Budzinski, H., Cousin, X., Morin, B. & Cachot, J. 2015. Environmental concentrations of benz[a]anthracene induce developmental defects and DNA damage and impair photomotor response in Japanese Medaka larvae. *Ecotoxicology and Environmental Safety*, 113: 321–328.

Lea-Langton, A.R., Spracklen, D.V., Arnold, S.R., Conibear, L.A., Chan, J., Mitchell, E.J.S., Jones, J.M. & Williams, A. 2018. PAH emissions from an African cookstove. *Journal of the Energy Institute*: 1–7. http://linkinghub.elsevier.com/retrieve/pii/S1743967117307341.

Lee, Y.-H., Wu, T.-C., Liaw, C.-W., Wen, T.-C., Feng, S.-W., Lee, J.-J., Wu, Y.-T. & Guo, T.-F. 2013. Non-doped active layer, benzo[k]fluoranthene-based linear acenes, for deep blue- to green-emissive organic light-emitting diodes. *Organic Electronics*, 14(4): 1064–1072.

Lefèvre, E., Bossa, N., Gardner, C.M., Gehrke, G.E., Cooper, E.M., Stapleton, H.M., Hsu-Kim, H. & Gunsch, C.K. 2018. Biochar and activated carbon act as promising amendments for promoting the microbial debromination of tetrabromobisphenol A. *Water Research*, 128: 102–110.

Lemaire, J., Buès, M., Kabeche, T., Hanna, K. & Simonnot, M.O. 2013. Oxidant selection to treat an aged PAH contaminated soil by *in situ* chemical oxidation. *Journal of Environmental Chemical Engineering*, 1: 1261–1268.

Li, B., Feng, C., Li, X., Chen, Y., Niu, J. & Shen, Z. 2012. Spatial distribution and source apportionment of PAHs in surficial sediments of the Yangtze Estuary, China. *Marine Pollution Bulletin*, 64(3): 636–643.

Li, B., Zeng, F., Ma, W., Dong, Q., Fan, H. & Deng, C. 2011. Vertical pollution characteristics of PAHs around an oil sludge storage site of Jianghan oil field of China. *Procedia Environmental Sciences*, 11: 1285–1290.

Li, H., Qu, R., Li, C., Guo, W., Han, X., He, F., Ma, Y. & Xing, B. 2014. Selective removal of polycyclic aromatic hydrocarbons (PAHs) from soil washing effluents using biochars produced at different pyrolytic temperatures. *Bioresource Technology*, 163: 193–198.

Li, J., Shang, X., Zhao, Z., Tanguay, R.L., Dong, Q. & Huang, C. 2010a. Polycyclic aromatic hydrocarbons in water, sediment, soil, and plants of the Aojiang River waterway in Wenzhou, China. *Journal of Hazardous Materials*, 173(1–3): 75–81.

Li, M., Hu, M., Du, B., Guo, Q., Tan, T., Zheng, J., Huang, X., He, L., Wu, Z. & Guo, S. 2017. Temporal and spatial distribution of PM2.5 chemical composition in a coastal city of Southeast China. *Science of The Total Environment*, 605–606: 337–346.

Li, W., Peng, J., Zhang, L., Xia, H., Li, N., Yang, K. & Zhu, X. 2008. Investigations on carbonisation processes of plain tobacco stems and H_3PO_4-impregnated tobacco stems used for the preparation of activated carbons with H_3PO_4 activation. *Industrial Crops and Products*, 28(1): 73–80.

Li, Y., Chen, B. & Zhu, L. 2010b. Enhanced sorption of polycyclic aromatic hydrocarbons from aqueous solution by modified pine bark. *Bioresource Technology*, 101: 7307–7313.

Liang, H.-D., Han, D.-M. & Yan, X.-P. 2006. Cigarette filter as sorbent for on-line coupling of solid-phase extraction to high-performance liquid chromatography for determination of polycyclic aromatic hydrocarbons in water. *Chromatograhy A*, 1103: 9–14.

Liao, C., Liang, X., Lu, G., Thai, T., Xu, W. & Dang, Z. 2015. Effect of surfactant amendment to PAHs-contaminated soil for phytoremediation by maize (*Zea mays* L.). *Ecotoxicology and Environmental Safety*, 112: 1–6.

Lide, D.R. & Miline, G.W. 1996. Properties of Organic Compounds. *CRC Press [CD-ROM]*.

Lin, Q. & Mendelssohn, I.A. 2009. Potential of restoration and phytoremediation with *Juncus roemerianus* for diesel-contaminated coastal wetlands. *Ecological Engineering*, 35: 85–91.

Ling, W., Jiang, G.-B., Ya-Qi, C., Bin, H., Ya-Wei, W. & Da-Zhong, S. 2007. Cloud point extraction coupled with HPLC-UV for the determination of phthalate esters in environmental water samples. *Journal of Environmental Sciences*, 19: 874–878.

Liu, M., Feng, J., Hu, P., Tan, L., Zhang, X. & Sun, J. 2016a. Spatial-temporal distributions, sources of polycyclic aromatic hydrocarbons (PAHs) in surface water and suspended particular matter from the upper reach of Huaihe River, China. *Ecological Engineering*, 95: 143–151.

Liu, Q.-S., Zheng, T., Wang, P., Jiang, J.-P. & Li, N. 2010. Adsorption isotherm, kinetic and mechanism studies of some substituted phenols on activated carbon fibers. *Chemical Engineering Journal*, 157: 348–356.

Liu, S., Liu, X., Liu, M., Yang, B., Cheng, L., Li, Y. & Qadeer, A. 2016b. Levels, sources and risk assessment of PAHs in multi-phases from urbanised river network system in Shanghai. *Environmental Pollution*, 219: 555–567.

Liu, Y., Chen, L., Jianfu, Z., Qinghui, H., Zhiliang, Z. & Hongwen, G. 2008. Distribution and sources of polycyclic aromatic hydrocarbons in surface sediments of rivers and an estuary in Shanghai, China. *Environmental Pollution*, 154(2): 298–305.

Liu, Y., Shen, J., Chen, Z., Ren, N. & Li, Y. 2013. Distribution of polycyclic aromatic hydrocarbons in surface water and sediment near a drinking water reservoir in Northeastern China. *Environmental Science and Pollution Research*, 20: 2535–2545.

López-Vizcaíno, R., Sáez, C., Cañizares, P. & Rodrigo, M. a. 2012. The use of a combined process of surfactant-aided soil washing and coagulation for PAH-contaminated soils treatment. *Separation and Purification Technology*, 88: 46–51.

Louis, M.R., Sorokhaibam, L.G., Bhandari, V.M. & Bundale, S. 2018. Multifunctional activated carbon with antimicrobial property derived from *Delonix regia* biomaterial for treatment of wastewater. *Journal of Environmental Chemical Engineering*, 6:169-181.

Luque de Castro, M.D. & Priego-Capote, F. 2012. 2.05 – Soxhlet Extraction Versus Accelerated Solvent Extraction. In: *Comprehensive Sampling and Sample Preparation*. 83–103.

Ma, B., He, Y., Chen, H., Xu, J. & Rengel, Z. 2010. Dissipation of polycyclic aromatic hydrocarbons (PAHs) in the rhizosphere: Synthesis through meta-analysis. *Environmental Pollution*, 158: 855–861.

Ma, F., Wu, B., Zhang, Q., Cui, D., Liu, Q., Peng, C., Li, F. & Gu, Q. 2018. An innovative method for the solidification/stabilisation of PAHs-contaminated soil using sulfonated oil. *Journal of Hazardous Materials*, 344: 742–748.

Ma, Q. & Lu, A.Y.H. 2007. CYP1A induction and human risk assessment: An evolving tale of *in vitro* and *in vivo* studies. *Drug Metabolism and Disposition*, 35(7): 1009–1016.

Ma, W.-L., Liu, L.-Y., Qi, H., Zhang, Z.-F., Song, W.-W., Shen, J.-M., Chen, Z.-L., Ren, N.-Q., Grabuski, J. & Li, Y.-F. 2013. Polycyclic aromatic hydrocarbons in water, sediment and soil of the Songhua River Basin, China. *Environmental Monitoring and Assessment*, 185: 8399–8409.

Machado, A.A. de S., Hoff, M.L.M., Klein, R.D., Cordeiro, G.J., Lencina Avila, J.M., Costa, P.G. & Bianchini, A. 2014. Oxidative stress and DNA damage responses to phenanthrene exposure in the estuarine guppy *Poecilia vivipara*. *Marine Environmental Research*, 98: 96–105.

Mackay, D. & Fraser, A. 2000. Bioaccumulation of persistent organic chemicals: mechanisms and models. *Environmental Pollution*, 110(3): 375–391.

MacLeod, C.T. & Daugulis, A.J. 2005. Interfacial effects in a two-phase partitioning bioreactor: Degradation of polycyclic aromatic hydrocarbons (PAHs) by a hydrophobic Mycobacterium. *Process Biochemistry*, 40: 1799–1805.

Mafejane, A., Belcher, A., Zingitwa, L. & Kempster, P. 2002. *Water resources management plan in the Diep River catchment: A situation assessment*. Institute for Water Quality studies Report # N/G210/REQ/1200, 1-150.

Mahanty, B., Pakshirajan, K. & Venkata Dasu, V. 2008. Biodegradation of pyrene by *Mycobacterium frederiksbergense* in a two-phase partitioning bioreactor system. *Bioresource technology*, 99: 2694–2698.

Maity, S., Mazumdar, P., Shyamal, M., Sahoo, G.P. & Misra, A. 2016. Crystal induced phosphorescence from Benzo[a]anthracene microcrystals at room temperature. *Spectrochimica Acta Part A: Molecular and Biomolecular Spectroscopy*, 157: 61–68.

Mal, T.K. & Narine, L. 2004. The biology of Canadian weeds. 129. *Phragmites australis* (Cav.) Trin. ex Steud. *Canadian Journal of Plant Science*, 84: 365–396.

Manneh, R., Abi Ghanem, C., Khalaf, G., Najjar, E., El Khoury, B., Iaaly, A. & El Zakhem, H. 2016. Analysis of polycyclic aromatic hydrocarbons (PAHs) in Lebanese surficial sediments: A focus on the regions of Tripoli, Jounieh, Dora, and Tyre. *Marine Pollution Bulletin*, 110: 578–583.

Manoli, E. & Samara, C. 1999. Polycyclic aromatic hydrocarbons in natural waters: Sources, occurrence and analysis. *Trends in Analytical Chemistry*, 18(6): 417–428.

Marcé, R. & Borrull, F. 2000. Solid-phase extraction of polycyclic aromatic compounds. *Journal of Chromatography A*, 885(1): 273–290.

Martorell, I., Nieto, A., Nadal, M., Perelló, G., Marcé, R.M. & Domingo, J.L. 2012. Human exposure to polycyclic aromatic hydrocarbons (PAHs) using data from a duplicate diet study in Catalonia, Spain. *Food and Chemical Toxicology*, 50(11): 4103–4108.

Marvin, C.H., Allan, L., McCarry, B.E. & Bryant, D.W. 1992. A comparison of ultrasonic extraction and soxhlet extraction of polycyclic aromatic hydrocarbons from sediments and air particulate material. *International Journal of Environmental Analytical Chemistry*, 49(4): 221–230.

Matamoros, V., Uggetti, E., García, J. & Bayona, J.M. 2016. Assessment of the mechanisms involved in the removal of emerging contaminants by microalgae from wastewater: A laboratory scale study. *Journal of Hazardous Materials*, 301: 197–205.

Maynard, A. 1970. *Methods in Food Analysis*. 2nd ed. New York: Academic Press.

Mcmichael, A.J. 2000. The urban environment and health in a world of increasing globalisation: Issues for developing countries. *Bulletin of the World Health Organisation*, 78(9): 1117–1126.

Megharaj, M., Ramakrishnan, B., Venkateswarlu, K., Sethunathan, N. & Naidu, R. 2011. Bioremediation approaches for organic pollutants: A critical perspective. *Environment International*, 37: 1362–1375.

Mendham, J., Denney, R.C., Barnes, J.D. & Thomas, M. 2000. *Vogel's textbook of quantitative chemical analysis*. 6th ed. Harlow, England: Pearson Education Limited.

Menzie, C.A., Potocki, B.B. & Santodonato, J. 1992. Exposure to Carcinogenic PAHs in the Environment. *Environmental Science & Technology*, 26(7): 1278–1284.

Meodor, J., Stein, J., Reichert, W. & Varanasi, U. 1995. Bioaccumulation of polycyclic aromatic hydrocarbons by marine organisms. *Reviews of Environmental Contamination and Toxicology*, 143: 79–165.

Miet, K., Le Menach, K., Flaud, P.M., Budzinski, H. & Villenave, E. 2009. Heterogeneous reactivity of pyrene and 1-nitropyrene with NO_2: Kinetics, product yields and mechanism. *Atmospheric Environment*, 43: 837–843.

Miller, J.S. & Olejnik, D. 2001. Photolysis of polycyclic aromatic hydrocarbons in water. *Water research*, 35(1): 233–243.

Moen, B.E., Nilsson, R., Nordlinder, R., Bleie, K., Skorve, A.H. & Hollund, B.E. 1996. Assessment of exposure to polycyclic aromatic hydrocarbons in engine rooms by measurement of urinary 1-hydroxypyrene. *Occupational and Environmental Medicine*, 53(10): 692–696.

Mohan, D., Pittman, C.U. & Steele, P.H. 2006. Pyrolysis of wood/biomass for bio-oil: A critical review. *Energy & Fuels*, 20(4): 848–889.

Molina-Sabio, M. & Rodríguez-Reinoso, F. 2004. Role of chemical activation in the development of carbon porosity. *Colloids and Surfaces A: Physicochemical and Engineering Aspects*, 241(1–3): 15–25.

Monte, M.J.S., Notario, R., Pinto, S.P., Lobo Ferreira, A.I.M.C. & Ribeiro da Silva, M.D.M.C. 2012. Thermodynamic properties of fluoranthene: An experimental and computational study. *The Journal of Chemical Thermodynamics*, 49: 159–164.

Moreda, J.M., Arranz, A., Fdez De Betoño, S., Cid, A. & Arranz, J.F. 1998. Chromatographic determination of aliphatic hydrocarbons and polyaromatic hydrocarbons (PAHs) in a sewage sludge. *Science of The Total Environment*, 220(1): 33–43.

Mozo, I., Stricot, M., Lesage, N. & Spérandio, M. 2011. Fate of hazardous aromatic substances in membrane bioreactors. *Water Research*, 45(15): 4551–4561.

Mujtaba, G. & Lee, K. 2017. Treatment of real wastewater using co-culture of immobilized *Chlorella vulgaris* and suspended activated sludge. *Water Research*, 120: 174–184.

Mulder, E., Brouwer, J.P., Blaakmeer, J. & Frénay, J.W. 2001. Immobilisation of PAH in waste materials. *Waste Management*, 21: 247–253.

Munir, M.T., Li, B., Boiarkina, I., Baroutian, S., Yu, W. & Young, B.R. 2017. Phosphate recovery from hydrothermally treated sewage sludge using struvite precipitation. *Bioresource Technology*, 239: 171–179.

Munyengabe, A., Mambanda, A. & Moodley, B. 2017. Polycyclic aromatic hydrocarbons in water, soils and surface sediments of the Msunduzi River. *Journal of Environmental Analytical Chemistry*, 4(4): 1–13.

Murakami, M., Abe, M., Kakumoto, Y., Kawano, H., Fukasawa, H., Saha, M. & Takada, H. 2012. Evaluation of Ginkgo as a biomonitor of airborne polycyclic aromatic hydrocarbons. *Atmospheric Environment*, 54: 9–17.

Murray, R.W., Singh, M. & Rath, N. 1996. The reaction of dimethyldioxirane with chrysene: Formation of a trioxide. *Tetrahedron Letters*, 37(48): 8671–8674.

Muthusamy, S., Peng, C. & Ng, J.C. 2016. Effects of binary mixtures of benzo[a]pyrene, arsenic, cadmium, and lead on oxidative stress and toxicity in HepG2 cells. *Chemosphere*, 165: 41–51.

Naidoo, G. & Naidoo, K. 2016. Uptake of polycyclic aromatic hydrocarbons and their cellular effects in the mangrove *Bruguiera gymnorrhiza*. *Marine Pollution Bulletin*, 113: 193–199.

Navarro, R.R., Ichikawa, H., Morimoto, K. & Tatsumi, K. 2009. Enhancing the release and plant uptake of PAHs with a water-soluble purine alkaloid. *Chemosphere*, 76: 1109–1113.

NCBI (National Center for Biotechnology Information). 2005. PAHs. *PubChem Compound Database*: 1–59.

NCBI (National Center for Biotechnology Information). 2004. PAHs. *PubChem Compound Database*: 1–44.

Neff, J.M., Stout, S.A. & Gunster, D.G. 2005. Ecological risk assessment of polycyclic aromatic hydrocarbons in sediments: Identifying sources and ecological hazard. *Integrated Environmental Assessment and Management*, 1(1): 22–33.

Nekhavhambe, T.J., van Ree, T. & Fatoki, O.S. 2014. Determination and distribution of polycyclic

aromatic hydrocarbons in rivers, surface runoff, and sediments in and around Thohoyandou, Limpopo Province, South Africa. *Water SA*, 40(3): 415–424.

Nguyen, C. & Do, D.D. 2001. The Dubinin-Radushkevich equation and the underlying microscopic adsorption description. *Carbon*, 39: 1327–1336.

Nieuwoudt, C., Pieters, R., Quinn, L.P., Kylin, H., Borgen, A.R. & Bouwman, H. 2011. Polycyclic aromatic hydrocarbons (PAHs) in soil and sediment from industrial, residential, and agricultural areas in Central South Africa: An initial assessment. *Soil and Sediment Contamination*, 20: 188–204.

Nleya, N. 2005. *Institutional overlaps in water management in the Eerste River catchment*. MSc thesis, University of the Western Cape, South Africa.

Nowack, B. 2008. *Pollution Prevention and Treatment Using Nanotechnology*. In: Krug, H.F. (edn), Nanotechnology: Environmental Aspects. Wiley, Weinheim, 2: 1-15.

NTP. 1992. PAHs. *CAMEO Chemicals*. https://cameochemicals.noaa.gov/search/simple 1 January 2016.

O'Connor, G.A. 1996. Organic compounds in sludge-amended soils and their potential for uptake by crop plants. *Science of The Total Environment*, 185(1–3): 71–81.

O'Mahony, M.M., Dobson, A.D.W., Barnes, J.D. & Singleton, I. 2006. The use of ozone in the remediation of polycyclic aromatic hydrocarbon contaminated soil. *Chemosphere*, 63(2): 307–14.

O'Neil, M.J. 2001. *The Merck index 13th edition: An encyclopedia of chemicals, drugs, and biologicals*. Merck Research Laboratories, Whitehouse Station, NJ, Merck & Co, pp 34 -135.

Okafor, E.C. & Opuene, K. 2007. Preliminary assessment of trace metals and polycyclic aromatic hydrocarbons in the sediments. *International Journal of Environmental Science and Technology*, 4(2): 233–240.

Okedeyi, O.O., Nindi, M.M., Dube, S. & Awofolu, O.R. 2013. Distribution and potential sources of polycyclic aromatic hydrocarbons in soils around coal-fired power plants in South Africa. *Environmental Monitoring and Assessment*, 185: 2073–2082.

Okuda, T., Naoi, D., Tenmoku, M., Tanaka, S., He, K., Ma, Y., Yang, F., Lei, Y., Jia, Y. & Zhang, D. 2006. Polycyclic aromatic hydrocarbons (PAHs) in the aerosol in Beijing, China, measured by aminopropylsilane chemically-bonded stationary-phase column chromatography and HPLC/fluorescence detection. *Chemosphere*, 65(3): 427–435.

Okuda, T., Okamoto, K., Tanaka, S., Shen, Z., Han, Y. & Huo, Z. 2010. Measurement and source identification of polycyclic aromatic hydrocarbons (PAHs) in the aerosol in Xi'an, China, by using automated column chromatography and applying positive matrix factorisation (PMF). *Science of the Total Environment*, 408(8): 1909–1914.

Olatunji, O.S., Fatoki, O.S., Opeolu, B.O. & Ximba, B.J. 2014. Determination of polycyclic aromatic hydrocarbons (PAHs) in processed meat products using gas chromatography-Flame ionisation detector. *Food Chemistry*, 156: 296–300.

Oleszczuk, P., Godlewska, P., Reible, D.D. & Kraska, P. 2017. Bioaccessibility of polycyclic aromatic hydrocarbons in activated carbon or biochar amended vegetated (*Salix viminalis*) soil. *Environmental Pollution*, 227: 406–413.

Oleszczuk, P., Hale, S.E., Lehmann, J. & Cornelissen, G. 2012. Activated carbon and biochar amendments decrease pore-water concentrations of polycyclic aromatic hydrocarbons (PAHs) in sewage sludge. *Bioresource Technology*, 111: 84–91.

Oleszczuk, P., Zielinska, A. & Cornelissen, G. 2014. Stabilisation of sewage sludge by different biochars towards reducing freely dissolved polycyclic aromatic hydrocarbons (PAHs) content. *Bioresource Technology*, 156: 139–145.

Oliferova, L., Statkus, M., Tsysin, G., Shpigun, O. & Zolotov, Y. 2005. On-line solid-phase extraction and HPLC determination of polycyclic aromatic hydrocarbons in water using fluorocarbon polymer sorbents. *Analytica Chimica Acta*, 538(1–2): 35–40.

Oliveira, A.M. de, Nascimento, M.F. do, Ferreira, M.R.A., Moura, D.F. de, Souza, T.G. dos S., Silva, G.C. da, Ramos, E.H. da S., Paiva, P.M.G., Medeiros, P.L. de, Silva, T.G. da, Soares, L.A.L., Chagas, C.A., Souza, I.A. de & Napoleão, T.H. 2016. Evaluation of acute toxicity, genotoxicity and inhibitory effect on acute inflammation of an ethanol extract of *Morus alba* L. (*Moraceae*) in mice. *Journal of Ethnopharmacology*, 194: 162–168.

Olivella, M.A., Ribalta, T.G., de Febrer, A.R., Mollet, J.M. & de las Heras, F.X.C. 2006. Distribution of polycyclic aromatic hydrocarbons in riverine waters after Mediterranean forest fires. *Science of The Total Environment*, 355(1): 156–166.

Olu-owolabi, B.I., Diagboya, P.N. & Adebowale, K.O. 2014. Evaluation of pyrene sorption-desorption on tropical soils. *Journal of Environmental Management*, 137: 1–9.

Opeolu, B.O., Bamgbose, O. & Fatoki, O.S. 2011. Zinc abatement from simulated and industrial wastewaters using sugarcane biomass. *Water SA*, 37(3): 313–320.

Opeolu, B.O., Fatoki, O.S. & Odendaal, J. 2010. Development of a solid-phase extraction method followed by HPLC-UV detection for the determination of phenols in water. *International Journal of Physical Sciences*, 5: 576–581.

Orecchio, S. 2010. Assessment of polycyclic aromatic hydrocarbons (PAHs) in soil of a Natural Reserve (Isola delle Femmine) (Italy) located in front of a plant for the production of cement. *Journal of Hazardous Materials*, 173(1): 358–368.

Othman, H. Ben, Leboulanger, C., Le Floc'h, E., Hadj Mabrouk, H. & Sakka Hlaili, A. 2012. Toxicity of benzo[a]anthracene and fluoranthene to marine phytoplankton in culture: Does cell size really matter? *Journal of Hazardous Materials*, 243: 204–211.

Oubina, A., Puig, D., Gascón, J. & Barceló, D. 1997. Determination of pentachlorophenol in certified waste waters, soil samples and industrial effluents using ELISA and liquid solid extraction followed by liquid chromatography. *Analytica Chimica Acta*, 346(1): 49–59.

Özcan, A.S., Erdem, B. & Özcan, A. 2004. Adsorption of Acid Blue 193 from aqueous solutions onto Na–bentonite and DTMA–bentonite. *Journal of Colloid and Interface Science*, 280(1): 44–54.

Ozcan, S., Tor, A. & Aydin, M.E. 2010. Determination of polycyclic aromatic hydrocarbons in waters by ultrasound-assisted emulsification-microextraction and gas chromatography-mass spectrometry. *Analytica Chimica Acta*, 665(2): 193–199.

Padmavathy, K.S., Madhu, G. & Haseena, P.V. 2016. A study on effects of pH, adsorbent dosage, time, initial concentration and adsorption isotherm study for the removal of hexavalent chromium (Cr (VI)) from wastewater by magnetite nanoparticles. *Procedia Technology*, 24: 585–594.

Palanikumar, L., Kumaraguru, A.K., Ramakritinan, C.M. & Anand, M. 2012. Biochemical response of anthracene and benzo[a]pyrene in milkfish *Chanos chanos*. *Ecotoxicology and Environmental Safety*, 75: 187–197.

Pan, L., Ren, J. & Liu, J. 2005. Effects of benzo[k]fluoranthene exposure on the biomarkers of scallop *Chlamys farreri*. *Comparative Biochemistry and Physiology Part C: Toxicology & Pharmacology*, 141(3): 248–256.

Panday, K.K., Prasas, G. & Singh, V.N. 1985. Copper(II) removal from aqueous solutions by fly ash. *Water Research*, 19: 869–873.

Pang, J., Sun, B., Li, H., Mehler, W.. . & You, J. 2012. Influence of bioturbation on bioavailability and toxicity of PAHs in sediment from an electronic waste recycling site in South China.

Ecotoxicology and environmental safety, 84: 227–233.

Park, J., Hung, I., Gan, Z., Rojas, O.J., Hun, K. & Park, S. 2013. Activated carbon from biochar: Influence of its physicochemical properties on the sorption characteristics of phenanthrene. *Bioresource Technology*, 149: 383–389.

Pathak, H., Kantharia, D., Malpani, A. & Madamwar, D. 2009. Naphthalene degradation by *Pseudomonas* sp. HOB1: *In vitro* studies and assessment of naphthalene degradation efficiency in simulated microcosms. *Journal of hazardous materials*, 166: 1466–1473.

Patra, D. & Mishra, A.K. 2001. Fluorescence quenching of benzo[k]fluoranthene in poly(vinyl alcohol) film: A possible optical sensor for nitro aromatic compounds. *Sensors and Actuators B: Chemical*, 80(3): 278–282.

Patrolecco, L., Ademollo, N., Capri, S., Pagnotta, R. & Polesello, S. 2010. Occurrence of priority hazardous PAHs in water, suspended particulate matter, sediment and common eels (*Anguilla anguilla*) in the urban stretch of the River Tiber (Italy). *Chemosphere*, 81(11): 1386–1392.

Paulse, A.N., Jackson, V.A. & Khan, W. 2009. Comparison of microbial contamination at various sites along the Plankenburg-and Diep Rivers, Western Cape, South Africa. *Water SA*, 35(4): 469–478.

Pavelkajr, J., Kocourek, V., Holadova, K., Klımova, I. & Tomaniova, M. 1998. Microwave-assisted solvent extraction — a new method for isolation of polynuclear aromatic hydrocarbons from plants. *Journal of Chromatography A*, 827: 21–29.

Peláez-Samaniego, M.R., Garcia-Perez, M., Cortez, L.B., Rosillo-Calle, F. & Mesa, J. 2008. Improvements of Brazilian carbonisation industry as part of the creation of a global biomass economy. *Renewable and Sustainable Energy Reviews*, 12(4): 1063–1086.

Pérez-Fernández, B., Viñas, L., Franco, M.Á. & Bargiela, J. 2015. PAHs in the Ría de Arousa (NW Spain): A consideration of PAHs sources and abundance. *Marine Pollution Bulletin*, 95(1): 155–165.

Peterson, J.S.K. & Bain, L.J. 2004. Differential gene expression in anthracene-exposed mummichogs (*Fundulus heteroclitus*). *Aquatic Toxicology*, 66(4): 345–355.

Phillips, D.H. 1999. Polycyclic aromatic hydrocarbons in the diet. *Mutation Research/Genetic Toxicology and Environmental Mutagenesis*, 443(1): 139–147.

Picó, Y. 2013. Ultrasound-assisted extraction for food and environmental samples. *Trends in Analytical Chemistry*, 43: 84–99.

Pieters, N., Koppen, G., Smeets, K., Napierska, D., Plusquin, M., De, S., Weghe, H. Van De, Nelen, V., Cox, B., Cuypers, A., Hoet, P., Schoeters, G. & Nawrot, T.S. 2013. Decreased mitochondrial DNA content in association with exposure to polycyclic aromatic hydrocarbons in house dust during wintertime: From a population enquiry to cell culture. *PLOS ONE*, 8(5): 1–8.

Pietzsch, R., Patchineelam, S.R. & Torres, J.P.M. 2010. Polycyclic aromatic hydrocarbons in recent sediments from a subtropical estuary in Brazil. *Marine Chemistry*, 118(1): 56–66.

Pinheiro, D., De Castro, C.S., Seixas De Melo, J.S., Oliveira, E., Nuñez, C., Fernández-Lodeiro, A., Capelo, J.L. & Lodeiro, C. 2014. From yellow to pink using a fluorimetric and colorimetric pyrene derivative and mercury (II) ions. *Dyes and Pigments*, 110: 152–158.

Platt, K.L., Grupe, S. & Fickler, M. 2008. The 3,4-oxide is responsible for the DNA binding of benzo[g, h, i]perylene, a polycyclic aromatic hydrocarbon without a “classic” bay-region. *Chemico-Biological Interactions*, 176(2): 179–187.

Plazinski, W., Dziuba, J. & Rudzinski, W. 2013. Modeling of sorption kinetics: The pseudo-second order equation and the sorbate intraparticle diffusivity. *Adsorption*, 19: 1055–1064.

Poster, D.L., Schantz, M.M., Sander, L.C. & Wise, S.A. 2006. Analysis of polycyclic aromatic hydrocarbons (PAHs) in environmental samples: A critical review of gas chromatographic (GC) methods. *Analytical and Bioanalytical Chemistry*, 386(4): 859–881.

Prahas, D., Kartika, Y., Indraswati, N. & Ismadji, S. 2008. Activated carbon from jackfruit peel waste by H_3PO_4 chemical activation: Pore structure and surface chemistry characterisation. *Chemical Engineering Journal*, 140: 32–42.

Priya, K.L. & Arulraj, G.P. 2011. A correlation-regression model for the physicochemical parameters of the groundwater in Coimbatore city, India. *Environmental Technology*, 32(7): 731–738.

Purwaningsih, I.S., Hill, G.A. & Headley, J. V. 2004. Mass transfer and bioremediation of naphthalene particles in a roller bioreactor. *Water research*, 38: 2027–2034.

Qiao, K., Tian, W., Bai, J., Dong, J., Zhao, J., Gong, X. & Liu, S. 2018. Preparation of biochar from *Enteromorpha prolifera* and its use for the removal of polycyclic aromatic hydrocarbons (PAHs) from aqueous solution. *Ecotoxicology and Environmental Safety*, 149: 80–87.

Qiao, M., Huang, S. & Wang, Z. 2008. Partitioning characteristics of PAHs between sediment and water in a shallow lake. *Journal of Soils and Sediments*, 8(2): 69–73.

Qin, G., Wu, M. & Sang, N. 2015. Sulfur dioxide and benzo[a]pyrene trigger apoptotic and anti-apoptotic signals at different post-exposure times in mouse liver. *Chemosphere*, 139: 318–325.

Qu, Y., Zhang, C., Li, F., Bo, X., Liu, G. & Zhou, Q. 2009. Equilibrium and kinetics study on the adsorption of perfluorooctanoic acid from aqueous solution onto powdered activated carbon. *Journal of Hazardous Materials*, 169: 146–152.

Quinn, L., Pieters, R., Nieuwoudt, C., Borgen, A.R., Kylin, H. & Bouwman, H. 2009. Distribution profiles of selected organic pollutants in soils and sediments of industrial, residential and agricultural areas of South Africa. *Journal of Environmental Monitoring*, 11(9): 1647–1657.

Quiroz, R., Popp, P., Urrutia, R., Bauer, C., Araneda, A., Treutler, H.-C. & Barra, R. 2005. PAH fluxes in the Laja Lake of south central Chile Andes over the last 50 years: Evidence from a dated sediment core. *Science of The Total Environment*, 349(1): 150–160.

Rabodonirina, S., Net, S., Ouddane, B., Merhaby, D., Dumoulin, D., Popescu, T. & Ravelonandro, P. 2015. Distribution of persistent organic pollutants (PAHs, Me-PAHs, PCBs) in dissolved, particulate and sedimentary phases in freshwater systems. *Environmental Pollution*, 206: 38–48.

Rad, R.M., Omidi, L., Kakooei, H., Golbabaei, F., Hassani, H., Loo, R.A. & Azam, K. 2014. Adsorption of polycyclic aromatic hydrocarbons on activated carbons: Kinetic and isotherm curve modeling. *International Journal of Occupational Hygiene*, 6: 43–49.

Rahim, A.A. & Garba, Z.N. 2016. Efficient adsorption of 4-Chloroguiacol from aqueous solution using optimal activated carbon: Equilibrium isotherms and kinetics modeling. *Journal of the Association of Arab Universities for Basic and Applied Sciences*, 21: 17–23.

Ramachandran, P., Vairamuthu, R. & Ponnusamy, S. 2011. Adsorption isotherms, kinetics, thermodynamics and desorption studies of Reactive Orange16 on activated carbon derived from *Ananas comosus* (L.) carbon. *Asian Research Publishing Network (ARPN) Journal of Engineering and Applied Sciences*, 6(11): 15–26.

Ramos, L. 2012. Critical overview of selected contemporary sample preparation techniques. *Journal of Chromatography A*, 1221: 84–98.

Ranc, B., Faure, P., Croze, V. & Simonnot, M.O. 2016. Selection of oxidant doses for *in situ* chemical oxidation of soils contaminated by polycyclic aromatic hydrocarbons (PAHs): A review. *Journal of Hazardous Materials*, 312: 280–297.

Rani, B.K. & John, S.A. 2016. A novel pyrene based fluorescent probe for selective detection of cysteine in presence of other bio-thiols in living cells. *Biosensors and Bioelectronics*, 83: 237–242.

Ranjbar Jafarabadi, A., Riyahi Bakhtiari, A. & Shadmehri Toosi, A. 2017. Comprehensive and comparative ecotoxicological and human risk assessment of polycyclic aromatic hydrocarbons (PAHs) in reef surface sediments and coastal seawaters of Iranian Coral Islands, Persian Gulf. *Ecotoxicology and Environmental Safety*, 145: 640–652.

Raptis, C.E., Boucher, J.M. & Pfister, S. 2017. Assessing the environmental impacts of freshwater thermal pollution from global power generation in LCA. *Science of The Total Environment*, 580: 1014–1026.

Rashidi, N.A., Yusup, S., Ahmad, M.M., Mohamed, N.M. & Hameed, B.H. 2012. Activated carbon from the renewable agricultural residues using single step physical activation: A preliminary analysis. *APCBEE Procedia*, 3: 84–92.

Ravindra, K., Bencs, L., Wauters, E., De Hoog, J., Deutsch, F., Roekens, E., Bleux, N., Berghmans, P. & Van Grieken, R. 2006. Seasonal and site-specific variation in vapour and aerosol phase PAHs over Flanders (Belgium) and their relation with anthropogenic activities. *Atmospheric Environment*, 40(4): 771–785.

Ravindra, K., Sokhi, R. & Van Grieken, R. 2008. Atmospheric polycyclic aromatic hydrocarbons: Source attribution, emission factors and regulation. *Atmospheric Environment*, 42(13): 2895–2921.

Ren, X., Pan, L. & Wang, L. 2015. The detoxification process, bioaccumulation and damage effect in juvenile white shrimp *Litopenaeus vannamei* exposed to chrysene. *Ecotoxicology and Environmental Safety*, 114: 44–51.

Reungoat, J., Escher, B.I., Macova, M., Argaud, F.X., Gernjak, W. & Keller, J. 2012. Ozonation and biological activated carbon filtration of wastewater treatment plant effluents. *Water Research*, 46: 863–872.

Rezaee, M., Assadi, Y., Milani Hosseini, M.-R., Aghaee, E., Ahmadi, F. & Berijani, S. 2006. Determination of organic compounds in water using dispersive liquid-liquid microextraction. *Journal of chromatography. A*, 1116(1–2): 1–9.

Rice, J.E., Coleman, D.T., Hosted, T.J., Lavoie, E.J., Mccaustland, D.J. & Wiley, J.C. 1985. Identification of mutagenic metabolites of Indeno[1, 2, 3-cd]pyrene formed *in vitro* with rat liver enzymes. *Cancer Research*, 45: 5421–5425.

Riva, M., Healy, R.M., Tomaz, S., Flaud, P.-M., Perraudin, E., Wenger, J.C. & Villenave, E. 2016. Gas and particulate phase products from the ozonolysis of acenaphthylene. *Atmospheric Environment*, 142: 104–113.

Rivas, F.J., Beltrán, F.J. & Acedo, B. 2000. Chemical and photochemical degradation of acenaphthylene. Intermediate identification. *Journal of Hazardous Materials B*, 75: 89–98.

Rizwan, M., Singh, M., Mitra, C.K. & Morve, R.K. 2014. Ecofriendly Application of nanomaterials: Nanobioremediation. *Journal of Nanoparticles*, 2014: 1–7.

Robinson, J.P., Kingman, S.W., Snape, C.E., Shang, H., Barranco, R. & Saeid, A. 2009. Separation of polyaromatic hydrocarbons from contaminated soils using microwave heating. , 69: 249–254.

Roshandel, G., Semnani, S., Malekzadeh, R. & Dawsey, S.M. 2012. Polycyclic aromatic hydrocarbons and esophageal squamous cell carcinoma. *Archives of Iran Medicine*, 15(11): 713–722.

Rossella, F., Campo, L., Pavanello, S., Kapka, L., Siwinska, E. & Fustinoni, S. 2009. Urinary polycyclic aromatic hydrocarbons and monohydroxy metabolites as biomarkers of exposure

in coke oven workers. *Occupational and Environmental Medicine*, 66(8): 509–516.

Ruggieri, R., Forti, P., Antoci, M.L. & De Waele, J. 2017. Accidental contamination during hydrocarbon exploitation and the rapid transfer of heavy-mineral fines through an overlying highly karstified aquifer (Paradiso Spring, SE Sicily). *Journal of Hydrology*, 546: 123–132.

Ruiz, Y., Suarez, P., Alonso, A., Longo, E., Villaverde, A. & San Juan, F. 2011. Environmental quality of mussel farms in the Vigo Estuary: Pollution by PAHs, origin and effects on reproduction. *Environmental pollution*, 159(1): 250–265.

Sabia, G., Petta, L., Moretti, F. & Ceccarelli, R. 2018. Combined statistical techniques for the water quality analysis of a natural wetland and evaluation of the potential implementation of a FWS for the area restoration: The Torre Flavia case study, Italy. *Ecological Indicators*, 84: 244–253.

Saeed, A., Sharif, M. & Iqbal, M. 2010. Application potential of grapefruit peel as dye sorbent: Kinetics, equilibrium and mechanism of crystal violet adsorption. *Journal of Hazardous Materials*, 179(1): 564–572.

Sallam, G.A.H. & Elsayed, E.A. 2015. Estimating the impact of air temperature and relative humidity change on the water quality of Lake Manzala, Egypt. *Journal of Natural Resources and Development*, 5: 76–87.

Salmon, J., Kohen, E., Kohen, C. & Bengtsson, G. 1974. A microspectrofluorometric approach for the study of benzo[a]pyrene and dibenzo[a , h]anthracene metabolisation in single living cells. *Histochemistry*, 42: 61–74.

Sánchez-Avila, J., Bonet, J., Velasco, G. & Lacorte, S. 2009. Determination and occurrence of phthalates, alkylphenols, bisphenol A, PBDEs, PCBs and PAHs in an industrial sewage grid discharging to a municipal wastewater treatment plant. *Science of the Total Environment*, 407: 4157–4167.

Sanchez-Prado, L., Garcia-Jares, C., Dagnac, T. & Llompart, M. 2015. Microwave-assisted extraction of emerging pollutants in environmental and biological samples before chromatographic determination. *Trends in Analytical Chemistry*, 71: 119–143.

Santos, C., de Oliveira, M.T., Cólus, I.M. de S., Sofia, S.H. & Martinez, C.B. dos R. 2018a. Expression of *cyp1a* induced by benzo[a]pyrene and related biochemical and genotoxic biomarkers in the neotropical freshwater fish *Prochilodus lineatus*. *Environmental Toxicology and Pharmacology*, 61: 30–37.

Santos, E., Souza, M.R.R., Vilela, A.R., Soares, L.S., Frena, M. & Alexandre, M.R. 2018b. Polycyclic aromatic hydrocarbons (PAHs) in superficial water from a tropical estuarine system: Distribution, seasonal variations, sources and ecological risk assessment. *Marine Pollution Bulletin*, 127: 352–358.

Santos, L.O., dos Anjos, J.P., Ferreira, S.L.C. & de Andrade, J.B. 2017. Simultaneous determination of PAHS, nitro-PAHS and quinones in surface and groundwater samples using SDME/GC-MS. *Microchemical Journal*, 133: 431–440.

Santos, R.C., Bernardes, C.E.S., Diogo, H.P., Piedade, M.F.M., Canongia Lopes, J.N. & Minas da Piedade, M.E. 2006. Energetics of the thermal dimerisation of acenaphthylene to heptacyclene. *The Journal of Physical Chemistry. A*, 110(6): 2299–2307.

Sarada, B., Prasad, M.K., Kumar, K.K. & Ramachandra Murthy, C.V. 2014. Cadmium removal by macro algae *Caulerpa fastigiata*: Characterisation, kinetic, isotherm and thermodynamic studies. *Journal of Environmental Chemical Engineering*, 2(3): 1533–1542.

Sarasidis, V.C., Plakas, K. V. & Karabelas, A.J. 2017. Novel water-purification hybrid processes involving *in-situ* regenerated activated carbon, membrane separation and advanced

oxidation. *Chemical Engineering Journal*, 328: 1153–1163.

Sartape, A.S., Mandhare, A.M., Jadhav, V.V, Raut, P.D., Anuse, M.A. & Kolekar, S.S. 2017. Removal of malachite green dye from aqueous solution with adsorption technique using *Limonia acidissima* (wood apple) shell as low cost adsorbent. *Arabian Journal of Chemistry*, 10: S3229–S3238.

Sasek, V., Bhatt, M., Cajthaml, T., Malachová, K. & Lednická, D. 2003. Compost-mediated removal of polycyclic aromatic hydrocarbons from contaminated soil. *Archives of environmental contamination and toxicology*, 44(3): 336–342.

Shahriari, M. & Frost, A. 2008. Oil spill cleanup cost estimation-Developing a mathematical model for marine environment. *Process Safety and Environmental Protection*, 86(3): 189–197.

Sharma, A., Kundu, S.S., Tariq, H., Kewalramani, N. & Yadav, R.K. 2017. Impact of total dissolved solids in drinking water on nutrient utilisation and growth performance of Murrah buffalo calves. *Livestock Science*, 198: 17–23.

Shi, Q., Li, A., Zhu, Z. & Liu, B. 2013. Adsorption of naphthalene onto a high-surface-area carbon from waste ion exchange resin. *Journal of Environmental Sciences (China)*, 25(1): 188–194.

Shou, M., Krausz, K.W., Gonzalez, F.J. & Gelboin, H. V. 1996. Metabolic activation of the potent carcinogen dibenzo[a, h]anthracene by cDNA-Expressed human cytochromes P450. *Archives of Biochemistry and Biophysics*, 328(1): 201–207.

Shuping, L.S., Snyman, R.G., Odendaal, J.P. & Ndakidemi, P.A. 2011. Accumulation and distribution of metals in *Bolboschoenus maritimus* (*Cyperaceae*), from a South African river. *Water, Air, and Soil Pollution*, 216(1–4): 319–328.

Sibiya, P., Chimuka, L., Cukrowska, E. & Tutu, H. 2013. Development and application of microwave assisted extraction (MAE) for the extraction of five polycyclic aromatic hydrocarbons in sediment samples in Johannesburg area, South Africa. *Environmental Monitoring and Assessment*, 185: 5537–5550.

Singh, B.K. & Rawat, N.S. 1994. Comparative sorption kinetic studies of phenolic compounds on fly ash and impregnated fly ash. *Journal of Chemical Technology and Biotechnology*, 61: 57–65.

Singh, V.K., Patel, D.K., Ram, S., Mathur, N., Siddiqui, M.K.J. & Behari, J.R. 2008. Blood Levels of Polycyclic Aromatic Hydrocarbons in Children of Lucknow, India. *Archives of Environmental Contamination and Toxicology*, 54: 348–354.

Siphugu, L. & Terry, L. 2011. *South Africa - Republic of Wine Annual*. Pretoria, South Africa. http://gain.fas.usda.gov/Recent GAIN Publications/Wine Annual_Pretoria_South Africa - Republic of_3-14-2011.pdf.

Sojinu, O.S., Sonibare, O.O., Ekundayo, O. & Zeng, E.Y. 2010. Biomonitoring potentials of polycyclic aromatic hydrocarbons (PAHs) by higher plants from an oil exploration site, Nigeria. *Journal of Hazardous Materials*, 184(1): 759–764.

Song, M.-K., Kim, Y.-J., Song, M., Choi, H.-S., Park, Y.-K. & Ryu, J.-C. 2012. Formation of a 3,4-diol-1,2-epoxide metabolite of benz[a]anthracene with cytotoxicity and genotoxicity in a human *in vitro* hepatocyte culture system. *Environmental Toxicology and Pharmacology*, 33(2): 212–225.

Song, Y., Jing, X., Fleischmann, S. & Wilke, B.-M. 2002. Comparative study of extraction methods for the determination of PAHs from contaminated soils and sediments. *Chemosphere*, 48: 993–1001.

Spinelli, R., Nati, C., Pari, L., Mescalchin, E. & Magagnotti, N. 2012. Production and quality of biomass fuels from mechanised collection and processing of vineyard pruning residues. *Applied Energy*, 89(1): 374–379.

Spink, D.C., Wu, S.J., Spink, B.C., Hussain, M.M., Vakharia, D.D., Pentecost, B.T. & Kaminsky, L.S. 2008. Induction of CYP1A1 and CYP1B1 by benzo[k]fluoranthene and benzo[apyrene in T-47D human breast cancer cells: Roles of PAH interactions and PAH metabolites. *Toxicology and Applied Pharmacology*, 226(3): 213–224.

Srogi, K. 2007. Monitoring of environmental exposure to polycyclic aromatic hydrocarbons: A review. *Environmental Chemistry Letters*, 5(4): 169–195.

Stogiannidis, E. & Laane, R. 2015. Source characterisation of polycyclic aromatic hydrocarbons by using their molecular indices: An overview of possibilities. In *Reviews of Environmental Contamination and Toxicology*. 49–133.

Su, D.C. & Wong, J.W.C. 2004. Selection of mustard oilseed rape (*Brassica juncea* L.) for phytoremediation of cadmium contaminated soil. *Bulletin of Environmental Contamination and Toxicology*, 72(5): 991–998.

Sudaryanto, Y., Hartono, S.B., Irawaty, W., Hindarso, H. & Ismadji, S. 2006. High surface area activated carbon prepared from cassava peel by chemical activation. *Bioresource Technology*, 97: 734–739.

Sugumaran, P., Susan, V.P., Ravichandran, P. & Seshadri, S. 2012. Production and characterisation of activated carbon from banana empty fruit bunch and *Delonix regia* fruit pod. *Journal of Sustainable Energy & Environment*, 3: 125–132.

Sun, F., Littlejohn, D. & David, M. 1998. Ultrasonication extraction and solid phase extraction clean-up for determination of US EPA 16 priority pollutant polycyclic aromatic hydrocarbons in soils by reversed-phase liquid chromatography with ultraviolet absorption detection. *Analytica Chimica Acta*, 364: 1–11.

Sun, J.-H., Wang, G.-L., Chai, Y., Zhang, G., Li, J. & Feng, J. 2009. Distribution of polycyclic aromatic hydrocarbons (PAHs) in Henan Reach of the Yellow River, Middle China. *Ecotoxicology and Environmental Safety*, 72(5): 1614–1624.

Sun, L. & Zang, S. 2013. Relationship between polycyclic aromatic hydrocarbons (PAHs) and particle size in dated core sediments in Lake Lianhuan, Northeast China. *Science of the Total Environment*, 461–462: 180–187.

Sun, T.-R., Cang, L., Wang, Q.-Y., Zhou, D.-M., Cheng, J.-M. & Xu, H. 2010. Roles of abiotic losses, microbes, plant roots, and root exudates on phytoremediation of PAHs in a barren soil. *Journal of Hazardous Materials*, 176(1): 919–925.

Sun, Y., Li, H., Li, G., Gao, B., Yue, Q. & Li, X. 2016. Characterisation and ciprofloxacin adsorption properties of activated carbons prepared from biomass wastes by H_3PO_4 activation. *Bioresource Technology*, 217: 239–244.

Sushkova, S.N., Vasilyeva, G.K., Minkina, T.M., Mandzhieva, S.S., Tjurina, I.G., Kolesnikov, S.I., Kizilkaya, R. & Askin, T. 2014. New method for benzo[a]pyrene analysis in plant material using subcritical water extraction. *Journal of Geochemical Exploration*, 144: 267–272.

Sylus, K.J. & Ramesh, H. 2015. The Study of sea water intrusion in coastal aquifer by electrical conductivity and total dissolved solid method in Gurpur and Netravathi River basin. *Aquatic Procedia*, 4: 57–64.

Takino, M., Daishima, S., Yamaguchi, K. & Nakahara, T. 2001. Determination of polycyclic aromatic hydrocarbons by liquid chromatography – electrospray ionisation mass spectrometry using silver nitrate as a post-column reagent. *Journal of Chromatography A*, 928: 53–61.

Tao, S., Cui, Y.H., Xu, F.L., Li, B.G., Cao, J., Liu, W.X., Schmitt, G., Wang, X.J., Shen, W.R., Qing, B.P. & Sun, R. 2004. Polycyclic aromatic hydrocarbons (PAHs) in agricultural soil and vegetables from Tianjin. *Science of the Total Environment*, 320(1): 11–24.

Tauhid Ur Rahman, M., Rasheduzzaman, M., Habib, M.A., Ahmed, A., Tareq, S.M. & Muniruzzaman, S.M. 2017. Assessment of fresh water security in coastal Bangladesh: An insight from salinity, community perception and adaptation. *Ocean and Coastal Management*, 137: 68–81.

Ter Laak, T.L., ter Bekke, M. a & Hermens, J.L.M. 2009. Dissolved organic matter enhances transport of PAHs to aquatic organisms. *Environmental Science & Technology*, 43(23): 7212–7217.

Tesar, M., Reichenauer, T.G. & Sessitsch, A. 2002. Bacterial rhizosphere populations of black poplar and herbal plants to be used for phytoremediation of diesel fuel. *Soil Biology and Biochemistry*, 34: 1883–1892.

Thamaga, K.H. & Dube, T. 2018. Remote Sensing Applications: Society and Environment Remote sensing of invasive water hyacinth (*Eichhornia crassipes*): A review on applications and challenges. *Remote Sensing Applications: Society and Environment*, 10: 36–46.

Thea, A.E., Ferreira, D., Brumovsky, L.A. & Schmalko, M.E. 2016. Polycyclic aromatic hydrocarbons (PAHs) in yerba maté (*Ilex paraguariensis St*. Hil) traditional infusions (*mate* and *tereré*). *Food Control*, 60: 215–220.

Thorwirth, S., Theule, P., Gottlieb, C.A., McCarthy, M.C. & Thaddeus, P. 2007. Rotational spectra of small PAHs : Acenaphthene, acenaphtylene, azulene, and fluorene. *The Astrophysical Journal*, 662: 1309–1314.

Titato, G. & Lancas, F. 2006. Optimisation and validation of HPLC-UV-DAD and HPLC-APCI-MS methodologies for the determination of selected PAHs in water samples. *Journal of Chromatographic Science*, 44: 35–41.

Tiwari, J.N., Mahesh, K., Le, N.H., Kemp, K.C., Timilsina, R., Tiwari, R.N. & Kim, K.S. 2013. Reduced graphene oxide-based hydrogels for the efficient capture of dye pollutants from aqueous solutions. *Carbon*, 56: 173–182.

Tomar, R.S. & Jajoo, A. 2014. Fluoranthene, a polycyclic aromatic hydrocarbon, inhibits light as well as dark reactions of photosynthesis in wheat (*Triticum aestivum*). *Ecotoxicology and Environmental Safety*, 109: 110–115.

Tomar, R.S. & Jajoo, A. 2015. Photomodified fluoranthene exerts more harmful effects as compared to intact fluoranthene by inhibiting growth and photosynthetic processes in wheat. *Ecotoxicology and Environmental Safety*, 122: 31–36.

Tongo, I., Ezemonye, L. & Akpeh, K. 2017. Distribution, characterisation, and human health risk assessment of polycyclic aromatic hydrocarbons (PAHs) in Ovia River, Southern Nigeria. *Environmental Monitoring and Assessment*, 5: 504–512.

Toyooka, T. & Ibuki, Y. 2007. DNA damage induced by coexposure to PAHs and light. *Environmental Toxicology and Pharmacology*, 23(2): 256–263.

Tran, N.H., Urase, T., Ngo, H.H., Hu, J. & Ong, S.L. 2013. Insight into metabolic and cometabolic activities of autotrophic and heterotrophic microorganisms in the biodegradation of emerging trace organic contaminants. *Bioresource Technology*, 146: 721–731.

Tromp, K., Lima, A.T., Barendregt, A. & Verhoeven, J.T.A. 2012. Retention of heavy metals and poly-aromatic hydrocarbons from road water in a constructed wetland and the effect of de-icing. *Journal of Hazardous Materials*, 203–204: 290–298.

UNECE (United Nations Economic Commission for Europe). 1998. The 1998 Aarhus protocol on persistent organic pollutants (POPs). *Protocol on persistent organic pollutants (POPs)*: 1–11. http://www.unece.org/env/lrtap/pops_h1.html.

Uno, S., Sakurai, K., Nebert, D.W. & Makishima, M. 2014. Protective role of cytochrome P450 1A1 (CYP1A1) against benzo[a]pyrene-induced toxicity in mouse aorta. *Toxicology*, 316: 34–42.

US EPA (United States Environmental Protection Agency). 1990. *Benz[a]anthracene (CASRN 56-55-3)* | *IRIS* | *US EPA*.

US EPA (United States Environmental Protection Agency). 2006. EPA region III BTAG freshwater sediment screening benchmarks.

US EPA (United States Environmental Protection Agency). 2014. Priority Pollutant List. *Toxic and Priority Pollutants Under the Clean Water Act*: 2.

Usman, M., Faure, P., Ruby, C. & Hanna, K. 2012. Remediation of PAH-contaminated soils by magnetite catalysed Fenton-like oxidation. *Applied Catalysis B: Environmental*, 117–118: 10–17.

Van Stempvoort, D. & Biggar, K. 2008. Potential for bioremediation of petroleum hydrocarbons in groundwater under cold climate conditions: A review. *Cold Regions Science and Technology*, 53(1): 16–41.

Van Veld, P.A., Vogelbein, W.K., Cochran, M.K., Goksøyr, A. & Stegeman, J.J. 1997. Route-specific cellular expression of cytochrome P4501A (CYP1A) in Fish (*Fundulus heteroclitus*) following exposure to aqueous and dietary benzo[a]pyrene. *Toxicology and Applied Pharmacology*, 142(2): 348–359.

VanRooij, J.G.M., Bodelier-Bade, M.M. & Jongeneelen, F.J. 1993. Estimation of individual dermal and respiratory uptake of polycyclic aromatic hydrocarbons in 12 coke oven workers. *British Journal of Industrial Medicine*, 50(7): 623–632.

Vymazal, J. 2009. The use constructed wetlands with horizontal sub-surface flow for various types of wastewater. *Ecological Engineering*, 35(1): 1–17.

Wakefield, J.C. 2007. Naphthalene - Toxicological overview. *Chemical Harzard and Poisons Division HQ, Health Protection Agency*: 1–9.

Wakx, A., Regazzetti, A., Dargère, D., Auzeil, N., Gil, S., Evain-Brion, D., Laprévote, O. & Rat, P. 2016. New *in vitro* biomarkers to detect toxicity in human placental cells: The example of benzo[a]pyrene. *Toxicology in Vitro*, 32: 76–85.

Walker, G.M. & Weatherley, L.R. 2001. Adsorption of dyes from aqueous solution — the effect of adsorbent pore size distribution and dye aggregation. *Chemical Engineering Journal*, 83(3): 201–206.

Wang, C., Wang, F., Wang, T., Bian, Y., Yang, X. & Jiang, X. 2010a. PAHs biodegradation potential of indigenous consortia from agricultural soil and contaminated soil in two-liquid-phase bioreactor (TLPB). *Journal of Hazardous Materials*, 176: 41–47.

Wang, J., Cao, J., Dong, Z., Guinot, B., Gao, M., Huang, R., Han, Y., Huang, Y., Ho, S.S.H. & Shen, Z. 2017a. Seasonal variation, spatial distribution and source apportionment for polycyclic aromatic hydrocarbons (PAHs) at nineteen communities in Xi'an, China: The effects of suburban scattered emissions in winter. *Environmental Pollution*, 231: 1330–1343.

Wang, J., Wang, H., Duan, C. & Guan, Y. 2010b. Micro-flame ionisation detector with a novel structure for portable gas chromatograph. *Talanta*, 82: 1022–1026.

Wang, J., Zhang, X., Ling, W., Liu, R., Liu, J., Kang, F. & Gao, Y. 2017b. Contamination and health risk assessment of PAHs in soils and crops in industrial areas of the Yangtze River Delta region, China. *Chemosphere*, 168: 976–987.

Wang, J.H. & Guo, C. 2010. Ultrasonication extraction and gel permeation chromatography clean-up for the determination of polycyclic aromatic hydrocarbons in edible oil by an isotope dilution gas chromatography-mass spectrometry. *Journal of Chromatography A*, 1217: 4732–4737.

Wang, X. & Qin, Y. 2005. Equilibrium sorption isotherms for of Cu^{2+} on rice bran. *Process Biochemistry*, 40(2): 677–680.

Wang, X., Zhao, L., Xu, H. & Zhang, X. 2018. Spatial and seasonal characteristics of dissolved heavy metals in the surface seawater of the Yellow River Estuary, China. *Marine Pollution Bulletin*, 137: 465–473.

Wang, Y., Tian, Z., Zhu, H., Cheng, Z., Kang, M., Luo, C., Li, J. & Zhang, G. 2012a. Polycyclic aromatic hydrocarbons (PAHs) in soils and vegetation near an e-waste recycling site in South China: Concentration, distribution, source, and risk assessment. *Science of the Total Environment*, 439: 187–193.

Wang, Y., Wei, X., Wang, S., Xie, R., Li, P., Liu, F. & Zong, Z. 2015a. A $FeCl_3$ -based ionic liquid for the oxidation of anthracene to anthraquinone. *Fuel Processing Technology*, 135: 157–161.

Wang, Y., Yang, B., Shu, J., Li, N., Zhang, P. & Sun, W. 2015b. Theoretical study on atmospheric reactions of fluoranthene and pyrene with $N_2O_5/NO_3/NO_2$. *Chemical Physics Letters*, 635: 146–151.

Wang, Y.Q., Tao, S., Jiao, X.C., Coveney, R.M., Wu, S.P. & Xing, B.S. 2008. Polycyclic aromatic hydrocarbons in leaf cuticles and inner tissues of six species of trees in urban Beijing. *Environmental Pollution*, 151: 158–164.

Wang, Z., Liu, Z., Yang, Y., Li, T. & Liu, M. 2012b. Distribution of PAHs in tissues of wetland plants and the surrounding sediments in the Chongming wetland, Shanghai, China. *Chemosphere*, 89(3): 221–227.

Wang, Z., Yang, C., Parrott, J.L., Frank, R.A., Yang, Z., Brown, C.E., Hollebone, B.P., Landriault, M., Fieldhouse, B., Liu, Y., Zhang, G. & Hewitt, L.M. 2014. Forensic source differentiation of petrogenic, pyrogenic, and biogenic hydrocarbons in Canadian oil sands environmental samples. *Journal of Hazardous Materials*, 271: 166–177.

Warmlander, S.K.T.S., Sholts, S.B., Erlandson, J.M., Gjerdrum, T. & Westerholm, R. 2011. Could the health decline of prehistoric California Indians be related to exposure to polycyclic aromatic hydrocarbons (PAHs) from natural bitumen ? *Environmental Health Perspectives*, 119(9): 1203–1207.

Weber, T.W. & Chakravorti, R.K. 1974. Pore and solid diffusion models for fixed-bed adsorbers. *American Institute of Chemical Engineers* (*AIChE) Journal*, 20(2): 228–238.

Weber, W.J. & Morris, J.C. 1963. Kinetics of adsorption on carbon from solution. *Journal of the Sanitary Engineering Division*, 89: 31–60.

Wei, M.-C. & Jen, J.-F. 2007. Determination of polycyclic aromatic hydrocarbons in aqueous samples by microwave assisted headspace solid-phase microextraction and gas chromatography/flame ionisation detection. *Talanta*, 72: 1269–1274.

Wen, C., Huang, X. & Qian, Y. 1999. Domestic wastewater treatment using an anaerobic bioreactor coupled with membrane filtration. *Process Biochemistry*, 35(3): 335–340.

White, J.E., Catallo, W.J. & Legendre, B.L. 2011. Biomass pyrolysis kinetics: A comparative critical review with relevant agricultural residue case studies. *Journal of Analytical and Applied Pyrolysis*, 91(1): 1–33.

WHO. 1998a. *Environmental Health Criteria 202: Selected Non-Heterocyclic Policyclic Aromatic Hydrocarbons*. Geneva, Switzerland.

WHO. 2006. *Guidelines for Drinking-water Quality: First addendum to Third Edition Volume 1*. Geneva, Switzerland.

WHO. 1998b. *Health Criteria and Other Supporting Information - Addendum*. Geneva.

Wiele, T. Van De, Vanhaecke, L., Boeckaert, C., Peru, K., Headley, J., Verstraete, W. & Siciliano, S. 2005. Human colon microbiota transform polycyclic aromatic hydrocarbons to estrogenic metabolites. *Environmental Geochemistry and Health*, 113(1): 6–10.

Wilcke, W., Amelung, W., Martius, C., Garcia, M.V.B. & Zech, W. 2000. Biological sources of polycyclic aromatic hydrocarbons (PAHs) in the Amazonian Rain Forest. *Journal of Plant Nutrition and Soil Science*, 163(1): 27–30.

Williams, P.T. & Reed, A.R. 2006. Development of activated carbon pore structure via physical and chemical activation of biomass fibre waste. *Biomass and Bioenergy*, 30(2): 144–152.

Williamson, K.S., Petty, J.D., Huckins, J.N., Lebo, J.A. & Kaiser, E.M. 2002. HPLC-PFD determination of priority pollutant PAHs in water, sediment, and semipermeable membrane devices. *Chemosphere*, 49: 703–715.

Wisniewski, C. & Grasmick, A. 1998. Floc size distribution in a membrane bioreactor and consequences for membrane fouling. *Colloids and Surfaces A: Physicochemical and Engineering Aspects*, 138(2): 403–411.

Wolf, M.A., Sfriso, A. & Moro, I. 2014. Thermal pollution and settlement of new tropical alien species: The case of *Grateloupia yinggehaiensis* (Rhodophyta) in the Venice Lagoon. *Estuarine, Coastal and Shelf Science*, 147: 11-16.

Wood, A.W., Levin, W., Thomas, P.E., Ryan, D., Karle, J.M., Yagi, H., Jerina, D.M. & Conney, A.H. 1978. Metabolic activation of dibenzo[a, h]anthracene and its dihydrodiols to bacterial mutagens. *Cancer Research*, 38(7): 1967–1973.

Wu, F.-C., Tseng, R.-L. & Juang, R.-S. 2009. Characteristics of Elovich equation used for the analysis of adsorption kinetics in dye-chitosan systems. *Chemical Engineering Journal*, 150(2–3): 366–373.

Wu, S. & Yu, W. 2012. Liquid-liquid extraction of polycyclic aromatic hydrocarbons in four different edible oils from China. *Food Chemistry*, 134: 597–601.

Wurts, W.A. & Durborow, R.M. 1992. Interactions of pH, carbon dioxide, alkalinity and hardness in fish ponds. Southern Regional Aquaculture Center (*SRAC) Publication*, (464): 1–4.

www.capetown.gov.za. 2017. City of Cape Town: Water Dashboard 24. www.capetown.gov.za 10 October 2017.

Xia, Y., Han, Y., Zhu, P., Wang, S., Gu, A., Wang, L., Lu, C., Fu, G., Song, L. & Wang, X. 2009. Relation between urinary metabolites of polycyclic aromatic hydrocarbons and human semen quality. *Environmental Science & Technology*, 43(12): 4567–4573.

Xiong, B., Zhang, Y., Hou, Y., Arp, H.P.H., Reid, B.J. & Cai, C. 2017. Enhanced biodegradation of PAHs in historically contaminated soil by *M. gilvum* inoculated biochar. *Chemosphere*, 182: 316–324.

Xiu, M., Pan, L. & Jin, Q. 2014. Bioaccumulation and oxidative damage in juvenile scallop *Chlamys farreri* exposed to benzo[a]pyrene , benzo[b]fluoranthene and chrysene. *Ecotoxicology and Environmental Safety*, 107: 103–110.

Xiu, M., Pan, L. & Jin, Q. 2016. Toxic effects upon exposure to polycyclic aromatic hydrocarbon (chrysene) in scallop *Chlamys farreri* during the reproduction period. *Environmental Toxicology and Pharmacology*, 44: 75–83.

Yamada, M., Takada, H., Toyoda, K., Yoshida, A., Shibata, A., Nomura, H., Wada, M., Nishimura, M., Okamoto, K. & Ohwada, K. 2003. Study on the fate of petroleum-derived polycyclic aromatic hydrocarbons (PAHs) and the effect of chemical dispersant using an enclosed ecosystem, mesocosm. *Marine Pollution Bulletin*, 47(1): 105–113.

Yan, B., Abrajano, T.A., Bopp, R.F., Benedict, L.A., Chaky, D.A., Perry, E., Song, J. & Keane, D.P. 2006. Combined application of $\delta^{13}C$ and molecular ratios in sediment cores for PAH source apportionment in the New York/New Jersey harbor complex. *Organic Geochemistry*, 37(6): 674–687.

Yang, B., Liu, S., Liu, Y., Li, X., Lin, X., Liu, M. & Liu, X. 2017. PAHs uptake and translocation in

Cinnamomum camphora leaves from Shanghai, China. *Science of the Total Environment*, 574: 358–368.

Yang, Y. & Hildebrand, F. 2006. Phenanthrene degradation in subcritical water. *Analytica Chimica Acta*, 555(2): 364–369..

Yao, C., Foster, W.G., Sadeu, J.C., Siddique, S., Zhu, J. & Feng, Y.-L. 2016. Screening for DNA adducts in ovarian follicles exposed to benzo[a]pyrene and cigarette smoke condensate using liquid chromatography-tandem mass spectrometry. *Science of The Total Environment*, 575: 742-749.

Yao, J.M., Sánchez-Pérez, J.M., Sauvage, S., Teissier, S., Attard, E., Lauga, B., Durant, R., Julien, F., Bernard-Jannin, L., Ramburn, H. & Gerino, M. 2017. Biodiversity, ecosystem purification function and service in an alluvial wetland. *Ecological Engineering*, 103: 359–371.

Ye, M., Sun, M.M., Xie, S.N., Liu, K., Feng, Y.F., Zhao, Y., Wan, J.Z., Hu, F., Li, H.X., Zong, L.G. & Jiang, X. 2017. Feasibility of tea saponin-enhanced soil washing in a soybean oil-water solvent system to extract PAHs/Cd/Ni efficiently from a coking plant site. *Pedosphere*, 27: 452–464.

Ye, Q., Zhuang, H. & Zhou, C. 2009. Detection of naphthalene by real-time immuno-PCR using molecular beacon. *Molecular and Cellular Probes*, 23(1): 29–34.

Ye, Q., Zhuang, H., Zhou, C. & Wang, Q. 2010. Real-time fluorescent quantitative immuno-PCR method for determination of fluoranthene in water samples with a molecular beacon. *Journal of Environmental Sciences*, 22(5): 796–800.

Yin, H., Tan, Q., Chen, Y., Lv, G. & Hou, X. 2011. Polycyclic aromatic hydrocarbons (PAHs) pollution recorded in annual rings of gingko *(Gingko biloba* L.): Determination of PAHs by GC/MS after accelerated solvent extraction. *Microchemical Journal*, 97(2): 138–143.

Yu, X.Z., Wu, S.C., Wu, F.Y. & Wong, M.H. 2011. Enhanced dissipation of PAHs from soil using mycorrhizal ryegrass and PAH-degrading bacteria. *Journal of Hazardous Materials*, 186: 1206–1217.

Yunker, M.B., Macdonald, R.W., Vingarzan, R., Mitchell, R.H., Goyette, D. & Sylvestre, S. 2002. PAHs in the Fraser River basin: A critical appraisal of PAH ratios as indicators of PAH source and composition. *Organic Geochemistry*, 33(4): 489–515.

Yunker, M.B., Perreault, A. & Lowe, C.J. 2012. Source apportionment of elevated PAH concentrations in sediments near deep marine outfalls in Esquimalt and Victoria, BC, Canada: Is coal from an 1891 shipwreck the source? *Organic Geochemistry*, 46: 12–37.

Zakeri-Milani, P., Barzegar-Jalali, M., Tajerzadeh, H., Azarmi, Y. & Valizadeh, H. 2005. Simultaneous determination of naproxen, ketoprofen and phenol red in samples from rat intestinal permeability studies: HPLC method development and validation. *Journal of Pharmaceutical and Biomedical Analysis*, 39(3): 624–630.

Zezulka, Š., Kummerová, M., Babula, P. & Váňová, L. 2013. Lemna minor exposed to fluoranthene: Growth, biochemical, physiological and histochemical changes. *Aquatic Toxicology*, 140: 37–47.

Zhang, F., Zhang, R., Guan, M., Shu, Y., Shen, L., Chen, X. & Li, T. 2016. Polycyclic aromatic hydrocarbons (PAHs) and Pb isotopic ratios in a sediment core from Shilianghe Reservoir , Eastern China : Implying pollution sources. *Applied Geochemistry*, 66: 140–148.

Zhang, P., Wang, Y., Bo, Y., Liu, C. & Shu, J. 2014. Heterogeneous reactions of particulate benzo[b]fluoranthene and benzo[k]fluoranthene with NO_3 radicals. *Chemos*, 99: 34–40.

Zhang, W., Zhang, S., Wan, C., Yue, D., Ye, Y. & Wang, X. 2008a. Source diagnostics of polycyclic aromatic hydrocarbons in urban road runoff, dust, rain and canopy throughfall. *Environmental pollution*, 153: 594–601.

Zhang, Y., Baoshan, C., Qijun, Z. & Xinhui, L. 2015. Polycyclic aromatic hydrocarbons in the food web of coastal wetlands: Distribution, sources and potential toxicity. *Clean - Soil, Air, Water*, 43(6): 881–891.

Zhang, Y., Wang, C., Huang, L., Chen, R., Chen, Y. & Zuo, Z. 2012. Low-level pyrene exposure causes cardiac toxicity in zebrafish (*Danio rerio*) embryos. *Aquatic Toxicology*, 114–115: 119–124.

Zhang, Z.L, Hong, H.S., Zhou, J.L. & Yu, G. 2004a. Phase association of polycyclic aromatic hydrocarbons in the Minjiang River Estuary, China. *Science of the Total Environment*, 323(1–3): 71–86.

Zhang, Z., Huang, J., Yu, G. & Hong, H. 2004b. Occurrence of PAHs, PCBs and organochlorine pesticides in the Tonghui River of Beijing, China. *Environmental pollution*, 130: 249–261.

Zhang, Z., Rengel, Z. & Meney, K. 2008b. Interactive effects of nitrogen and phosphorus loadings on nutrient removal from simulated wastewater using *Schoenoplectus validus* in wetland microcosms. *Chemosphere*, 72(11): 1823–1828.

Zhang, Z., Rengel, Z. & Meney, K. 2010. Polynuclear aromatic hydrocarbons (PAHs) differentially influence growth of various emergent wetland species. *Journal of Hazardous Materials*, 182: 689–695.

Zhao, N., Zhang, Q. & Wenxing, W. 2016. Atmospheric oxidation of phenanthrene initiated by OH radicals in the presence of O_2 and NO_x — A theoretical study. *Science of the Total Environment*, 563-564: 1008-1015.

Zhao, Y., Chen, X., Liu, X., Ding, Y., Gao, R., Qiu, Y., Wang, Y. & He, J. 2014a. Exposure of mice to benzo[a]pyrene impairs endometrial receptivity and reduces the number of implantation sites during early pregnancy. *Food and Chemical Toxicology*, 69: 244–251.

Zhao, Z., Zhang, L., Cai, Y. & Chen, Y. 2014b. Distribution of polycyclic aromatic hydrocarbon (PAH) residues in several tissues of edible fishes from the largest freshwater lake in China, Poyang Lake, and associated human health risk assessment. *Ecotoxicology and Environmental Safety*, 104: 323–331.

Zhou, J., Hong, H., Zhang, Z., Maskaoui, K. & Chen, W. 2000. Multi-phase distribution of organic micropollutants in Xiamen Harbour, China. *Water Research*, 34(7): 2132–2150.

APPENDICES

Appendix A: Calibration plots for the 16 US EPA priority PAHs

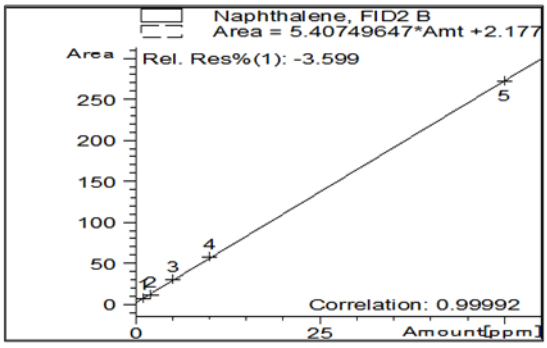

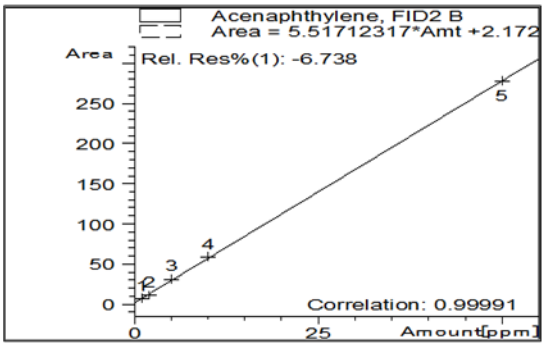

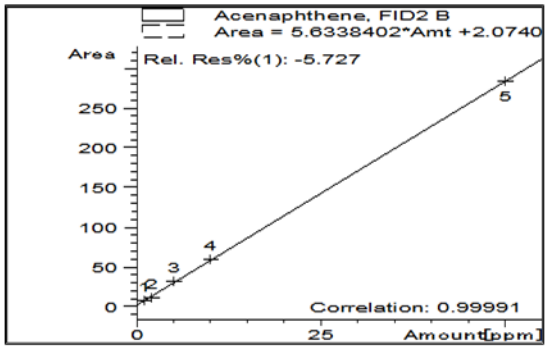

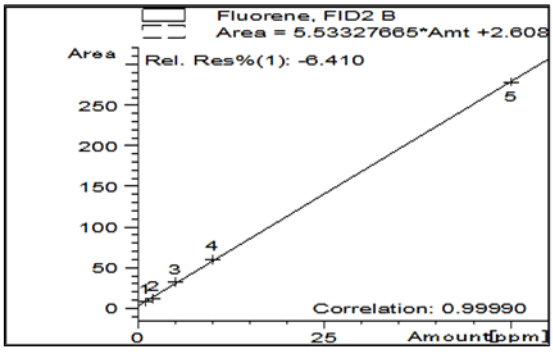

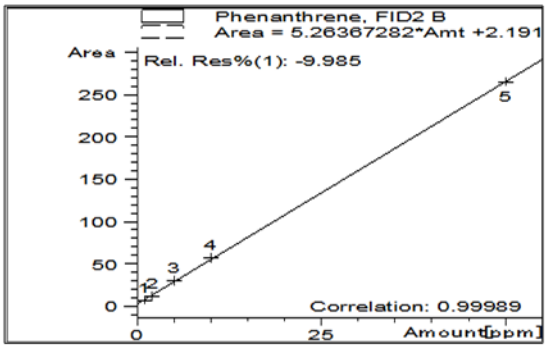

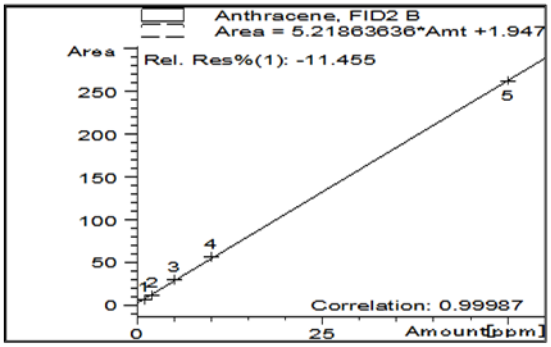

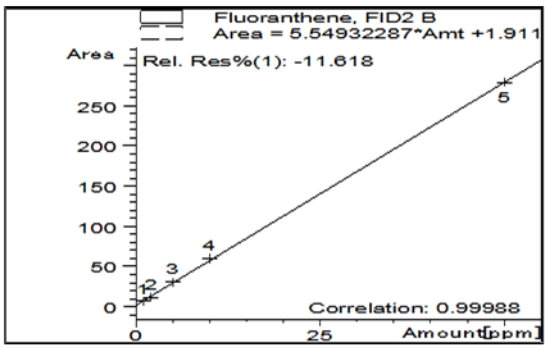

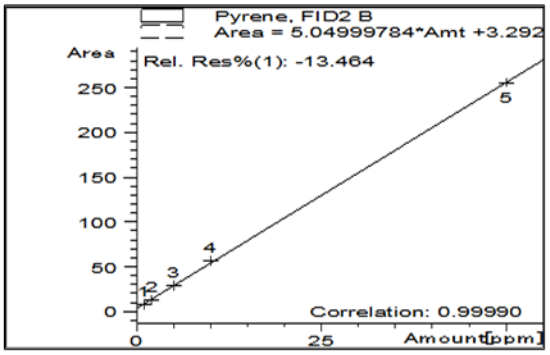

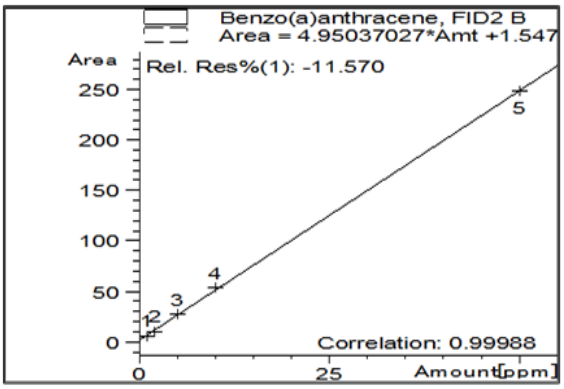
Benzo(a)anthracene, FID2 B
Area = 4.95037027*Amt +1.547
Area
Rel. Res%(1): -11.570
Correlation: 0.99988
Amount[ppm]

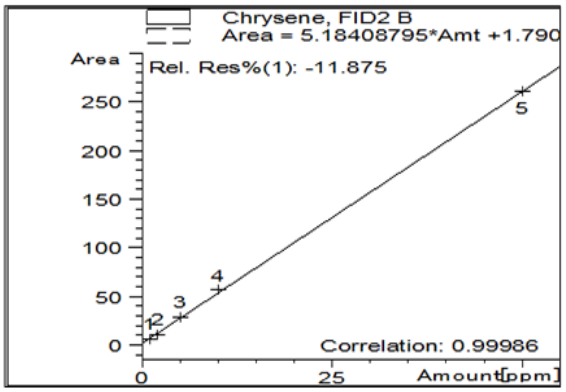
Chrysene, FID2 B
Area = 5.18408795*Amt +1.790
Area
Rel. Res%(1): -11.875
Correlation: 0.99986
Amount[ppm]

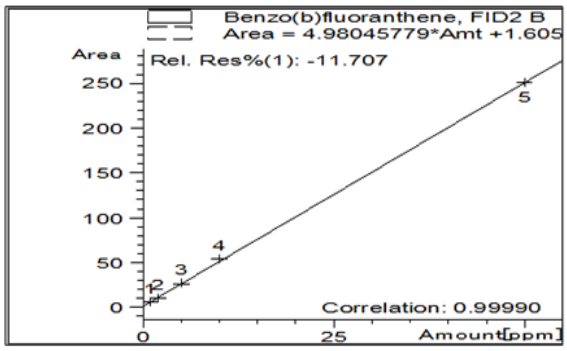
Benzo(b)fluoranthene, FID2 B
Area = 4.98045779*Amt +1.605
Area
Rel. Res%(1): -11.707
Correlation: 0.99990
Amount[ppm]

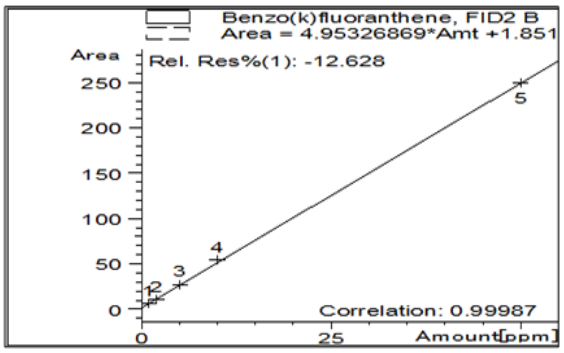
Benzo(k)fluoranthene, FID2 B
Area = 4.95326869*Amt +1.851
Area
Rel. Res%(1): -12.628
Correlation: 0.99987
Amount[ppm]

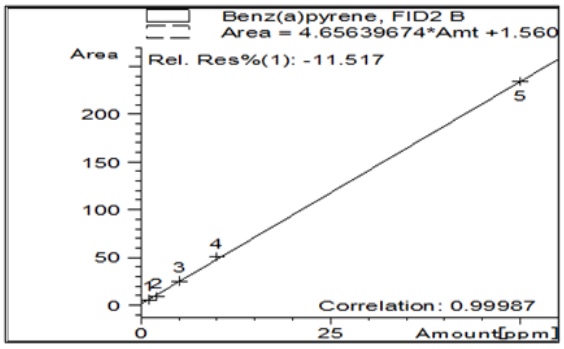
Benz(a)pyrene, FID2 B
Area = 4.65639674*Amt +1.560
Area
Rel. Res%(1): -11.517
Correlation: 0.99987
Amount[ppm]

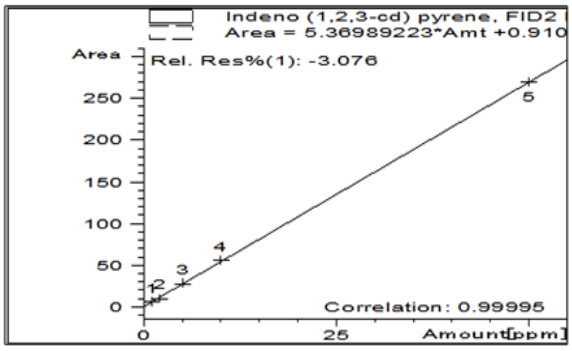
Indeno (1,2,3-cd) pyrene, FID2
Area = 5.36989223*Amt +0.910
Area
Rel. Res%(1): -3.076
Correlation: 0.99995
Amount[ppm]

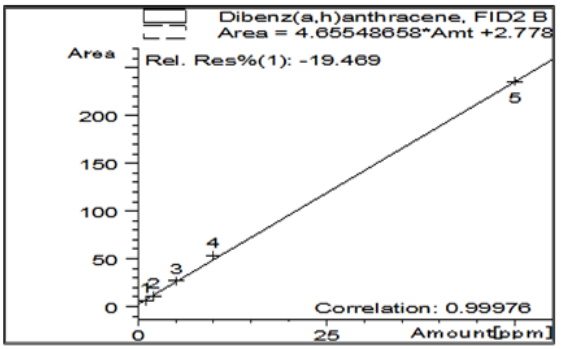
Dibenz(a,h)anthracene, FID2 B
Area = 4.65548658*Amt +2.778
Area
Rel. Res%(1): -19.469
Correlation: 0.99976
Amount[ppm]

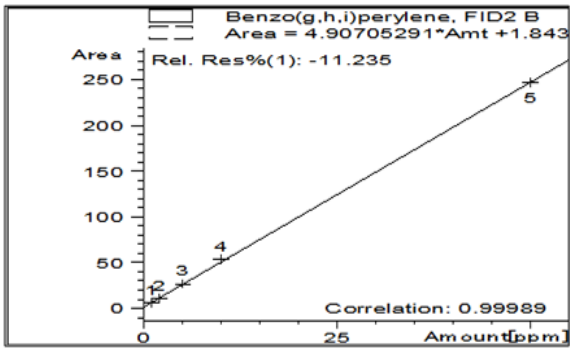
Benzo(g,h,i)perylene, FID2 B
Area = 4.90705291*Amt +1.843
Area
Rel. Res%(1): -11.235
Correlation: 0.99989
Amount[ppm]

Appendix B: Pictures from sampling sites

A: Sampling site PA, with sign of eutrophication
B: Dumping site close to sampling point PB
C: Industrial drain into sampling point PC
D: Site PD
E: Pile of used plastics at site PD
F: Site DA showing sign of eutrophication
G: Refinery close to site DB
H: Drain into site DB
I: Recreation activity around site DC

Appendix C1: Seasonal occurrence (average ±SD) of PAHs in the Diep River water samples (sites DA and DB)

PAHs (µg/L)	Site DA				Site DB			
	Summer (Dec to Feb)	Autumn (Mar to May)	Winter (June to Aug)	Spring (Sept to Nov)	Summer (Dec to Feb)	Autumn (Mar to May)	Winter (June to Aug)	Spring (Sept to Nov)
Nap	10.14 ± 3.65	nd	nd	3.11 ± 1.49	14.28 ± 2.51	nd	0.91 ± 1.08	6.17 ± 4.80
Acy	0.82 ± 0.74	2.22 ± 1.35	2.91 ± 0.68	2.45 ± 1.48	8.97 ± 3.95	11.44 ± 2.11	0.43 ± 0.16	2.49 ± 2.05
Can	0.95 ± 0.21	0.86 ± 0.30	1.58 ± 0.91	0.64 ± 0.60	4.22 ± 3.82	6.88 ± 2.02	8.68 ± 7.36	0.60 ± 0.14
Flu	2.07 ± 1.97	4.34 ± 0.72	1.28 ± 1.35	3.57 ± 1.71	10.43 ± 6.75	10.34 ±3.58	1.72 ± 2.30	1.57 ± 0.88
Phe	3.16 ± 2.87	5.46 ± 1.02	2.07 ± 1.19	6.45 ± 0.88	31.04 ± 13.89	37.93 ± 1.99	8.31 ± 11.33	1.38 ± 0.73
Ant	2.90 ± 1.51	3.54 ± 0.46	1.44 ± 0.12	3.63 ± 2.86	23.00 ± 10.26	19.79 ± 15.82	1.25 ± 0.40	1.44 ± 1.38
Flt	6.61 ± 0.18	nd	1.30 ± 1.61	3.83 ± 1.22	6.95 ± 2.16	7.30 ± 2.73	10.28 ± 3.00	3.13 ± 1.59
Pyr	0.52 ± 0.48	0.23 ± 0.20	5.76 ± 9.97	0.49 ± 0.85	5.44 ± 4.44	nd	0.12 ± 0.20	5.89 ± 7.73
BaA	6.57 ± 1.89	8.62 ± 1.92	16.60 ± 5.65	24.57 ± 14.06	46.73 ± 19.02	34.99 ± 21.57	18.03 ± 16.85	8.88 ± 8.56
Chy	19.58 ± 3.56	11.16 ± 1.73	17.19 ± 2.44	25.54 ± 17.92	72.38 ± 9.58	42.58 ± 27.06	18.54 ± 6.14	3.55 ± 1.75
BbF	Nd	nd	nd	nd	nd	nd	15.47 ± 17.17	1.14 ± 1.23
BkF	1.55 ± 0.27	nd	nd	2.78 ± 1.20	6.16 ± 2.00	nd	Nd	2.73 ± 2.38
BaP	1.29 ± 0.21	1.06 ± 0.92	1.14 ± 1.09	1.98 ± 0.37	5.34 ± 3.77	nd	Nd	2.74 ± 1.14
IcP	4.69 ± 1.26	4.17 ± 3.71	4.87 ± 3.56	15.67 ± 19.02	37.98 ± 12.81	17.30 ± 9.05	11.24 ± 2.90	3.04 ± 3.33
DBA	6.75 ± 1.40	4.45 ± 1.27	10.47 ± 3.52	7.55 ± 2.36	19.71 ± 12.27	17.58 ± 3.52	6.48 ± 3.16	2.35 ± 1.26
BgP	1.65 ± 0.30	1.87 ± 0.44	3.87 ± 0.81	5.66 ± 4.58	17.91 ± 16.29	8.80 ± 3.78	2.59 ± 0.55	1.27 ± 0.19
∑16 PAHs	69.25 ± 4.98	47.97 ± 3.30	70.48 ± 5.56	107.92 ± 8.05	310.52 ± 19.31	214.94 ± 14.15	104.05 ± 6.64	48.35 ± 2.21
% C PAHs	58.38	61.41	71.32	72.36	60.64	52.32	67.05	50.52

Site DA: Nature reserve (upstream). Site DB: Theo Marais Sports Club – industrial and residential area. nd: not detected. C PAHs: Carcinogenic PAHs (BaA, Chy, BbF, BkF, BaP IcP and DBA).

Appendix C2: Seasonal occurrence (average ±SD) of PAHs in the Diep River water samples (site DC)

PAHs (µg/L)	Site DC			
	Summer (Dec to Feb)	Autumn (Mar to May)	Winter (June to Aug)	Spring (Sept to Nov)
Nap	4.95 ± 4.96	11.12 ± 8.78	nd	2.49 ± 1.11
Acy	0.89 ± 1.30	7.86 ± 2.24	2.65 ± 2.05	2.95 ± 1.50
Can	0.79 ± 1.37	0.57 ± 0.42	2.58 ± 2.87	0.88 ± 0.29
Flu	0.65 ± 0.67	3.38 ± 3.00	nd	0.16 ± 0.27
Phe	8.97 ± 1.82	9.52 ± 4.31	0.71 ± 0.27	1.25 ± 1.37
Ant	7.36 ± 2.27	1.78 ± 0.59	3.94 ± 1.14	1.52 ± 0.77
Flt	6.93 ± 1.85	24.36 ± 11.66	0.90 ± 0.86	8.73 ± 7.47
Pyr	nd	5.39 ± 2.08	9.00 ± 3.58	0.37 ± 0.20
BaA	30.56 ± 48.89	7.86 ± 3.18	19.01 ± 12.55	12.36 ± 9.50
Chy	41.96 ± 39.96	5.36 ± 3.12	15.87 ± 6.38	7.87 ± 9.08
BbF	1.82 ± 1.13	nd	nd	nd
BkF	2.85 ± 1.91	nd	1.85 ± 3.20	1.48 ± 1.31
BaP	nd	nd	1.93 ± 0.55	1.92 ± 1.58
IcP	11.21 ± 8.45	4.11 ± 2.09	6.29 ± 2.49	3.40 ± 1.85
DBA	23.65 ± 12.71	19.28 ± 20.65	4.67 ± 2.78	3.83 ± 4.77
BgP	29.16 ± 11.78	1.44 ± 1.91	4.61 ± 2.85	2.26 ± 0.69
∑16 PAHs	171.75 ± 13.18	102.03 ± 7.04	73.99 ± 5.61	51.47 ± 3.49
% C PAHs	65.24	35.88	67.06	59.96

Site DC: Woodbridge (downstream). nd: not detected. C PAHs: Carcinogenic PAHs.

Appendix D: ANOVA statistical analysis (multivariate tests) of data from the Diep River water samples

Multivariate Tests[b]

Effect		Value	F	Hypothesis df	Error df	Sig.
Sites	Pillai's Trace	.679	14.787[a]	2.000	14.000	.000
	Wilks' Lambda	.321	14.787[a]	2.000	14.000	.000
	Hotelling's Trace	2.112	14.787[a]	2.000	14.000	.000
	Roy's Largest Root	2.112	14.787[a]	2.000	14.000	.000
Seasons	Pillai's Trace	.496	4.268[a]	3.000	13.000	.026
	Wilks' Lambda	.504	4.268[a]	3.000	13.000	.026
	Hotelling's Trace	.985	4.268[a]	3.000	13.000	.026
	Roy's Largest Root	.985	4.268[a]	3.000	13.000	.026
Sites * Seasons	Pillai's Trace	.591	2.413[a]	6.000	10.000	.105
	Wilks' Lambda	.409	2.413[a]	6.000	10.000	.105
	Hotelling's Trace	1.448	2.413[a]	6.000	10.000	.105
	Roy's Largest Root	1.448	2.413[a]	6.000	10.000	.105

a. Exact statistic

b. Design: Intercept
Within Subjects Design: Sites + Seasons + Sites * Seasons

Appendix E1: Seasonal occurrence (average ±SD) of PAHs in the Plankenburg River water samples (sites PA and PB)

PAHs (µg/L)	Site PA				Site PB			
	Summer (Dec to Feb)	Autumn (Mar to May)	Winter (June to Aug)	Spring (Sept to Nov)	Summer (Dec to Feb)	Autumn (Mar to May)	Winter (June to Aug)	Spring (Sept to Nov)
Nap	4.07 ± 2.99	nd	0.58 ± 0.52	2.83 ± 2.52	4.12 ± 2.58	0.79 ± 1.14	3.42 ± 2.38	3.55 ± 2.14
Acy	5.97 ± 4.37	5.57 ± 5.07	0.39 ± 0.67	1.04 ± 1.52	10.97 ± 5.45	0.91 ± 1.14	0.89 ± 1.54	2.48 ± 1.49
Can	0.98 ± 0.97	2.92 ± 2.66	0.63 ± 1.08	0.96 ± 1.04	2.43 ± 3.17	4.26 ± 2.75	1.46 ± 0.55	1.42 ± 0.67
Flu	8.10 ± 1.99	8.86 ± 5.07	nd	nd	9.16 ± 5.69	11.98 ± 5.52	1.20 ± 0.53	7.00 ± 3.73
Phe	16.79 ± 1.99	9.51 ± 6.40	2.11 ± 2.96	1.58 ± 1.48	26.05 ± 10.97	26.05 ± 10.96	1.73 ± 1.32	14.22 ± 9.17
Ant	7.36 ± 5.78	5.57 ± 6.88	1.60 ± 0.55	1.41 ± 0.82	19.75 ± 24.18	20.00 ± 23.88	3.31 ± 1.55	4.31 ± 5.38
Flt	5.34 ± 4.35	2.09 ± 6.88	1.01 ± 1.11	3.55 ± 0.44	12.95 ± 9.42	12.95 ± 4.54	3.10 ± 3.76	4.17 ± 3.06
Pyr	nd	5.66 ± 4.24	5.93 ± 3.64	nd	4.15 ± 2.16	4.15 ± 2.90	10.05 ± 8.43	nd
BaA	36.47 ± 25.89	14.75 ± 9.66	25.43 ± 24.44	20.33 ± 23.96	20.66 ± 13.28	18.50 ± 10.03	18.85 ± 4.43	28.98 ± 5.02
Chy	57.90 ± 19.33	25.35 ± 14.70	19.74 ± 23.54	15.65 ± 18.31	13.21 ± 14.51	11.80 ± 8.90	23.60 ± 11.66	36.30 ± 31.84
BbF	nd	nd	21.78 ± 5.67	1.70 ± 2.15	nd	nd	31.93 ± 29.50	1.43 ± 0.59
BkF	nd	nd	nd	2.84 ± 2.34	0.54 ± 0.93	1.75 ± 3.02	1.87 ± 1.47	2.99 ± 2.86
BaP	6.37 ± 2.92	nd	1.76 ± 0.35	1.89 ± 1.79	nd	nd	2.23 ± 0.40	nd
IcP	26.65 ± 6.79	6.47 ± 5.24	15.75 ± 4.25	15.34 ± 2.89	23.61 ± 23.44	6.15 ± 5.55	10.97 ± 5.35	41.43 ± 8.91
DBA	11.94 ± 5.60	11.14 ± 6.67	1.74 ± 0.68	2.35 ± 1.57	26.14 ± 31.39	16.42 ± 10.00	3.24 ± 1.94	4.49 ± 2.44
BgP	9.90 ± 9.34	3.10 ± 2.31	2.96 ± 1.93	4.57 ± 4.16	2.98 ± 1.93	3.022 ± 1.87	3.52 ± 1.85	8.4 ± 2.17
∑16 PAHs	197.83 ± 15.73	100.97± 22.38	101.42 ± 8.85	76.04 ± 6.33	176.71 ± 9.59	138.73 ± 8.27	121.37 ± 9.32	161.21 ± 13.32
% C PAHs	70.43	57.16	85.00	79.04	47.63	39.36	76.37	71.72

Site PA: Agricultural and residential areas. Site PB: Informal settlement of Kayamandi. nd: not detected. C PAHs: Carcinogenic PAHs.

Appendix E2: Seasonal occurrence (average ±SD) of PAHs in the Plankenburg River water samples (sites PC and PD)

PAHs (µg/L)	Site PC				Site PD			
	Summer (Dec to Feb)	Autumn (Mar to May)	Winter (June to Aug)	Spring (Sept to Nov)	Summer (Dec to Feb)	Autumn (Mar to May)	Winter (June to Aug)	Spring (Sept to Nov)
Nap	5.64 ± 0.32	nd	0.86 ± 0.52	4.29 ± 1.72	6.02± 2.99	nd	2.37 ± 2.09	2.95 ± 1.78
Acy	4.18 ± 4.59	4.44 ± 4.55	3.95 ± 2.21	1.08 ± 1.21	0.59 ± 0.18	1.55 ± 0.78	1.33 ± 2.09	1.61 ± 1.39
Can	1.51 ± 0.81	2.85 ± 1.99	1.88 ± 1.39	1.52 ± 0.46	0.52 ± 0.13	nd	1.21 ± 1.07	1.07 ± 1.26
Flu	8.02 ± 2.30	6.27 ± 0.69	4.07 ± 4.18	7.00 ± 2.46	10.43 ± 2.32	10.43 ± 3.31	0.78 ± 1.08	0.93 ± 0.50
Phe	10.26 ± 3.19	14.44 ± 2.61	5.89 ± 2.80	14.22 ± 3.52	27.02 ± 7.88	19.42 ± 7.92	1.68 ± 1.44	0.68 ± 0.84
Ant	7.26 ± 5.09	8.25 ± 2.19	5.87 ± 3.20	5.50 ± 2.51	14.62 ± 4.84	9.61 ± 4.24	2.68 ± 0.93	1.94 ± 1.78
Flt	4.15 ± 2.72	4.13 ± 1.93	3.60 ± 0.41	4.17 ± 1.20	7.96± 1.53	7.96 ± 1.60	nd	1.50 ± 1.30
Pyr	2.13 ± 2.22	1.69 ± 0.73	4.07 ± 4.16	nd	2.03 ± 1.17	1.45 ± 1.48	3.91 ± 1.16	0.91 ± 0.81
BaA	49.24 ± 29.30	13.33 ± 7.68	19.39 ± 4.71	67.50 ± 18.05	20.68 ± 5.40	16.15 ± 4.73	9.98 ± 2.75	48.25 ± 12.57
Chy	52.57 ± 19.25	20.51 ± 13.71	30.87 ± 5.12	59.55 ± 12.20	45.70 ± 9.95	23.51 ± 5.72	12.65 ± 5.22	32.40 ± 8.50
BbF	5.00 ± 3.85	5.85 ± 2.97	15.94 ± 3.07	18.05 ± 13.26	4.01 ± 1.85	2.47 ± 0.78	2.37 ± 0.85	4.26 ± 2.97
BkF	5.32 ± 3.51	5.30 ± 3.25	11.14 ± 1.64	22.92 ± 18.16	3.93 ± 1.00	2.49 ± 1.34	1.97 ± 1.07	6.63 ± 2.76
BaP	4.13 ± 2.04	nd	1.45 ± 1.33	3.87 ± 2.85	1.68 ± 0.56	nd	1.04 ± 0.72	3.52 ± 2.46
IcP	34.03 ± 10.59	4.25 ± 2.17	12.28 ± 6.45	36.91 ± 9.23	4.19 ± 3.43	6.11 ± 2.00	3.03 ± 1.77	23.51 ± 5.48
DBA	8.65 ± 5.17	12.45 ± 6.11	9.97 ± 1.20	5.33 ± 0.97	16.76 ± 6.06	7.64 ± 2.48	8.44 ± 4.60	4.28 ± 1.57
BgP	12.18 ± 11.48	2.67 ± 1.23	6.75 ± 6.43	37.86 ± 9.68	3.65 ± 2.41	2.63 ± 1.23	2.73 ± 0.90	6.51 ± 0.97
∑16 PAHs	214.27 ± 16.46	106.45 ± 5.75	137.96 ± 7.96	289.77 ± 21.39	169.77 ± 12.16	111.43 ± 7.30	56.15 ± 3.61	140.94 ± 13.77
% C PAHs	74.18	57.96	73.24	73.90	57.11	52.39	70.30	87.17

Site PC: Substation in industrial area. Site PD: Industrial area at Adam Tas bridge. nd: Not detected. C PAHs: Carcinogenic PAHs.

Appendix F: ANOVA statistical analysis (multivariate tests) of data from the Plankenburg River water samples

Multivariate Tests[b]

Effect		Value	F	Hypothesis df	Error df	Sig.
Sites	Pillai's Trace	.680	9.223[a]	3.000	13.000	.002
	Wilks' Lambda	.320	9.223[a]	3.000	13.000	.002
	Hotelling's Trace	2.128	9.223[a]	3.000	13.000	.002
	Roy's Largest Root	2.128	9.223[a]	3.000	13.000	.002
Seasons	Pillai's Trace	.387	2.733[a]	3.000	13.000	.086
	Wilks' Lambda	.613	2.733[a]	3.000	13.000	.086
	Hotelling's Trace	.631	2.733[a]	3.000	13.000	.086
	Roy's Largest Root	.631	2.733[a]	3.000	13.000	.086
Sites * Seasons	Pillai's Trace	.690	1.727[a]	9.000	7.000	.242
	Wilks' Lambda	.310	1.727[a]	9.000	7.000	.242
	Hotelling's Trace	2.221	1.727[a]	9.000	7.000	.242
	Roy's Largest Root	2.221	1.727[a]	9.000	7.000	.242

a. Exact statistic

b. Design: Intercept
Within Subjects Design: Sites + Seasons + Sites * Seasons

Appendix G1: Seasonal occurrence (average ±SD) of PAHs in the Diep River sediment samples (sites DA and DB)

PAHs (µg/g)	Site DA				Site DB			
	Summer (Dec to Feb)	Autumn (Mar to May)	Winter (June to Aug)	Spring (Sept to Nov)	Summer (Dec to Feb)	Autumn (Mar to May)	Winter (June to Aug)	Spring (Sept to Nov)
Nap	1.809 ± 0.171	0.631 ± 0.367	0.034 ± 0.031	0.960 ± 0.816	2.148 ± 0.150	nd	nd	1.802 ± 1.057
Acy	0.047 ± 0.022	nd	0.040 ± 0.032	0.284 ± 0.333	0.338 ± 0.265	0.364 ± 0.200	nd	0.439 ± 0.548
Can	0.056 ± 0.034	0.080 ± 0.075	0.079 ± 0.008	0.187 ± 0.030	0.044 ± 0.044	1.915 ± 1.237	0.483 ± 0.422	0.635 ± 0.369
Flu	nd	0.243 ± 0.138	0.027 ± 0.023	0.058 ± 0.067	0.009 ± 0.016	0.632 ± 0.257	1.839 ± 1.374	0.220 ± 0.164
Phe	0.033 ± 0.007	nd	0.061 ± 0.012	1.103 ± 1.407	0.036 ± 0.031	15.005±3.223	13.029±2.749	0.197 ± 0.253
Ant	0.084 ± 0.022	nd	0.115 ± 0.061	0.204 ± 0.090	0.078 ± 0.068	3.013 ± 1.036	0.051 ± 0.045	0.097 ± 0.050
Flt	0.059 ± 0.015	0.666 ± 0.629	0.527 ± 0.234	0.624 ± 0.380	6.445 ±10.658	3.831 ± 2.015	0.221 ± 0.205	2.948 ± 2.089
Pyr	0.006 ± 0.010	0.197 ± 0.111	0.041 ± 0.016	0.157 ± 0.102	0.555 ± 0.907	1.364 ± 0.340	2.356 ± 1.641	0.294 ± 0.127
BaA	0.267 ± 0.033	0.687 ± 0.294	0.305 ± 0.174	0.289 ± 0.225	0.878 ± 1.049	2.555 ± 1.923	2.302 ± 2.298	0.788 ± 0.262
Chy	0.080 ± 0.072	1.528 ± 1.522	0.243 ± 0.168	0.714 ± 1.024	1.924 ± 1.049	2.100 ± 0.778	2.938 ± 0.544	1.207 ± 1.035
BbF	nd	1.188 ± 0.192	0.176 ± 0.138	0.148 ± 0.089	2.897 ± 4.400	16.652±2.626	5.065 ± 2.573	0.809 ± 0.678
BkF	0.144 ± 0.069	2.256 ± 1.387	0.334 ± 0.107	0.495 ± 0.664	3.461 ± 5.071	12.276±6.287	5.092 ± 4.045	1.237 ± 1.026
BaP	0.124 ± 0.017	1.299 ± 0.448	0.238 ± 0.032	0.304 ± 0.257	0.133 ± 0.230	5.789 ± 2.239	6.541 ± 2.876	0.515 ± 0.537
IcP	0.070 ± 0.065	0.895 ± 0.357	0.205 ± 0.032	0.665 ± 0.992	2.331 ± 2.299	2.393 ± 1.864	1.654 ± 1.348	0.295 ± 0.204
DBA	0.065 ± 0.071	0.959 ± 0.596	0.180 ± 0.052	0.371 ± 0.402	1.898 ± 1.394	1.217 ± 0.596	3.322 ± 2.715	0.354 ± 0.302
BgP	0.136 ± 0.151	0.750 ± 0.537	0.263 ± 0.041	0.407 ± 0.333	nd	1.601 ± 1.431	2.020 ± 0.989	0.209 ± 0.090
∑16 PAHs	2.980 ± 0.438	11.379 ± 0.639	2.867 ± 0.138	6.968 ± 0.303	23.175 ±1.768	70.706±5.321	46.914±3.342	12.046±0.750
% C PAHs	25.16	77.44	58.62	42.84	58.35	60.79	57.37	43.20

Site DA: Nature reserve (upstream). Site DB: Theo Marais Sports Club – industrial and residential area. nd: not detected. C PAHs: Carcinogenic PAHs.

Appendix G2: Seasonal occurrence (average ±SD) of PAHs in the Diep River sediment samples (site DC)

PAHs (µg/g)	Site DC			
	Summer (Dec to Feb)	Autumn (Mar to May)	Winter (June to Aug)	Spring (Sept to Nov)
Nap	1.633 ± 0.547	0.276 ± 0.827	0.674 ± 0.629	0.853 ± 0.456
Acy	0.098 ± 0.169	0.230 ± 0.128	0.121 ± 0.096	nd
Can	0.342 ± 0.521	0.244 ± 0.305	0.046 ± 0.079	0.161 ± 0.081
Flu	0.128 ± 0.116	0.015 ± 0.074	0.050 ± 0.087	0.115 ± 0.067
Phe	1.285 ± 1.128	0.080 ± 0.742	0.119 ± 0.106	0.060 ± 0.015
Ant	0.089 ± 0.077	0.122 ± 0.052	0.056 ± 0.025	0.136 ± 0.033
Flt	0.200 ± 0.204	1.169 ± 0.989	0.547 ± 0.491	1.586 ± 1.955
Pyr	0.002 ± 0.004	0.085 ± 0.068	0.063 ± 0.055	0.052 ± 0.057
BaA	0.507 ± 0.613	0.538 ± 0.515	0.308 ± 0.073	0.627 ± 0.600
Chy	0.213 ± 0.219	0.483 ± 0.308	0.221 ± 0.127	0.778 ± 1.149
BbF	1.560 ± 1.698	1.023 ± 0.248	0.646 ± 0.303	0.304 ± 0.156
BkF	1.439 ± 1.181	1.632 ± 0.539	0.859 ± 1.020	0.708 ± 0.300
BaP	1.991 ± 1.101	1.598 ± 0.198	1.221 ± 0.480	0.624 ± 0.110
IcP	0.080 ± 0.139	0.502 ± 0.534	0.240 ± 0.210	0.101 ± 0.175
DBA	0.059 ± 0.101	0.785 ± 0.555	0.223 ± 0.221	0.145 ± 0.066
BgP	0.189 ± 0.328	0.793 ± 0.630	0.144 ± 0.103	0.156 ± 0.106
∑16 PAHs	9.814 ± 0.698	9.575 ± 0.525	5.535 ± 0.346	6.404 ± 0.430
% C PAHs	59.59	68.52	67.13	51.31

Site DC: Woodbridge (downstream). nd: not detected. C PAHs: Carcinogenic PAHs.

Appendix H1: Seasonal occurrence (average ±SD) of PAHs in the Plankenburg River sediment samples (sites PA and PB)

PAHs (µg/g)	Site PA				Site PB			
	Summer (Dec to Feb)	Autumn (Mar to May)	Winter (June to Aug)	Spring (Sept to Nov)	Summer (Dec to Feb)	Autumn (Mar to May)	Winter (June to Aug)	Spring (Sept to Nov)
Nap	1.788 ± 1.273	0.470 ± 0.160	0.099 ± 0.171	1.837 ± 0.819	1.803 ± 1.021	0.652 ± 0.479	1.506 ± 0.938	2.169 ± 1.331
Acy	0.307 ± 0.379	0.666 ± 0.178	0.020 ± 0.004	0.431 ± 0.254	0.045 ± 0.040	0.219 ± 0.192	nd	0.160 ± 0.138
Can	0.442 ± 0.394	1.262 ± 0.421	nd	0.075 ± 0.068	0.070 ± 0.120	0.053 ± 0.053	nd	0.065 ± 0.082
Flu	0.351 ± 0.222	0.839 ± 0.433	nd	0.129 ± 0.086	0.046 ± 0.080	0.238 ± 0.206	0.757 ± 0.788	0.086 ± 0.126
Phe	0.311 ± 0.461	9.697 ± 7.761	0.051 ± 0.028	0.074 ± 0.045	0.040 ± 0.035	13.416 ± 5.869	3.788 ± 2.750	0.151 ± 0.076
Ant	0.593 ± 0.156	nd	0.102 ± 0.005	0.509 ± 0.227	0.217 ± 0.188	0.177 ± 0.175	nd	0.159 ± 0.025
Flt	2.437 ± 1.672	4.717 ± 4.083	0.080 ± 0.042	0.507 ± 0.450	0.929 ± 1.107	1.093 ± 0.953	1.916 ± 1.445	0.335 ± 0.141
Pyr	0.332 ± 0.476	0.913 ± 0.183	nd	0.523 ± 0.458	0.006 ± 0.010	0.389 ± 0.339	0.367 ± 0.324	0.021 ± 0.036
BaA	0.944 ± 0.605	1.365 ± 0.698	0.577 ± 0.065	0.804 ± 0.960	0.472 ± 0.370	0.573 ± 0.359	1.954 ± 1.343	0.387 ± 0.161
Chy	1.035 ± 1.261	1.753 ± 1.189	0.160 ± 0.160	1.129 ± 0.811	0.519 ± 0.385	0.937 ± 0.553	1.888 ± 1.131	0.465 ± 0.322
BbF	27.869 ± 9.637	6.479 ± 2.704	0.790 ± 0.042	7.362 ± 4.969	2.750 ± 1.962	7.453 ± 4.299	8.154 ± 2.252	1.111 ± 1.494
BkF	6.774 ± 3.896	5.638 ± 2.310	0.876 ± 0.028	3.215 ± 1.163	3.967 ± 2.035	3.77 ± 2.032	4.385 ± 3.484	0.757 ± 0.836
BaP	3.284 ± 4.347	5.369 ± 2.626	0.116 ± 0.012	1.172 ± 0.966	0.639 ± 0.653	1.685 ± 0.909	7.316 ± 4.323	0.256 ± 0.302
IcP	0.612 ± 0.776	2.252 ± 0.983	0.680 ± 0.034	0.999 ± 0.833	0.494 ± 0.445	0.576 ± 0.113	0.583 ± 0.398	0.621 ± 0.654
DBA	2.320 ± 3.294	6.744 ± 1.208	1.046 ± 0.015	0.448 ± 0.624	0.331 ± 0.321	0.762 ± 0.253	1.505 ± 0.899	0.138 ± 0.056
BgP	0.864 ± 1.289	2.472 ± 1.410	0.088 ± 0.039	0.376 ± 0.298	0.269 ± 0.465	0.291 ± 0.261	1.193 ± 0.952	0.060 ± 0.034
∑16 PAHs	50.262 ± 6.802	50.635 ± 2.886	4.683 ± 0.364	19.588 ±1.818	12.596 ± 1.122	32.285 ± 3.574	35.312 ± 2.499	6.940 ± 0.550
% C PAHs	85.23	58.46	90.61	77.23	72.82	48.81	73.02	53.82

Site PA: Agricultural and residential areas. Site PB: Informal settlement of Kayamandi. nd: not detected. C PAHs: Carcinogenic PAHs.

Appendix H2: Seasonal occurrence (average ±SD) of PAHs in the Plankenburg River sediment samples (sites PC and PD)

PAHs (µg/g)	Site PC				Site PD			
	Summer (Dec to Feb)	Autumn (Mar to May)	Winter (June to Aug)	Spring (Sept to Nov)	Summer (Dec to Feb)	Autumn (Mar to May)	Winter (June to Aug)	Spring (Sept to Nov)
Nap	1.773 ± 0.301	0.471 ± 0.162	nd	2.316 ± 2.133	2.001 ± 0.533	0.240 ± 0.054	0.348 ± 0.150	1.692 ± 0.874
Acy	0.095 ± 0.164	0.207 ± 0.069	0.026 ± 0.025	0.275 ± 0.238	0.084 ± 0.043	0.120 ± 0.080	0.054 ± 0.026	0.422 ± 0.497
Can	0.025 ± 0.043	nd	0.086 ± 0.040	0.140 ± 0.143	0.451 ± 0.374	0.067 ± 0.084	0.017 ± 0.029	0.180 ± 0.162
Flu	0.058 ±0.016	0.155 ± 0.093	0.054 ± 0.040	0.128 ± 0.120	0.139 ± 0.027	0.034 ± 0.014	0.024 ± 0.009	0.167 ± 0.151
Phe	0.068 ± 0.033	8.460 ± 3.866	0.033 ± 0.028	6.494 ± 11.109	0.471 ± 0.273	17.886 ± 5.274	0.036 ± 0.020	0.186 ± 0.139
Ant	0.282 ± 0.048	2.779 ± 3.216	0.112 ± 0.012	0.229 ± 0.080	0.573 ± 0.039	4.856 ± 2.367	0.110 ± 0.030	0.208 ± 0.061
Flt	0.220 ± 0.098	0.738 ± 0.377	0.205 ± 0.239	1.362 ± 1.681	0.608 ± 0.332	0.737 ± 0.446	0.379 ± 0.250	0.930 ± 1.034
Pyr	0.011 ± 0.003	0.313 ± 0.147	0.014 ± 0.016	0.350 ± 0.293	0.612 ± 0.505	0.767 ± 0.458	0.044 ± 0.038	0.225 ± 0.240
BaA	0.140 ± 0.029	0.370 ± 0.235	0.303 ± 0.165	0.668 ± 0.451	0.797 ± 0.903	0.718 ± 0.459	0.304 ± 0.184	0.547 ± 0.618
Chy	0.248 ± 0.178	0.683 ± 0.103	0.418 ± 0.144	0.816 ± 0.803	0.494 ± 0.668	0.685 ± 0.251	0.149 ± 0.016	0.688 ± 0.620
BbF	19.047 ± 4.671	20.388 ± 6.131	15.497± 7.593	22.446 ± 10.820	10.466 ± 6.402	16.300 ± 8.264	3.631 ± 2.673	18.230 ± 7.417
BkF	8.992 ± 4.240	6.997 ± 5.064	6.562 ± 2.618	17.972 ± 9.591	8.544 ± 6.640	5.842 ± 0.843	2.331 ± 2.406	8.502 ± 3.187
BaP	0.881 ± 0.467	1.668 ± 1.013	1.052 ± 1.396	2.277 ± 1.959	1.670 ± 0.973	2.882 ± 2.296	0.370 ± 0.314	1.374 ± 1.152
IcP	0.184 ± 0.144	0.269 ± 0.098	0.234 ± 0.189	0.721 ± 0.268	0.456 ± 0.507	0.420 ± 0.326	0.375 ± 0.396	0.323 ± 0.358
DBA	0.130 ± 0.104	0.814 ± 0.194	0.095 ± 0.025	0.804 ± 1.002	0.434 ± 0.575	0.503 ± 0.301	0.102 ± 0.039	0.471 ± 0.343
BgP	0.100 ± 0.048	nd	0.114 ± 0.083	0.256 ± 0.076	0.253 ± 0.239	0.348 ± 0.179	0.063 ± 0.033	0.114 ± 0.066
∑16 PAHs	32.253 ± 5.052	44.311 ± 5.331	24.805 ± 4.052	57.254 ± 6.729	28.053 ± 3.088	52.405 ± 5.673	8.336 ± 0.999	34.257 ± 4.749
% C PAHs	91.84	70.39	97.41	79.83	81.49	52.19	87.11	87.96

Site PC: Substation in industrial area. Site PD: Industrial area at Adam Tas bridge. nd: Not detected. C PAHs: Carcinogenic PAHs.

Appendix I: ANOVA statistical analysis (multivariate tests) of data from the Diep and Plankenburg River sediment samples (compound Vs sites)

Multivariate Tests[c]

Effect		Value	F	Hypothesis df	Error df	Sig.
Sites	Pillai's Trace	.895	8.484[a]	6.000	6.000	.010
	Wilks' Lambda	.105	8.484[a]	6.000	6.000	.010
	Hotelling's Trace	8.484	8.484[a]	6.000	6.000	.010
	Roy's Largest Root	8.484	8.484[a]	6.000	6.000	.010
Compounds	Pillai's Trace	.[b]	.	.	.	.
	Wilks' Lambda	.[b]	.	.	.	.
	Hotelling's Trace	.[b]	.	.	.	.
	Roy's Largest Root	.[b]	.	.	.	.
Sites * Compounds	Pillai's Trace	.[b]	.	.	.	.
	Wilks' Lambda	.[b]	.	.	.	.
	Hotelling's Trace	.[b]	.	.	.	.
	Roy's Largest Root	.[b]	.	.	.	.

a. Exact statistic

b. Cannot produce multivariate test statistics because of insufficient residual degrees of freedom.

c. Design: Intercept
Within Subjects Design: Sites + Compounds + Sites * Compounds

Appendix J: ANOVA statistical analysis (multivariate tests) of data from the Diep and Plankenburg River sediment samples (compound Vs seasons)

Multivariate Tests[c]

Effect		Value	F	Hypothesis df	Error df	Sig.
Compounds	Pillai's Trace	.[a]	.	.	.	.
	Wilks' Lambda	.[a]	.	.	.	.
	Hotelling's Trace	.[a]	.	.	.	.
	Roy's Largest Root	.[a]	.	.	.	.
Seasons	Pillai's Trace	.661	2.600[b]	3.000	4.000	.189
	Wilks' Lambda	.339	2.600[b]	3.000	4.000	.189
	Hotelling's Trace	1.950	2.600[b]	3.000	4.000	.189
	Roy's Largest Root	1.950	2.600[b]	3.000	4.000	.189
Compounds * Seasons	Pillai's Trace	.[a]	.	.	.	.
	Wilks' Lambda	.[a]	.	.	.	.
	Hotelling's Trace	.[a]	.	.	.	.
	Roy's Largest Root	.[a]	.	.	.	.

a. Cannot produce multivariate test statistics because of insufficient residual degrees of freedom.

b. Exact statistic

c. Design: Intercept

Within Subjects Design: Compounds + Seasons + Compounds * Seasons

Appendix K: Sediment physicochemical properties

Sediment	Fractional Organic Carbon (%)	Organic matter (%)	Percentage of sand particle size	Percentage of silt particle size	Percentage of clay particle size
PA	0.5357	15.23	29.29	9.06	2.03
PB	2.3096	13.42	24.68	1.58	4.41
PC	0.9013	3.89	61.58	1.31	0.80
PD	0.8650	2.69	79.52	1.09	0.10
DA	2.0402	15.23	62.68	5.99	2.95
DB	1.1172	11.86	67.00	3.01	1.70
DC	0.6706	2.02	0.47	51.59	6.61

Appendix L: Weibull plots of PAHs levels in water samples from the Diep and Plankenburg Rivers

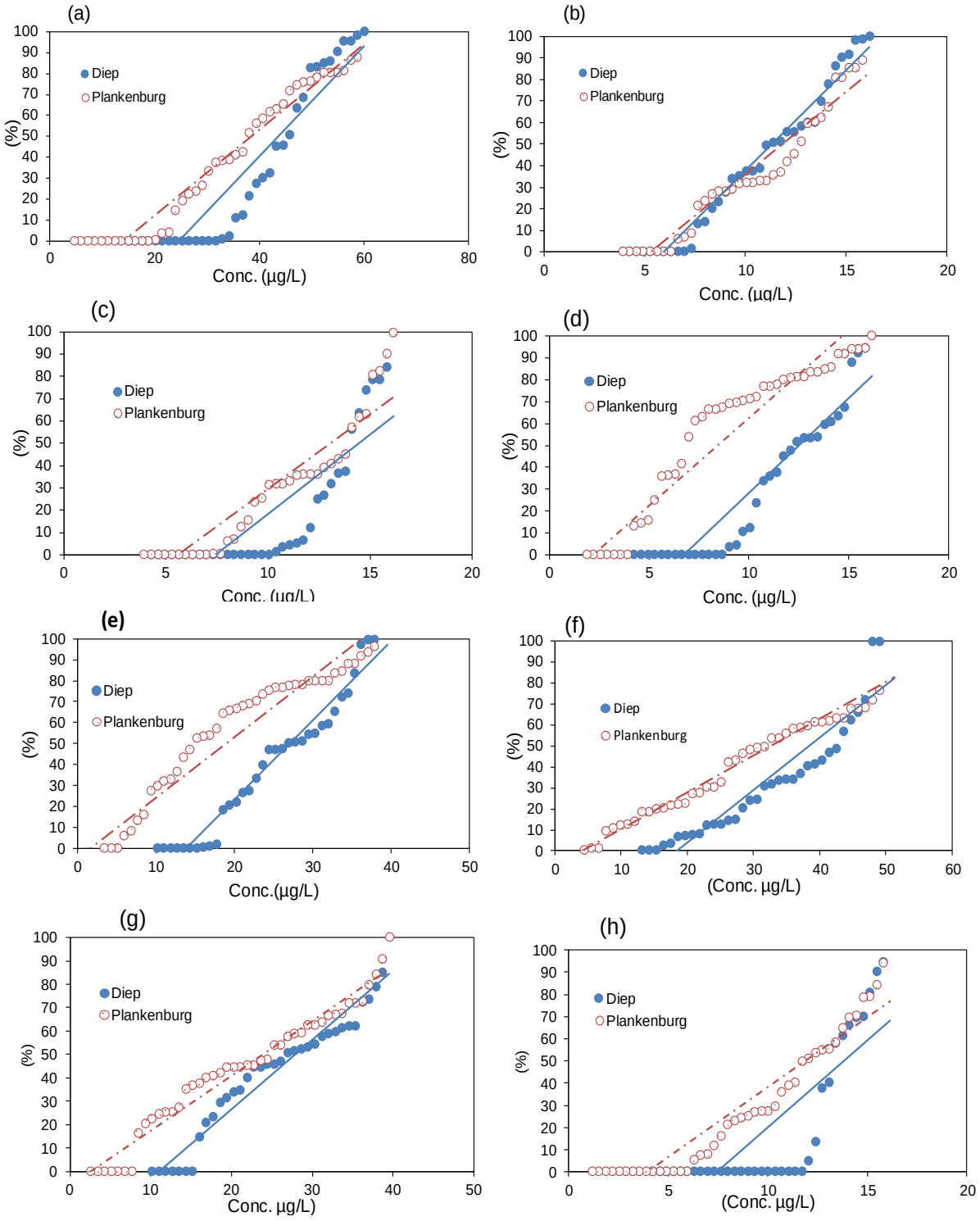

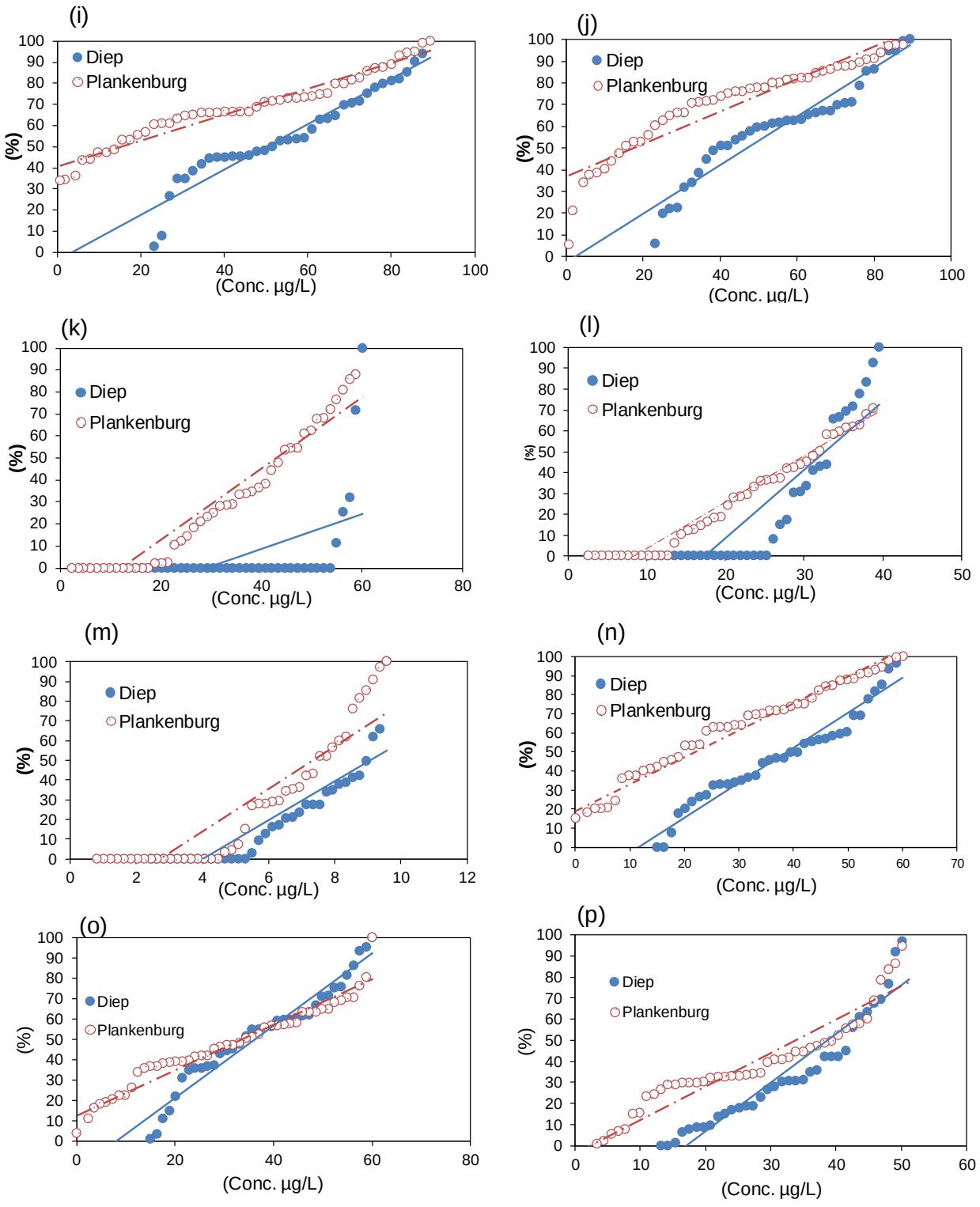

a = naphthalene. b= acenaphthylene. c = acenaphthene. d = fluorene.
e = phenanthrene. f = anthracene. g = fluoranthene. h = pyrene.
i = benzo[a]anthracene. j = chrysene. k = benzo[b]fluoranthene. l = benzo[k]fluoranthene.
m = benzo[a]pyrene. n = indeno[1,2,3-cd]pyrene o = dibenzo[a, h]anthracene. p = benzo[g, h, i]perylene.

Appendix M: Weibull plots of PAHs levels in sediments from the Diep and Plankenburg Rivers

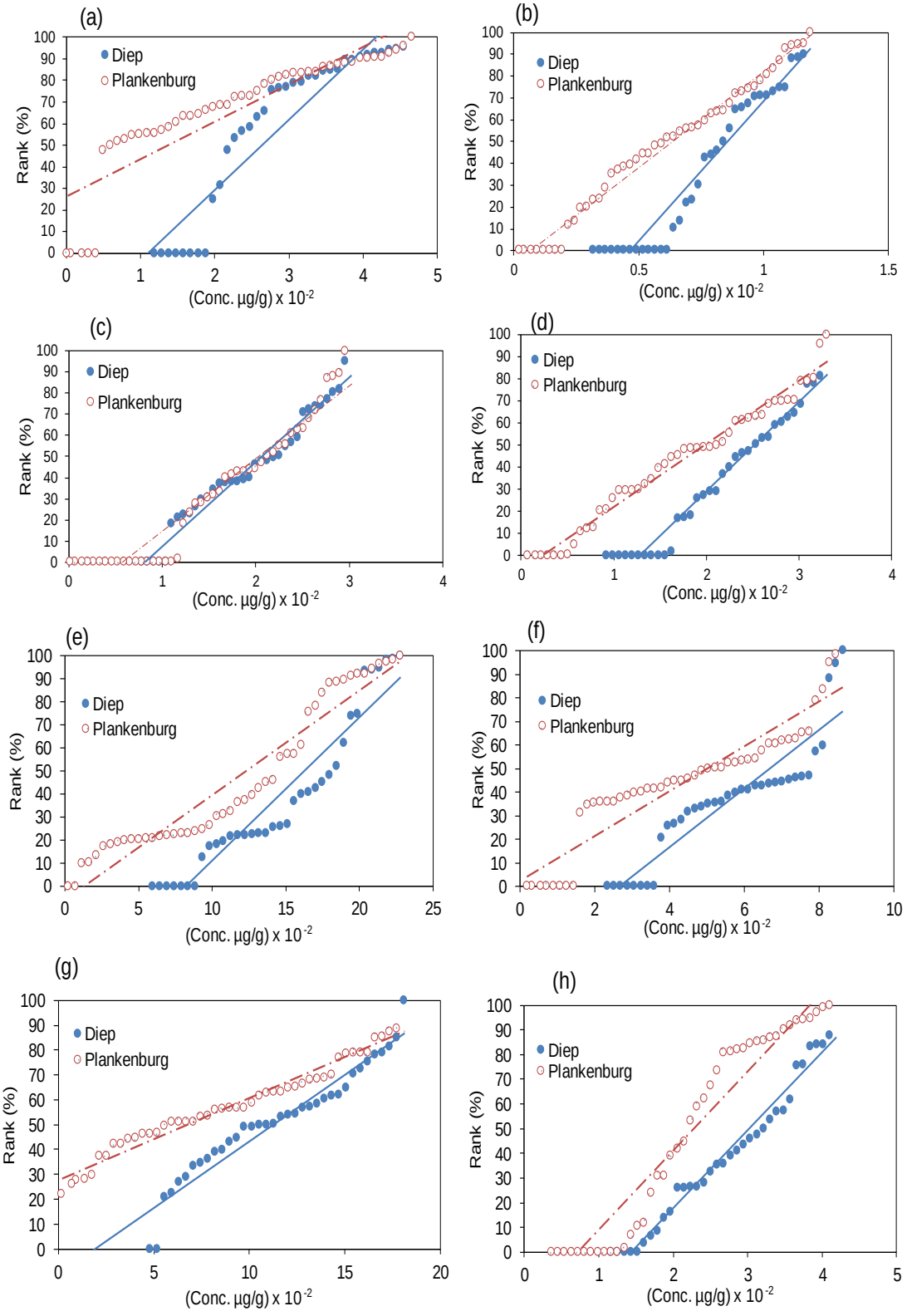

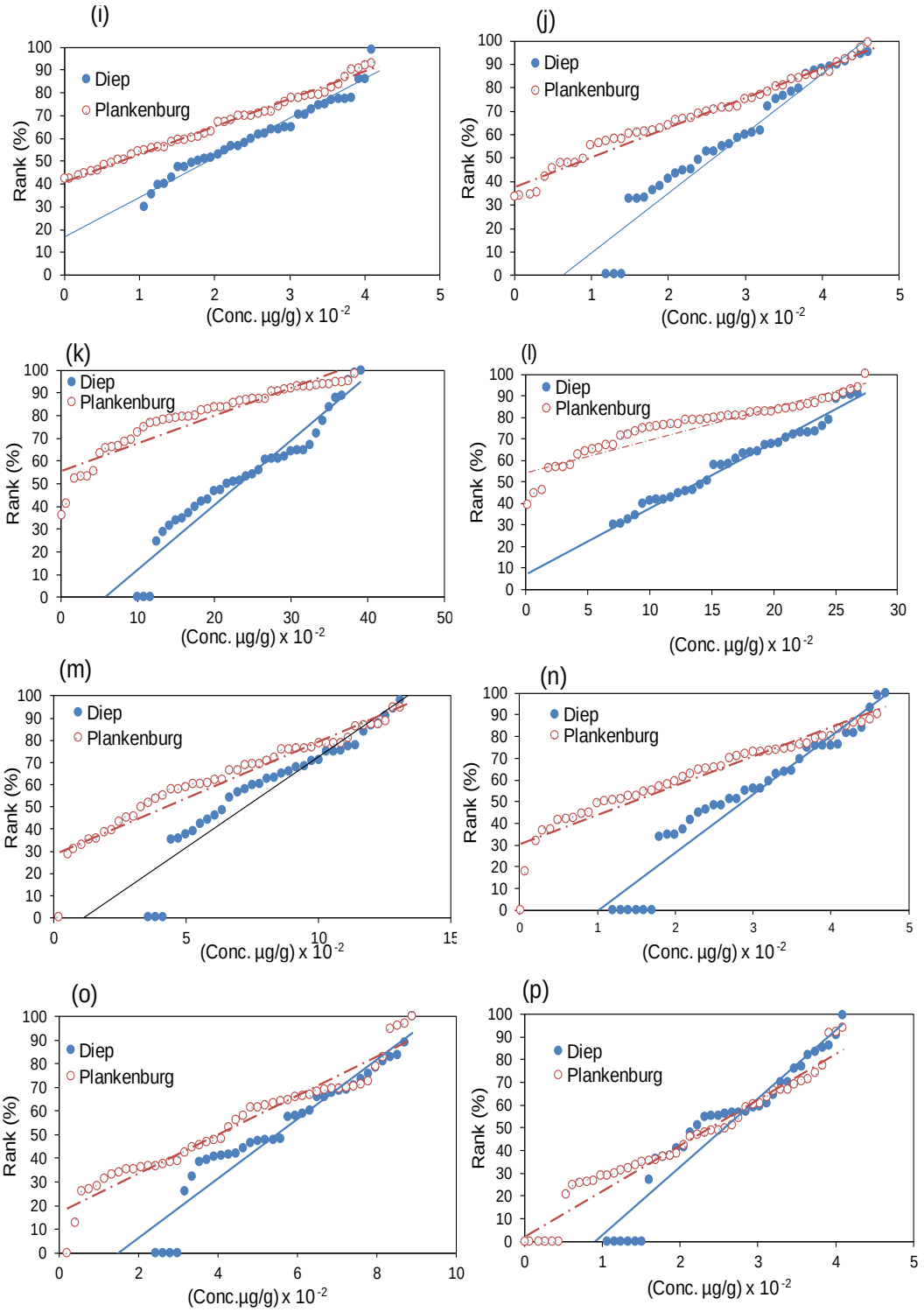

a = naphthalene. b= acenaphthylene. c = acenaphthene. d = fluorene.
e = phenanthrene. f = anthracene. g = fluoranthene. h = pyrene.
i = benzo[a]anthracene. j = chrysene. k = benzo[b]fluoranthene. l = benzo[k]fluoranthene.
m = benzo[a]pyrene. n = indeno[1,2,3-cd]pyrene o = dibenzo[a, h]anthracene. p = benzo[g, h, i]perylene.